ANALYTICA CHIMICA ACTA

International monthly devoted to all branches of analytical chemistry
Revue mensuelle internationale consacrée à tous les domaines de la chimie analytique
Internationale Monatsschrift für alle Gebiete der analytischen Chemie

ELSEVIER SCIENTIFIC PUBLISHING COMPANY

AMSTERDAM

✓ *Anal. Chim. Acta*, Vol. 67, No. 2, 253–496, December 1973
Published monthly
Completing Volume 67

Publication Schedule for 1973

Vol. **63,** No. **1**	January 1973	
Vol. **63,** No. **2**	February 1973	**(completing Vol. 63)**
Vol. **64,** No. **1**	March 1973	
Vol. **64,** No. **2**	April 1973	
Vol. **64,** No. **3**	May 1973	**(completing Vol. 64)**
Vol. **65,** No. **1**	June 1973	
Vol. **65,** No. **2**	July 1973	**(completing Vol. 65)**
Vol. **66,** No. **1**	August 1973	
Vol. **66,** No. **2**	September 1973	
Vol. **66,** No **3**	October 1973	**(completing Vol. 66)**
Vol. **67,** No. **1**	November 1973	
Vol. **67,** No. **2**	December 1973	**(completing Vol. 67)**

Subscription price: Dfl. 410.00 plus Dfl. 30.00 postage. Subscribers in the U.S.A. and Canada receive their copies by airmail. Additional charges for airmail to other countries are available on request. For advertising rates apply to the publishers.

GENERAL INFORMATION

Languages

Papers will be published in English, French or German.

Submission of papers

Papers should be sent to:

PROF. PHILIP W. WEST,
Coates Chemical Laboratories,
College of Chemistry and Physics,
Louisiana State University,
Baton Rouge 3,
La. 70803 (U.S.A.)

or to:

DR. A. M. G. MACDONALD,
Department of Chemistry,
The University,
P.O. Box 363
Birmingham B15 2TT (Great Britain)

Reprints

Fifty reprints will be supplied free of charge. Additional reprints (minimum 100) can be ordered at quoted prices. They must be ordered on order forms which are sent together with the proofs.

PRINTED IN THE NETHERLANDS

Ready-for-use Buffer Solutions

Analytica Chimica Acta, 67 (1973) 253–258

THE DETERMINATION OF BORON IN SOLUTION TO SUB-p.p.b. CONCENTRATIONS BY HOLLOW-CATHODE EMISSION

E. H. DAUGHTREY and W. W. HARRISON

Department of Chemistry, University of Virginia, Charlottesville, Va. 22901 (U.S.A.)

(Received 4th April 1973)

Trace analysis methods for the determination of boron in solution have generally lacked the sensitivity to operate at parts-per-billion concentration levels. Yet many potential applications[1,2] fall within this range, requiring pretreatment and concentration steps to comply with sensitivity limitations.

A comprehensive account of the analytical chemistry of boron through 1964 is available[3]. Spectrophotometric and fluorimetric methods have provided reasonable sensitivity but may involve considerable chemical pretreatment to produce the chromophore. They are also subject to many interferences[4–6]. Conventional atomic absorption has rather poor sensitivity[7], although non-flame atomization sources such as the Kranz d.c. arc[8] offer some improvement. A nitrous oxide–acetylene flame also evidently reduces the formation of refractory oxides, which are suggested as a chief cause of unsatisfactory sensitivity by atomic absorption[9]. Advances in emission spectrometry, especially the use of an inert argon atmosphere for the d.c. arc[10], and the high-frequency plasma source[11] have yielded improved sensitivity.

The use of a hollow-cathode emission source for the analysis of cathode surface films deposited from solution suggests an application to elements such as boron which form refractory oxides in atmospheric discharges. A hollow-cathode source has been used to determine boron in zirconium[12]. A report from this laboratory[13] showed the application of hollow-cathode emission to lead, copper, tin, and boron; the determination of lead in biological materials[14] was also demonstrated. A commercially available hollow-cathode source was used in trace analysis for gold in solution[15].

The same source, with only slight modification, has now been applied to the study of boron atomic emission for p.p.b. and sub-p.p.b. solutions deposited onto a hollow cathode.

EXPERIMENTAL

Hollow-cathode source

The Glomax demountable hollow-cathode lamp (Barnes Engineering Co., Stamford, Conn.), operating in the flow mode, was used with two modifications. The gas port modification has been previously described[15]. Inadequate cathode cooling with resultant tube current limitations led to the second modification, a replacement of the constricted flow concentric tubing (serving as both cooling water source and drain to the heat exchange block) with a Swagelok Tee-joint fitting

and a short length of thin wall stainless steel tubing joined to the heat exchange block by a machine fitting. This arrangement allows higher water flow rates, greater cathode cooling, and use of tube currents up to several hundred milliamperes for the hollow-cathode emission.

The tube was mounted on an Ealing vertical and transverse motion carrier which provided translation along two axes for optical alignment with the spectrometer slit.

The hollow-cathode tube was powered by a Kepco model HB power supply which can provide regulated current up to 500 mA, with a maximal operating potential of 600 V.

Vacuum system

The vacuum system was previously described for a static mode[15]. The flow system was operated by bleeding fill gas through the manifold (flow controlled by a metering valve) into the hollow-cathode tube and pumped out by an oil rotary pump. The pressure was monitored on both sides of the tube by thermocouple gauges and a differential oil manometer filled with apiezon oil. The gauge on the pump side of the tube gave the most accurate indication of actual pressure within the hollow cathode, because of the constriction of a stopcock on the fill side between the oil manometer and the tube.

Measurement system

The spectrometer, amplifier, and readout system have been previously described[15].

Reagents

Reagent-grade chemicals were used throughout the investigation. Boron standards were prepared by dilution of a 100 p.p.m. stock solution made by dissolving either boric acid or sodium tetraborate in distilled, deionized water, followed by proper dilution. All boron standards were stored in polyethylene bottles. Distilled, deionized water was used for all standard solutions.

Procedure

A series of standard boron solutions was prepared and a 100-μl portion of the test solution transferred to the cathode cavity by syringe. After evaporation to dryness under an infrared lamp, the cathode was placed in the cathode block, and the system evacuated and flushed with the desired fill gas. The pressure was adjusted by the metering valve, reaching an equilibrium value in 1–2 min. The discharge was initiated at low current and rapidly increased to its operating value.

The spectrometer and associated readout produced a display of emission intensity as a function of time. The recorder trace showed a rapid rise in emission intensity followed by an exponential-like decay to a background level. This peak intensity was taken in each case; 10–20% r.s.d. was observed. Blanks were run to determine the contribution to the emission intensity from the cathode material.

Copper cathodes were re-used by sputtering them in the discharge at high current until the emission intensity reached the background level.

RESULTS AND DISCUSSION

The strongest analytical emission lines for boron are listed[16] as 249.68 nm and 249.77 nm, a doublet unresolved by the spectrometer used. These resonance lines were the most sensitive for hollow-cathode emission and were used for all atomic boron emission in this study.

Flow vs. static operation

The use of the gas flow system offered several advantages over a static system. Discharge stability was obtained for a wider current and pressure range. An improvement was observed for long-term stability; this was necessary for the boron determination because the emission peak arose more slowly than for previous elements studied. With the static system, increased localized pressure in the discharge could cause stability problems within a few minutes of initiation. The flow system eliminated this pressure rise and thus the instability. A flow system suggests possible sensitivity loss by rapid removal of the sputtered analyte from the discharge, but comparisons with the static mode showed no such effects except at very high gas flow rates.

Cathode selection and cleanup

Stainless steel and copper were investigated as possible cathode materials. Stainless steel produced good sensitivity, but the boron sputtered very slowly, and the emission intensity required an inordinate time to return to background. Also, the background was higher for stainless steel than copper, partly because of the slight overlap of an iron line with the boron doublet. Copper proved to be an excellent cathode material, owing to low background and ease of boron sputtering from the surface. Thus, copper was chosen as the cathode material for this study.

Clean-up of the cathode is a critical factor in reproducibility of hollow-cathode emission. Traces of residual boron must be removed after each run, but perhaps more important is the reproducible conditioning of the cathode surface to remove contaminants and surface oxidation. Dilute nitric acid washing was too destructive of the cathode surface. However, the sputtering process itself at vigorous conditions could be used to clean the cathode cavity. A sputtering current of 150 mA for 3–4 min not only cleaned the metal surface but also created a more reproducible cathode response.

Fill gas parameters

Helium, neon, and argon were investigated as fill gases. Helium and neon both gave much lower signal-to-background ratios than argon, owing to their lower sputtering rates. Even after several minutes of firing a boron sample with either helium or neon, a subsequent discharge of the same cathode with argon would result in a substantial emission peak from boron. Also, neither helium nor neon gave the reproducible cavity surface provided by argon. For argon as a fill gas, the response of emission intensity as a function of fill gas pressure is given in Fig. 1. The best signal-to-background intensity was at 0.7 torr pressure of argon, measured on the exit side of the tube. Below 0.2 torr, the discharge was difficult to maintain at reasonable currents, because of the voltage limit of the power supply. At pressures

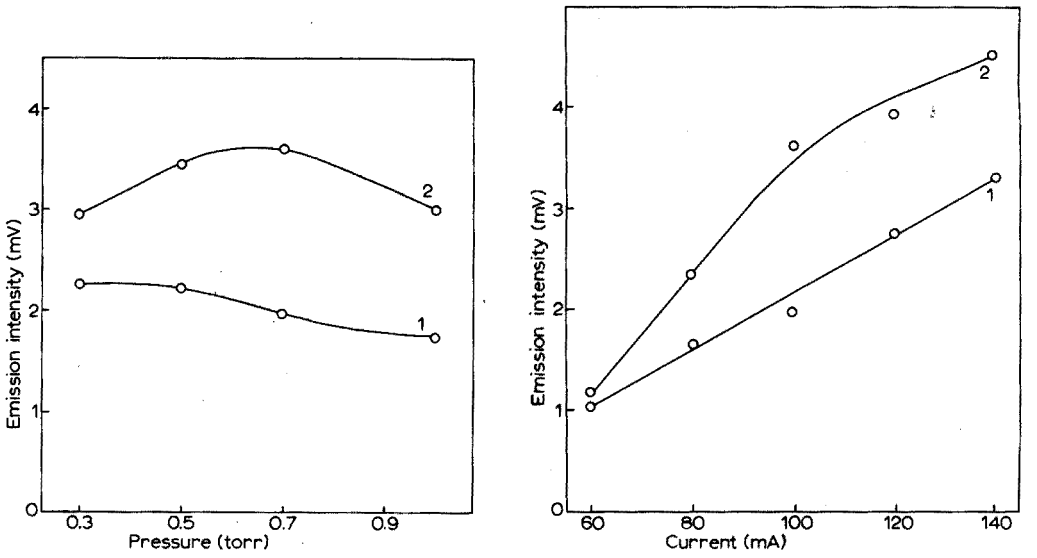

Fig. 1. Plot of 249.8-nm boron emission line intensity *vs.* argon filler gas pressure for (1) cathode background and (2) signal plus background for 0.4 p.p.b. boron solution. Tube current, 100 mA.

Fig. 2. Plot of 249.8-nm boron emission line intensity *vs.*, tube current for (1) cathode background and (2) signal plus background for 0.4 p.p.b. solution. Filler gas, argon at 0.7 torr.

above 0.9 torr, the flow rate necessary to maintain the pressure can cause sensitivity losses.

Figure 2 shows the effect of tube current on both boron intensity and background. Optimal current was taken to be 100 mA, as higher currents gave no increase in net peak height above background. Thus, an argon fill at 0.7 torr pressure and a current of 100 mA were selected as standard conditions yielding the best sensitivity and reproducibility.

Studies with boron solutions

The type of signal obtained from the discharge is shown in Fig. 3. Within the first minute after initiation, maximum boron emission is reached and then drops more slowly to the background emission level. Since the "tail" of the peak is rather long, the clean-up procedure (high tube current) is normally initiated shortly after the emission peaks appear, in order to rid the cathode of any trace of boron. The background response is also shown in Fig. 3; the slight peaking is due to broad-band emission and not to boron impurity in the cathode or in the distilled deionized water.

A working curve for boron was constructed from standard solutions prepared from boric acid. Figure 4 shows the lower limits of effective working range for the hollow-cathode technique.

The relative magnitude of boron oxide present in the discharge was observed by measuring the BO_2 band emission at 546.0 nm, a wavelength used for flame emission analysis[17]. The sensitivity by hollow-cathode emission was estimated as 20 ng, a 200-fold decrease relative to boron line emission.

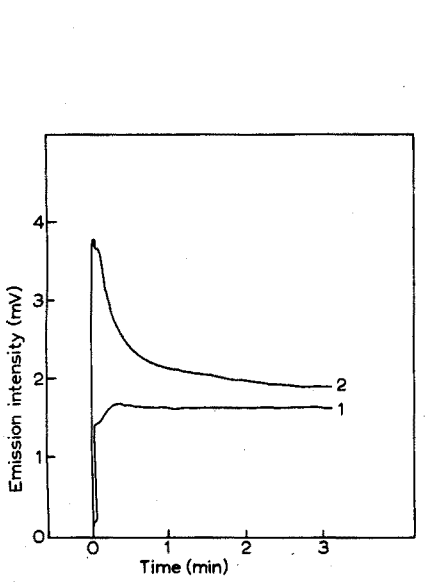

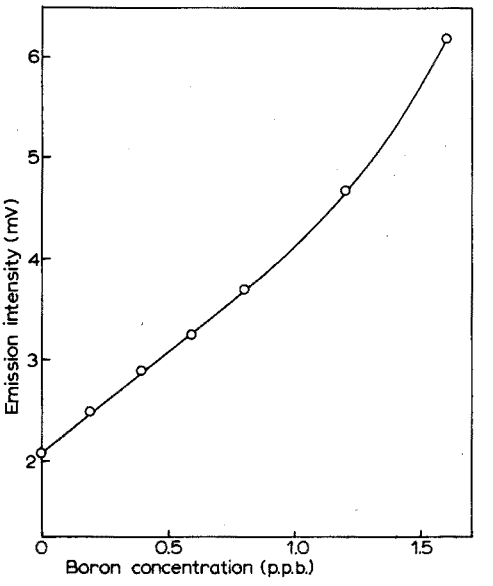

Fig. 3. Recorder tracing of 249.8-nm boron emission line intensity as a function of time for (1) cathode background and (2) signal plus background for 1.0 p.p.b. boron solution. Filler gas, argon at 0.7 torr; tube current, 100 mA.

Fig. 4. Working curve for boron at 249.8 nm; conditions as in Fig. 3.

The lower limit of atomic emission detection is about 10 pg, although the sensitivity could be improved by multiple sample applications. The sensitivity for boron by hollow-cathode emission can be attributed to three main factors: (*a*) the ease of sputtering of the copper matrix by argon effectively strips the boron from the surface and into the discharge; (*b*) the high energy available in the discharge atomizes the boron with apparently good efficiency; and (*c*) the inert argon atmosphere prevents oxide formation of the boron, one of the major reasons cited to explain the low sensitivity for elements which form refractory compounds, in atomic absorption and conventional emission spectrometry.

The attainable sensitivity compares favorably with those reported for fluorescence[4,5] where 0.5 and 10 p.p.b. sensitivities were attained, and for spectrophotometry[6] where 2 p.p.b. was achieved. The hollow-cathode emission sensitivity is much better than that by atomic absorption, 1 p.p.m.[9], flame emission, 0.1 p.p.m.[17], and d.c. arc emission, 0.5 p.p.m.[10].

This work was supported by grant no. GM-14569, U.S.P.H.S.

SUMMARY

The determination of boron in solutions to sub-p.p.b. concentrations by hollow-cathode emission is demonstrated. The effects of cathode material, clean-up procedure, fill gas, and tube current were investigated to determine the conditions yielding optimal sensitivity. The boron atomic line emission is 200 times as intense as boron oxide band emission.

RÉSUMÉ

On propose une méthode de dosage très sensible (sub-p.p.b.) pour le bore par émission à cathode creuse. On examine diverse paramètres permettant de déterminer les conditions les meilleures pour une sensibilité optimale. La raie d'émission du bore atomique est 200 fois plus intense que celle de l'oxyde de bore.

ZUSAMMENFASSUNG

Die Bestimmung von Bor in Lösungen bei Sub-p.p.b.-Konzentrationen durch Hohlkathodenemission wird beschrieben. Der Einfluss von Kathodenmaterial, Aufbereitungsverfahren, Füllgas und Lampenstrom wurde zur Ermittlung der Bedingungen untersucht, unter denen die Empfindlichkeit optimal ist. Die Bor-Atomlinien-Emission ist um den Faktor 200 intensiver als die Bandenemission von Boroxid.

REFERENCES

1 H. J. M. Bowen, *Trace Elements in Biochemistry*, Academic Press, New York, 1966.
2 J. F. Kipp and R. C. Kroner, *Trace Metals in Waters of the United States*, United States Department of the Interior (Survey 1962–1967), Washington, D.C.
3 A. A. Nemodrux and Z. K. Karojova, *Analytical Chemistry of Boron*, Ann Arbor-Humphey Science Publishers, Ann Arbor, 1969 (translated from the Russian).
4 M. Marcantonatos, G. Gamba and D. Monnier, *Helv. Chim. Acta*, 52 (1969) 538.
5 B. Liebich, D. Monnier and M. Marcantonatos, *Anal. Chim. Acta*, 52 (1970) 305.
6 J. W. Mair and H. G. Day, *Anal. Chem.*, 44 (1972) 2015.
7 G. D. Christian and F. J. Feldman, *Atomic Absorption Spectroscopy*, Wiley–Interscience, New York, 1970.
8 M. Malinek and H. Massman, *Can. Spectrosc.*, 15 (3) (1970) 1.
9 S. J. Weger, L. R. Hossner and L. W. Ferrara, *J. Agric. Food Chem.*, 17 (1969) 1276.
10 K. Takahoshi, T. Takahoshi and E. Sudo, *Bunko Kenkyu*, 18 (1969) 311; *Chem. Abstr.*, 73 (1970) 31245.
11 R. M. Dagnall, D. J. Smith, T. S. West and S. Greenfield, *Anal. Chim. Acta*, 54 (1971) 397.
12 L. V. Lipis and Yu. I. Koroium, *Opt. Spektrosk.*, 5 (1958) 334.
13 W. W. Harrison and N. J. Prakash, *Anal. Chim. Acta*, 49 (1970) 151.
14 N. J. Prakash and W. W. Harrison, *Anal. Chim. Acta*, 53 (1971) 421.
15 W. W. Harrison and E. H. Daughtrey, *Anal. Chim. Acta*, 65 (1973) 35.
16 *Experimental Transition Probabilities for Spectral Lines of Seventy Elements*, NBS Monograph 53, U.S. Government Printing Office, Washington, D.C., 1962.
17 *Atomic Absorption Methods Manual*, Jarrell-Ash Company, Waltham, Mass.

Analytica Chimica Acta, 67 (1973) 259–267

ELECTRONIC ABSORPTION AND FLUORESCENCE STUDY OF IONIZATION AND INTRAMOLECULAR HYDROGEN-BONDING IN THE α, β-*o*-HYDROXYNAPHTHOIC ACIDS

STEPHEN G. SCHULMAN and PETER J. KOVI
College of Pharmacy, University of Florida, Gainesville, Fla. 32610 (U.S.A.)
(Received 29th March 1973)

The *o*-hydroxynaphthoic acids are of considerable analytical significance as chelating agents, fluorescent indicators and in the manufacture of dyestuffs. Fluorescence spectroscopy affords a sensitive method for the detection and determination of these compounds; and because each of these compounds contains two ionizing groups, it would be desirable to study the variations of fluorescent properties with respect to solution acidity in order to be able to obtain maximal selectivity in fluorimetric analysis. From the photochemical point of view, it has been shown that in salicylic acid, the simplest of the *o*-arylhydroxycarboxylic acids, proton transfer from the hydroxyl group to the carboxyl group occurs during the lifetime of the lowest excited singlet state[1,2] in both amphiprotic and aprotic solvents; a result that indicates that excited-state proton transfer is truly unimolecular in salicylic acid. In a similar study of 3-hydroxy-2-naphthoic acid[3], Hirota found that an anomalous long-wavelength fluorescence appeared in basic solvents and in aprotic solvents doped with small amounts of basic solvents. From this, he concluded that intramolecular proton transfer occurred during the lifetime of the lowest excited singlet state of 3-hydroxy-2-naphthoic acid. Recently, the hypothesis of true intramolecular proton transfer in the excited state of 3-hydroxy-2-naphthoic acid has been refuted by Ware *et al.*[4], who employed fluorescence quenching and singlet-state lifetime measurement techniques, in a variety of solvents, to show that the phototautomerization of 3-hydroxy-2-naphthoic acid, in the lowest excited singlet state involves intermolecular hydrogen bonding with the solvent in the ground electronic state. However, of the four possible prototropic species extant in the ground state of 3-hydroxy-2-naphthoic acid, two (the uncharged molecule and the singly charged anion) are capable of demonstrating phototautomerism and it was shown by Kovi and Schulman[5] that, in fact, the neutral molecule does not phototautomerize but the singly charged anion does in the ^1L_b state.

The two remaining *o*-hydroxynaphthoic acids, 1-hydroxy-2-naphthoic acid and 2-hydroxy-1-naphthoic acid, have not been systematically investigated. In light of the fact that there are substantial differences in fluorimetric titration behavior between salicylic acid and 3-hydroxy-2-naphthoic acid, it appeared that a study of the pH and Hammett acidity dependences of 1-hydroxy-2-naphthoic and 2-hydroxy-1-naphthoic acids might yield considerable information of general chemical interest.

EXPERIMENTAL

Apparatus

Absorption spectra were taken on a Beckman DB-GT spectrophotometer. Fluorescence spectra were taken on a Perkin–Elmer MPF-2A fluorescence spectrophotometer whose monochromators were calibrated against the xenon line emission spectrum and whose output was corrected for instrumental response by means of a rhodamine-B quantum counter. pH measurements were made on an Orion 801 pH meter with a Sargent–Welch combination Ag/AgCl–glass electrode.

Reagents

1-Hydroxy-2-naphthoic acid (1-HNA) and 2-hydroxy-1-naphthoic acid (2-HNA) (Aldrich Chemical Co., Milwaukee, Wisc.) were purified by multiple recrystallizations from chloroform. Analytical reagent-grade sulfuric acid (Mallinckrodt Chemical Works, Inc., St. Louis, Mo.) and chloroform (Matheson, Coleman and Bell, Inc., East Rutherford, N. J.) were used without further purification. Sulfuric acid solutions were prepared by dilution with distilled, deionized water and were calibrated by the corrected Hammett acidity scale of Jorgenson and Hartter[6]. Solutions on which fluorescence spectra were taken were *ca.* $1 \cdot 10^{-5}$ *M* in 1-HNA or 2-HNA; for absorption measurements, *ca.* $1 \cdot 10^{-4}$ *M* solutions were used.

RESULTS AND DISCUSSION

The long-wavelength absorption (^1L_a and ^1L_b) maxima and fluorescence maxima of the various prototropic species derived from the *o*-hydroxynaphthoic acids are presented in Table I. The assignments of the spectral maxima to the species from which they originated were based on the pH-dependent transformations of the electronic spectra and the assumptions that in the most concentrated acid solutions the cations were the predominant species in ground and excited states and in the most concentrated solutions the doubly charged anions were the predominant species in ground and electronically excited states. These assumptions are justifiable on the basis of the results of previous studies of *o*-arylhydroxycarboxylic acids[2,5].

The identification of the sites of dissociation in ground and electronically excited states of 1-HNA and 2-HNA from spectral shifts is slightly more complicated than in the case of 3-hydroxy-2-naphthoic acid (3-HNA)[5]. In 3-HNA both the carboxyl and hydroxyl groups are in β-positions in the naphthalene ring; in all prototropic species derived from 3-HNA, the ^1L_b band is the longest wavelength absorption band in the absorption spectrum and all prototropic reactions in the ground state can be followed by observing the shifts of this band with protonation and dissociation. Moreover, in 3-HNA fluorescence always arises from the ^1L_b state and the study of excited-state prototropic reactivity in 3-HNA is facilitated by the substantial shifting of the ^1L_b fluorescence band under the positive and negative polarizing influences of protonation and dissociation[5].

In 1-HNA, the carboxyl group is in a β-position of naphthalene but the hydroxyl group is in an α-position. In this case, ground-state protolytic reactions at the carboxyl group have the greatest effect on the position of the ^1L_b band

TABLE I

LOW FREQUENCY ABSORPTION ($\bar{\nu}_{^1L_a}$ AND $\bar{\nu}_{^1L_b}$) AND FLUORESCENCE ($\bar{\nu}_f$) SPECTRAL MAXIMA (IN $cm^{-1} \cdot 10^{-4}$) OF 1-HYDROXY-2-NAPHTHOIC ACID AND 2-HYDROXY-1-NAPHTHOIC ACID IN AQUEOUS AND SULFURIC ACID MEDIA

(The assignments of the spectral bands are discussed in the text)

	$\bar{\nu}_{^1L_a}$	$\bar{\nu}_{^1L_b}$	$\bar{\nu}_f$
1-HNA			
Cation ($H_0 - 10$)	3.33	2.61	2.27
Zwitterion ($H_0 - 5.8$)	[a]	[a]	2.14
Neutral molecule (pH 0.8)	3.48	2.92	2.43
Singly charged anion (pH 6.0) (dissociated carboxyl group)	3.46	3.00	2.43
Doubly charged anion ($H - 15.2$)	2.92	[b]	2.20
2-HNA			
Cation ($H_0 - 10$)	2.92	[b]	2.30
Zwitterion ($H_0 - 5.8$)	[a]	[a]	1.91
Neutral molecule (pH 0.8)	3.41	3.01	2.53
Singly charged anion (pH 6.0) (dissociated carboxyl group)	3.48	2.99	2.46
Doubly charged anion ($H - 15.2$)	3.48	2.84	2.36

[a] The zwitterions are not detectable as ground-state species.
[b] The ^1L_b band is eclipsed by the more intense ^1L_a band.

but dissociation of the hydroxyl group has the greatest effect on the position of the ^1L_a band. In 2-HNA the prototropic reactions of the carboxyl group have the greatest effect on the ^1L_a band while the dissociation of the hydroxyl group has the greatest effect on the ^1L_b band.

Table I shows that in 1-HNA, the dissociation of the cation (C), results in a substantial blue shift of the ^1L_b band and a smaller shift of the ^1L_a band, suggesting that dissociation occurs, in the ground state, from the protonated carboxyl group to form the neutral molecule (N). Dissociation of the neutral molecule (N) produces a further blue shift of the ^1L_b band with practically no effect on the ^1L_a band and thus corresponds to dissociation of the carboxyl group to form the singly charged anion (A). Dissociation of the anion (A) results in a large red shift of the ^1L_a band so that in the absorption spectrum of the doubly charged anion (D) the ^1L_b band is eclipsed by the more intense ^1L_a band. This final dissociation must of course occur from the hydroxyl group. The sequence of ground-state protolytic dissociations of 1-HNA and the pK_a values for each equilibrium, estimated from the acidity dependences of the absorption spectra, are as follows:

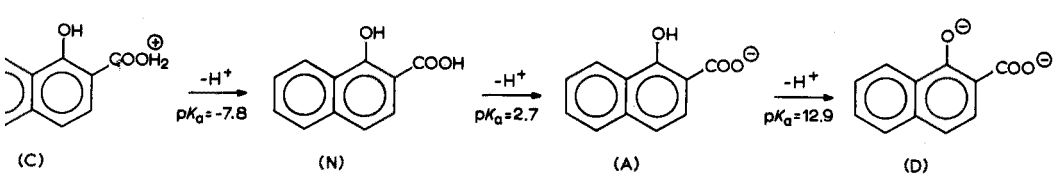

In 2-HNA, dissociation of the cation (C) yields a large blue shift of the ^1L_a band indicating dissociation from the protonated carboxyl group. The dissociation of the neutral molecule (N) yields a further blue shift of the ^1L_a band and a very small red shift of the ^1L_b band. Thus the singly charged anion (A) derived from 2-HNA is also charged at the carboxyl group. Dissociation of the anion (A) to give the dianion (D) is accompanied by a red shift of the ^1L_b band and no change in the position of the ^1L_a band, indicating dissociation, this time, from the hydroxyl group. The sequence of ground-state dissociations and absorptiometrically estimated pK_a values of 2-HNA, are as follows:

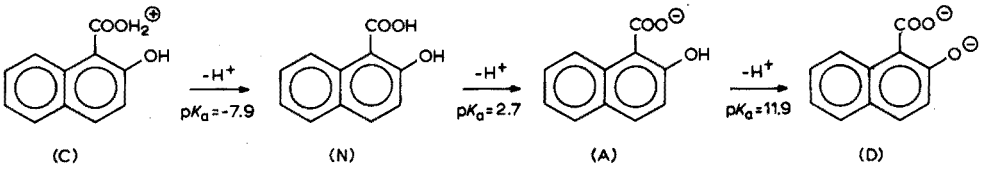

The pK_a values for the equilibria between the neutral molecules and the singly charged anions and those for the equilibria between the singly charged anions and the doubly charged anions are similar to the corresponding pK_a values of salicylic[2] and 3-hydroxy-2-naphthoic[5] acids and are anomalous for the dissociation constants of arylcarboxylic acids and phenols[7], respectively. In the cases of the latter two compounds, the anomalously high acidities of the neutral molecules and the anomalously low acidities of the singly charged anions are the result of intramolecular hydrogen bonding between the phenolic proton and the carboxyl group[7]. That the same phenomenon is operative in 1-HNA and 2-HNA is a conclusion supported by the anomalously small spectral shifts for carboxylic acids, accompanying the N⇌A interconversions[7].

The interpretations of the pH and H_0 dependent shifts of the fluorescences of 1-HNA and 2-HNA are complicated by the possibility of phototautomerism of the uncharged and singly charged anion species, which, for 1-HNA, can be depicted:

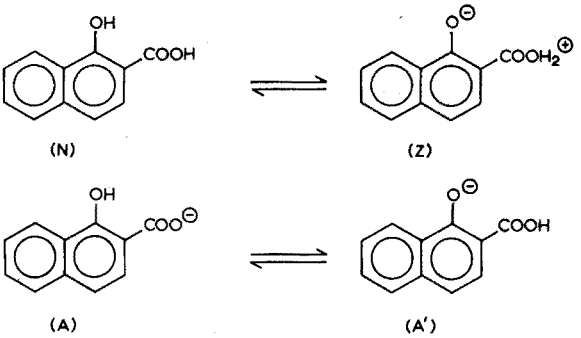

The fluorescences of the cations of 1-HNA and 2-HNA in the region H_0–10 to −6 both shift to lower frequencies as a result of dissociation even though the corresponding absorption spectra shift to higher frequencies. This

suggests that the site of dissociation in both cations, in the lowest excited singlet state, is the hydroxyl group rather than the carboxyl group as in the ground state, and thus, that the predominant uncharged species, in the lowest excited singlet state, are the zwitterions (Z). In the range H_0-2 to pH 1 the fluorescenses of both isomers shift to higher frequencies. No changes in the absorption spectra occur in this acidity region, indicating that only the neutral species is excited and that excited-state processes are responsible for the shifting of fluorescence. Two processes could conceivably account for the blue shifts of the fluorescences in the H_0-2 to pH 1 region. First, the excited neutral species could phototautomerize to the excited zwitterion and then dissociate, during the lifetime of the excited state, to the excited, singly charged anion, dissociated from the phenolic group (A'). Alternatively, if the phototautomerism of the excited neutral molecule (N) to the excited zwitterion (Z) was not intramolecular, but rather, required the diffusion-limited protonation of the carboxyl group followed by dissociation of the hydroxyl group, the critical chemical condition necessary to produce phototautomerization would be the concentration of protonating species (*i.e.*, the sulfuric acid concentration). Presumably, below a certain region of sulfuric acid concentration, the probability of an excited neutral molecule encountering a protonating species within its diffusion volume (*i.e.* during the lifetime of the excited state) is small, so that fluorescence or non-radiative deactivation of the excited neutral molecule is more probable than phototautomerism in the lowest excited singlet state. In this case the midpoint of the fluorimetric titration represents the Hammett acidity or pH at which an excited neutral molecule has an equal probability of fluorescing, as such, or of undergoing phototautomerism to the excited zwitterion, rather than the acidity at which half of the equilibrium population of excited molecules exists as the zwitterions and half as the singly dissociated anions. In order to distinguish between the excited-state equilibrium dissociation and diffusion-limited tautomerism processes it is necessary briefly to examine the rest of the pH region with regard to subsequent protolytic phenomena in the hydroxynaphthoic acids.

Between pH 1 and pH 5 the fluorescence of 1-HNA undergoes about a threefold increase in quantum yield and a slight increase in bandwidth, although the position of the fluorescence maximum is hardly affected. In this pH region the fluorescence of 2-HNA shows a shift to lower frequency and a doubling in quantum yield of fluorescence with increasing pH. Although the lack of shifting of the fluorescence of 1-HNA and the red shift in the fluorescence of 2-HNA in this pH region are somewhat unexpected, the changes in relative fluorescence quantum yield as the absorbing species is changed from the neutral molecule to the singly charged anion (A), clearly indicate that in this pH interval, the identity of the fluorescing species derived from each isomer has changed, most likely through protolytic dissociation. In the pH regions 11–15 and 10–14 the fluorescences of 1-HNA and 2-HNA, respectively, shift to lower frequencies, indicating in both cases dissociation of the singly charged anions (A), from the hydroxyl group, to form the doubly charged anions (D) with no phototautomerism of the singly charged anion or approach to equilibrium in the lowest excited singlet state (*i.e.* the conversions of the fluorescences follow the ground-state thermodynamics).

That two prototropic processes, both following the titrimetry of the ground-state dissociations, follow the blue shifting of the zwitterion fluorescences in the

$H_0 - 2$ to pH 1 region clearly indicates that the shifts in this acidity region are due to the diffusion-limited nature of the biprotonic phototautomerism of the neutral molecules. If the shifting corresponded to protolytic dissociation in the excited state, only one more dissociative process, that of the singly charged anion to the doubly charged anion, would be possible. However, if the short-wavelength emission at pH 1 corresponds to that of the neutral molecule two more dissociations, as observed, would be expected at higher pH.

TABLE II

FLUORESCENCE MAXIMA ($\bar{\nu}_f$) (IN $cm^{-1} \cdot 10^{-4}$) OF THE NEUTRAL MOLECULES AND ANIONS DERIVED FROM THE METHYL ETHERS AND METHYL ESTERS OF 1-HNA AND 2-HNA

	$\bar{\nu}_f$	
	Neutral molecules	*Anions*
1-Methoxy-2-naphthoic acid	2.40	2.77
2-Methoxy-1-naphthoic acid	2.55	2.79
1-Hydroxy-2-carbomethoxynaphthalene	2.42	2.19
2-Hydroxy-1-carbomethoxynaphthalene	2.57	2.36

In order to examine more closely the failure of the fluorescence of the neutral molecule derived from 1-HNA to shift, and the anomalous red shift of the fluorescence of neutral 2-HNA, upon dissociation from their respective carboxyl groups, the methyl ethers[8] and the methyl esters[9] of 1-HNA and 2-HNA were prepared. The fluorescence spectra of the neutral ethers and esters were taken in water at pH 2.0 and are similar in frequency to the corresponding neutral molecules derived from 1-HNA and 2-HNA, respectively. The fluorescence spectra of the anions derived from the methyl esters were taken at pH 10.5 and their maxima (Table II) are much lower in frequency than the anions derived from 1-HNA and 2-HNA. This result is reasonable, because the anions derived from the esters should be similar in electronic structure to the anions (A′) and having their hydroxyl groups fully dissociated and carboxyl groups undissociated, should, and do, fluoresce at frequencies comparable to or lower than the fluorescences of the dianions derived from 1-HNA and 2-HNA. The fluorescence spectra of the anions derived from the methyl ethers fluoresce at frequencies considerably greater than either the corresponding neutral molecules (as expected for carboxyl dissociation) or the anions derived from 1-HNA and 2-HNA. The singly charged anions (A) derived from 1-HNA and 2-HNA, and the anions derived from the corresponding ethers differ predominantly in that the intramolecular hydrogen bonds between the hydroxyl protons and the carboxylate anions, present in the anions of 1-HNA and 2-HNA are absent in the ether anions. Probably, the internal hydrogen bonds in the anions derived from 1-HNA and 2-HNA, which are especially strong in the lowest excited singlet state, effect partial deprotonation of the hydroxyl groups, in the anions, enhancing intramolecular charge transfer from the hydroxyl groups to the naphthalene ring, causing a reversal of the excited states and anomalous shifting

of the fluorescence in the anions relative to the neutral molecules. That is, if the ^1L_a state is the state from which fluorescence originates in 2-HNA, fluorescence originates from the ^1L_b state in the anion derived from 2-HNA. Correspondingly, if the neutral 1-HNA fluoresces from the ^1L_b state, the anion derived from 1-HNA fluoresces from the ^1L_a state. This will now be discussed.

TABLE III

FLUORESCENCE MAXIMA ($\bar{\nu}_f$) (IN $cm^{-1} \cdot 10^{-4}$) OF THE NEUTRAL MOLECULES AND ANIONS DERIVED FROM 1- AND 2-NAPHTHOIC ACID AND 1- AND 2-NAPHTHOL, AND THE ELECTRONIC STATES FROM WHICH THEY ORIGINATE[10,11]

	Neutral molecules	*Anions*
1-Naphthoic acid	2.58 (^1L_a)	2.86 (?)
2-Naphthoic acid	2.65 (^1L_b)	2.84 (^1L_b)
1-Naphthol	2.60 (^1L_a)	2.19 (^1L_a)
2-Naphthol	2.74 (^1L_b)	2.38 (^1L_b)

Although naphthalene itself and its monofunctionally β-substituted derivatives fluoresce from the ^1L_b state, monofunctionally α-substituted naphthalenes may fluoresce from the ^1L_a state if the α-substituents interact strongly enough (by intramolecular charge transfer) with the ^1L_a state of naphthalene. Thus, in aqueous solutions 2-naphthoic acid, its anion and cation[10] and 2-naphthol and its anion[11] all fluoresce from the ^1L_b state (Table III). Although the nature of the fluorescing state of the 1-naphthoate anion is unknown, the ^1L_a state is lowest in aqueous solutions of 1-naphthoic acid and its conjugate cation[10] and 1-naphthol and its conjugate anion[11] (Table III). In 1-HNA and 2-HNA, the hydroxyl and carboxyl functions (and their ionized derivatives) compete with each other for the stronger influence in lowering the ^1L_a or ^1L_b states. In 1-HNA, the hydroxyl group is in an α-position and the carboxyl group in a β-position. Dissociation of the hydroxyl group, as in the dianion, favors the ^1L_a state being lowest while protonation of the carboxyl group as in the cation, favors the ^1L_b state being lowest. When the hydroxyl group is undissociated, the carboxyl group being neutral or dissociated is likely to have a substantial effect on the relative positions of the ^1L_a and ^1L_b states. This conclusion is based on the data of Table III, which show the carboxylate anion to have a small, and the neutral carboxyl and hydroxyl groups to have a substantial, effect on the energies of the $\pi^* \rightarrow \pi$ fluorescences of naphthalene.

In 1-HNA, the dissociation of the carboxyl group substantially raises the energy of the ^1L_b state which is the fluorescing state in the neutral molecule. However, the partial release of the hydroxylic proton to the carboxyl group in the excited anion lowers the energy of the ^1L_a state. If the ^1L_a state in the anion dropped fortuitously to the level of the ^1L_b state in the neutral molecule, thereby becoming the lowest excited singlet state in the anion, fluorescence would occur from the ^1L_a state of the anion with the same frequency at which fluorescence was observed in the neutral molecule. In 2-HNA, the dissociation of the carboxyl

group raises the energy of the ^1L_a state while the partial release of the hydroxylic proton to the carboxyl group, accompanying dissociation of the carboxyl group lowers the energy of the ^1L_b state (the intramolecular hydrogen-bond should also diminish the extent to which the ^1L_a state is raised by carboxyl dissociation). If the ^1L_b state of the anion lies below the ^1L_a state of the neutral molecule, dissociation would produce a red shift of the fluorescence spectrum even though the effect of dissociation of the carboxyl group may be greater in magnitude on the ^1L_a state than on the ^1L_b state. For 2-HNA these arguments would explain the red shift of the fluorescence spectrum even if the ^1L_b state was lowest in both the neutral molecule and the singly charged anion. However, in 1-HNA, for no shift to be observed upon dissociation of the neutral molecule, from the carboxyl group, the ^1L_b state of the neutral molecule and the ^1L_a state of the anion must have the same energy. In 3-HNA[5], the dissociation of the carboxyl group and the readjustment of the hydroxylic proton toward the carboxyl group both affect the energy of the ^1L_b state which is the fluorescing state in the neutral molecule and singly charged anion (A). Since dissociation occurs from the carboxyl group, the magnitude of the blue shifting effect of dissociation of the carboxyl group is greater than the red shifting effect of partial loss of the hydroxylic proton. Thus the observed effect in 3-HNA is the anticipated blue shift of the fluorescence, accompanying dissociation.

It is thus apparent that the neutral molecules derived from 1-HNA and 2-HNA undergo biprotonic phototautomerization to the respective zwitterions, a process not observed in 3-HNA[5] (nor is intramolecular phototautomerism observed in 3-HNA). However, phototautomerism of the singly charged anion occurs in 3-HNA but not in 1-HNA or 2-HNA. The reasons for this are not yet understood.

The characteristic patterns of acidity-dependent changes of the fluorescences of these molecules suggest that for aromatic acids and bases of analytical interest, fluorimetric acid–base titrimetry may provide the means for reasonably rapid identification, at trace levels. The combination of fluorescence frequencies of various prototropic species pK_a and pK_a^* values should provide a "fingerprint" of a given compound, of selectivity comparable to that in infrared spectroscopy but of much greater sensitivity and ease of sampling. However, in order to appreciate the significance and utility of acidity-dependent shifts of electronic spectra, the present study makes it apparent that simple generalizations about spectral shifts accompanying the ionizations of acids and bases will often be inaccurate and that a reasonably detailed understanding of the interplay of spectroscopic, chemical and photochemical phenomena is highly desirable.

From the standpoint of quantitative analysis, the fluorescences of the singly charged anions (A) derived from 1-HNA and 2-HNA are the most intense relative to the fluorescences of all other species derived from either compound. Moreover, the fluorescence intensities of both anions are constant from pH 6 to 10. Consequently, it is suggested that assay of these ligands be carried out in this pH range.

SUMMARY

The electronic absorption and fluorescence spectra of 1-hydroxy-2-naphthoic acid and 2-hydroxy-1-naphthoic acid were studied throughout the pH range in

water and the Hammett acidity range in sulfuric acid. As in salicylic acid and 3-hydroxy-2-naphthoic acid an intramolecular hydrogen bond between the hydroxyl proton and the carboxyl group is evident from the small pH dependent shifts of the spectra of the neutral molecules, upon dissociation, and the anomalous pK_a values. The neutral molecules undergo biprotonic phototautomerizations to the zwitterions, in their lowest excited singlet states, in moderately concentrated sulfuric acid. The anomalous shifts of the fluorescences of the neutral molecules upon dissociation, are attributed to the effects of dissociation and intramolecular hydrogen bonding, upon the ^1L_a and ^1L_b states. Mention is made of the possible utility of fluorimetric titrimetry for qualitative analysis at trace levels.

RÉSUMÉ

Une étude est effectuée sur les spectres de fluorescence et d'absorption électronique de l'acide hydroxy-1-naphtoïque-2 et de l'acide hydroxy-2-naphtoïque-1. On a pu mettre en évidence la liaison hydrogène intramoléculaire entre le proton hydroxyle et le groupe carboxyle, comme pour l'acide salicylique et l'acide hydroxy-3-naphtoïque-2. On fait mention de l'utilité possible d'une titrimétrie fluorimétrique pour l'analyse quantitative de traces.

ZUSAMMENFASSUNG

Die elektronischen Absorptions- und Fluoreszenzspektren von 1-Hydroxy-2-naphthoesäure und 2-Hydroxy-1-naphthoesäure wurden über den ganzen pH-Bereich in Wasser und den ganzen Hammett-Aciditätsbereich in Schwefelsäure untersucht. Die kleinen pH-abhängigen Verschiebungen der Spektren der neutralen Moleküle nach Dissoziation und die anomalen pK_a-Werte weisen darauf hin,dass wie in Salicylsäure und 3-Hydroxy-2-naphthoesäure eine intramolekulare Wasserstoffbindung zwischen dem Hydroxylproton und der Carboxylgruppe vorliegt. Die neutralen Moleküle unterliegen in mässig konzentrierter Schwefelsäure biprotonigen Phototautomerisierungen zu den Zwitterionen in deren niedrigsten angeregten Singulettzuständen. Die anomalen Verschiebungen der Fluoreszenz der neutralen Moleküle nach Dissoziation werden dem Einfluss von Dissoziation und intramolekularer Wasserstoffbindung auf die ^1L_a- und ^1L_b-Zustände zugeschrieben. Es wird erwähnt, dass eine fluorimetrische Titration für die quantitative Analyse in Spurenbereichen von Nutzen sein kann.

REFERENCES

1 A. Weller, *Z. Elektrochem.*, 60 (1956) 1144.
2 P. J. Kovi, C. L. Miller and S. G. Schulman, *Anal. Chim. Acta*, 61 (1972) 7.
3 K. Hirota, *Z. Phys. Chem. (N.F.)*, 35 (1961) 222.
4 W. R. Ware, P. R. Shukla, P. J. Sullivan and R. V. Bremphis, *J. Chem. Phys.*, 55 (1971) 4048.
5 P. J. Kovi and S. G. Schulman, *Anal. Chem.* 45 (1973) 989.
6 M. J. Jorgenson and D. R. Hartter, *J. Amer. Chem. Soc.*, 85 (1963) 878.
7 S. G. Schulman and H. Gershon, *J. Phys. Chem.*, 72 (1968) 3297.
8 C. N. Vyas and N. M. Shah, *Organic Synthesis*, Collective Vol. 4 (1963) 837.
9 J. B. Cohen and H. W. Dudley, *J. Chem. Soc.*, (1910) 1748.
10 P. J. Kovi and S. G. Schulman, *Anal. Chim. Acta*, 63 (1973) 39.
11 S. G. Schulman, *Spectrosc. Lett.*, 6 (1973) 197.

Analytica Chimica Acta, 67 (1973) 269–275

DETERMINATION OF STOICHIOMETRY OF VANADIUM OXIDES BY 14-MeV NEUTRON ACTIVATION

P. LIEVENS, A. SPEECKE and J. HOSTE
Institute for Nuclear Sciences, Rijksuniversiteit, Ghent (Belgium)
(Received 10th May 1973)

In an investigation of the kinetics of chemisorption of oxygen and electrical conductivity changes on vanadium pentoxide catalysts, a rapid method for determining the oxygen/vanadium ratio was required.

Several methods have been used for determining the number of defect centres or oxygen vacancies in vanadium pentoxide, *e.g.* e.p.r., susceptibility and conductivity measurements, i.r. spectroscopy and chemical analyses. Most analyses dealing with the determination of vanadium have been carried out by spectrochemical and spectrophotometric techniques whereas the inert gas fusion has been used for determining oxygen. Most of these methods for vanadium and oxygen require a series of chemical analytical procedures and are therefore time-consuming in addition to being destructive. The order of magnitude for the oxygen deficiency ranges from 0.01–0.06% (e.p.r. and chemical analysis[1–4]) to 0.2–0.8% (conductivity and susceptibility measurements[5–13]).

Activation analysis with a neutron generator is capable of analyzing suitable samples at both minor and major levels of concentration. This technique was found to give results for vanadium and oxygen with a precision which compared favorably with conventional methods.

Vanadium and oxygen can easily be determined with 14-MeV neutrons, the following reactions being commonly used: $^{51}V(n, p)^{51}Ti$ and $^{16}O(n, p)^{16}N$. Both reactions give rise to short-lived radionuclides; the $T_{\frac{1}{2}}$ values are 5.8 min and 7.15 s, respectively. Measuring the counts accumulated in the region 4.5–6.5 MeV for oxygen and under the 320-keV photopeak for vanadium with a single-channel analyzer is the simplest method.

Persiani and Cosgrove[14] analyzed for oxygen and vanadium separately; irradiation times were 30 s and 1 min, respectively. Oxygen was irradiated to saturation *versus* a long-lived copper flux monitor. Measurements were made by a multichannel analyzer.

When vanadium was used as an internal standard, however, multiple sources of error such as flux variations (intensity, geometry) and inaccurate positioning of standard and sample at the measuring site were minimized.

In addition, no corrections for neutron attenuation[18] were required because the ^{51}Ti–^{16}N ratio is independent of flux intensity.

Nuclear data

Irradiation of oxygen and vanadium with 14-MeV neutrons gives rise to

TABLE I

NUCLEAR REACTION ON OXYGEN AND VANADIUM

Reaction	*Isotopic abundance (%)*	*Cross-section (mb)*	*Half-life*	*γ-Energy (MeV)*	*β-Energy (MeV)*
$^{16}O(n, p)^{16}N$	99.759	40	7.15 s	6.13 (68%) 7.12 (5%)	10.4 (26); 4.3 (68)
$^{16}O(n, 2n)^{15}O$	99.759	0.5	122 s	0.511 (100)	
$^{17}O(n, p)^{17}N$	0.0374	112	4.14 s	0.87; 2.19	
$^{18}O(n, \alpha)^{15}C$	0.2039	11	2.3 s	5.3	
$^{51}V(n, p)^{51}Ti$	99.76	35	5.8 min	0.320 (100) 0.605 (1.5) 0.928 (4.4)	1.5 (6) 2.17 (94)
$^{51}V(n, \gamma)^{52}V$	99.76	0.35	3.77 min	1.44 (100)	2.47
$^{51}V(n, \alpha)^{48}Sc$	99.76	40	44 h	0.99; 1.04; 1.32	0.65

several reactions summarized in Table I. The most frequently employed nuclide for oxygen determination is ^{16}N whose high-energy γ-rays can be counted practically free of interference above 4.5 MeV; for vanadium the prominent 320-keV photopeak of 5.8-min ^{51}Ti is the most convenient.

EXPERIMENTAL

Apparatus

The neutron generator was a Sames Type J accelerator (150 kV, 2.5 mA) with a 100 MHz–60 W radiofrequency ion source; 14-MeV neutrons were produced by the $^{3}H(d, n)^{4}He$ reaction from a 90-Ci rotating water-cooled tritium target (Nukem Type RTE-1). The neutron production was controlled by means of a pneumatically operated removable tantalum screen. The pneumatic transfer system consisted of a pair of aluminium tubes with rectangular section (26.5 × 9.5 mm).

The neutron generator, transfer system and counting equipment have been described in detail elsewhere[15,16]. Irradiated samples were counted with a 7.6 cm × 7.6 cm NaI(Tl) detector (resolution *ca.* 8%) coupled to a NE-5288 preamplifier and two NE-4603 amplifiers. The differentiated output of the amplifiers was fed to two NE-4602 single-channel analyzers and scalers. A 400-channel analyzer was included as a supplementary facility. The timing program was completely automatic. Neutron monitoring was performed by means of an oxygen flux monitor[16].

Preparation of samples and standards

Several standards with increasing vanadium/oxygen ratios were prepared from vanadium carbide powder (Ventron, Beverly, Mass., U.S.A.) and oxalic acid (E. Merck, Darmstadt). The vanadium content of vanadium carbide was determined by titration with 0.05 *M* cerium(IV) sulfate and potentiometric determination of the end-point; the electrode system used consisted of a platinum indicator electrode and a saturated calomel reference electrode[17]. The vanadium content was

found to be 80.18 ± 0.15% (theor. 80.92%). An absolute oxygen analysis with 14-MeV neutrons of vanadium carbide showed an oxygen content of 1.22 ± 0.02%. The standardization method for the determination of oxygen has been described in detail elsewhere[18].

From decay curve analysis of the long-lived component of irradiated vanadium carbide powder it appeared that the activity decays with a half-life of 5.75 ± 0.03 min, which is in good agreement with the literature value of 5.8 min for ^{51}Ti. Six standard mixtures were prepared by successive addition of oxalic acid to the vanadium carbide. The mixtures were ground in an agate mortar for 1 h and homogenized by tumbling for 8 h. The vanadium/oxygen ratios are shown in Table II.

TABLE II

COMPOSITION OF THE VANADIUM CARBIDE–OXALIC ACID MIXTURES

	Vanadium carbide (g)	*Oxalic acid (g)*	*V/O ratio*
A	6.1783	2.5745	$VO_{1.3085}$
B	5.5438	2.7758	$VO_{1.5625}$
C	5.4133	3.0707	$VO_{1.7637}$
D	5.2707	3.5169	$VO_{2.0661}$
E	4.9354	4.1138	$VO_{2.5689}$
F	4.8473	4.4497	$VO_{2.8242}$

Seven samples were analyzed: (I) vanadium pentoxide (Ventron); (II) vanadium pentoxide (BDH, Poole, England); (III) vanadium tetroxide (Ventron); (IV) vanadium trioxide (Ventron); (V) powdered yellow oxide; (VI) powdered yellow oxide; (VII) powdered green oxide. The last three oxides were supplied by the Laboratory for Solid State Physics, Rijksuniversiteit, Ghent, Belgium and were previously used for studying catalytic mechanisms.

The sample holders were polyethylene cylindrical transfer rabbits (9 mm thickness, 26 mm diameter, 2.20 cm^3 internal volume) fitting the pneumatic system. The density of samples and standards varied between 0.9 and 1.3 g cm^{-3}.

Since the oxygen content of the irradiation boxes was not negligible, a blank correction was performed by irradiating and counting empty sample holders in the same way as the samples and standards, normalizing the results with an oxygen flux monitor. For vanadium, this correction corresponds to a background subtraction.

Procedure

When the analysis cycle was started sample and monitor were transferred pneumatically to the irradiation position. Both were irradiated during 5 s by pneumatic removal of the tantalum screen. After the 5-s irradiation time, a saturation of 40% for the ^{16}O(n, p)^{16}N reactions and of 1% for the ^{51}V(n, p)^{51}Ti reaction was reached.

At the end of the irradiation, the sample was returned to the counting room. Exactly 4 s after irradiation, the induced ^{16}N activity of sample and monitor

was automatically counted for 15 s, which is about the optimal counting time of two half-life times[19]. The window of the single-channel analyzer was adjusted to correspond to the 4.5–6.5 MeV energy range. After 75 s, which was necessary for complete decay of ^{16}N, the induced ^{51}Ti activity was counted for 600 s on a second single-channel analyzer with window between 280 and 360 keV.

This adjustment of the window corresponded to an optimal signal-to-background ratio. Before every analysis, energy calibration with ^{51}Cr (same γ-energy of 320 keV) was carried out by means of the multi-channel analyzer to correct for possible gain shifts of the amplifier. After 1 h the ^{51}Ti activity has completely decayed and the analysis of the same sample can be repeated.

Attenuation of γ- and β-radiation

Attenuation of γ-radiation can be expressed as a simple exponential absorption law of the general form:

$$I = I_0 e^{-\mu d} \tag{1}$$

where I_0 is the γ-intensity without attenuation and μ is the linear γ-ray attenuation coefficient (cm^{-1}).

A thickness d_y can be defined in the sample so that, if all the activity were concentrated in that layer, as many γ-rays would leave the sample as with the real homogeneous activity distribution. Thus:

$$I = I_0 e^{-\mu d_y} \tag{2}$$

where I_0 is the activity counted by the detector for a hypothetical sample with the same activity distribution as an actual sample, but without γ-ray attenuation; and I is the activity counted by the detector system for a real sample, including γ-ray attenuation.

d_y was experimentally determined by Vandecasteele *et al.*[18] to be 0.33 ± 0.02. Taking into account this correction, one can set up the following equation:

$$\frac{\text{activity } ^{51}\text{Ti}}{\text{activity } ^{16}\text{N}} \cdot \exp(\mu_{0.32} - \mu_6) d_y = K \frac{\text{weight vanadium}}{\text{weight oxygen}} \tag{3}$$

where $\mu_{0.32}$ = linear attenuation coefficient (cm^{-1}) for γ-rays of 320 keV; μ_6 = linear attenuation coefficient (cm^{-1}) for γ-rays of 6 MeV.

For a mixture or compound the linear attenuation coefficient is calculated as follows:

$$\mu = \sum_{i=1}^{n} \frac{w_i (\mu/\rho)_i}{V} \tag{4}$$

where w_i = weight of element i; $(\mu/\rho)_i$ = mass attenuation coefficient ($cm^2\ g^{-1}$) of element i; V = volume.

The β-contribution of the ^{16}N activity was about 18% for a density of 1 g cm^{-3}. No β-ray absorption was applied, however, because the absorber to remove the high-energy electrons of ^{16}N, would reduce considerably the detection of the low γ-energy rays of ^{51}Ti. Therefore the induced ^{16}N activity was normalized to a

density of 1 g cm^{-3} with the aid of the relationship between β-contribution and sample density as determined by Vandecasteele[20].

RESULTS AND DISCUSSION

With the corrected $^{51}Ti/^{16}N$ activity ratios as a function of the vanadium/oxygen weight ratios, a calibration line was set up. The separate results for each standard mixture with the standard deviation on the mean is given in Table III. The number of samples and the total number of analyses for each standard mixture are also given. A significant difference between the samples of one standard mixture could not be detected by means of a *t*-test. The standard deviation for a single determination was always about 1.4%. The deviation on the mean varied between 0.24 and 0.33%.

TABLE III

ACTIVITY RATIOS FOR THE DIFFERENT STANDARD MIXTURES WITH MEAN DEVIATION

Standard	*Number of samples*	*Number of analyses*	$\frac{Act.\ ^{52}Ti}{Act.\ ^{16}N}$
A	3	20	1.8799 ± 0.0053
B	4	36	1.5706 ± 0.0047
C	4	23	1.3980 ± 0.0041
D	4	26	1.2017 ± 0.0029
E	3	19	0.9658 ± 0.0032
F	4	28	0.8749 ± 0.0027

Least-squares fitting of the calibration line allows the determination of K from eqn. (3). The result for K, the slope of the calibration curve, was $0.774_2 \pm 0.0014$. The intercepts of the ordinate and the abscissa were 0.016 ± 0.007 and -0.021 ± 0.010, respectively. The *t*-tests and *F*-tests showed that these values were statistically insignificant.

From the standard error on the slope, the correlation coefficient and the intercepts on abscis and ordinate, it is evident that the two variables are linearly related and that the equation should pass through the origin, *i.e.*:

$$\frac{\text{act.}\ ^{51}\text{Ti}}{\text{act.}\ ^{16}\text{N}} = 0.774_2 \frac{\text{weight vanadium}}{\text{weight oxygen}}$$

The final results from analyses of seven vanadium oxides are shown in Table IV. From these results it is clear that the stoichiometry deviations are larger than 2% for vanadium pentoxide. Sample III, which was found to be a V_2O_6 compound, was in fact a vanadium tetroxide dihydrate, which has been proved to exist[21]. The real stoichiometric formula therefore is $V_2O_{4.03} \cdot 2\,H_2O$.

The precision of these analyses (0.53%–1.09%) is satisfactory. The accuracy can certainly compete with that obtained with chemical methods because 14-MeV

TABLE IV

V/O RATIOS OF ANALYZED SAMPLES

Sample	*V/O ratio*	*Standard error*
I	$VO_{2.445}$	±0.018
II	$VO_{2.422}$	±0.013
III	$VO_{3.015}$	±0.018
IV	$VO_{1.980}$	±0.012
V	$VO_{2.418}$	±0.026
VI	$VO_{2.374}$	±0.020
VII	$VO_{2.400}$	±0.013

neutron activation analysis allows the determination of both vanadium and oxygen. Moreover, as the analysis is nondestructive, the same sample can be analyzed repeatedly in a very short time.

SUMMARY

A method was developed for the determination of oxygen/vanadium ratios in vanadium oxides by 14-MeV neutron activation analysis by means of the reactions $^{51}V(n, p)^{51}Ti$ and $^{16}O(n, p)^{16}N$. A linear relationship between activity ratios and weight ratios of six mixtures composed of vanadium carbide and oxalic acid was obtained with a precision of 0.18% after suitable corrections for γ- and β-ray absorption. Four commercial vanadium oxides and three specially prepared vanadium oxides were analyzed. The V/O ratio varied between 1.980 and 3.015. The percent standard deviation on these values was between 0.53% and 1.09%.

RÉSUMÉ

Une méthode est décrite pour la détermination du rapport oxygène/vanadium dans des oxydes de vanadium, par activation neutronique (14-MeV) basée sur les réactions $^{51}V(n, p)^{51}Ti$ et $^{16}O(n, p)^{16}N$. On arrive à une relation linéaire entre rapports d'activité et rapports de poids de six mélanges composés de carbure de vanadium et d'acide oxalique, avec une précision de 0.18%, après correction pour absorption γ et β. Quatre oxydes de vanadium du commerce et trois oxydes spécialement préparés ont été analysés. Le rapport V/O varie de 1.980 à 3.015 et la déviation standard de 0.53 à 1.09%.

ZUSAMMENFASSUNG

Es wurde eine Methode für die Bestimmung von Sauerstoff/Vanadin-Verhältnissen in Vanadinoxiden mittels 14 MeV-Neutronenaktivierungsanalyse unter Anwendung der Reaktionen $^{51}V(n, p)^{51}Ti$ und $^{16}O(n, p)^{16}N$ entwickelt. Eine lineare Beziehung wurde zwischen den Aktivitätsverhältnissen und den Gewichtsverhältnissen von sechs aus Vanadincarbid und Oxalsäure zusammengesetzten Gemischen mit einer Reproduzierbarkeit von 0.18% erhalten, wenn geeignete Korrekturen für

die γ- und β-Strahlen-Absorption vorgenommen wurden. Vier im Handel erhältliche Vanadinoxide und drei besonders hergestellte Vanadinoxide wurden analysiert. Die V/O-Verhältnisse variierten zwischen 1.980 und 3.015. Die prozentuale Standardabweichung bei diesen Werten lag zwischen 0.53% und 1.09%.

REFERENCES

1 E. Gillis and E. Boesman, *Phys. Status Solidi*, 14 (1966) 349.
2 H. Takahashi, M. Shiotani, H. Kobyashi and J. Sohna, *J. Catal.*, 14 (1969) 134.
3 V. A. Joffe and I. B. Patrina, *Phys. Status Solidi*, 40 (1970) 389.
4 M. Colpaert, *Ph.D. Thesis*, Rijksuniversiteit, Ghent, 1972.
5 S. K. Bhattacharya and P. Mahanti, *J. Catal.*, 20 (1971) 10.
6 T. Allersma, R. Hakim, T. N. Kennedy and J. D. Mackenzie, *J. Chem. Phys.*, 46 (1967) 154.
7 P. Nagels and M. Denayer, preprint to the *10th Int. Conf. on the Physics of Semiconductors, Cambridge, Aug. 17, 1970.*
8 F. Khan, L. N. Blinov and L. P. Strakkov, *Fiz. Tekh. Poluprov.*, 2 (1968) 457.
9 J. Rock, *C.R.*, 250 (1960) 2167.
10 G. Grossman, O. W. Proskurenka and S. M. Arija, *Z. Anorg. Allg. Chem.*, 305 (1960) 121.
11 K. Kosuge, T. Takada and S. Kachi, *J. Phys. Soc. Jap.*, 18 (1963) 318.
12 M. J. Sienko and J. V. Sohn, *J. Chem. Phys.*, 44 (1966) 1369.
13 G. Tridot and J. Tudo, *C.R.*, 263C (1966) 421.
14 C. Persiani and J. F. Cosgrove, *Anal. Chem.*, 40 (1968) 1350.
15 J. Hoste, D. De Soete and A. Speecke, *Euratom Report EUR 3565e*, 1967.
16 R. Gijbels, A. Speecke and J. Hoste, *Anal. Chim. Acta*, 43 (1968) 183.
17 I. M. Kolthoff and P. J. Elving (Editors), *Treatise on Analytical Chemistry*, Part II, Vol. 8, Wiley, New York, 1963, p. 226.
18 C. Vandecasteele, A. Speecke and J. Hoste, *The Determination of Oxygen in Non-ferrous Metals by 14 MeV Neutron Activation Analysis*, Eurisotop Office Information Booklet 68, Brussels, 1972.
19 Sl. Sterlinski, *Nucl. Instr. Methods*, 42 (1966) 219.
20 C. Vandecasteele, personal communication.
21 Ref. 17, p. 194.

Analytica Chimica Acta, 67 (1973) 277–282

INSTRUMENTAL NEUTRON ACTIVATION ANALYSIS FOR BROMINE IN PIG TISSUES

MELVIN H. FRIEDMAN, THEODORE M. FARBER and JAMES T. TANNER

Bureau of Foods, Food and Drug Administration, Department of Health, Education, and Welfare, Washington, D.C. 20204 (U.S.A.)

(Received 26th February 1973)

Brominated oils derived from olive, sesame, cottonseed and soybean oils have been used in beverages and certain manufactured foods for many years. In fruit-based beverages, they are used primarily to enhance the cloud-stability so that the appearance is similar to that of the natural juice and ring formation in the bottles is prevented. Recent studies indicate thathhigh levels of brofinated oils in the diet of rats can produce a number of adverse toxicological effects such as cardiac myocytolysis, thyroid hyperplasia, fatty liver, testicular atrophy and renal damage[1,2]. Additionally, brominated vegetable oils may inhibit the oxidation of palmitic acid in cardiac tissue[3].

A study of the subacute toxicity of brominated sesame oil in the miniature pig has been completed in one of our laboratories[4] to determine if similar toxicological changes appeared in a species having a cardiovascular system similar to that of man. The analytical results and the methodology employed for that study are presented in this paper. Although neutron activation analysis has previously been used for the determination of bromine[5], an unusual feature of the technique described here was the use of an automatic data analysis system consisting of a sample changer modified for use with a high resolution Ge(Li) detector and data reduction program[6].

Tissues taken from pigs fed brominated vegetable oil were analyzed for total (inorganic and organic) and hexane-soluble bromine content. The latter values represent compounds possessing lipophilic character (*i.e.*, long-chained fatty acids) and were expected to be extensively deposited in adipose tissue.

EXPERIMENTAL

Sample preparation

Five groups of four miniature Hormel-Hanford pigs were fed brominated sesame oil (Abbott Laboratories, Chicago, Ill.) in the diet at dose levels of 0, 5, 25, 50, and 500 mg kg^{-1} of body weight day^{-1}. After the pigs had been fed this diet for 17 weeks, they were sacrificed and samples of their organs and tissue were taken.

The tissues had to be dried to minimize pressure buildup when the samples, sealed in polyethylene containers, were placed in the reactor. For the determination of total bromine content of the heart, liver, muscle, spleen, thyroid, kidney, and brain, aqueous homogenates (1+3) of the various tissues were prepared with a

Polytron homogenizer. A 0.5-ml aliquot of the homogenate (166 mg of tissue) was placed into a polyvial and allowed to dry in a vacuum desiccator over concentrated sulfuric acid. With adipose tissue, a homogenate with water was difficult to obtain; accordingly, 670 mg of adipose tissue was digested in 2 ml of alcoholic potassium hydroxide in a 60° water bath for 30 min. The sample was cooled slightly and the volume was adjusted to 3 ml with absolute methanol. After the solution had been mixed, 2 ml of hexane was added to prevent the solidification of the fatty acids when the solution was cooled to room temperature. A 0.5-ml portion of this solution was placed into a polyvial and allowed to dry overnight at room temperature.

For the determination of the hexane-soluble bromine content of tissues other than adipose tissue, 2.0 g of the aqueous homogenate prepared above was mixed with 10 ml of hexane by shaking for 1 h in screwcap centrifuge tubes. A 1-ml portion of the hexane layer was transferred to a polyvial and the solvent was allowed to evaporate. To prepare adipose tissue for this determination, 670 mg of tissue was homogenized with 10 ml of hexane with a Polytron homogenizer, 1.4 ml of water was added to the centrifuge tube, and the mixture was shaken for 1 h. A 1-ml portion of the hexane layer was placed into a polyvial and the solvent was allowed to evaporate.

The polyvials were heat-sealed to prevent any losses from the sample. Six samples and three standards, each of which contained 100 μg of bromine, were packaged in an irradiation container in three layers. Inhomogeneities in the neutron flux were compensated for in the data reduction by comparing the activity of a sample with that of the standard adjacent to it.

Irradiation and data acquisition

The dried tissues were irradiated for 30 min at a flux of $1 \cdot 10^{13}$ n cm^{-2} s^{-1} in the 10-MW research reactor at the National Bureau of Standards. The samples and standards were then left for 1–2 days to allow short-lived nuclides to decay.

A Ge(Li) detector with 16% efficiency and a resolution of 2.2 keV was used for the measurements. With these levels of bromine, a counting time of 10 min was adequate. An automatic counting system[6] was used with the Ge(Li) detector for the measurements, which were based on the 554, 619, and 777-keV γ-rays of ^{82}Br ($t_{\frac{1}{2}}$=35.4 h). Through the use of a biased amplifier to expand this region of interest, each peak could occupy several channels and the total number of channels which had to be read out and later reduced was kept to 256.

Data reduction

For any given peak, the amount of bromine in the sample was found by the equation:

p.p.m. Br=(μg Br in standard/g of sample)·(activity of sample/activity of standard)

The data reduction was done directly from the magnetic tape with the computer program MTELMT[6]. The bromine γ-ray peak locations varied by no more than a channel; therefore, the peak locations and the number of channels to average on the left and right wings of the γ-ray peaks to subtract the background were specified at the beginning of the data reduction sequence rather than having

the program search for the peaks. The continuous background under the peak was found by averaging four channels on the left and right wings of the peak and drawing a straight line through these points; this method yielded a more reproducible value for the background. The corresponding areas of the sample were then found by the same procedure, and the amount of bromine in the sample was computed independently by the above equation from the three most prominent peaks (554, 619, and 777 keV) of ^{82}Br. The amount of bromine computed with these three peaks differed slightly, but was within the range expected on the basis of counting statistics.

RESULTS AND DISCUSSION

The bromine concentrations in organs and tissues of pigs given brominated sesame oil are shown in Table I, and are the average of the values computed from the three γ-ray peaks. A dose-related increase in total bromine content was seen with all tissues examined. The highest concentrations of total and hexane-soluble bromine were found in adipose tissue from the pigs given the brominated oil at 500 mg kg^{-1} day^{-1}; one animal had a level of 62,000 p.p.m. In this group, the total bromine content was very high in kidney, liver, heart, and thyroid tissue, and significant concentrations were also observed in the spleen and skeletal muscle; high levels of hexane-soluble bromine were found in kidney and liver tissue. Even in pigs given the brominated oil at 5 mg kg^{-1} day^{-1}, the average concentrations of total and hexane-soluble bromine in all tissues were higher than those observed in the control pigs.

To determine the validity of the analysis, a standard sample (NBS orchard leaf SRM 1571) was analyzed periodically and a value of 9.8 ± 0.6 p.p.m. of bromine was obtained. This value is in agreement with the neutron activation analysis value obtained by the National Bureau of Standards[7] of 9.8 ± 0.4 p.p.m. bromine.

The limit of detection for the instrumental measurement was estimated to be 1 μg of bromine. No effort was made to obtain a more sensitive measurement, as this was more than adequate for these samples. The limit of detection, based on work by Currie[8], was estimated to be 4.65 times the standard deviation of the background.

Because of the high levels of bromine found in the tissues, the error from counting statistics was negligible. Aside from biological variation between the animals, which is the largest error in these experiments, the accuracy of the measurements was estimated to be about 10%.

Instrumental activation analysis has several advantages as a method for the quantitative analysis of bromine; perhaps the most important is that the sample is not treated chemically and therefore bromine losses during analysis are avoided. In addition, the analyses were done automatically with the use of an automatic sample changer and data reduction program. The good agreement between the analyses based on the three most prominent peaks in the bromine spectrum indicated that this measurement technique was free from interference. Interferences from other nuclides such as ^{24}Na were circumvented by the use of a high-resolution Ge(Li) detector and a 1–2-day decay time. A sensitivity of 1 μg was easily achieved. No difficulties were

TABLE I

BROMINE DISTRIBUTION IN TISSUES AND ORGANS OF PIGS GIVEN BROMINATED SESAME OIL IN THE DIET FOR 17 WEEKS

Pig. no.	*Dose (mg kg^{-1} day^{-1})*	*Bromine concentration (p.p.m.)*[a]							
		Heart	*Liver*	*Muscle*	*Spleen*	*Thyroid*	*Kidney*	*Brain*	*Adipose*
4205	500	2500(600)	8000(3600)	950(300)	1500(150)	3200(1400)	8600(1900)	940(33)	30,000(26,000)
4265		2300(330)	19000(4900)	2100(200)	1700(100)	2300(430)	5600(1500)	1400(60)	62,000(41,000)
4187		2800(220)	12000(2300)	960(180)	1300(100)	2000(220)	7200(1900)	930(45)	37,000(26,000)
4203		1700(180)	11000(3300)	1500(190)	—	—	7900(5200)	—	35,000 —
4204	50	—	340(58)	190(53)	350(19)	460(110)	600(27)	180(15)	2300 —
4181		400(60)	270(38)	160(21)	260(30)	320(58)	540(82)	140(14)	2900(2400)
4255		300(82)	320(51)	160(44)	250(15)	470(81)	490(46)	140(21)	2500(2000)
4251		450(58)	410(50)	220(27)	310(21)	220(32)	460(18)	170(15)	2800(2500)
4263	25	230(62)	250(30)	130(18)	260(18)	180(38)	350(27)	140(26)	1800(1800)
4261		230(36)	240(30)	110(16)	200(21)	200(38)	160(32)	100(21)	2000(1200)
4257		160(74)	210(54)	160(38)	230(26)	160(26)	270(27)	160(22)	1100(950)
4262		130(16)	170(20)	90(21)	200(14)	170(16)	250(16)	84(12)	1000(1000)
4281	5	78(21)	78(22)	36(14)	72(14)	110(22)	120(21)	54(12)	530 —
4184		52(12)	73(12)	25(12)	53(12)	94(12)	97(27)	34(27)	270(270)
4193		78(22)	100(20)	42(16)	54(16)	110(24)	130(16)	72(12)	310(370)
4272		54(15)	66(30)	42(34)	72(10)	72(15)	78(15)	42(14)	470(410)
4243	0	30(10)	18(12)	18(10)	24(9)	18(14)	54(12)	30(9)	40(34)
4192		18(12)	12(9)	12(8)	24(14)	—	24(18)	12(10)	27(22)
4241		—	30(14)	12(12)	—	—	—	—	130(120)
4194		12(12)	24(14)	12(12)	24(9)	—	36(12)	18(12)	40(36)

[a] Numbers in parentheses are the concentration of hexane-soluble bromine (*i.e.*, the "organic" bromine content of the tissue).

encountered in the subtraction of the Compton background, since in all cases the such as ^{24}Na were circumvented by the use of a high-resolution Ge(Li) detector and concentration of bromine in the sample was much greater than the limit of detection. The observation that the bromine concentrations in the tissues of the control animals were much smaller than those in the animals that were given a bromine dose indicates that any possible reagent contamination could be disregarded in this work.

We thank D. N. Lincoln, R. E. Simpson, W. Forbes and N. Tandy of the Food and Drug Administration, H. Yule of the NUS Corporation, and the personnel of the NBS Reactor Radiation Division, National Bureau of Standards, for their contributions to various phases of this work.

SUMMARY

Bromine was determined by instrumental neutron activation analysis in tissues and organs of pigs as an indicator of brominated vegetable oil residues. The bromine content was found to be dose-related. An advantage of this technique is that the sample was not treated chemically. The analyses were done with the aid of an automatic sample changer and computer reduction of the data. Rapid and reliable analyses were obtained at the p.p.m. level.

RÉSUMÉ

Une méthode est proposée pour le dosage du brome dans la viande et les organes de porcs, par activation neutronique. Un avantage de cette technique est que l'échantillon à analyser n'est pas traité chimiquement. L'analyse se fait automatiquement avec ordinateur. On peut obtenir des résultats rapidement et sûrement, pour des quantités de l'ordre du p.p.m.

ZUSAMMENFASSUNG

In Geweben und Organen von Schweinen wurde mittels instrumenteller Neutronenaktivierungsanalyse Brom als ein Indikator für Rückstände von bromiertem Pflanzenöl bestimmt. Der Bromgehalt erwies sich als dosisabhängig. Ein Vorteil dieses Verfahrens ist, dass die Probe nicht chemisch behandelt wird. Die Analysen wurden unter Anwendung eines automatischen Probenwechslers und Auswertung der Messwerte durch einen Computer ausgeführt. Es waren schnelle und zuverlässige Analysen im p.p.m.-Bereich möglich.

REFERENCES

1 I. C. Munro, E. J. Middleton and H. C. Grice, *Food Cosmet. Toxicol.*, 7 (1969) 25.
2 I. F. Gaunt, P. Grasso and S. D. Gangolli, *Food Cosmet. Toxicol.*, 9 (1970) 1.
3 I. C. Munro, F. A. Salem, T. Goodman and S. H. Hasnain, *Toxicol. Appl. Pharmacol.*, 19 (1971) 62.
4 T. M. Farber, D. L. Ritter and G. W. Bierbower, *Abstracts of the 5th Int. Pharmacological Congr., San Francisco, 1972*, p. 66.
5 G. J. Lutz, R. J. Boreni, R. S. Maddock and J. Wing, *Activation Analysis: A Bibliography Through 1971*, NBS Tech. Note 467, National Bureau of Standards, 1972.

6 M. H. Friedman and J. T. Tanner, *86th Ann. Meet. Assoc. Off. Anal. Chem., Washington, D.C., October 1972*, Abstract No. 25; M. H. Friedman, Abstract No. 26.
7 P. Lafleur, private communication, 1972.
8 L. A. Currie, *Anal. Chem.*, 40 (1968) 586.

Analytica Chimica Acta, 67 (1973) 283–288

FUSION WITH BORON TRIOXIDE FOR SILICATE ANALYSIS BY ATOMIC ABSORPTION SPECTROMETRY: DETERMINATION OF POTASSIUM

O. A. OHLWEILER, J. O. MEDITSCH and CLARISSE M. S. PIATNICKI
Istituto de Quimica, U.F.R.G.S., Pôrto Alegre, RS (Brasil)
(Received 22nd March 1973)

Atomic absorption spectrometry has been extensively applied to the analysis of silicate rocks for both major and minor constituents. The introduction of the nitrous oxide–acetylene flame for the determination of refractory elements, has considerably enlarged the possibilities of the method. Silicate minerals are conventionally decomposed by acid or fusion techniques. However, the overall efficiency of the atomic-absorption method can be seriously diminished by the time-consuming modifications which are often necessary to overcome ionization, chemical and matrix interferences. For example, chemical separations of interfering species or additions of releasing, compensating, and/or complexing agents to samples and standards alike, are often essential. An ideal decomposition technique would yield sample solutions entirely free from chemical, ionization and matrix interferences. With such solutions, a given constituent could be determined by comparison with standards only, and reagent addition or close matching of samples and standards would be unnecessary.

Acid attack of silicates is usually based on the use of hydrofluoric acid, either alone or in mixtures, especially with sulfuric acid. After decomposition, the hydrofluoric acid must be eliminated by volatilization, or otherwise made innocuous. Several authors have recommended the use of hydrofluoric acid in Teflon vessels to decompose silicates and refractory minerals[1–5].

The decomposition of silicates by fusion is generally done with alkaline fluxes, such as hydroxides, carbonates and borates of sodium or potassium. Obviously, the use of such fluxes precludes the determination of the cation in the flux. The determination of sodium and potassium in silicate rocks is often required. Since the determination of lithium is not commonly required in routine analysis, the use of lithium salts as fusion agents is therefore advantageous. In the recent literature, lithium tetraborate has been mentioned as a very effective decomposition agent[6,7]. Biskupsky[8] recommended, for the decomposition of rocks, refractory silicates and minerals, fusing the sample (0.5 g) with a mixture of lithium fluoride (3 g) and boric acid (2 g). In general, interferences caused by lithium ionization are less than those caused by sodium and potassium in atomic-absorption measurements; however, a very high concentration of lithium, as introduced in the lithium fluoride–boric acid fusion, could cause significant ionization interference[9].

A critical feature of the usual fusion techniques is that the flux must be generally used in a 10–20 fold excess over the sample weight. Bernas[5] pointed out that the

resultant high concentrations may cause, with respect to silicate analysis by atomic absorption spectrometry, solution instability as well as high and fluctuating background readings; light scattering and/or molecular absorption phenomena which may occur in such environments are also detrimental in determinations of trace elements.

The method described by Bernas[5] for the decomposition and analysis of silicates by atomic absorption spectrometry, is based on attack by hydrofluoric acid at 110° in a specially designed Teflon vessel. Subsequently, an excess of boric acid is added to produce a solution containing fluoroboric acid and borid acid. The introduction of cations to the sample solution is thus avoided. The system permits contamination-free sample handling in glass equipment, and is said to diminish significantly or eliminate entirely chemical, ionization and matrix interferences. Sodium, potassium, calcium, magnesium and iron were determined by using an air–acetylene flame, and silicon, aluminum, titanium and vanadium, by using a nitrous oxide–acetylene flame.

Apparently, an even more satisfactory sample solution for atomic absorption would be obtained by fusion of the silicate sample with boron trioxide. It has been known for a long time that boron trioxide is a powerful non-oxidizing flux[10], but its advantages have not been recognized[11]. Recently, Ohlweiler *et al.*[12] determined silica in silicates after decomposition by fusion with a mixed flux consisting principally of boron trioxide; the sample (0.1000 g) was fused with a mixture of boron trioxide (1.0 g) and lithium carbonate (0.10 g) in a platinum crucible at 1000° for 30 min. The addition of lithium carbonate to the boron trioxide in a 1:10 ratio was necessary to ensure complete decomposition of the silicates.

This paper reports the results obtained in an attempt to apply the boron trioxide–lithium carbonate (10:1) fusion to the analysis of silicates by atomic absorption spectrometry. Ultrasonic waves were used to detach the fusion melt from the crucible. The sample solution was prepared by dissolving the cake in dilute hydrochloric acid containing hydrogen peroxide; the peroxide served to maintain any titanium in solution as the peroxy complex. The boron trioxide–lithium carbonate (10:1) fusion was applied to the determination of potassium in standard silicates.

EXPERIMENTAL

Reagents

Boron trioxide. Dehydrate boric acid by fusing the reagent in a platinum dish. When the formation of bubbles has ceased, cool suddenly to cause the resultant boron trioxide to crack into pieces. Then crush the material in a Plattner mortar and, finally, powder it in a mullite mortar. Boron trioxide is hygroscopic and must be stored in an air-tight vessel.

Stock solution for potassium. Weigh out 1.583 g of potassium chloride, previously dried at 150°, dissolve in distilled water, transfer to a 1 l volumetric flask and dilute to the mark; this stock solution contains 1.00 g of K_2O per liter. Prepare a 10 μg ml^{-1} solution by 100-fold dilution with distilled water and store in a polyethylene container.

Matrix system. Dissolve 10.0 g of boron trioxide and 1.00 g of lithium carbonate in 1 l of 1 *M* hydrochloric acid. Store in a polyethylene container.

Apparatus

Ultrasonic generator. Operating frequency, 20 kHz. Cavitation bath: diameter, 16 cm; height, 10 cm. Power density in the cavitation bath, 2 W cm^{-2}.

· *Atomic absorption spectrometer.* Measurements were carried out on a Perkin–Elmer (Model 290) instrument with a potassium hollow-cathode lamp and an air–acetylene flame. The current for the lamp and the monochromator slitwidth used were those suggested by the manufacturer.

Procedure

Transfer 0.1000 g of the finely powdered sample (< 200 mesh) to a 30-ml platinum crucible. Add 1.0 g of boron trioxide and 0.10 g of lithium carbonate and mix intimately with a short glass rod with rounded ends. Set the crucible in a silica triangle and heat carefully with a small flame until any water is completely expelled. Then, cover the crucible and heat with a strong oxidizing flame (*ca.* 1000°) for 30 min. Remove the burner and allow the crucible to cool to room temperature, so that the fused mass solidifies forming a transparent glass. Then proceed as described below.

(a) For samples containing more than 1% of K_2O. Transfer 800–900 ml of 0.1 *M* hydrochloric acid to a 1-l beaker and add 2 ml of 30% hydrogen peroxide. Introduce the platinum crucible into the solution contained in the beaker. Rinse the cover of the crucible with a stream of 0.1 *M* hydrochloric acid. Put the beaker in the cavitation bath of the ultrasonic generator; usually 1–2 min suffice to detach completely the cake from the crucible. Then, place the beaker on a magnetic stirrer. Place a magnetic bar in the liquid, suspend the crucible in the solution (if necessary), cover the beaker and run the stirrer at a convenient rate until dissolution of the cake is complete; generally, no more than 20 min are required. (The dissolution may be greatly hastened by maintaining the ultrasonic wave in action until it is complete.) Remove and rinse the crucible with 0.1 *M* hydrochloric acid. Transfer the solution to a 1-l volumetric flask, and dilute with 0.1 *M* hydrochloric acid to the mark. If the atomic absorption measurement is not to be done immediately, transfer the solution to a polyethylene container.

Prepare the working standard solutions for potassium determination by adding 10.00 ml of the matrix system solution to each of four 100-ml volumetric flasks, and then 10.00, 20.00, 30.00 and 40.00 ml of the standard 10 μg ml^{-1} solution for potassium to successive flasks. Dilute with distilled water to the mark. These working standards contain 1, 2, 3 and 4 μg of K_2O per ml (1, 2, 3 and 4 p.p.m.), respectively.

Aspirate the sample solution and the working standard solutions into the air–acetylene flame. Calculate the concentration for potassium as K_2O from the calibrated graph or by narrow range bracketing.

(b) For samples containing less than 1% of K_2O. In this case, it is better to dissolve the cake so as to obtain a sample solution measuring 500 ml. Prepare the working standard solutions for potassium by adding 20.00 ml of the matrix system solution to each of three 100-ml volumetric flasks, adding 10.00, 15.00 and 20.00

ml of the standard 10 μg ml^{-1} solution for potassium to successive flasks and dilute to the mark with distilled water.

RESULTS AND CONCLUSIONS

The method described was tested by determining potassium in three silicate standards issued by the U.S. National Bureau of Standards, which were treated as unknown samples. The results obtained (Table I) agree with the established values within the normal precision level of atomic absorption measurements. The high reliability achieved shows that the proposed method of decomposition provides satisfactory accuracy and reproducibility for potassium. No interelemental interferences were observed. The results indicate that the major refractory-forming constituents—silicon, aluminum and titanium—have no detrimental effects on the determination of potassium. It was shown that addition of lithium to the matrix system solution was not essential; however, it seemed advisable to match the matrix composition of the unknowns and standards.

TABLE I

RESULTS OBTAINED IN THE DETERMINATION OF POTASSIUM IN SILICATE STANDARD SAMPLES

Sample	*Composition (%)*	*K_2O found (%)*	*Relative error (%)*
Plastic clay (NBS no. 98)	SiO_2, 59.11; Al_2O_3, 25.54; Fe_2O_3, 2.05; TiO_2, 1.43; ZrO_2, 0.041; P_2O_5, 0.08; V_2O_5, 0.025; Cr_2O_3, 0.021; CaO, 0.21; MgO, 0.72; K_2O, 3.17; Na_2O, 0.28; SO_3, 0.07; MnO, 0.005; CuO, 0.009	3.13 3.21 3.19 3.18	−1.3 +1.3 +0.6 +0.3
Flint clay (NBS no. 97)	SiO_2, 42.87; Al_2O_3, 38.77; Fe_2O_3, 0.98; TiO_2, 2.38; ZrO_2, 0.25; P_2O_5, 0.08; V_2O_5, 0.040; Cr_2O_3, 0.079; CaO, 0.10; MgO, 0.26; K_2O, 0.54; Na_2O, 0.33; SO_3, 0.042; MnO, 0.002; CuO, 0.003	0.55	+2.0
Burnt refractory (NBS no. 76)	SiO_2, 54.69; Al_2O_3, 37.67; Fe_2O_3, 2.38; TiO_2, 2.21; ZrO_2, 0.07; MgO, 0.58; CaO, 0.27; K_2O, 1.54; Na_2O, 0.38; P_2O_5, 0.069; V_2O_5, 0.021	1.52 1.54 1.52 1.52	−1.4 0 −1.4 −0.7

Sample solutions of silicate standards to which sodium chloride was added in various amounts were also analysed; results were not affected by up to 20 p.p.m. of Na_2O. Similarly, no effects were observed with additions of magnesium, calcium and iron up to 10 p.p.m. of MgO, CaO and Fe_2O_3, respectively.

The new approach seems to be a satisfactory solution to the problem of the preparation of sample solutions for the analysis of silicate rocks by atomic absorption spectrometry. The dissolution of the fusion melt, after detaching it from the crucible by the action of ultrasonic waves, is simple and rapid. No filtration

or separation steps are necessary; determinations are carried out directly without any further treatment. The matrix was found to keep the sample solution free from colloidal precipitation of silica and no other type of precipitation was observed over a period of some days. Although the decomposition method has been used in this work for the determination of potassium in silicate samples, the technique surely must be applicable to the determination of other major and minor constituents, probably with identical advantages. The fact that no cations are introduced by reagents, except a little lithium, contributes to signal stability of the atomic absorption measurements and to a decrease in background readings. This is an important point for the determination of trace elements.

The authors gratefully acknowledge the help received from the Conselho Nacional de Pesquisas.

SUMMARY

A boron trioxide–lithium carbonate (10:1) fusion is proposed for silicate analysis by atomic absorption spectrometry. The fusion melt is detached from the platinum crucible by the action of ultrasonic waves and dissolved in dilute hydrochloric acid containing hydrogen peroxide. The method was applied to the determination of potassium in standard silicate samples. No matrix effects were observed and the results obtained show very good accuracy and reproducibility.

RÉSUMÉ

Une fusion au mélange trioxyde de bore–carbonate de lithium (10:1) est proposée pour l'analyse des silicates par spectrométrie d'absorption atomique. Le produit de la fusion est détaché du creuset de platine par action d'ultrasons et dissous dans de l'acide chlorhydrique dilué contenant du peroxyde d'hydrogène. Cette méthode a été appliquée au dosage de potassium dans des échantillons de silicates étalons. Aucun effet de matrice n'est observé. L'exactitude et la reproductibilité des résultats obtenus sont très bonnes.

ZUSAMMENFASSUNG

Für den Aufschluss von Silicaten, die mittels Atomabsorptionsspektrometrie analysiert werden sollen, wird eine Bortrioxid–Lithiumcarbonat-Schmelze vorgeschlagen. Der Schmelzkuchen wird mit Hilfe von Ultraschallwellen aus dem Tiegel entfernt und in verdünnter wasserstoffperoxidhaltiger Salzsäure gelöst. Die Methode wurde auf die Bestimmung von Kalium in Standard-Silicatproben angewendet. Es wurden keine Matrixeffekte beobachtet, und die Ergebnisse sind sehr genau und gut reproduzierbar.

REFERENCES

1 J. Ito, *Bull. Chem. Soc. Jap.*, 35 (1962) 225.
2 I. May and J. J. Rowe, *Anal. Chim. Acta*, 33 (1965) 648.

3 F. J. Langmyhr and S. Sveen, *Anal. Chim. Acta*, 32 (1965) 1.
4 F. J. Langmyhr and P. R. Graff, *A Contribution to the Analytical Chemistry of Silicate Rocks*, Universitetsforlaget, Oslo, 1965.
5 B. Bernas, *Anal. Chem.*, 40 (1968) 1682.
6 M. S. Wang, *Appl. Spectrosc.*, 16 (1962) 141.
7 E. E. Welday, A. R. Baird, D. B. Intyre and K. W. Madlem, *Amer. Mineral.*, 49 (1964) 889.
8 V. S. Biskupsky, *Anal. Chim. Acta*, 33 (1965) 334.
9 A. M. Bond and D. R. Canterford, *Anal. Chem.*, 43 (1971) 134.
10 W. F. Hillebrand and G. E. F. Lundell, *Applied Inorganic Analysis*, Wiley, New York, 1944, p. 703.
11 I. M. Kolthoff and P. J. Elving, *Treatise on Analytical Chemistry*, Part I, Vol. 2, Interscience, New York, 1961, p. 1047.
12 O. A. Ohlweiler, J. O. Meditsch, L. P. Silveira and S. Silva, *Anal. Chim. Acta*, 61 (1972) 57.

Analytica Chimica Acta, 67 (1973) 289–295

DETERMINATION OF CHROMIUM IN SEA WATER BY ATOMIC ABSORPTION SPECTROMETRY

THOMAS R. GILBERT and ALICE M. CLAY
Research Department, New England Aquarium, Boston, Mass. 02110 (U.S.A.)
(Received 9th March 1973)

The determination of chromium in sea water can be difficult and time-consuming, owing to its very low concentration (*ca.* 0.05 $\mu g\ l^{-1}$) in the open ocean[1–3]. Three of the analytical methods which have been used previously include neutron activation analysis, atomic absorption spectrometry and a spectrophotometric analysis in which the diphenylcarbazide derivative is measured. Of these processes only neutron activation requires a simple one-step preconcentration: freeze-drying of the sample. Among the drawbacks of activation analysis are the reactor facilities needed and the time required for sample irradiation, cooling off and counting[4]. In the spectrophotometric method, chromium is preconcentrated by coprecipitation from the sample with iron(III) hydroxide[4]; the chromium must then be separated from the iron before it can be measured. Coprecipitation with iron(III) hydroxide followed by extraction with acetylacetone in MIBK has been employed to preconcentrate chromium before atomic absorption spectrometry[5]. Coprecipitation of chromium(III) with 5,7-dibromo-8-hydroxyquinoline has been used, but the literature differs concerning the feasibility of redissolving the precipitate and aspirating it directly into the flame. Chau *et al.*[5] report unstable flame conditions, while Riley and Topping[6] indicate that the precipitate can be dissolved in nitric acid and sprayed into the flame, but the authors offer no analytical results using this procedure.

In the present paper, chromium(VI) is extracted from sea water with ammonium pyrrolidine dithiocarbamate (APDC) and methyl isobutyl ketone (MIBK) as the second phase. Mansell and Emmel[7] have described a method for the extraction of p.p.m. levels of chromium(VI) from 25% brine with APDC and MIBK. The sample is heated to incipient boiling to achieve complexation. Midgett and Fishman[8] have reported a modification of this procedure in which a 10:1 volume ratio of brine to MIBK was used to give a detection limit of 1 $\mu g\ l^{-1}$ in the original sample. Sample preparation in their procedure included 3 changes in pH and a filtration step before extraction. In the procedure described here, sample preparation has been reduced to filtration, a 30-min oxidation, acidification and extraction. The volume ratio of sample to MIBK was increased for greater sensitivity.

EXPERIMENTAL

Reagents and apparatus

Chromium stock solutions (1000 p.p.m.) were prepared from reagent grade

chromium nitrate and potassium chromate. Working standards (100 p.p.m.) were prepared as needed by dilution with (distilled deionized) water. Aqueous 5% solutions of APDC were extracted three times with equal volumes of MIBK to remove impurities. The MIBK, hydrochloric acid, and hydrogen peroxide used were ACS reagent grade. A 0.5% potassium permanganate solution was prepared from mercury-free 5% potassium permanganate reagent (No. 1-50-101, Coleman Instruments, Maywood, Ill.).

Measurements were made with an Instrumentation Laboratories dual-beam atomic absorption spectrophotometer, Model 153. The fuel and aspiration rates through the single-slot titanium steel burner were adjusted to give a fuel-rich air/acetylene flame. The light source was an IL chromium–copper hollow-cathode lamp No. 63208; the 357.9-nm resonance line for chromium was used.

Sampling

All laboratory ware used for the collection and analysis of sea-water samples was thoroughly washed in detergent, rinsed with tap water and distilled water, and soaked in 3 *M* hydrochloric acid for several days. Before use, the acid-soaked vessel was washed thoroughly with water.

Sea-water samples (4 l) were collected in conditioned polypropylene bottles. Within 2–3 h, each sample was filtered through a glass fiber filter (Millipore No. AP2004700) which had been soaking in 6 *M* hydrochloric acid for several days before use.

Procedures

Aqueous phase. Collect the filtrate in a propylene flask, and separate into four 800-ml portions. To three of these, add spikes of chromium(III) working standard, to increase the sample chromium concentration by 1, 2 and 3 $\mu g\, l^{-1}$. Then heat the samples in a hot water bath to 50° and add drops of permanganate solution as needed to maintain a pink color. After 30 min, remove the samples from the bath, acidify to pH 2.0 with 6 *M* hydrochloric acid, and add 0.3% hydrogen peroxide solution dropwise, with swirling between additions, until the solutions are colorless. Then cool to room temperature, transfer to 1-l Pyrex separatory funnels, and extract with 4 ml of 5% APDC into 20 ml of MIBK. After vigorous shaking for 1 min, allow the phases to separate, and collect the MIBK extract for analysis in recappable polypropylene test tubes. For the final step, carefully adjust the burner height and fuel/oxidant ratio to optimize sensitivity. Aspirate the extract into the flame at a rate of 3 ml min^{-1}, and measure the chromium absorbance over a 10-s integration period against a water-saturated MIBK blank. Use the absorbance values of the four portions of each sample to construct a standard addition curve.

Particulate phase. During filtration, measure the total sample volume which passes through the filter. Then place the filter in a conditioned Pyrex petri dish and soak with 5 ml of 12 *M* hydrochloric acid. After 1 h, wash the acid extract into a 25-ml volumetric flask with several water rinses, and dilute to volume. Measure the absorbance as with the aqueous phase, but against a distilled water blank. Prepare a calibration curve using 5-ml portions of 12 *M* hydrochloric acid spiked with 0, 0.16, 0.32 and 0.48 mg Cr(III) l^{-1}, in final volumes of 25 ml. These concentra-

tions correspond to 0, 1, 2 and 3 μg Cr l^{-1} in the particulate phase of an original filtered volume of 4 l.

RESULTS AND DISCUSSION

Loss of chromium on storage

Upon storage, sea-water samples are known to lose trace metals, probably because of adsorption on container walls[9]. The rate of chromium(III) loss was measured from unacidified sea water stored in containers made of Nalge polyethylene (CPE), Pyrex, Kimax polypropylene and Nalge polypropylene. Portions (1 l) of harbor water spiked with 10 μg Cr(III) l^{-1} were stored in three bottles of each type. After 1, 2 and 3 days, 200-ml samples were poured from each container and analyzed for soluble chromium as described above. Results showed little difference in the rate of loss of chromium between samples stored in different container materials. Polypropylene ware was selected because it is less breakable than Pyrex and has a higher melting point than polyethylene and thus can be autoclaved. In a second study, a 4-l sample of sea water was spiked with 10 μg Cr(III) l^{-1} and stored in a polypropylene bottle; 400-ml portions were poured from the bottle and analyzed for soluble chromium after 0, 1, 2, 3, 7, and 14 days. The results are shown in Fig. 1; the best fitting curve of the form

$$y = \beta_1 e^{-\beta_2 t} + \beta_3$$

was solved and drawn through the points with the aid of a computer. The data show that chromium in the sample approaches an equilibrium concentration not equal to zero. From the value of β_2 and the standard deviation of its determination, the half-life of chromium(III) in the sample was found to be 1.8 ± 0.3 days. Other sea-water samples will have to be studied to determine how representative this number is, but it does indicate that a significant loss of chromium may occur from samples stored only a few hours.

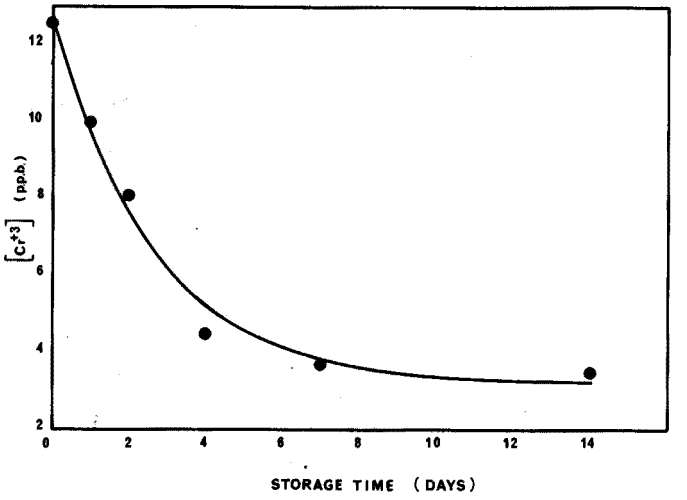

Fig. 1. Loss of chromium(III) from sea water stored in polypropylene. .

Since unacidified sea-water samples must not be stored for more than a few hours, oxidation and extraction should be carried out as soon after collection as possible. The stability of the APDC–chromium(VI) complex in MIBK then determines the maximum allowable time before sample analysis. A 200-ml sample spiked with 10 μg Cr(VI) l^{-1} was extracted and analyzed. The extract was stored in a capped polypropylene test tube and analyzed again after 1, 2, and 7 days. The results of these analyses (Table I) show that the complex is stable for at least a week. Since no effort was made to separate all traces of water from the MIBK layer, the results indicate that back-extraction into the aqueous phase was negligible.

TABLE I

STABILITY OF CHROMIUM(VI)–APDC COMPLEX IN MIBK

(200-ml samples, 10 p.p.b. Cr(VI). Added: 2 ml 5% APDC, 10 ml MIBK)

Time (days)	0	1	2	7
Absorbance	0.0264 ±0.0024	0.0280 ±0.0014	0.0274 ±0.0020	0.0284 ±0.0018

Oxidation and extraction of chromium

Preliminary studies indicated that several common oxidants, *e.g.* chlorine, 5% ammonium persulfate and 30% hydrogen peroxide, were not suitable for the oxidation of chromium(III) in sea water at pH 8. When samples were heated to 50° persulfate only partially oxidized a 10 μg l^{-1} spike of chromium(III) after 2 h. At the same temperature a few drops of permanganate solution completely oxidized a 10 μg l^{-1} spike in less than 30 min. Under similar conditions, but at pH 2.3, the permanganate oxidation was not complete (Table II).

TABLE II

EFFECT OF pH ON CHROMIUM(III) OXIDATION IN SEA WATER

(200-ml sample oxidized with permanganate at 50° for 30 min)

pH	*Cr(III) added (μg l^{-1})*	*Cr(VI) added (μg l^{-1})*	*Absorbance*
2.3	10	0	0.0116±0.0016
2.3	0	10	0.0296±0.0028
7.8	10	0	0.0312±0.0020

The extraction of chromium(VI) with APDC into MIBK is strongly dependent on sample pH (Fig. 2). Approximately 50% of maximum efficiency is achieved at pH 4. Since literature values for the pK_2 of chromic acid are about 6.5, extraction efficiency is apparently not determined by the protonation of chromate. One explanation for the observed acid dependence may be that the rate-determining step in complex formation is acid-catalyzed. Another possibility is that the dithio acid group must be protonated before APDC complexes chromium(VI). A mechanism consistent with the latter theory is that an APDC sulfur atom formally bonds with

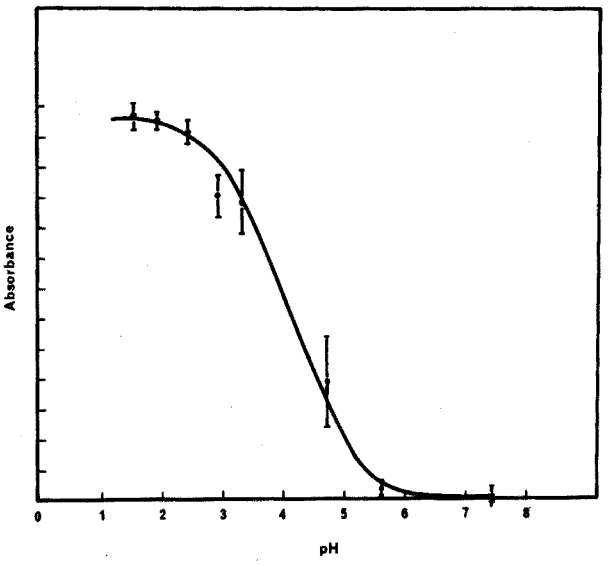

Fig. 2. Absorbance of MIBK extract at 357.9 nm as a function of sample pH. Sample Cr(VI) concentration = 10 p.p.b.

chromium displacing the protonated tetrahedral oxygen of hydrogen chromate, $HCrO_4^-$. The displaced hydroxyl group condenses with the thio acid proton to form water.

Application to sea water

A number of samples of Boston Harbor water were collected and analyzed for chromium. The results of some of these analyses are listed in Table III with standard deviation values of triplicate determinations. The high concentration of commercial and industrial activity in the Inner Harbor is reflected in high levels of both soluble and particulate chromium. Generally lower levels were found through-

TABLE III

CHROMIUM IN BOSTON HARBOR WATERS AT HIGH TIDE

Date	*Location*	*Chromium concentration (p.p.b.)*	
		Soluble	*Particulate*
	Inner Harbor		
9/19/72	New England Aquarium Dock	1.97 ± 0.06	2.23 ± 0.06
9/19/72	Charles River (mouth)	2.24 ± 0.01	2.56 ± 0.09
9/19/72	Fort Point Channel	3.69 ± 0.04	4.15 ± 0.08
	Outer Harbor		
9/11/72	Neponset River (mouth)	0.44 ± 0.02	0.59 ± 0.06
9/8/72	Deer Island Light	2.10 ± 0.02	5.4 ± 0.2
9/8/72	e. of Thompson Island	0.27 ± 0.03	0.70 ± 0.03

out the Outer Harbor with the exception of samples collected near Deer Island Light, the site of several sewage outfalls from a metropolitan primary treatment plant.

The described procedure requires much less time and is free from the major interferences encountered with neutron activation[4]. Additions of 10 p.p.t. Na^+ and K^+, 2 p.p.t. Mg^{2+}, 500 p.p.m. Ca^{2+} and 10 p.p.m. Sr^{2+}, Fe^{3+} and Mn^{2+} did not interfere with the determination of 10 p.p.b. chromium(III).

To evaluate the detection limit of the method, twice the standard deviation of 26 successive blank measurements was converted to sample chromium concentration. These values were 0.05 $\mu g\ l^{-1}$ for the aqueous and 0.06 $\mu g\ l^{-1}$ for the particulate phase. This sensitivity is comparable to or better than that obtained by other a.a.s. procedures[3,5,8] and is achieved in a procedure which is faster, requires less sample manipulation, and so reduces the likelihood of sample contamination.

SUMMARY

A method for the determination of chromium in sea water is described which requires minimal sample preparation. The chromium from filtered samples is oxidized with permanganate, extracted with ammonium pyrrolidine dithiocarbamate into MIBK, and analyzed by atomic absorption spectrometry in a fuel-rich air–acetylene flame. Non-filterable solids are extracted with 12 *M* hydrochloric acid and analyzed. Detection limits for the methods are 0.05 $\mu g\ l^{-1}$ in the soluble phase and 0.06 $\mu g\ l^{-1}$ in the particulate phase.

RÉSUMÉ

Une méthode est décrite pour le dosage du chrome dans l'eau de mer, par spectrométrie d'absorption atomique. Le chrome, après filtration des échantillons, est oxydé par le permanganate, extrait au moyen de pyrrolidine dithiocarbamate d'ammonium dans la méthylisobutylcétone et analysé par absorption atomique dans une flamme air–acétylène riche en acétylène. Des solides non-filtrables sont extraits par l'acide chlorhydrique 12 *M* et analysés. Les limites de détection de ces méthodes sont 0.05 $\mu g\ l^{-1}$ dans la phase soluble et 0.06 $\mu g\ l^{-1}$ dans l'autre cas.

ZUSAMMENFASSUNG

Es wird eine Methode für die Bestimmung von Chrom in Meerwasser beschrieben, die eine minimale Probenvorbereitung erfordert. Das Chrom in filtrierten Proben wird mit Permanganat oxidiert, mit Ammoniumpyrrolidindithiocarbamat in MIBK extrahiert und durch Atomabsorptionsspektrometrie in einer brenngasreichen Luft–Acetylen-Flamme bestimmt. Nichtfiltrierbare Feststoffe werden mit 12 *M* Salzsäure ausgezogen und analysiert. Die Nachweisgrenzen für die Methoden sind 0.05 $\mu g\ l^{-1}$ in der löslichen Phase und 0.06 $\mu g\ l^{-1}$ in der unterteilten Phase.

REFERENCES

1 K. B. Krauskopf, *Geochim. Cosmochim. Acta*, 9 (1956) 1.
2 B. Mason, *Principles of Geochemistry*, Wiley, New York, 1966, p. 195.
3 L. Chuecas and J. P. Riley, *Anal. Chim. Acta*, 35 (1966) 240.
4 D. Z. Piper and G. G. Goles, *Anal. Chim. Acta*, 47 (1969) 560.
5 Y. Chau, S. Sim and Y. Wong, *Anal. Chim. Acta*, 43 (1968) 13.
6 J. P. Riley and G. Topping, *Anal. Chim. Acta*, 44 (1969) 234.
7 R. E. Mansell and H. W. Emmel, *At. Absorption Newslett.*, 4 (1965) 365.
8 M. R. Midgett and M. J. Fishman, *At. Absorption Newslett.*, 6 (1967) 128.
9 D. E. Robertson, *Anal. Chim. Acta*, 42 (1968) 533.

Analytica Chimica Acta, 67 (1973) 297–306

THE EXTRACTION-SPECTROPHOTOMETRIC DETERMINATION OF CHROMIUM(III) WITH 4-(2-PYRIDYLAZO)-RESORCINOL

TAKAO YOTSUYANAGI, YASUO TAKEDA, RYUJI YAMASHITA and KAZUO AOMURA
Laboratory of Analytical Chemistry, Faculty of Engineering, Hokkaido University, Sapporo-shi 060 (Japan)
(Received 9th March 1973)

The metallochromic indicator 4-(2-pyridylazo)-resorcinol (PAR) proposed by Pollard *et al.*[1] has since found many applications as a highly sensitive reagent for the colorimetric determination of the number of metals including cobalt[1,2], nickel(II)[3], iron(II)[4], iron(III)[5], manganese(II)[6], vanadium(V)[7,8], etc.[9]. It is evident, however, that PAR shows only a slight selectivity, and can be used only after separation of interfering metals by solvent extraction, ion-exchange chromatography, etc. In the course of studies on the selective colorimetric determination of metals with PAR, it was found that ions of the d^6 and d^8 type, *e.g.* Fe^{2+}, Co^{2+} and Ni^{2+}, form PAR complexes which are very inert against ligand substitution reactions with polyaminopolycarboxylates (*e.g.* EDTA, CDTA)[4,10]; this property has made it possible to develop selective methods for these metals ions[4,10–12].

In this paper are described studies on the color reaction forming the inert PAR–chromium(III) (d^3 ion) complex and the extraction of the complex with a quaternary ammonium compound (tetradecyldimethylbenzylammonium chloride, $TDBA^+$–Cl^-). Based on these studies, a highly sensitive and selective colorimetric method for chromium(III) was developed; the sensitivity is much greater than that of the diphenylcarbazide method[13].

EXPERIMENTAL

Apparatus and reagents

A Hitachi model 124 double-beam recording spectrophotometer with 10-mm cells was used for the absorbance measurement and for recording the spectra. A Toa Electronic Ltd. model HM-5A meter was used for pH measurements.

0.1% PAR solution. Dissolve 0.100 g of PAR (Dojindo Co. Ltd., Japan) in 10 ml of 0.1 *M* sodium hydroxide solution and dilute to 100 ml with water.

0.005 M tetradecyldimethylbenzylammonium chloride solution. Dissolve 1.84 g of $TDBA^+$ chloride (Dojindo Co. Ltd., Japan) in 80 ml of water and dilute to 100 ml.

Procedures

Color development. Pipette a sample aliquot containing 0–50 μg of chromium(III) into a 50-ml volumetric flask. Add, in the following order and with mixing, 2.0 ml of 2 *M* acetate buffer pH 5.0 solution and 1.0 ml of PAR solution, and

dilute to about 45 ml with water. Transfer the mixture to a 100-ml flask equipped with a ground-glass joint. Attach a reflux condenser to the flask and heat under reflux for 135 min. After cooling to room temperature, add 2.0 ml of aqueous 0.05 *M* EDTA (disodium salt) solution and allow to stand for 2 min. Then, dilute to 50 ml with water and measure the color at 530 nm against a reagent blank.

Extraction. Pipette the colored mixture containing 0–9 μg of chromium(III) prepared as described above into a 100-ml separating funnel. Add 1.0 ml of $TDBA^+$ solution, shake with 10.0 ml of chloroform for 10 min, and allow the phases to separate. Run the chloroform layer into a test tube containing a small amount of anhydrous sodium sulfate crystals to remove droplets of water. Measure the color of the chloroform layer at 540 nm against a reagent blank.

RESULTS

General study on the formation of chromium(III)–PAR complex

Absorption spectra and adherence to Beer's law. The absorption spectra of PAR–chromium(III) complexes in water and in chloroform which were extracted with $TDBA^+$ are shown in Fig. 1. Extraction with $TDBA^+$ produced a small red shift, the wavelength of maximal absorbance for the extracted ion-association complex being 540 nm compared with 530 nm for the complex in water. The molar absorptivities of these complexes at the wavelengths of maximum absorbance are $4.8 \cdot 10^4$ in water and $4.7 \cdot 10^4$ in chloroform, respectively.

Beer's law was obeyed from zero to 1.0 absorbance unit (0–1.0 μg Cr^{3+} ml^{-1}) in water, and from zero to 0.9 absorbance unit (0–0.9 μg Cr^{3+} ml^{-1}) in chloroform.

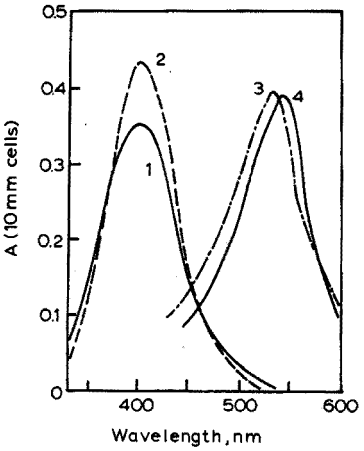

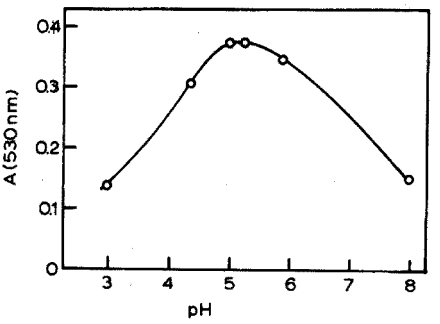

Fig. 1. Absorption spectra of solutions at pH = 5.0. (1) Free PAR in H_2O; (2) PAR–TDBA complex in $CHCl_3$; (3) PAR–Cr^{3+} complex ($8 \cdot 10^{-6}$ *M vs.* blank) in H_2O; (4) PAR–Cr^{3+}–TDBA complex ($8 \cdot 10^{-6}$ *M vs.* blank) in $CHCl_3$.

Fig. 2. Effect of pH on the color reaction of PAR and chromium(III). (Cr^{3+}): 25 μg per 50 ml.

Effect of pH. The effect of pH on the formation of the complex was investigated by changing the pH value of the acetate buffer solution. The results are shown in Fig. 2. Buffers of pH between 4.8 and 5.2 gave maximal absorbance. After completion of the complex formation, the absorbance was not influenced by any change in pH ranging from 4 to 13 at room temperature.

Influence of the nature of buffer solution and effect of time on the stability of the complex. The effect of the nature of the buffer solution on the color reaction was examined at pH 5.0 ± 0.1 (Fig. 3). The color developed slowly and attained a constant value after heating for 135 min. A reproducible maximal absorbance was obtained when acetate buffer solution was added (curve A). When no buffer (curve C) or hexamine buffer (curve B) solution was used, however, only part of the chromium(III) formed the complex with PAR. An oxalate buffer solution or an acetate buffer solution containing EDTA completely suppressed the color reaction. But, when EDTA and potassium cyanide were added after the completion of the color reaction, the color remains unchanged for at least 24 h at room temperature. This behavior may be mainly attributed to the inert nature of the chromium(III) ion. The favorable effect of acetate suggests that the acetate ion forms relatively labile acetato–chromium(III) complexes and prevents the formation of very inert polynuclear-hydroxo-complexes of chromium(III) ion.

Composition and stability of the chromium(III)–PAR complex

Continuous variation plots (Fig. 4), which were confirmed by molar ratio plots, indicated the formation of a 1:3 chromium:PAR complex. From these plots, the conditional stability constant, $K_{Cr(HR)_3}$, in acetate buffer solution ($[OAc^-]_{total} = 8 \cdot 10^{-3}$ *M*, pH 5.0, 25°) at boiling point, was evaluated as 18.5 by the usual method:

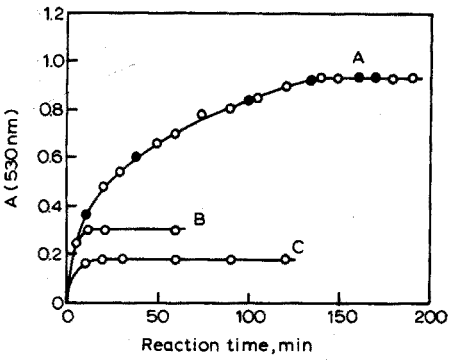

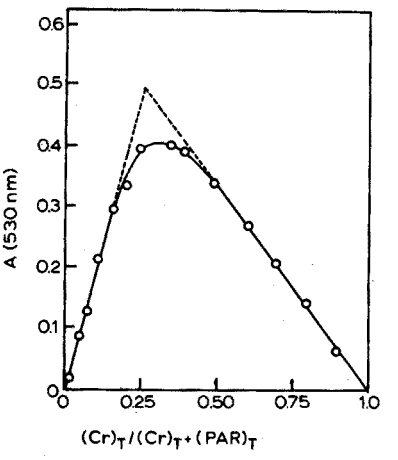

Fig. 3. Influence of the nature of buffer solutions on the color reaction at pH 5.0 ± 0.1. (A) Acetate buffer solution: (○) Cr^{3+} + buffer, boil for 5 min, add PAR and boil; (●) Cr^{3+} + PAR + buffer, mix at room temperature and boil; (B) hexamine buffer solution, and (C) no buffer solution and pH was adjusted by HCl solution and NaOH solution. Each solution contained 50 μg Cr^{3+} per 50 ml.

Fig. 4. Continuous variation plots for Cr–PAR complex. $(Cr^{3+})_T + (PAR)_T = 4 \cdot 10^{-5}$ *M*.

$$K_{Cr(HR)_3} = \frac{[Cr(HR)'_3][H^+]^3}{(C_{Cr}-[Cr(HR)'_3])(C_{H_2R}-3[Cr(HR)'_3])^3} \quad (1)$$

where C_{Cr} and C_{H_2R} are the total concentrations of chromium(III) and PAR, respectively. The total concentration of chromium(III)–PAR complexes, $[Cr(HR)'_3]$, is given by $[Cr(HR)'_3]=[Cr(HR)_3]+[Cr(R)(HR)_2^-]=C_{Cr}A/A_{ex}$, A being the observed absorbance and A_{ex} the extrapolated absorbance, because both chromium complexes have effectively the same molar absorptivity.

The stability constant, $\beta_3^{*HR^-}$, of the reaction,

$$Cr^{3+}+3\ *HR^- \rightleftharpoons Cr(HR)_3 \quad (2)$$

can be calculated by following equation:

$$\log \beta_3^{*HR^-} = \log K_{Cr(HR)_3} + \log \alpha_{Cr}(OH^-, OAc^-) + 3 \log \alpha_{H_2R}(H) - \log \alpha_{Cr(HR)_3}(H) - 3 \log K^*_{a\,H_2R} \quad (3)$$

where $\alpha_{Cr}(OH^-, OAc^-)$ is the coefficient of side reactions of metal ion with hydroxide and acetate ions (*i.e.*, $Cr(OH)^{2+}$, $Cr(OH)_2^+$, $Cr(OAc)^+$ and $Cr(OAc)_2^+$), $\alpha_{H_2R}(H)$ is that of PAR with hydrogen ion, $\alpha_{Cr(HR)_3}(H)$ is that of proton dissociation of $Cr(HR)_3$ to $Cr(R)(HR)_2^-$ (see eqn. 5), and $K^*_{a\cdot H_2R}$ is the dissociation constant of H_2R to form a hypothetical ligand $*HR^-$ in which the *o*-hydroxyl proton of the resorcinol group is dissociated:

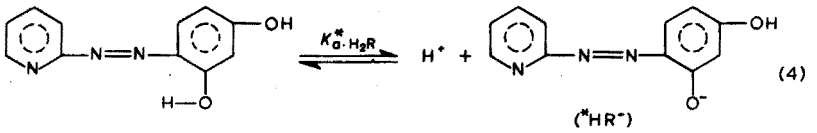

(4)

Because equilibrium constants of the side reactions under boiling conditions are lacking, $\beta_3^{*HR^-}$ cannot be calculated precisely, but an approximate value can be found based on the data at 25° taken from the tables of Sillén and Martell[14]. At pH 5.0 and $[OAc^-]=8\cdot10^{-2}$ *M*, the α coefficients are $\log \alpha_{Cr}(OH^-, OAc^-)=1.22$, $\log \alpha_{H_2R}(H)=0.097$, $\log \alpha_{Cr(HR)_3}(H)=0.12$, and $pK^*_{a\cdot H_2R}$ is taken[15] as 11.9, which is the last acid dissociation constant of PAR, according to the proposal of Freiser *et al.*[16,17]. Thus, the value of $\log \beta_3^{*HR^-}$ was estimated as 38.4.

Extraction of chromium(III)–PAR complex

Extraction without TDBA$^+$. At pH 5, the complex can be partially extracted into the chloroform layer even in the absence of $TDBA^+$. This result would be expected from the fact that chromium(III) forms a 1:3 neutral complex $[Cr(HR)_3]^0$ with PAR as discussed above. The extractability of the chromium complex was a function of pH, since the concentration of the extractable species, $Cr(HR)_3$, changed according to the dissociation of acidic hydrogen atoms in the complex.

$$Cr(HR)_3 \overset{K'_a}{\rightleftharpoons} Cr(R)(HR)_2^- + H^+ \quad (5)$$

$$K'_a = [Cr(R)(HR)_2^-][H^+]/[Cr(HR)_3] \quad (6)$$

The distribution of the chromium complex between chloroform and water is described by,

$$D = [Cr(HR)_3]_o/[Cr(HR)_3] \quad (7)$$

and by the material balance of chromium,

$$C_{Cr} = \frac{V_o}{1000}[Cr(HR)_3]_o + \frac{V_w}{1000}\sum_0^3 [Cr(OH)_m^{(3-m)+}] + \sum_0^3 [Cr(R)_n(HR)_{3-n}^{n-}] \quad (8)$$

where $[Cr(HR)_3]_o$ is the concentration of the chromium complex in chloroform, and V_o and V_w are the volumes of the chloroform and water layers, respectively. When purified chromium complex, $Cr(HR)_3$, is used for the distribution experiment, the term $\Sigma_0^3[Cr(OH)_m^{(3-m)+}]$ in eqn. (8) can be dropped because of the inert nature of the chromium complex. And, under acidic conditions (pH 3.5–5.6), the acid dissociation of the 1-hydroxyl group of PAR in the chromium complex occurs only in its first step as shown in eqn. (5). Therefore, from eqns. (6)–(8), one can write:

$$\frac{C_{Cr}}{[Cr(HR)_3]_o} \cdot \frac{1000}{V} = \frac{K_a'}{D} \cdot \frac{1}{[H^+]} + \frac{1}{D} + \frac{V_o}{V} \quad (9)$$

From the plot of $C_{Cr}/[Cr(HR)_3]_o$ *vs.* $[H^+]^{-1}$ (Fig. 5), constants K_a' and D (at 25°, $I=0.1$) were determined as follows

$$D = \frac{[Cr(HR)_3]_o}{[Cr(HR)_3]} = 1.17 \quad (10)$$

$$K_a' = \frac{[Cr(R)(HR)_2^-][H^+]}{[Cr(HR)_3]} = 10^{-5.49} \quad (11)$$

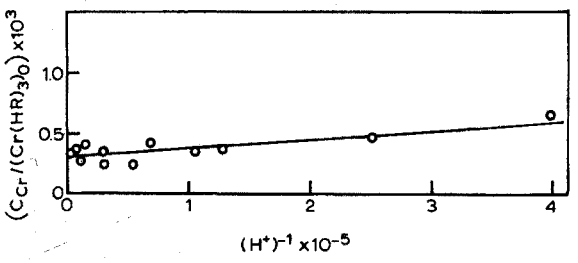

Fig. 5. Plots of $C_{Cr}/[Cr(HR)_3]_o$ *vs.* $[H^+]^{-1}$. $V_o=10$ ml of chloroform, $V=25$ ml of 0.1 M acetate buffer solution and $C_{Cr}=4.68\cdot10^{-5}$ M.

Extraction with TDBA$^+$. A study of the kinetics of the extraction of the chromium–PAR complex showed that equilibrium was reached after 10 min, and that EDTA ($2\cdot10^{-3}$ M) in the aqueous phase did not affect the extractability of the complex. The complex can be extracted quantitatively in the presence of suitable amounts of $TDBA^+$ at pH 5 (Fig. 6).

This molar ratio plot (Fig. 6) is useful for determining extraction conditions, but does not provide much information on the stoichiometry of the extracted ion-association complex, the aqueous phase used in this experiment was a mixture

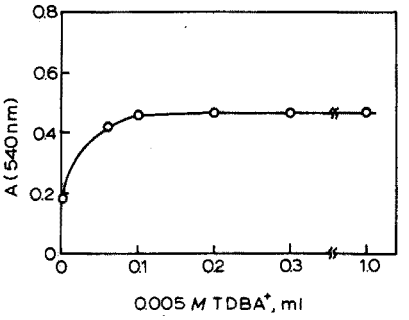

Fig. 6. Effect of $TDBA^+$ concentration on the extractability from acetate buffer solution (pH 5.0). (Cr^{3+}): 5 μg per 10 ml $CHCl_3$.

containing many species such as $Cr(HR)_3$, $Cr(R)(HR)_2^-$, H_2R and EDTA which could form ion-association complexes with $TDBA^+$. Therefore, in the studies described below, purified chromium(III)–PAR complex solutions were used: the complex was prepared by reacting PAR with excess of chromium(III) nitrate in boiling acetate buffer solution (pH 5) and was purified by repeated extraction with chloroform at pH 5 and back-extraction with 0.05 *M* borate buffer solution at pH 9.3.

The molar ratio plots with the purified complex solution (Fig. 7) clearly show the occurrence of two constant absorbance regions; one occurs in the $[TDBA^+]/[Cr(HR)_3]$ range of 5–100, and the other above 1000. It seems very likely that the first step in Fig. 7 indicates the formation of a 1:1 $Cr(HR)_3$:$TDBA^+$ ion-association compound. In order to confirm this result, continuous variation plots were made in a concentration region of $TDBA^+$ where the first constant absorbance was observed in Fig. 7. The plots for PAR and its chromium(III) complex (Fig. 8) indicate that the stoichiometry of the extraction reaction with $TDBA^+$ can be described as

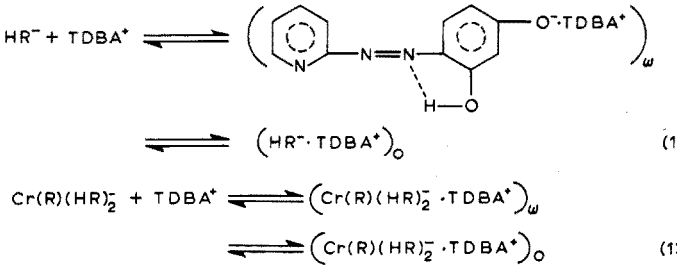

The extraction constant of these ion-association reaction at 25° can be calculated by the usual method from the data in Fig. 8 as:

$$K_{ex}^{L} = \frac{[HR^- \cdot TDBA^+]_o}{[HR^-][TDBA^+]} = 10^{5.41} \tag{14}$$

$$K_{ex}^{c} = \frac{[Cr(R)(HR)_2^- \cdot TDBA^+]_o}{[Cr(R)(HR)_2^-][TDBA^+]} = 10^{6.93} \tag{15}$$

where subscript o indicates the concentration of the chloroform layer.

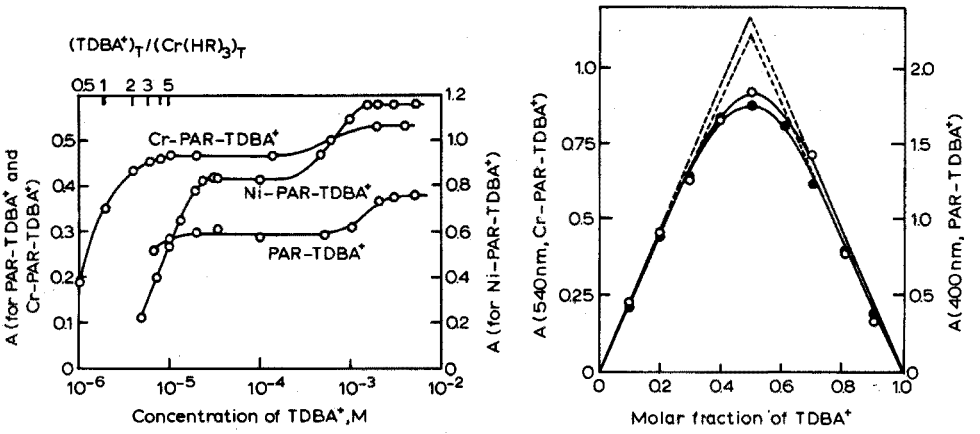

Fig. 7. Effect of $TDBA^+$ concentration on the absorbance of the complex in $CHCl_3$. [Cr–PAR complex]$_0 = 1 \cdot 10^{-5}$ *M*, [Ni–PAR complex]$_0 = 1.7 \cdot 10^{-5}$ *M* and [PAR]$_0 = 1.1 \cdot 10^{-4}$ *M*. Extracted from borate buffer solution (pH 9.3).

Fig. 8. Continuous variation plots for Cr–PAR–TDBA complex and PAR–TDBA complex. (●) Cr–PAR–TDBA complex ([Cr–PAR complex]$_T$ + [$TDBA^+$]$_T = 1 \cdot 10^{-5}$ *M*) and (○) PAR–TDBA complex ([PAR]$_T$ + [$TDBA^+$]$_T = 3.5 \cdot 10^{-4}$ *M*). Extracted from borate buffer solution (pH 9.3).

Effect of excess $TDBA^+$ on the absorbance. In the presence of a large excess of $TDBA^+$, the absorbance of the chloroform layer increased again (Fig. 7). The chromium complex was completely extracted both in the first and the second constant absorbance regions. Therefore, the second increase in the absorbance must be attributed to an increase in the molar absorptivity of the ion-association complex in chloroform. A very similar increase in absorbance was also observed for PAR and the nickel(II)–PAR complex (Fig. 7) at a $TDBA^+$ concentration range of $2 \cdot 10^{-4}$–$2 \cdot 10^{-3}$ *M*. The formation of higher-order association complexes with $TDBA^+$ such as ($R^{2-} \cdot 2TDBA^+$), ($Cr(R)_2(HR)^{2-} \cdot 2TDBA^+$) and ($Cr(R)_3^{3-} \cdot 3TDBA^+$) might account for this phenomenon. However, in the case of PAR, there was very little shift in the wavelength of maximal absorbance (400 nm) before and after the increase in the absorbance, whereas the 1:2 complex ($R^{2-} \cdot 2TDBA^+$) extracted at pH 13 had its absorbance maximum at 500 nm, as shown in the following diagram.

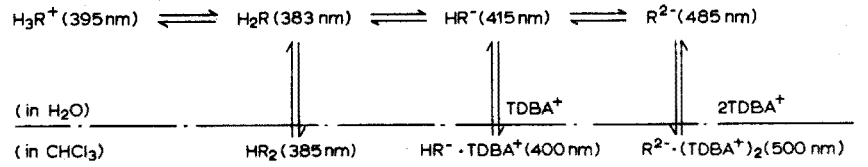

The $TDBA^+$ concentration of about 10^{-3} *M* corresponds to that of $TDBA^+$ forming its micelle[18] in the aqueous solution. This suggests that the observed increases in the absorbance are due to the effects of micelle formation of $TDBA^+$, but the detailed mechanism requires further study.

Interference studies

The influence of foreign ions on the proposed method was ascertained. The ions Al(III), Ba(II), Ca(II), Cd(II), Cu(II), Mg(II), Mn(II), Mo(VI), Pb(II), Sn(II), Sr(II), V(V), and Zn(II) in moderate amounts (0–500 μg) are masked by EDTA and do not interfere. These ions form labile PAR complexes, which are decomposed completely by EDTA within 2 min at room temperature. Sodium and potassium ions also do not interfere. However, iron, cobalt and nickel form inert complexes with PAR at pH 5 and seriously interfere with the determination. These interfering ions can be removed by extracting twice with cupferron from acetate buffer solution (pH 5.0) into a (1+1) mixture of benzene and iso-amyl alcohol[13], leaving chromium(III) in the aqueous phase.

DISCUSSION

According to the molar ratio plots and continuous variation plots (Fig. 4). PAR and chromium(III) form a 1:3 complex, $Cr(HR)_3$. Chromium(III) complexes with d^3 electronic configuration commonly have octahedral configuration. Thus, in forming the chromium(III) complex, PAR is functioning as a bidentate ligand. The extraction study shows that the 1:3 complex can be partly extracted into chloroform without $TDBA^+$ from a slightly acidic solution. This suggests the presence of an uncharged complex, which is consistent with the 1:3 complex suggested by the stoichiometric studies.

The first acid dissociation constant of the complex $Cr(HR)_3$, which was determined by the extraction method, was $pK_{a_1} = 5.49$. This value seems to be quite reasonable compared with that of the copper chelate ($Cu(HR)_2$, $pK_{a_1} = 5.3$)[19] and that of zinc chelate ($Zn(HR)_2$, $pK_{a_1} = 5.90$)[20].

Studies on the stoichiometry of the extraction reaction of free PAR ligand and the PAR–chromium(III) complex with $TDBA^+$ show that 1:1 ion-association compounds are formed (eqns. 4 and 5). These extractable compounds still contain dissociatable phenolic hydrogen atoms; which indicates that in the case of complexes having phenolic hydroxy groups, the displacement of all the hydrogen atoms with organic bases is not essential for extraction.

Thus, the extraction scheme of the PAR–chromium system can be summarized as:

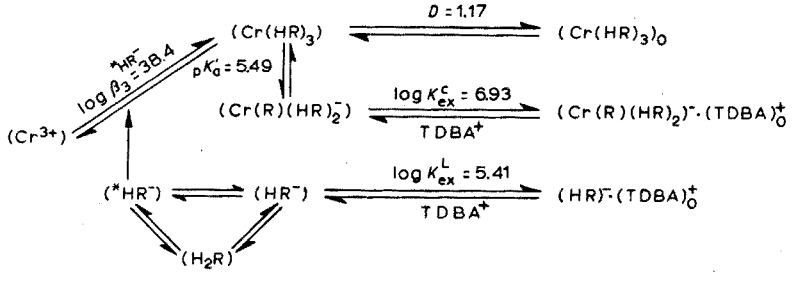

For the spectrophotometric determination, the complex ($Cr(R)(HR)_2^-$–$TDBA^+$) used is the one formed in a $TDBA^+$ concentration range of 10^{-5} *M*–$2 \cdot 10^{-4}$ *M*. Above $2 \cdot 10^{-3}$ *M* $TDBA^+$, a complex with a larger molar absorptivity

was formed, but the application of this complex to the spectrophotometric determination of chromium(III) was limited by poor reproducibility and by difficulties in phase separation.

The selectivity of the proposed procedure is based on the inert nature of the d^3 electron configuration of the chromium ion. The chromium(III)–PAR complex can be separated from many other metal–PAR complexes, except those of iron, cobalt and nickel, owing to the very large difference in the rate of the substitution reaction of PAR complexes with EDTA. The interferences of iron, cobalt and nickel can be avoided by preliminary extraction of these metal ions with cupferron[13], by means of the difference in the rate of the cupferrate formation at room temperature.

The extractable species, $Cr(R)(HR)_2^-$–$TDBA^+$, has a very large molar absorptivity of $4.7 \cdot 10^4$ in chloroform, which classifies the color reaction as one of the most sensitive available for chromium(III). According to the proposed extraction procedure, in which 50 ml of aqueous solution is extracted with 10 ml of chloroform, the sensitivity (Sandell index) is 0.00022 $\mu g\ Cr^{3+}\ cm^{-2}$ at 540 nm, which is seven times more sensitive than that of the diphenylcarbazide method[21].

SUMMARY

The extraction-spectrophotometric determination of chromium(III) with 4-(2-pyridylazo)-resorcinol (PAR) is described. $PAR(H_2R)$ forms a 1:3 complex with chromium(III) in a boiling acetate buffer solution at pH 5. The complex forms an ion-association compound with tetradecyldimethylbenzylammonium ion $(TDBA^+):Cr(R)(HR)_2^-$–$TDBA^+$ which can be extracted into chloroform, the molar absorptivity being $4.7 \cdot 10^4$ at 540 nm. If EDTA is added as a masking agent after the $Cr(HR)_3$ has been formed, only iron, cobalt and nickel interfere seriously, and the method can be made specific for chromium by a preliminary extraction of these metals with cupferron. The sensitivity of the method is seven times higher than that of the diphenylcarbazide method.

RÉSUMÉ

On décrit une méthode de dosage du chrome(III) par extraction et spectrophotométrie au moyen de 4-(2-pyridylazo)-résorcinol (PAR). $PAR(H_2R)$ donne un complexe 1:3 avec le chrome(III) en solution tampon acétique à pH 5 et à ébullition. Ce complexe forme un composé d'association avec l'ion tétradécyldiméthylbenzylammonium $(TDBA^+):Cr(R)(HR)_2^- - TDBA^+$ qu'on peut extraire dans le chloroforme. Le coefficient d'extinction molaire est $4.7 \cdot 10^4$ à 540 nm. L'EDTA est utilisé comme agent masquant après qu $Cr(HR)_3$ soit formé. Seuls fer, cobalt et nickel interfèrent sérieusement. La méthode peut être rendue spécifique pour le chrome en procédant à une extraction préliminaire de ces métaux au moyen de cupferron. La sensibilité de cette méthode est sept fois supérieure à celle obtenue avec la diphénylcarbazide.

ZUSAMMENFASSUNG

Die extraktions-spektrophotometrische Bestimmung von Chrom(III) mit 4-(2-Pyridylazo)-resorcin (PAR) wird beschrieben. PAR (H_2R) bildet mit Chrom-

(III) in einer siedenden Pufferlösung bei pH 5 einen 1:3-Komplex. Der Komplex bildet eine Ionenassoziationsverbindung mit Tetradecyldimethylbenzylammonium-Ion ($TDBA^+$):$Cr(R)(HR)_2^-$–$TDBA^+$ kann mit Chloroform extrahiert werden; der molare Extinktionskoeffizient beträgt bei 540 nm $4.7 \cdot 10^4$. Wenn nach der Bildung von $Cr(HR)_3$ EDTA als Maskierungsreagenz hinzugefügt wird, stören nur Eisen, Kobalt und Nickel ernsthaft; die Methode wird für Chrom spezifisch, wenn diese Metalle vorher mit Cupferron extrahiert werden. Die Empfindlichkeit der Methode ist siebenmal höher als die der Diphenylcarbazid-Methode.

REFERENCES

1 F. H. Pollard, P. Hanson and W. J. Geary, *Anal. Chim. Acta*, 26 (1959) 20.
2 Y. Shijo and T. Takeuchi, *Jap. Anal.*, 13 (1964) 536.
3 Y. Shijo and T. Takeuchi, *Jap. Anal.*, 14 (1965) 511.
4 T. Yotsuyanagi, K. Goto and Nagayama, *Jap. Anal.*, 18 (1969) 184.
5 T. Takeuchi and Y. Shijo, *Jap. Anal.*, 14 (1965) 930.
6 T. Yotsuyanagi, K. Goto, M. Nagayama and K. Aomura, *Jap. Anal.*, 18 (1969) 477.
7 W. J. Geary and C. N. Larson, *S.A.C. Conference 1965*, Heffer, Cambridge, p. 455.
8 T. Yotsuyanagi, J. Ito and, K. Aomura, *Talanta*, 16 (1969) 1611.
9 L. Sommer and H. Nilockova, *Anal. Chim. Acta*, 27 (1962) 241; R. Belcher, T. V. Ramakrishna and T. S. West, *Talanta*, 9 (1962) 934; P. Pakalns and A. B. Ivanfy, *Anal. Chim. Acta*, 31 (1968) 139, etc.
10 T. Yotsuyanagi, R. Yamashita and K. Aomura, *Jap. Anal.*, 19 (1970) 981.
11 R. Yamashita, T. Yotsuyanagi and K. Aomura, *Jap. Anal.*, 20 (1971) 1282.
12 T. Yotsuyanagi, R. Yamashita and K. Aomura, *Anal. Chem.*, 44 (1972) 1091.
13 J. S. Fritz, M. J. Richard and A. S. Bystroff, *Anal. Chem.*, 29 (1957) 577.
14 L. G. Sillén and A. E. Martell, *Stability Constants of Metal-Ion Complexes*, The Chem. Soc., Burlington House, London, 1964 and its supplement No. 1, 1971.
15 M. Huilićková and L. Sommer, *Collect. Czech. Chem. Commun.*, 26 (1961) 2189.
16 A. Corsini, Q. Fernando and H. Freiser, *Inorg. Chem.*, 2 (1963) 224.
17 A. Corsini, I. M. Yih, Q. Fernando and H. Freiser, *Anal. Chem.*, 34 (1962) 1090.
18 H. Kobara, N. Ishibashi and T. Masuzaki, *Jap. Anal.*, 19 (1970) 467.
19 T. Iwamoto, *Bull. Chem. Soc. Jap.*, 34 (1961) 605.
20 M. Tanaka, S. Funahashi and K. Shirai, *Inorg. Chem.*, 7 (1968) 573.
21 E. B. Sandell, *Colorimetric Determination of Traces of Metals*, Interscience, New York, 2nd Ed., 1950, p. 260.

Analytica Chimica Acta, 67 (1973) 307–315

THE SPECTROPHOTOMETRY AND SOLVENT-EXTRACTION BEHAVIOUR OF IRON(III), VANADIUM(IV AND V) AND TITANIUM-(IV) CHELATES OF 1-(*o*-CARBOXYPHENYL)-3-HYDROXY-3-METHYLTRIAZENE

A. K. MAJUMDAR, B. C. BHATTACHARYYA and B. C. ROY
Department of Chemistry, Jadavpur University, Calcutta-32 (India)
(Received 26th March 1973)

1-(*o*-Carboxyphenyl)-3-hydroxy-3-methyltriazene has been proposed[1] as a reagent for the direct gravimetric determination of titanium in the presence of even niobium and tantalum, in addition to other cations and anions. In this paper, an account of the solvent-extraction behaviour of the iron(III), vanadium-(IV and V) and titanium(IV) chelates of the reagent is given and a spectrophotometric method for the determination of titanium after separation from a large amount of iron and other cations is suggested.

The iron(III) and titanium(IV) chelates

With an ethanolic solution of the reagent, iron(III) forms a green cationic 1:1 complex at pH 1.5–2.0, and an anionic violet 1:2 complex at pH 4.0–9.4. The green complex, which has a molar absorptivity of $1.3 \cdot 10^3$ at 660 nm, obeys Beer's law over the range 1.1–35.8 p.p.m. of iron, whereas the violet complex with a molar absorptivity of $3.6 \cdot 10^3$ at 570 nm, obeys the law over the range 1.1–17.9 p.p.m. of iron. The optimal ranges as evaluated from the standard curves[2] are 8.9–35.8 and 3.9–11.2 p.p.m., respectively.

The golden-yellow titanium(IV) complex on extraction into chloroform at pH 1.0–3.5 shows an absorption maximum at 410 nm. The colour system obeys Beer's law in the range 0.1–7.7 p.p.m. of titanium, the optimal range being 0.8–5.7 p.p.m.; the molar absorptivity is $7.3 \cdot 10^3$.

The titanium chelate can be back-extracted from its chloroform solution into concentrated sulphuric acid when it gives a violet solution, the stability of which depends on the amount of water present in the acid. This violet coloured product which shows maximal absorption at 530 nm, obeys Beer's law from 2.0 to 23.9 p.p.m. of titanium, the optimal range being 3.4–19.2 p.p.m. The molar absorptivity is $2.4 \cdot 10^3$.

The extraction behaviour of the iron(III) complex in chloroform is quite different (see Fig. 2). The green complex is cationic, since it is absorbed by the cation-exchange resin Amberlite IR-120 (NH_4^+-form), whereas the anionic violet complex is absorbed by the anion-exchanger Dowex 1-X 8 (Cl^--form). The green cationic complex has the same absorption maximum and molar absorptivity, irrespective of the anion (*e.g.* Cl^-, SO_4^{2-}, NO_3^-, ClO_4^-) present in solution, and so the anion can be said to be present outside the co-ordination zone. At a

higher pH (*ca.* 2.7), iron(III) reacts with the reagent in aqueous ethanolic medium to produce a bluish-violet colour which is slowly discharged by either of the ion-exchangers; this suggests the formation of an ion-pair type of complex such as $[Fe\,L(H_2O)_3]^+[Fe\,L_2]^-$, where LH_2 is the ligand molecule. The anionic complex, however, is completely extracted between pH 3.0 and 9.0 in chloroform containing n-octylamine.

The violet iron(III) complex isolated from an ammoniacal medium has the formula $NH_4[Fe(C_8H_7O_3N_3)_2]$. The molar conductance of a $1\cdot10^{-3}$ *M* solution in water was found to be 83. The cationic complex formed at a lower pH (*ca.* 1.5) could not be isolated. However, an acid form of the 1:2 complex, $H[Fe(C_8H_7O_3N_3)_2]$, precipitated at that pH. The latter in dimethylformamide solution ($1\cdot10^{-3}$ *M*) had a molar conductance of 66.

The vanadium chelates

The freshly precipitated vanadium(V and IV) complexes of the reagent were partially extracted into chloroform at any pH. Moreover, on back-extraction with 98% sulphuric acid from their chloroform solution, violet complexes with absorption maxima at 550–560 nm for vanadium(V) and 550 nm for vanadium-(IV), which are stable for a few hours, were obtained. The vanadium chelates thus appear to be identical species in strongly acidic solutions. However, two types of vanadium(V) complexes were isolated. The yellow variety is anionic (the molar conductance with a $1\cdot10^{-3}$ *M* solution in water was 88), being absorbed by an anion-exchange resin, and may be formulated as $H[VO(OH)_2(C_8H_7O_3N_3)]$. The apparently black complex is neutral, with the composition $VO_2(C_8H_8O_3N_3)$. Both produce violet solutions in 98% sulphuric acid, with the same absorption maximum at 550–560 nm and a molar absorptivity of 533. The apparently black paramagnetic vanadium(IV) complex, $VO(C_8H_7O_3N_3)$, which after isolation is completely insoluble in chloroform, also produces the same colour in 98% sulphuric acid with a molar absorptivity of 702 at 550 nm, the region of maximal absorption.

EXPERIMENTAL AND RESULTS

Apparatus, reagents and solutions

A Hilger u.v. spectrophotometer with 10-mm glass cells, and a Cambridge pH meter (bench type), were used for measurements of absorbance and pH, respectively. Conductance experiments were made with a Philips PR 9500 conductivity bridge. Magnetic measurements were done in a Gouy balance, with mercury tetrathiocyanato cobaltate(II) as the standard.

Standard solutions of iron(III) chloride, nitrate, sulphate and perchlorate, titanium(IV) sulphate, and ammonium metavanadate were prepared and subsequently diluted to obtain solutions of appropriate strength. The vanadium(IV) solution was obtained by reducing the standard vanadium(V) solution with hydroxyammonium chloride in acidic medium by boiling. The standard solutions of other cations and anions were prepared from analytical-grade reagents.

Absorbance curves for iron(III)

To every 5 ml of a $1\cdot10^{-3}$ *M* solution of iron(III) chloride, were added

5 ml of a $1 \cdot 10^{-2}$ *M* solution of the reagent in ethanol and about 5 ml of water. After suitable adjustment of pH, each of these solutions was transferred quantitatively with an ethanol–water mixture to a 25-ml volumetric flask and diluted to the mark, the alcohol content of the final solution being maintained at 50% (v/v). The pH of the solution was recorded after measuring the absorbance at 400–800 nm of the coloured complex against a reagent blank. The absorbance spectra are shown in Fig. 1. The absorption maximum and the colour intensity of the system remained the same in the pH ranges 1.5–2.0 for the green complex and 4.0–9.4 for the violet complex.

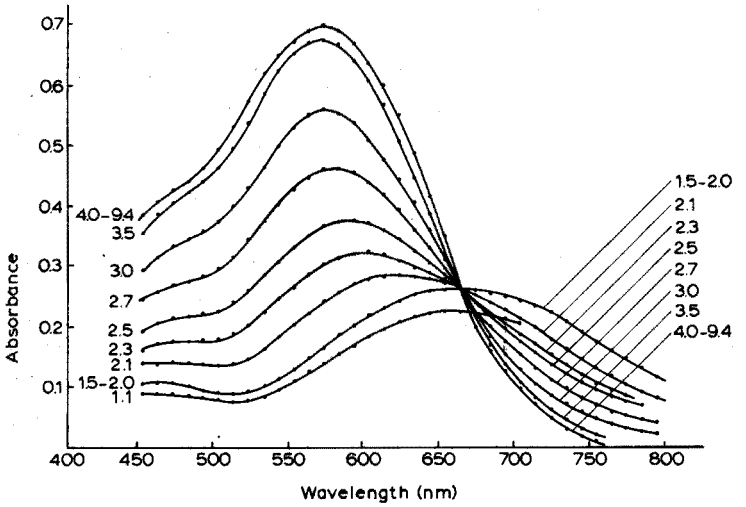

Fig. 1. Absorbance curves of iron(III) chelates at different pH values.

The same experiment was repeated in the pH range 1.5–2.0 with iron(III) nitrate, sulphate and perchlorate solutions; for pH adjustment the corresponding acids and sodium hydroxide solutions were used. The colour intensities and the absorption maxima were the same as before. However, when the metal nitrate and nitric acid solutions were used, the colour system was less stable, probably because of oxidation.

Extraction of iron(III)

For the extraction of the iron(III) complexes in chloroform, the colour was developed at different pH values as stated above, and then the solution (20 ml) was shaken with two 10-ml portions of chloroform. To the aqueous phase, 2 ml of the reagent solution were added, the pH was adjusted to 5.0 and the absorbance was measured at 570 nm after diluting to 50 ml. From this, the amount of the metal ion extracted into the organic layer was calculated (*cf.* Fig. 2).

For extraction in presence of n-octylamine, to 5 ml of a $1 \cdot 10^{-3}$ *M* iron(III) solution, 1 ml of a 2% tartaric acid solution and about 10 ml of water were added, the pH of the solution was adjusted to a certain value, and the

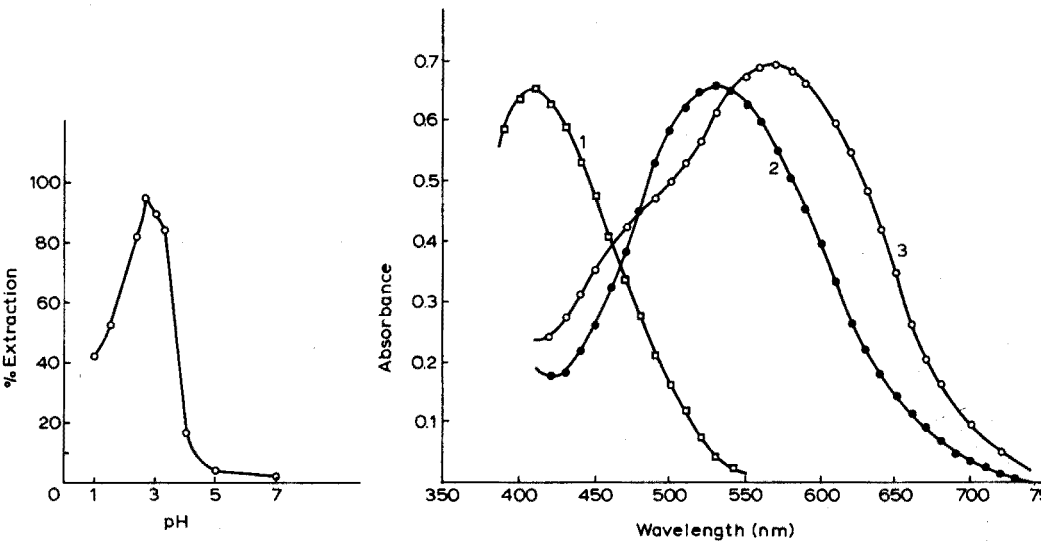

Fig. 2. Extraction of iron(III) chelates in chloroform at different pH values.

Fig. 3. Absorbance curves. (1) Titanium(IV) chelate in chloroform. (2) Titanium(IV) chelate in 98% sulphuric acid. (3) Iron(III) chelate in chloroform–octylamine.

aqueous layer (25 ml) was extracted 2–3 times with 5-ml portions of a $2 \cdot 10^{-2}$ *M* solution of the reagent in chloroform which was also $2 \cdot 10^{-2}$ *M* in n-octylamine. The extracts were collected in a 25-ml flask and diluted to the mark with chloroform. The region of maximal absorption was found to be at 560 nm (Fig. 3, Curve 3) and the colour intensity remained the same between pH 3.0 and 9.0.

Extraction of titanium(IV)

To extract the titanium(IV) complex, 3 ml of a $5 \cdot 10^{-4}$ *M* titanium(IV) solution were mixed with 5 ml of an ethanolic 1% solution of the reagent, 2 ml of a 5% tartaric acid and 10 ml of water. After the adjustment of the pH to a definite value, the solution was heated on a boiling water bath for about 15 min, cooled to room temperature and transferred quantitatively to a separating funnel. About 8 ml of chloroform were added to the beaker to dissolve out completely the adhering complex, which was then added to the separating funnel and shaken. The process was repeated 3 times and the extracts were collected in a 25-ml flask and diluted to the mark with chloroform. The absorbance of the extract was measured against a reagent blank. The region of maximum absorption was found to be at 410 nm (Fig. 3, Curve 1) and the colour intensity remained the same at pH 1.0–3.5.

For back-extraction into concentrated sulphuric acid, the above procedure for the extraction of the titanium complex into chloroform was followed, with 5 ml of $5 \cdot 10^{-4}$ *M* metal solution. The chloroform extract was then shaken thrice, each time with a 5-ml portion of 98% sulphuric acid. A few drops of the reagent solution were added which aided in the complete extraction of the colour. The resultant violet complex with absorption maximum at 530 nm (Fig. 3, Curve

2) was found to be stable for more than 2 h in 98% sulphuric acid. With more dilute acid, though the absorption maximum and the colour intensity remained the same, the coloured product was less stable; in 80% acid the complex was stable only for about 30 min.

The optimal ranges for determination according to Ringbom[2] are shown in Fig. 4.

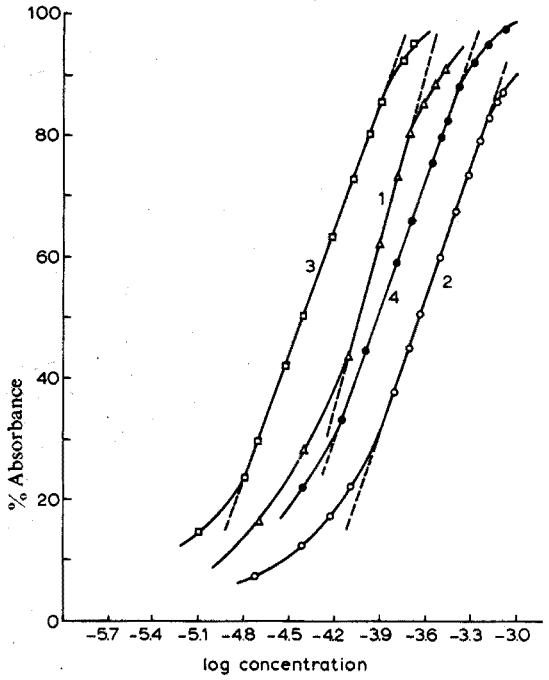

Fig. 4. Standard curves. (1) Iron(III) at higher pH range. (2) Iron(III) at lower range. (3) Titanium(IV) in chloroform. (4) Titanium(IV) in 98% sulphuric acid.
% Absorbance

Composition of the complexes

The compositions of the green and the violet iron complexes were determined by Job's method[3] of continuous variations and also by the mole ratio method[4], and were found to be 1:1 and 1:2, respectively, by both methods. The composition of the titanium complex could not, however, be determined by the above two methods, because the complex was highly dissociated unless a large excess of the reagent was present in the solution.

Effect of various ions

To evaluate the tolerance limits for different ions, 5 ml of a $1 \cdot 10^{-3}$ *M* solution of iron(III), or 3 or 5 ml of a $5 \cdot 10^{-4}$ *M* solution of titanium, respectively, for chloroform and sulphuric acid extractions, were separately mixed with varying quantities of other ions and then the procedures for their determinations were followed as described above.

Tartaric acid, citrate, oxalate (each 500 mg) do not interfere with the iron

system; in presence of an excess of tartaric acid (200 mg), the system then tolerates (in p.p.m.): VO_3^- (100), Co^{2+} (50), Ni^{2+} (100), Mn^{2+} (100), Cr^{3+} (50) and Cu^{2+} (30). The interference of fluoride is eliminated by adding a large excess of beryllium(II). There is no interference from 200 p.p.m. of each of the ions, WO_4^{2-}, MoO_4^{2-}, Ce^{3+}, La^{3+}, lanthanides, Nb^{5+}, UO_2^{2+}, BO_3^{3-}, AsO_3^{3-}, Zr^{4+}, Th^{4+}, Zn^{2+}, Cd^{2+}, Hg^{2+}. However, when Co^{2+}, Ni^{2+}, Cr^{3+} or Mn^{2+} is present, the pH must be adjusted between 4 and 5.

Only Fe^{3+}, Cu^{2+}, Cr^{3+}, VO_3^- and EDTA interfere seriously with the titanium system in chloroform, but the interference of even 200 p.p.m. of Fe^{3+}, Cu^{2+} or Cr^{3+} is eliminated when the chloroform layer is back-extracted into 98% sulphuric acid. No interference was observed from 100 p.p.m. of each of the following ions: Ni^{2+}, Co^{2+}, Mn^{2+}, UO_2^{2+}, Ce^{3+}, Ce^{4+}, MoO_4^{2-}, WO_4^{2-}, $C_2O_4^{2-}$, citrate, La^{3+}, Nb^{5+}, Ta^{5+}, Zr^{4+}, Th^{4+}, PO_4^{3-}, AsO_3^{3-}, F^- (in presence of excess of Be^{2+}), Zn^{2+}, Cd^{2+}, Hg^{2+}, BO_3^{3-}; or from 150 mg of tartaric acid. When the chelate is back-extracted into 98% sulphuric acid, only vanadium(IV) and V) interfere.

Separation procedures

Method A. For the separation of a large amount of iron, the solution (20 ml) containing 0.25–5.0 mg of iron(III) together with 50–125 μg of titanium and 200 mg of tartaric acid, was adjusted to above pH 7.8; then 5 ml of an ammonium chloride–ammonia buffer solution were added. The iron in the solution was extracted repeatedly with 10-ml portions of a 0.5% solution of the reagent in chloroform which was also 0.5% with respect to n-octylamine, until the last portion of the extract was colourless. The pH of the aqueous layer was then lowered to 1.0–3.5, so that the titanium content could be determined at 410 nm by the above procedure.

In this way, 2–5 p.p.m. of titanium could be separated from 200 p.p.m. of iron and determined accurately.

Method B. Alternatively, to a 20 ml of the solution of iron, titanium and tartaric acid, were added 5 ml of an 1% reagent solution in ethanol. After adjusting the pH to 1.0–3.5, the solution was digested on a boiling water bath for 15 min, cooled and extracted 5 times with 10-ml portions of chloroform; both the titanium and a part of the iron were extracted. To eliminate the influence of iron, the titanium from the chloroform phase was back-extracted with three 5-ml portions of 98% sulphuric acid, which were collected in a 25-ml flask, diluted to the mark with the acid. The absorbance at 530 nm was measured as before.

Method C. When a much larger amount of iron (25 mg) was present, it was extracted as in method A, and the titanium after extraction from the aqueous phase into chloroform, was re-extracted with three 5-ml portions of 98% sulphuric acid. The extract was diluted to 25 ml with the acid and the absorbance was measured to determine titanium as above.

When a small quantity of iron (8–10 p.p.m.) was present with a relatively large amount of titanium (100 p.p.m.), the iron content was determined in the aqueous ethanolic medium at pH 4.0–9.4, in the presence of tartaric acid. The separation of this small amount of iron from such a large quantity of titanium was

quite difficult, and because of this, titanium was determined by the sulphuric acid extraction procedure (Method B). Vanadium(IV or V) could not be separated from titanium.

In this connection, it should be mentioned that in a previous communication[5] it was reported that titanium was separated from vanadium by extracting its complex with 1-(*o*-carboxyphenyl)-3-hydroxy-3-phenyltriazene into chloroform at pH 1.0, after reduction of vanadium(V) to vanadium(IV) with hydroxyammonium chloride and subsequent masking with thiocyanate. However, on reinvestigation, it was found that the titanium complex of the reagent was quantitatively extracted into chloroform not at pH 1.0 but at and above pH 1.2. Moreover, the vanadium(IV) complex of the reagent in the presence or absence of thiocyanate was also very slightly extracted at pH 1.0 and the extent of extraction increased with the increasing pH and the amount of vanadium. Therefore, it may be argued that at pH 1.0 the amount of titanium left unextracted in chloroform was compensated by the extraction of a very small amount of vanadium complex.

Preparation of the solid complexes

$H[Fe(C_8H_7O_3N_3)_2]$. Iron(III) chloride hexahydrate (2.7 g) was dissolved in the minimal quantity of 95% ethanol and was then added to a hot ethanolic solution of the reagent (2.0 g). The pH was adjusted to about 1.5, and the solution was digested for a few minutes and then kept overnight. The shining crystals were filtered and washed with ice-cold ethanol and dried in air. (Found: Fe 12.59%, N 18.68%; required: Fe 12.60%, N 18.97%.) The compound (μ_{eff} = 5.91 B.M.) does not melt or decompose upto 320°. It has a molar conductance value of 66 with $1 \cdot 10^{-3}$ *M* solution in DMF. It is very slightly soluble in methanol and chloroform, appreciably soluble in pyridine, but insoluble in benzene.

$NH_4[Fe(C_8H_7O_3N_3)_2]$. To a mixture of the solutions of 2.7 g of $FeCl_3 \cdot 6H_2O$ and 4.0 g of the reagent in absolute ethanol, was added a strong solution of ammonia to make the solution ammoniacal. It was then kept for a few days when deep violet crystals were separated. These were filtered and washed with ice-cold ethanol and dried in the air. (Found: Fe 11.71%, N 21.31%; required: Fe 12.19%, N 21.40%.) The compound decomposes at 220° and has a magnetic moment of 6.02 B.M. It is soluble in water, methanol and pyridine, and slightly so in chloroform, but insoluble in benzene. The molar conductance is 83 with a $1 \cdot 10^{-3}$ *M* solution in water.

$VO(C_8H_7O_3N_3)$. The vanadium(IV) complex was obtained as a green precipitate by adding an ethanolic solution of vanadyl chloride (0.01 mole in 20 ml) to a solution of the ligand (0.01 mole) also in ethanol (50 ml). The compound was filtered, washed with ethanol and dried in the air. (Found: V 20.14%, N 15.83%; required: V 19.60%, N 16.15%.) The compound (μ_{eff} = 1.67 B.M.) does not melt or decompose upto 340°. It is insoluble in methanol, benzene or chloroform, and feebly soluble in hot pyridine. The V=O stretch appears at 995 cm^{-1}.

$H[VO(OH)_2(C_8H_7O_3N_3)]$. Ammonium metavanadate (0.6 g) was dissolved by boiling in about 20 ml of water containing a few drops of ammonia solution

and was then mixed with an ethanolic solution of the reagent (1.0 g in 20 ml). The pH was adjusted to 5.0, the solution was evaporated completely on a boiling water bath, and the solid mass was dissolved in about 30 ml of hot 95% ethanol and kept overnight. The shining yellow crystals which separated were filtered, washed with ice-cold ethanol and dried in air. (Found: V 17.11%, N 13.66%; required: V 17.29%, N 14.24%.) The diamagnetic complex, m.p. 193°, with $\chi_g = -0.474$, is soluble in water and also in ethanol but insoluble in chloroform and benzene. The O–H stretch appears as a doublet at 3077 and 3000 cm^{-1} and the asymmetric stretch of the carboxyl group and V=O stretch are at 1617 and 925 cm^{-1}, respectively.

$VO_2(C_8H_8O_3N_3)$. Ammonium metavanadate (0.6 g) was dissolved in water as stated above and mixed with a solution of the reagent (1.0 g) in 30 ml of acetone. The pH was adjusted to 1.0 and then the solution was evaporated on a boiling water bath. When the crystals began to separate, the solution was cooled and the apparently black crystals were filtered, washed with water and dried in air. (Found: V 18.73%, N 14.31%; required: V 18.40%, N 15.16%.) The complex (m.p. 214°) is slightly paramagnetic ($\chi_{M_{corr}} = 386 \cdot 10^{-6}$ c.g.s. unit) and is slightly soluble in chloroform producing a violet solution and also in water giving a yellow solution. The carboxyl group is free, since its asymmetric stretch is at 1686 cm^{-1}, and the V=O stretch appears to be at 995 cm^{-1}.

SUMMARY

1-(*o*-Carboxyphenyl)-3-hydroxy-3-methyltriazene is proposed as an excellent reagent for the spectrophotometric determination of iron(III) and titanium(IV), and also for the separation of titanium from a large quantity of iron as well as other cations and anions. Iron(III) forms an anionic violet 1:2 complex at pH 4.0–9.4, and a cationic green 1:1 complex at pH 1.5–2.0, with absorption maxima at 570 nm and 660 nm, respectively. The violet complex is quantitatively extracted in chloroform containing n-octylamine at pH 3.0–9.0. The green and the violet iron(III) complexes obey Beer's law, the respective optimal ranges being 8.9–35.8 and 3.9–11.2 p.p.m. The yellow titanium chelate extracted into chloroform (absorption maximum at 410 nm) between pH 1.0 and 3.5, can be re-extracted into concentrated sulphuric acid a violet colour being produced with absorption maximum at 530 nm. Beer's law is obeyed in the ranges 0.8–5.7 p.p.m. for the titanium complex in chloroform and 3.4–19.2 p.p.m. when extracted in concentrated sulphuric acid. Interferences from diverse ions are not severe. Procedures for the separation and determination of titanium in the presence of a large quantity of iron are given. The isolation of the iron(III) and vanadium(IV and V) complexes, and their properties, are described.

RÉSUMÉ

Le 1-(*o*-carboxyphényl)-3-hydroxy-3-méthyltriazène est proposé comme un réactif excellent pour le dosage spectrophotométrique du fer(III) et du titane(IV) et également pour la séparation du titane d'avec de grandes quantités de fer de même que d'avec d'autres cations et anions. Le fer(III) donne un complexe

anionique violet (1:2) à pH 4.0–9.4 et un complexe cationique vert (1:1) à pH 1.5–2.0 avec maximum d'absorption respectivement à 570 et 660 nm. Le complexe violet est quantitativement extrait dans le chloroforme en présence de n-octylamine à pH 3.0–9.0. Ces complexes vert et violet de fer(III) obéissent à la loi de Beer de 8.9 à 35.8 et de 3.9 à 11.2 p.p.m. respectivement. Le chélate jaune du titane est extrait dans le chloroforme avec maximum d'absorption à 410 nm. Il peut être ré-extrait dans l'acide sulfurique concentré en donnant une coloration violette (maximum d'absorption 530 nm). La loi de Beer s'applique de 0.8 à 5.7 p.p.m. (chloroforme) et de 3.4 à 19.2 p.p.m. (acide sulfurique).

ZUSAMMENFASSUNG

1-(*o*-Carboxyphenyl)-3-hydroxy-3-methyltriazen wird als ein ausgezeichnetes Reagenz für die spektrophotometrische Bestimmung von Eisen(III) und Titan(IV) und ebenso für die Abtrennung von Titan von einer grossen Menge Eisen sowie von anderen Kationen und Anionen vorgeschlagen. Eisen(III) bildet einen violetten anionischen 1:2-Komplex bei pH 4.0–9.4 und einen grünen kationischen 1:1-Komplex bei pH 1.5–2.0 mit Absorptionsmaxima bei 570 nm bzw. 660 nm. Der violette Komplex wird bei pH 3.0–9.0 mit einer Lösung von n-Octylamin in Chloroform quantitativ extrahiert. Beide Eisen(III)-Komplexe gehorchen dem Beerschen Gesetz; der optimale Bereich ist 8.9–35.8 p.p.m. beim grünen und 3.9–11.2 p.p.m. beim violetten Komplex. Das zwischen pH 1.0 und 3.5 mit Chloroform extrahierte gelbe Titanchelat (Absorptionsmaximum bei 410 nm) kann mit konz. Schwefelsäure reextrahiert werden, wobei eine violette Färbung mit einem Absorptionsmaximum bei 530 nm entsteht. Die Bereiche der Gültigkeit des Beerschen Gesetzes für den Titankomplex sind 0.8–5.7 p.p.m. in Chloroform und 3.4–19.2 p.p.m. in konz. Schwefelsäure. Störungen durch andere Ionen sind nicht ernsthaft. Arbeitsvorschriften für die Abtrennung und Bestimmung von Titan in Gegenwart einer grossen Menge Eisen werden angegeben. Die Isolierung der Eisen(III)- und Vanadin(IV und V)-Komplexe und deren Eigenschaften werden beschrieben.

REFERENCES

1 A. K. Majumdar, B. C. Bhattacharyya and B. C. Roy, *Anal. Chim. Acta*, 57 (1971) 425.
2 A. Ringbom, *Z. Anal. Chem.*, 115 (1938/39) 332.
3 P. Job, *C. R.*, 180 (1925) 928; *Ann. Chim. (Paris)*, 9 (1928) 113.
4 J. H. Yoe and A. L. Jones, *Ind. Eng. Chem., Anal. Ed.*, 16 (1944) 111.
5 A. K. Majumdar and S. C. Saha, *Anal. Chim. Acta*, 44 (1969) 85.

Analytica Chimica Acta, 67 (1973) 317–323

A NEW SOLVENT EXTRACTION SCHEME FOR THE SEPARATION OF PLATINUM, PALLADIUM, RHODIUM AND IRIDIUM

A. DIAMANTATOS

J.C.I. Minerals Processing Research Laboratory, Knights, Transvaal (South Africa)

(Received 29th March 1973)

The analysis of the platinum-group metals is complicated by the fact that very rarely does only one of them occur in the material to be analyzed. Frequently all six of them, and gold, have to be determined. Therefore, whatever merit a method of separation or determination of individual members of the group may possess, its value will eventually depend on the readiness with which it can be incorporated with other reliable methods into a systematic scheme for the determination of all members individually. Usually, before the determination of each metal, a separation is imperative and the separation step definitely represents the most difficult problem of the analysis, especially in the case of micro amounts. From this point of view, the solvent extraction technique holds a prominent position because of its speed, ease and selectivity. The chemical literature shows basically only two schemes for the separation of platinum, palladium, rhodium and iridium. In the first published paper, Gupta and Beamish[1] combined the methods of Yoe and Kirkland[2] and of Tertipis and Beamish[3] to separate simultaneously platinum and palladium from rhodium and iridium, by extracting the former pair as their diethyldithiocarbamate complexes in the presence of potassium iodide and then separate rhodium from iridium in 1 *M* hydrochloric acid by reduction–precipitation of rhodium with copper powder. In the second paper, Faye and Inman[4] extracted simultaneously the platinum and palladium iodide complexes into tributyl phosphate, thus separating them from rhodium and iridium, and finally separated iridium from rhodium by extracting the former with tributyl phosphate, using a modified method of Wilson and Jacobs[5].

The present author recently[6] showed the potential utility of the 2-mercaptobenzothiazole for the extraction of all the platinum metals.

This paper describes a new solvent extraction scheme for the separation of platinum, palladium, rhodium and iridium by using the above-mentioned thio compound.

EXPERIMENTAL

Apparatus

Spectrophotometric measurements were made with a Carl Zeiss spectrophotometer model PMQ II, and 1-cm quartz cells.

The pH adjustments were made with a Radiometer model pH meter.

Reagents

Standard platinum solution. Johnson-Matthey "Specpure" platinum wire (1 g) was dissolved in aqua regia and the nitrogen compounds were expelled by three evaporations with hydrochloric acid; the solution was standardized gravimetrically by precipitating the platinum with mercury(II) chloride and hypophosphorous acid as follows. An aliquot of the above stock solution, containing *ca.* 50 mg of the metal, was diluted to 200 ml in 1 *M* hydrochloric acid, 10 ml of aqueous 5% (w/v) mercury(II) chloride solution was added, and the solution was brought to the boil. Slowly and while stirring, 5 ml of 4% hypophosphorous acid solution was added, and the solution was simmered for *ca.* 1 h until the black precipitate of platinum and elemental mercury settled, leaving a water-clear supernatant liquid. The precipitate was collected in a No. 40 Whatman filter paper, washed well with hot 10% hydrochloric acid solution and then with hot water, charred and ignited at 800° for 1 h in a platinum crucible. The residue was weighed as pure platinum without any hydrogen reduction treatment.

Standard palladium solution. This solution was prepared by dissolving 0.5 g of "Specpure" palladium wire as described above for platinum. The concentration of the stock solution was determined gravimetrically by the dimethylglyoxime method[8].

Standard rhodium and iridium solutions. The solutions were prepared from Johnson-Matthey ammonium chlororhodite and ammonium chloroiridate "Specpure" reagents, by dissolving them in diluted hydrochloric acid and standardizing them gravimetrically with thiobarbituric acid[9] and 2-mercaptobenzothiazole[10] respectively.

Stock hydrochloric acid solutions of ruthenium, osmium and gold were prepared from "Specpure" ruthenium chloride, osmium tetroxide and gold foil, respectively.

Hydrochloric acid stock solutions of interfering base metals, containing 0.1 mg of test metal per ml were used.

Reagent solution. A 0.5% (w/v) solution of 2-mercaptobenzothiazole (Merck recrystallized reagent) in ethanol was used.

Chloroform was distilled before use.

Separation of platinum and palladium from rhodium and iridium

Evaporate the hydrochloric acid solution containing the platinum metals to incipient dryness in the presence of a few milligrams of sodium chloride. Add 10 ml of concentrated hydrochloric acid and five drops of 20-vol. hydrogen peroxide, and boil for 5 min. Transfer the solution to a 250-ml separatory funnel and dilute to *ca.* 100 ml in 6 *M* hydrochloric acid. Add 10 ml of the 2-mercaptobenzothiazole solution and leave standing for 5 min. Add 1 g of potassium iodide, dissolved in a minimum of water, mix and leave standing for another 5 min. Extract the platinum and palladium complexes simultaneously with 100-ml and 50-ml portions of chloroform after shaking for 4–5 min each time. Keep the aqueous phase for the separation of rhodium and iridium as described below.

Separation of palladium from platinum

Evaporate off the combined chloroform extracts, containing the platinum

and palladium, on a steam bath by blowing air onto the surface of the solvent. Destroy the iodides by boiling with 10 ml of concentrated nitric acid, then add 5 ml of concentrated hydrochloric acid, boil and evaporate to incipient dryness. Add 5 ml of 60% (w/v) perchloric acid and 3 ml of concentrated sulphuric acid, and evaporate to dryness in the presence of a little sodium chloride. Convert the metals to their chloro complexes by boiling with hydrochloric acid. Finally add 10 ml of concentrated hydrochloric acid and 2–3 drops of 20-vol. hydrogen peroxide, and boil for 3–5 min. Cool, transfer the solution to a separatory funnel and dilute to 100 ml with water. Add 3 drops of concentrated nitric acid and then 5 ml of an ethanolic 1% (w/v) solution of dimethylglyoxime. Leave standing for 45 min and extract the yellow palladium complex with three 50-ml portions of chloroform.

Determination of palladium

Evaporate the combined chloroform extracts on a steam bath as described above, add 2 ml of concentrated nitric acid and 5 ml of 60% perchloric acid, boil and evaporate to complete dryness in the presence of a little sodium chloride. Add 10 ml of concentrated hydrochloric acid, 1–2 drops of 20-vol. hydrogen peroxide, boil and evaporate to dryness again. Determine palladium spectrophotometrically by the potassium bromide method[11].

Determination of platinum

Transfer the aqueous phase from the above palladium extraction to a suitable volumetric flask, adjust the acidity to 1 *M* with hydrochloric acid, and determine platinum photometrically by the tin(II) chloride method[12].

Separation of rhodium from iridium

Transfer the aqueous phase after the simultaneous extraction of platinum and palladium to a beaker and evaporate to dryness. Decompose the iodides with concentrated nitric acid and destroy the organic residue with sulphuric acid as usual. To the dry residue add 20 ml of concentrated hydrochloric acid and 4–5 drops of 20-vol. hydrogen peroxide, boil and evaporate to dryness. Finally add 10 ml of concentrated hydrochloric acid and 1–2 drops of 20-vol. hydrogen peroxide, and boil for 2–3 min to decompose the peroxides. Transfer the solution to a separatory funnel and dilute to *ca.* 100 ml with water. Add 10 ml of the 2-mercaptobenzothiazole reagent solution, mix and then add 15–20 drops of 20% (w/v) tin(II) chloride solution and mix again. Leave standing for 30 min and extract the orange rhodium complex with 60-ml and 30-ml portions of chloroform.

Determination of rhodium

Evaporate the combined chloroform extracts and destroy the organic matter first with nitric and then with perchloric and sulphuric acids, as described in the Separation of palladium from platinum. Convert to chloro complexes by boiling with concentrated hydrochloric acid and a few drops of hydrogen peroxide. Pipette an aliquot, containing 0.2–0.3 mg of rhodium, into a 25-ml volumetric flask and determine the metal photometrically by the tin(II) chloride method[13].

Determination of iridium

Transfer the aqueous phase remaining after the extraction of rhodium to a

beaker, and evaporate to dryness. Add 10 ml of concentrated nitric acid and 5 ml of 60% perchloric acid, boil and evaporate to dryness again. Dissolve the residue in 20 ml of concentrated hydrobromic acid by boiling and evaporate to low volume. Dilute to a suitable volume with concentrated hydrobromic acid such that the concentration is *ca.* 8 μg Ir ml^{-1}. Pipette 5 ml of this solution into a 25-ml volumetric flask, and determine iridium photometrically by a modification[4] of the tin(II) chloride–hydrobromic acid method[14].

RESULTS AND DISCUSSION

Extraction of platinum

The addition of potassium iodide to a hydrochloric acid solution of platinum results in the appearance of a pink colour, thus indicating some reaction. If then 2-mercaptobenzothiazole solution is added, a yellow precipitate is formed which is extractable in chloroform. When the order of adding the reagents was reversed, no coloration appeared with the addition of the thio compound and only after the potassium iodide had been added did the yellow precipitate appear.

The platinum solution was transferred to a separatory funnel, and potassium iodide, dissolved in a minimum of water, was added and left to react for 5 min; 10 ml of the reagent solution was then added and the solution left standing again for another 10 min. The yellow precipitate was extracted into chloroform by shaking for 4–5 min. This extraction test was performed at different acid concentrations and with different amounts of potassium iodide, but in all cases with 10 ml of the reagent solution. The aqueous phases were individually analyzed for any unextracted platinum. The experimental data and results are shown in Table I. The results suggest that by using an excess of potassium iodide and avoiding low acid concentrations, a quantitative extraction of platinum can be achieved. The 1–6 *M* hydrochloric acid range concentration, and 1 g of potassium iodide are

TABLE I

PLATINUM EXTRACTION WITH 2-MERCAPTOBENZOTHIAZOLE AND POTASSIUM IODIDE

(1 mg of Pt, 10 ml of 0.5% (w/v) 2-mercaptobenzothiazole, 100 ml of final volume, 100 ml of chloroform)

Molarity, HCl	*KI added (g)*	*Pt extracted (%)*
0.1	0.5	52.3
0.1	2	95.1
0.1	5	>99.8
0.25	2	>99.8
0.5	0.5	83.4
0.5	1	98.0
0.5	2	>99.8
0.5	5	>99.8
1.0	1	>99.8
1.0	2	>99.8
6.0	0.5	>99.8
6.0	2	>99.8

therefore recommended. This extraction test was repeated, but the order of adding the reagents was reversed. The results, however, were almost identical to those indicated in Table I.

Extraction of palladium

Although 2-mercaptobenzothiazole itself forms with palladium a chelate extractable in chloroform[6], the addition of potassium iodide may cause some complications, some palladium iodide, which is insoluble in chloroform, being precipitated. When to a 1 *M* hydrochloric acid solution, containing 1 mg of palladium, 1 g of potassium iodide was added followed by 10 ml of the reagent solution, as described above for the extraction of platinum, a small red skin appeared at the interface between the chloroform and the aqueous phases. The analysis of the insoluble skin showed that some 8–10% of the palladium was retained by the skin, although the rest of the palladium was extracted into chloroform. This test was repeated in a 6 *M* hydrochloric acid solution. This time the skin was much less. For a complete elimination of this drawback, it was thought worthwhile to reverse the order of the addition of the reagents, in order to complex palladium first with the 2-mercaptobenzothiazole before the addition of potassium iodide, thus inhibiting the formation of any insoluble PdI_2. Indeed when this idea was applied to a 1 *M* hydrochloric acid solution, only a thin skin appeared at the interface. Finally when 4–6 *M* solutions were used, excellent and sharp separations were accomplished and not even traces of any skin appeared. Furthermore, on analysis of the aqueous phases, no palladium could be detected, thus confirming the quantitative extraction of palladium from 4–6 *M* hydrochloric acid solutions.

Behaviour of rhodium, iridium, ruthenium, osmium and gold

The above-described extraction procedure for platinum and palladium was applied to the rest of the noble metals separately, at acidities ranging from 0.1 *M* to 6 *M* hydrochloric acid. No rhodium or iridium was found to be extracted. Ruthenium, osmium and gold, however, were partially extracted. This co-extraction is, in fact, of no importance, because ruthenium and osmium are completely volatilized as their tetroxides when the organic residue, containing platinum and palladium, is treated with perchloric acid. Gold, on the other hand, is always easily extracted in advance before the extraction of the platinum metals.

Effect of diverse base metals (Ni, Cu, Fe, Co, Cr, Te)

The extraction procedure involving 2-mercaptobenzothiazole and potassium iodide was carried through with each base metal individually, in 4–6 *M* hydrochloric acid solutions. Ni, Fe, Co and Cr were not extracted but Cu and Te were. Tellurium as well as most of the copper, are eliminated by coextracting them at the beginning while extracting gold by methyl isobutyl ketone from 6 *M* hydrochloric acid solution, as is described below in the analysis of the synthetic solution; moderate amounts of copper, however, have no effect on the colorimetric determination of platinum with tin(II) chloride.

Separation of rhodium from iridium

A study of the extraction of rhodium with 2-mercaptobenzothiazole and

tin(II) chloride into chloroform and its separation from iridium, has been recently published[6]. The results obtained showed that a quantitative extractive separation of rhodium could be accomplished by extracting its complex from 0.25–6 *M* hydrochloric acid solutions.

Application of the proposed scheme in synthetic solutions

Four synthetic solutions containing platinum, palladium, rhodium and iridium at varying ratios, as well as 0.5 mg each of gold, ruthenium and osmium, were prepared from the hydrochloric acid stock solutions. Each solution was evaporated to near dryness in presence of a few milligrams of sodium chloride; 10 ml of concentrated hydrochloric acid and 2–3 drops of 20-vol. hydrogen peroxide were then added and the mixture was boiled for a few minutes. Each solution was transferred to a separatory funnel and made up to 100 ml in 6 *M* hydrochloric acid. Gold was first extracted with methyl isobutyl ketone. The residual solvent dissolved in the aqueous phase was removed by shaking with two 50-ml portions of chloroform and discarding the solvent. The above recommended procedures were then followed for the separation and determination of platinum, palladium, rhodium and iridium. The results (Table II) indicated very satisfactory recoveries in all cases.

TABLE II

ANALYSIS OF SYNTHETIC MIXTURES

Added (mg)				*Recovered (mg)*			
Pt	*Pd*	*Rh*	*Ir*	*Pt*	*Pd*	*Rh*	*Ir*
2.010	1.016	0.256	0.231	2.010	1.016	0.250	0.226
0.502	0.508	0.512	0.462	0.500	0.508	0.512	0.460
0.502	1.016	0.256	0.092	0.502	1.010	0.252	0.090
0.201	0.203	0.512	0.924	0.200	0.201	0.506	0.905

The author acknowledges his indebtedness to the Johannesburg Consolidated Investment Company for permission to publish this work.

SUMMARY

A new scheme is proposed for the separation of platinum, palladium, rhodium and iridium in hydrochloric acid solutions, by solvent extraction. Platinum and palladium are complexed with 2-mercaptobenzothiazole and potassium iodide and simultaneously extracted into chloroform, thus separating them from rhodium and iridium. Palladium is separated from platinum by extracting its dimethylglyoxime complex into chloroform, while rhodium is separated from iridium by extracting its 2-mercaptobenzothiazole complex into chloroform after reduction with tin(II) chloride.

RÉSUMÉ

Un nouveau schéma est proposé pour la séparation platine, palladium,

rhodium et iridium, en milieu acide chlorhydrique, par extraction dans un solvant. Le platine et le palladium sont complexés au moyen de 2-mercaptobenzothiazole et d'iodure de potassium; ils sont ensuite extraits simultanément dans le chloroforme et ainsi séparés d'avec rhodium et iridium. Le palladium est séparé d'avec le platine par extraction de son complexe diméthylglyoxime, dans le chloroforme. Tandis que le rhodium est séparé d'avec l'iridium par extraction de son complexe 2-mercaptobenzothiazole dans le chloroforme, après réduction au chlorure d'étain(II).

ZUSAMMENFASSUNG

Für die Trennung von Platin, Palladium, Rhodium und Iridium in salzsauren Lösungen mittels Extraktion wird ein neues Schema vorgeschlagen. Platin und Palladium werden mit 2-Mercaptobenzothiazol und Kaliumjodid komplexiert und gleichzeitig mit Chloroform extrahiert, wodurch sie von Rhodium und Iridium abgetrennt werden. Palladium wird von Platin abgetrennt, indem es als Dimethylglyoxim-Komplex mit Chloroform extrahiert wird. Rhodium wird von Iridium abgetrennt, indem es nach Reduktion mit Zinn(II)-chlorid als 2-Mercaptobenzothiazol-Komplex mit Chloroform extrahiert wird.

REFERENCES

1 J. G. Sen Gupta and F. E. Beamish, *Anal. Chem.*, 34 (1962) 1761.
2 J. H. Yoe and J. J. Kirkland, *Anal. Chem.*, 26 (1954) 1335.
3 G. G. Tertipis and F. E. Beamish, *Anal. Chem.*, 32 (1960) 486.
4 G. H. Faye and W. R. Inman, *Anal. Chem.*, 35 (1963) 985.
5 R. B. Wilson and W. D. Jacobs, *Anal. Chem.*, 33 (1961) 1650.
6 A. Diamontatos, *Anal. Chim. Acta*, 66 (1973) 147.
7 W. R. Schoeller and A. R. Powell, *The Analysis of Minerals and Ores of the Rarer Elements*, Charles Griffin, London, 3rd Ed., 1955, p. 357.
8 A. I. Vogel, *A Textbook of Quantitative Analysis*, Longmans Green, London, 2nd Ed., 1951, p. 445.
9 J. E. Currah, W. A. E. McBryde, A. J. Cruikshank and F. E. Beamish, *Ind. Eng. Chem., Anal. Ed.*, 18 (1946) 120.
10 R. R. Barefoot, W. J. McDonnell and F. E. Beamish, *Anal. Chem.*, 23 (1951) 514.
11 A. Diamantatos, *Anal. Chim. Acta*, 63 (1973) 220.
12 G. H. Ayres and A. S. Meyer, *Anal. Chem.*, 23 (1951) 299.
13 E. B. Sandell, *Colorimetric Determination of Traces of Metals*, Interscience, New York, 3rd Ed., 1959, p. 769.
14 S. S. Berman and W. A. E. McBryde, *Analyst*, 81 (1956) 566.

Analytica Chimica Acta, 67 (1973) 325–330

SYNERGIC SOLVENT EXTRACTION OF DIVALENT CATIONS WITH DECAFLUOROHEPTANEDIONE AND DI-n-BUTYLSULFOXIDE*

CHARLES A. BURGETT
Hewlett-Packard, Avondale Division, Avondale, Pa. 19311 (U.S.A.)
(Received 28th March 1973)

With the development of the gas chromatography of β-diketonates several methods for the rapid preparation of stable, volatile chelates have been investigated. Solvent extraction has been extensively used for the preparation of β-diketonates; however, when the coordination number of the metal ion exceeds twice the charge, the extraction is usually less than quantitative. The extraction inefficiency is undoubtedly caused by coordination of water molecules which decreases phase partitioning. The formation of hydrated diketonates has been a significant problem in the extraction of the divalent metals, cobalt, iron, nickel and lead. Recently, Mitchell and Banks[1,2] reported the successful solvent extraction of the lanthanides, uranium and thorium utilizing a synergic system incorporating various β-diketones and sulfur and phosphorus bases. Several workers[3–7] have reported the extracted mixed-ligand complexes of the lanthanides, uranium and thorium as thermally stable and considerable gas-chromatographic success has been achieved. Scribner and Kotecki[8] studied the synergic solvent extraction of the divalent transition metals, palladium, copper, nickel, cobalt, zinc and cadmium. They reported quantitative extraction with trifluoroacetylacetone and isobutylamine, but the organic phase was unstable and could not be used after 2 h.

The present paper describes the synergic solvent extraction of iron(II), cobalt(II), nickel(II) and lead(II) with 1,1,1,2,2,6,6,7,7,7-decafluoro-3,5-heptanedione (H(FHD)) and di-n-butylsulfoxide (DBSO) into cyclohexane. The optimal pH, equilibration time, stoichiometry and stability of the extracted species were studied.

EXPERIMENTAL

Instrumentation

A Burrell wrist-action shaker was used for extractions. Analytical data for the extracted species were obtained with a Hewlett-Packard Model 185 CHN analyzer. All pH measurements were made with a Beckman Zeromatic pH meter and an A. H. Thomas 4094-L5 combination electrode.

Reagents

The ligand 1,1,1,2,2,6,6,7,7,7-decafluoro-3,5-heptanedione was synthesized as previously described[6] and was used to prepare stock 0.3 *M* solutions in cyclo-

* Presented in part at the 24th Pittsburgh Conference, 6th March, 1972.

hexane. Di-n-butylsulfoxide (K&K Laboratories) was used without further purification to prepare a stock 0.3 *M* solution in cyclohexane.

Approximately 0.01 *M* solutions of nickel, cobalt and lead were prepared from reagent-grade salts. Solutions *ca.* 0.01 *M* in iron(II) were prepared from reagent-grade iron(II) ammoniumsulfate hexahydrate and used immediately to prevent formation of iron(III).

Aqueous acetate buffers were prepared by mixing 0.2 *M* solutions of sodium acetate and acetic acid. Ionic strength was maintained constant by the addition of sodium chloride.

Extraction procedure

Approximately 0.01 *M* solutions of the cations were prepared by dissolving the appropriate salt in deionized water. The stock solutions were then standardized

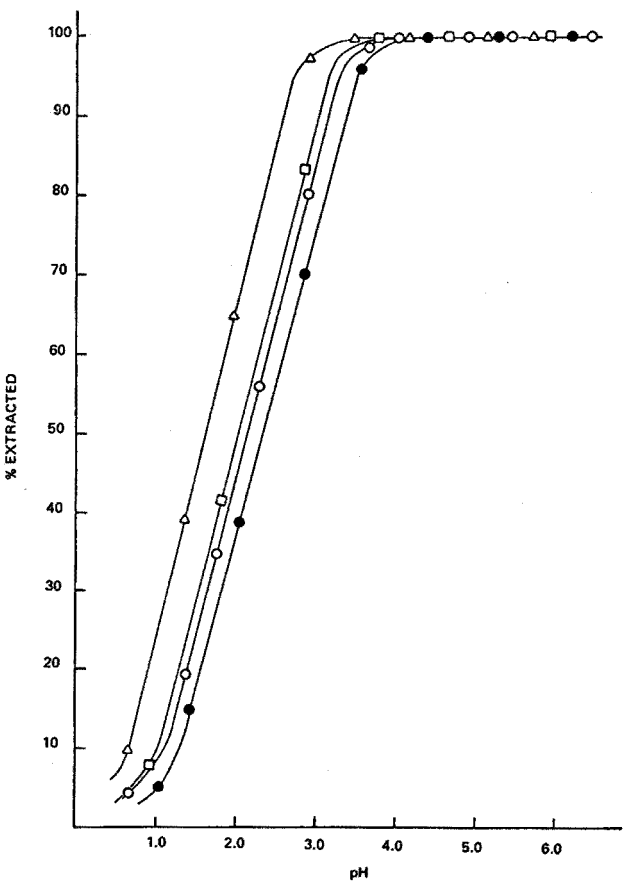

Fig. 1. Extraction of divalent cations with solutions of H(FHD) and DBSO in cyclohexane. (△) Fe; (○) Co; (□) Ni; (●) Pb.

by titration with EDTA, NAS serving as the indicator[9]. Exactly 1.00 ml of the 0.01 *M* metal solutions was pipeted into a 15-ml screw-cap glass test tube. Then 1.00 ml of the appropriate buffer solution was added to each test tube. To each test tube 1.00 ml of a cyclohexane solution of DBSO and 1.00 ml of a cyclohexane solution of H(FHD) was added. The mixture was shaken for 1 h and the phases were allowed to separate. The equilibrium pH of the aqueous phase was measured. A 1.00-ml aliquot of the aqueous phase was removed for determination of the amount of unextracted metal by titration with EDTA as described above.

The organic layers possessed the following colors: the cobalt was wine-red; the nickel was emerald-green; the iron was deep blue; and the lead was colorless.

RESULTS AND DISCUSSION

pH dependence

Results for the extraction of the various metals are presented in Fig. 1. For all of the metals studied, highly efficient extraction occurred at equilibrium pH values of 4.5–6.0. No detrimental effect from the presence of chloride, acetate, sodium or acetic acid was observed.

The extraction was found to be quantitative after equilibration times of 15 min or more. All of the extracted species, except the iron(II) complex, were stable for a period of two weeks and could be dried at 100°. The iron(II) complex was stable after one day at low pH, but at pH 6.0 the complex was stable for one week. As suggested by the change in color of the organic phase, from deep blue to rust, it is probable that decomposition caused by the oxidation of iron(II) to iron(III) occurred.

Characterization of the extracted species

The mass action effect was applied to the H(FHD)–DBSO system in order to determine the exact stoichiometry of the extracted species. A plot of log of the distribution ratio, K_D, *versus* the concentration of H(FHD) is shown in Fig. 2. The slopes approach the value 2, which indicates the formation of a species containing 2 β-diketone molecules. This is necessary for electrical neutrality in the molecule and is expected for divalent metal β-diketonates. The dependence of the distribution ratio on the concentration of DBSO is shown in Fig. 3. The slopes of these plots also approach 2, which indicates the formation of the bis adducts. A bis adduct is consistent with the preferred coordination number of six for these metals, and is in agreement with the results found by Scribner and Kotecki[8]. On the basis of these studies the following equation can be written to describe the extraction process:

$$M^{2+}_{aq} + 2\,H(FHD)_o + 2DBSO_o \rightarrow M(FHD)_2 \cdot 2DBSO_o + 2\,H^+_{aq}$$

The two phases were separated and the organic layer was evaporated. At room temperature the excess of DBSO present from the extraction was not removed by evaporation; it was therefore necessary to heat the samples to 100° for 1 h, in order to obtain a pure solid for microanalysis. No visible decomposition occurred. The analytical results (Table I) confirm the stoichiometry of the extracted species as $M(FHD)_2 \cdot 2DBSO$.

An attempt to extract copper(II) proved interesting. Apparent extraction of

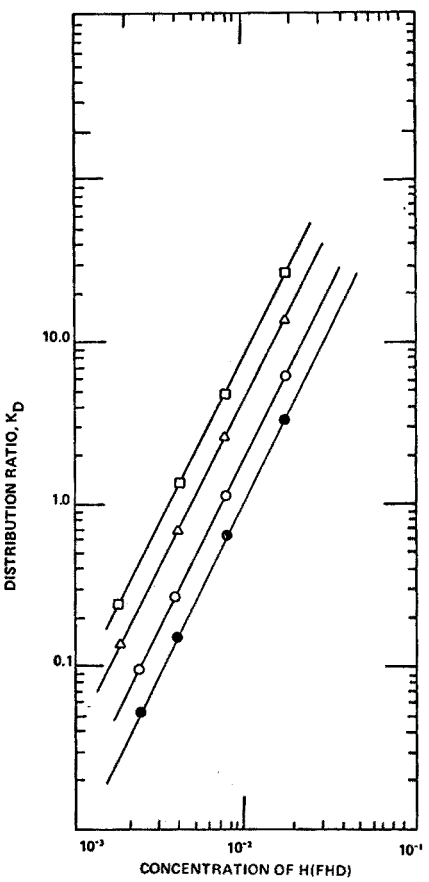

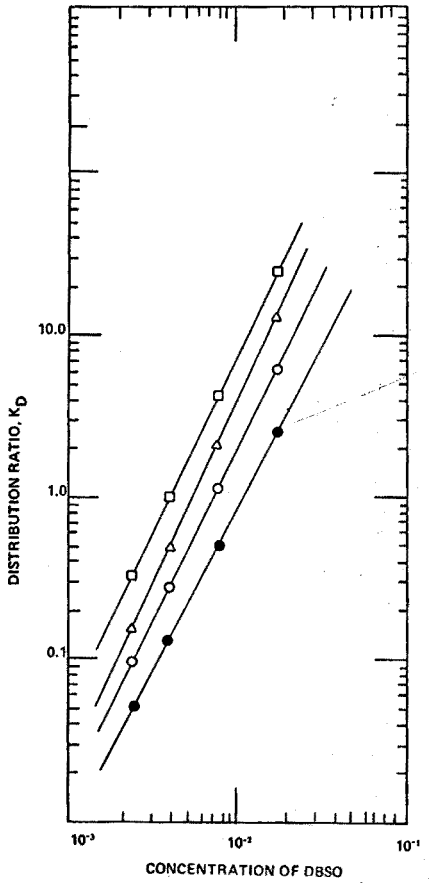

Fig. 2. Dependence of the distribution ratio on the molar concentration of H (FHD). (□) Co; (△) Fe; (○) Ni; (●) Pb.

Fig. 3. Dependence of the distribution ratio on the molar concentration of DBSO. (□) Co; (△) Fe; (○) Ni; (●) Pb.

copper(II) occurred immediately after the addition of H(FHD), as observed by the green color of the organic phase. The addition of DBSO to the system had the effect of improving the extraction, particularly at low pH. Subsequent analysis showed the copper species to be void of DBSO (Table I). In this instance, the DBSO seems to act synergically by aiding the distribution of H(FHD) and the $Cu(FHD)_2$ species without actual formation of an adduct with the copper. Because the copper complex was green, it was expected that the complex would be hydrated, but microanalysis failed to give any indication of the presence of water. In addition, the chelate appeared to be extremely volatile, with significant loss of material evident after heating to 100°. This increased volatility would be expected for a complex which contained no DBSO. The apparent failure of the $Cu(FHD)_2$ complex to form an adduct with DBSO is not consistent with reports in the literature of mono adducts[10,11] and bis adducts[8] and is therefore a subject for further investigation.

TABLE I

ELEMENTAL ANALYSIS OF DIVALENT METAL DECAFLUOROHEPTANEDIONE–DI-n-BUTYLSULFOXIDE ADDUCTS

		Percent	
		Calcd.	*Found*
$Fe(FHD)_2 \cdot 2$ DBSO	C	36.23	37.41
	H	3.85	4.01
$Co(FHD)_2 \cdot 2$ DBSO	C	36.12	36.54
	H	3.84	3.92
$Ni(FHD)_2 \cdot 2$ DBSO	C	36.13	36.48
	H	3.84	3.91
$Pb(FHD)_2 \cdot 2$ DBSO	C	31.44	30.98
	H	3.34	3.47
$Cu(FHD)_2$	C	24.81	25.10
	H	2.98	2.63

Further studies regarding the thermal stability of these mixed-ligand complexes and the application of the extraction system to the preparation of complexes suitable for gas-chromatographic analysis are presently in progress and will be reported later.

SUMMARY

The synergic solvent extraction of iron(II), cobalt(II), nickel(II) and lead(II) with 1,1,1,2,2,6,6,7,7,7-decafluoro-3,5-heptanedione (H(FHD)) and di-n-butylsulfoxide (DBSO), is described. The divalent cations are extracted with 99.9% efficiency at pH 5.5 in extraction times of less than 15 min. The extracted species was shown to be $M(FHD)_2 \cdot 2$ DBSO by mass action studies and elemental analyses. The extraction of copper(II) was also studied. No DBSO adduct was found in the copper extraction.

RÉSUMÉ

On décrit une méthode synergétique d'extraction dans un solvant du fer(II), du cobalt(II), du nickel(II) et du plomb(II) au moyen de décafluoro-1,1,1,2,2,6,6,7,7,7-heptanedione-3,5 (H(FHD)) et de di-n-butylsulfoxyde (DBSO). Les cations divalents sont extraits avec un rendement de 99.9%, à pH 5.5 et des durées d'extraction inférieures à 15 min. La substance extraite correspond à $M(FHD)_2 \cdot 2$DBSO, d'après l'étude d'action de masse et l'analyse élémentaire. L'extraction du cuivre(II) est également examinée. On ne retrouve pas de DBSO dans le produit d'extraction.

ZUSAMMENFASSUNG

Die synergetische Extraktion von Eisen(II), Kobalt(II), Nickel(II) und Blei(II) durch 1,1,1,2,2,6,6,7,7,7-Decafluor-3,5-heptandion (H(FHD)) und Di-n-

butylsulfoxid (DBSO) wird beschrieben. Die zweiwertigen Kationen werden bei pH 5.5 zu 99.9% in Extraktionszeiten von weniger als 15 min extrahiert. Die extrahierte Spezies erwies sich aufgrund von Massenwirkungsuntersuchungen und Elementaranalysen als $M(FHD)_2 \cdot 2DBSO$. Die Extraktion von Kupfer(II) wurde ebenfalls untersucht. Bei der Kupferextraktion wurde kein DBSO-Addukt gefunden.

REFERENCES

1 J. W. Mitchell and C. V. Banks, *Anal. Chim. Acta*, 57 (1971) 415.
2 J. W. Mitchell and C. V. Banks, *Talanta*, 19 (1972) 1157.
3 W. C. Butts and C. V. Banks, *Anal. Chem.*, 42 (1970) 1133.
4 R. F. Sieck and C. V. Banks, *Anal. Chem.*, 44 (1972) 2307.
5 R. F. Sieck, J. J. Richard, K. Iverson and C. V. Banks, *Anal. Chem.*, 43 (1971) 913.
6 C. A. Burgett and J. S. Fritz, *Anal. Chem.*, 44 (1972) 1738.
7 C. A. Burgett and J. S. Fritz, *J. Chromatogr. Sci.*, in press.
8 W. A. Scribner and A. M. Kotecki, *Anal. Chem.*, 37 (1965) 1304.
9 J. S. Fritz, J. E. Abbink and M. A. Payne, *Anal. Chem.*, 33 (1961) 1381.
10 R. D. Gillard and G. Wilkinson, *J. Chem. Soc.*, (1963) 5885.
11 N. C. Li, S. M. Wang and W. R. Walker, *J. Inorg. Nucl. Chem.*, 27 (1965) 2263.

Analytica Chimica Acta, 67 (1973) 331–340

EFFECT OF SOLVENTS AND SUBSTITUENTS ON THE DISTRIBUTION COEFFICIENTS OF ALKYL-SUBSTITUTED β-DIKETONES AND THEIR COPPER CHELATES

HIDEO KOSHIMURA

Tokyo Metropolitan Industrial Technical Institute, Tokyo (Japan)

TEIJI OKUBO

National Chemical Laboratory for Industry, Tokyo (Japan)

(Received 16th May 1973)

Solvent extraction is one of the most widely used separation method of metals[1,2]. The choice of the solvent is as important as that of extractant. Several workers[3–5] have attempted to relate the distribution coefficient to such parameters of the solvent as its dielectric constant, dipole moment and solubility parameter, and to formulate selection rules based on the functional dependence obtained.

It is well known generally that the extent of extraction is much affected by solubility characteristics of chelates in the solvent. The effect of the alkyl chain length on extractive power has been studied for various model systems[6–9].

In the previous paper of this series[10], it was reported that the logarithm of the distribution coefficient of the alkyl-substituted β-diketones and their chelates was a linear function of the number of carbon atoms in the molecule in benzene systems. In this paper, nine alkyl-substituted β-diketones were investigated in order to establish the effects of substituents on the properties of these extractants in other solvents. In addition, the effects of the solvents on the solvent extraction of copper(II) were examined.

EXPERIMENTAL

The alkyl-substituted β-diketones used were acetylacetone (AA), propionylacetylmethane (PrAM), dipropionylmethane (DPrM), di-n-butyrylmethane (DNBM), di-n-valerylmethane (DNVM), di-n-caproylmethane (DNCM), di-isobutyrylmethane (DIBM), pivaloylacetylmethane (PAM) and dipivaloylmethane (DPM). These materials were the same as those used previously[10,11].

The experimental procedures for establishing the distribution ratio of the β-diketone and metal ion were exactly the same as previously described[11]. The distribution ratios of the β-diketones were determined spectrophotometrically; in some cases, the solvent itself absorbed at the wavelength used, and this interference was avoided by using an aqueous solution equilibrated with the same solvent free from β-diketone as a blank.

All solvents were purified by ordinary methods. Redistilled water was used. Other reagents were all analytical-reagent quality. All aqueous solutions and solvents were suitably equilibrated with each other before distribution experiments. All experiments were carried out in a room thermostatted at $20 \pm 1°$.

TABLE I

THE DISTRIBUTION COEFFICIENTS FOR ALKYL-SUBSTITUTED β-DIKETONES

Solvent	δ_o	*log* P_{HA}								
		AA	*PrAM*	*DPrM*	*PAM*	*DNBM*	*DNVM*	*DNCM*	*DIBM*	*DPM*
n-Hexane	7.24	−0.36	0.30	0.96	1.64	2.28	3.59	4.90	2.46	3.78
Cyclohexane	8.18	−0.27	0.38	1.05	1.73	2.36	3.70	5.05	2.65	3.90
Carbon tetrachloride	8.6	0.46		1.32	2.03	2.66	3.95	5.17	2.85	3.97
Toluene	8.91	0.61		1.54	2.11	2.81	4.09	5.40	2.96	3.98
Benzene	9.15	0.65	1.05	1.61	2.18	2.88	4.15	5.46	3.04	3.98
o-Dichlorobenzene	10.0	0.71		1.63	2.16	2.86	4.13	5.43	3.00	3.96
Chloroform	9.3	1.37	1.80	2.23	2.65	3.18	4.46	5.74	3.35	4.02
n-Octanol	10.3	0.14		1.12	1.67	2.23	3.56	4.88	2.22	
Chlorobenzene	9.5	0.72				2.88				
Nitrobenzene	10.0	0.86								
Isoamyl acetate	8.1					2.89				
n-Heptane	7.48					2.25				
n-Hexanol		0.25								

RESULTS AND DISCUSSION

The distribution coefficients of β-diketones

The distribution coefficient, P_{HA}, of a β-diketone is represented by

$$P_{HA} = D_{HA}[(K_a/H^+)+1] \quad (1)$$

where D_{HA} and K_a denote the distribution ratio and the acid dissociation constant of the β-diketone. The distribution coefficients found in various solvents were shown in Table I. The log P_{HA} values increase regularly with the carbon number of the alkyl chain in the β-diketone molecule, but the change is much less pronounced when normal groups are compared with branched ones with the same number of carbon atoms. The log P_{HA} value for each of the β-diketones determined was plotted as a function of the number of carbon atoms in β-diketone molecule. In practice, however, it is well known that β-diketone derivatives undergo keto–enol tautomerism, and that the keto–enol ratio and the enthalpy change in a tautomeric conversion depend to a certain extent on the structure of the β-diketone molecule and also on the solvent environment. Burdett and Rogers[12] have pointed out that β-diketones are principally found in the enol form in inert solvents, since the internal hydrogen-bonded molecule is less polar than the keto molecule. Powling and Bernstein[13] have also pointed out that the proton of solvents such as chloroform or alcohol is bonded with the carbonyl oxygen in β-diketone molecules, so that the amount of the keto form increases. For the alkyl-substituted β-diketones used in this study, the keto–enol ratio[14] and the enthalpy change[15] in a tautomeric conversion were measured in the pure liquid state (Table II). The keto–enol ratio was greatly influenced by the substituents in the β-diketone molecule, and the conversion enthalpy also differed. However, since the keto–enol ratio and the conversion enthalpy for enolization in the pure liquid state were the same for DNBM, DNVM and DNCM, it would be expected that the influence of solvents on the keto–enol ratio would also be the same in each case. The three points of log P_{HA} for DNBM, DNVM and DNCM fall almost on a straight line with slope of 0.61–0.65 as shown in Fig. 1 depending

TABLE II

THE ACID DISSOCIATION CONSTANT, ENOL–KETO RATIO AND CONVERSION ENTHALPY FOR ALKYL-SUBSTITUTED β-DIKETONES[a]

β-Diketone	*pK_a*	*Enol/keto ratio*	*$-\Delta H$ (kcal mol^{-1})*
AA	8.84	4.32	2.7
PrAM	9.11	4.59	2.7
DPrM	9.55	4.00	2.6
DNBM	9.67	11.05	3.2
DNVM	9.72	11.05	3.2
DNCM	9.71	11.05	3.2
DIBM	9.82	22.81	3.9
DPM	11.57	49.00	4.6
PAM	10.00	14.87	3.8

[a] $\ln K = -\Delta H/R(1/T)+C$. K = [enol]/[keto] (ref. 16).

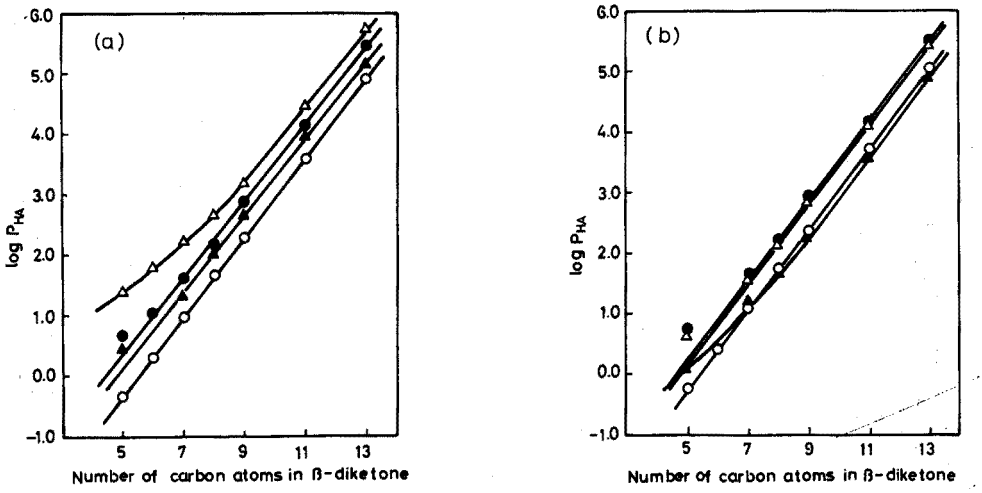

Fig. 1. Correlation between the distribution coefficient of a β-diketone and the number of carbon atoms in its molecule. (a) (○) n-Hexane; (△) chloroform; (▲) carbon tetrachloride; (●) benzene. (b) (▲) n-Octanol; (△) toluene; (○) cyclohexane; (●) *o*-dichlorobenzene.

on the solvents used. The equations of the lines are

$$\log P_{HA} = an + b \tag{2}$$

where P_{HA} is the distribution coefficient of the β-diketone, n is the number of carbon atoms in the molecule, and a and b are constants which depend only on the solvents. The value a can be assumed to be the same for each of solvents.

The distribution coefficients of copper chelates

The distribution ratios of copper were determined at various initial β-diketone concentrations and at different hydrogen concentrations for each of the solvents. The results obtained for various solvents were plotted as log D *vs.* pH or log D *vs.* log HA; straight lines with slopes of 1.9–2.0 were obtained for each of the β-diketones in various solvents. Even when different initial concentrations of β-diketone solutions were used and the pH values differed, straight lines with the same slope were obtained. Consequently, under these experimental conditions, the extractable copper chelate is CuA_2 (A is the anionic species of β-diketone) and there is no adduct formation with the β-diketone. Some typical examples are shown in Figs. 2–4. As can be seen from these Figures, the distribution ratios of these β-diketone chelates increase as the number of carbon atoms in the aliphatic chain increases. From the distribution data for copper(II), the values of the extraction constants, K_{ex}, were calculated; Table III gives these values and the aqueous pH values needed for 50% extraction. In the cases of AA, PrAM and DPrM, the plots deviated from the straight line with the theoretical slope of 2.0. The deviations are assumed to be due to chelate formation in the aqueous phase. Because of these deviations, the extraction constants were obtained by the curve-fitting method[17].

TABLE III

EXTRACTION CONSTANTS AND $pH_{\frac{1}{2}}$ VALUES FOR COPPER CHELATES OF ALKYL-SUBSTITUTED β-DIKETONES

Solvent	*AA*	*PrAM*	*DPrM*	*PAM*	*DNBM*	*DNVM*	*DNCM*	*DIBM*	*DPM*
$-log\ K_{ex}$									
n-Hexane	—	4.02	3.83	4.54	3.83	3.88	3.91	4.26	4.73
Cyclohexane	—	3.95	3.90	4.54	3.96	3.99	4.00	4.23	4.86
Carbon tetrachloride	3.41		4.02	4.15	3.68	3.75	3.74	4.28	5.04
Toluene	3.73		4.23	4.43	3.95	4.02	4.01	4.31	5.21
Benzene	3.60	3.86	4.34	4.44	3.94	3.96	3.92	4.42	5.19
o-Dichlorobenzene	3.30		4.13	4.45	3.96	3.94	3.90	4.52	5.41
Chloroform	2.98	3.62	4.00	4.54	3.96	4.01	3.98	4.89	6.10
n-Octanol	3.10				3.52			4.08	
Chlorobenzene	3.35				3.92				
Nitrobenzene	3.73								
$(pH_{\frac{1}{2}})_{0.1}$									
n-Hexane	—	3.73	3.23	3.27	3.04	2.96	2.92	3.09	3.45
Cyclohexane	—	3.50	3.13	3.27	3.05	3.01	3.00	3.12	3.43
Carbon tetrachloride	3.36		2.97	3.10	2.88	2.88	2.87	3.14	3.52
Toluene	3.48		3.10	3.22	3.05	3.01	3.00	3.12	3.61
Benzene	3.35	3.03	3.17	3.31	2.98	2.98	2.96	3.20	3.60
o-Dichlorobenzene	3.04		3.08		3.02	2.97	2.95	3.26	3.71
Chloroform	2.50	2.82	3.00	3.26	3.02	3.01	3.00	3.40	4.10
n-Octanol	3.08				2.76			3.04	
Chlorobenzene	3.16				2.96				
Nitrobenzene	3.24								

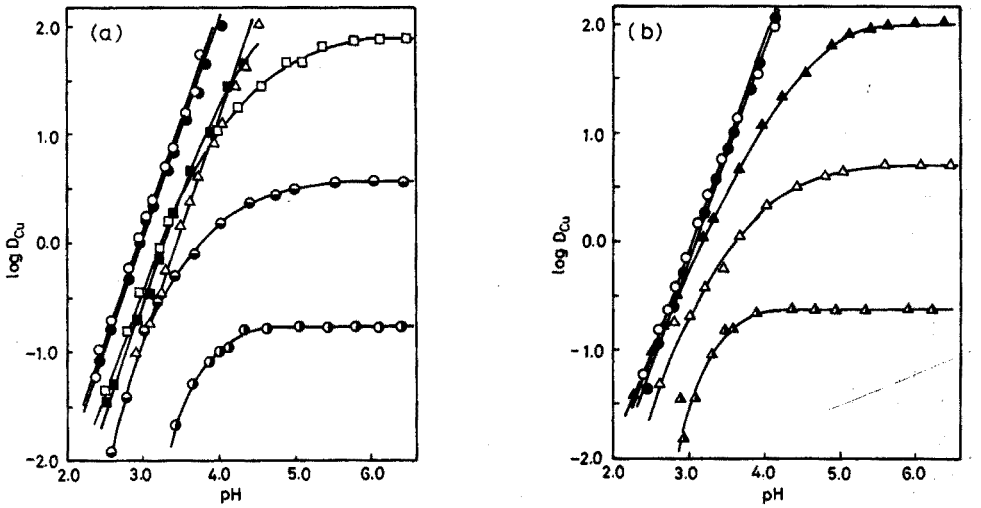

Fig. 2. Distribution ratio of copper as a function of pH. (a) *n-Hexane system.* (○) DNCM, (●) DNVM, (■) PAM, (△) DPM, (□) DPrM, (◒) PrAM, (◑) AA. (b) *n-Hexane system:* (○) DNBM, (●) DIBM; *cyclohexane system:* (▲) AA, (△) PrAM, (▲) DPrM.

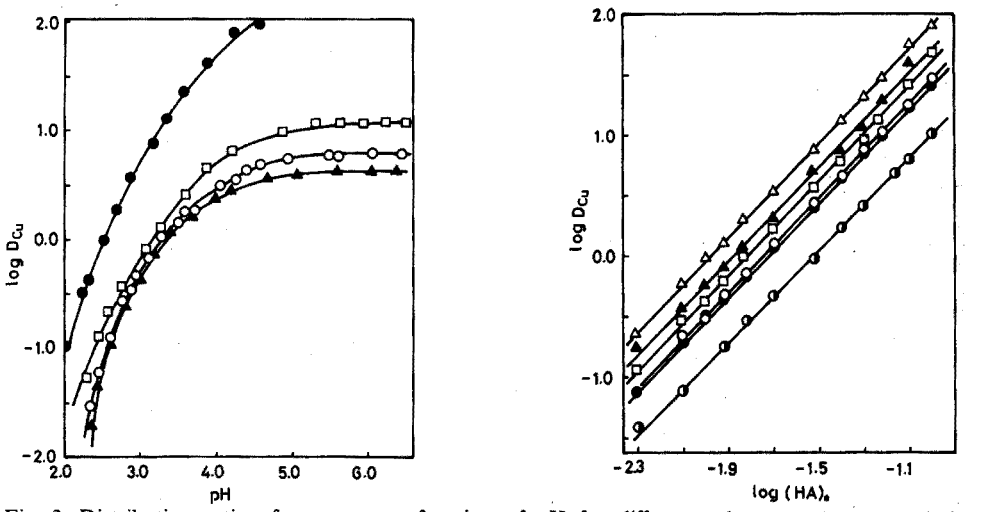

Fig. 3. Distribution ratio of copper as a function of pH for different solvents. *AA system:* (●) chloroform, (▲) carbon tetrachloride, (□) chlorobenzene, (○) benzene.

Fig. 4. Distribution ratio of copper as a function of the concentration of β-diketone. *DNBM system:* (◑) n-hexane (pH 3.50 aqueous phase), (●) chloroform (pH 3.76 aqueous phase), (○) *o*-dichlorobenzene (pH 3.77 aqueous phase), (□) toluene (pH 3.83 aqueous phase), (▲) cyclohexane (pH 3.85 aqueous phase), (△) carbon tetrachloride (pH 3.89 aqueous phase).

The distribution coefficients for the AA chelate in various solvent systems were determined by measuring the limiting distribution ratios in a pH-independent range of the extraction curves. The PrAM and DPrM chelates in n-hexane and cyclohexane systems were also studied. These results are shown in Table IV.

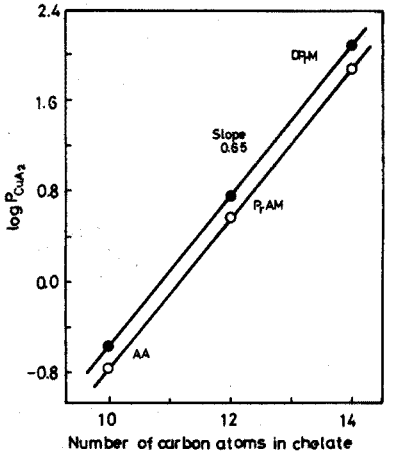

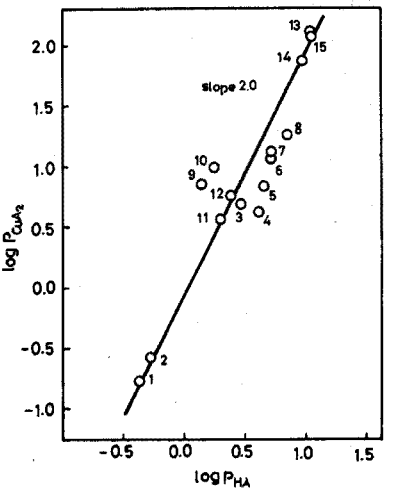

Fig. 5. Correlation between the distribution coefficient for the copper chelate and the number of carbon atoms in the molecule. (○) n-Hexane, (●) cyclohexane.

Fig. 6. Correlation between the distribution coefficients of β-diketones and their copper chelates. Numbered points correspond to entries in Table IV.

TABLE IV

THE DISTRIBUTION COEFFICIENTS AND SOLUBILITY PARAMETERS FOR ALKYL-SUBSTITUTED β-DIKETONES AND THEIR COPPER CHELATES

No.	*β-Diketone*	*Solvent*	*log* P_{HA}	*log* P_{CuA_2}	δ_{HA}[a]	δ_{CuA_2}[b]
1	AA	n-Hexane	−0.36	−0.77	11.36	11.37
2		Cyclohexane	−0.27	−0.57	11.71	11.72
3		Carbon tetrachloride	0.41	0.70	11.38	11.46
4		Toluene	0.61	0.63	11.32	11.54
5		Benzene	0.65	0.85	11.42	11.59
6		*o*-Dichlorobenzene	0.71	1.08	11.59	11.73
7		Chlorobenzene	0.72	1.14	11.41	11.53
8		Nitrobenzene	0.86	1.27	11.39	11.58
9		n-Octanol	0.14	0.85	—	—
10		n-Hexanol	0.25	0.99	—	—
11	PrAM	n-Hexane	0.30	0.57	10.97	10.97
12		Cyclohexane	0.38	0.76	11.29	11.29
13		Benzene	1.05	2.14	11.22	11.20
14	DPrM	n-Hexane	0.96	1.92	10.67	10.67
15		Cyclohexane	1.05	2.08	10.97	10.97

[a] V_{HA} values for AA, PrAM and DPrM from ref. 15.
[b] Calculated as $V_{CuA_2} = 2\ V_{HA}$ (ref. 18).

Table III shows that the extent of the solvent extraction of the copper chelate, as expressed by the value of log K_{ex} or $pH_{\frac{1}{2}}$, does not depend strongly on the nature of the solvent; increases in the distribution coefficients of both the

chelating reagent and the chelate compensate each other. That this is true has been shown by Alimarin and Zolotov[19] in the extraction of coordinatively saturated compounds. However, the chloroform system for AA is capable of extracting copper from solutions of greater acidity than any other, despite the higher value for the distribution coefficient of AA itself.

The distribution coefficient for the copper chelate is extremely large, as shown in Figs. 2–4, and cannot be obtained experimentally. If the effects of the interacting solvent are the same for the chelating reagent and its chelate, the distribution coefficients of the chelate and chelating agent should increase proportionately. Since the pK_a and log K_{ex} values for DNBM, DNVM and DNCM are the same, it would be expected that a linear relationship with a slope of 0.65 would exist between the distribution coefficients of these chelates and the number of carbon atoms in the chelate molecules, as shown previously[10]. This was further confirmed by the correlation between the experimental values for log P_{CuA_2} and the additional carbon atoms of AA, PrAM and DPrM chelate (Fig. 5); the points fall on a straight line with a slope of 0.65 in both the n-hexane and cyclohexane systems. The equation of the straight line is

$$\log P_{CuA_2} = AN + B \tag{3}$$

where N is the number of carbon atoms and A and B are constants which depend on the solvent.

From eqns. (2) and (3), the value a and A can be assumed to be the same for different solutions. Since two molecules of chelating reagent are coordinated in one molecule of the copper(II) chelate, the number of carbon atoms in the chelate molecule is twice that in the reagent molecule. Consequently, the relationship may be written as follows:

$$\log P_{CuA_2} = 2 \log P_{HA} + (B - 2b) \tag{4}$$

where $(B-2b)$ depends on the solvent. In order to confirm this relationship, the log P_{CuA_2} values were plotted against the log P_{HA} values. As shown in Fig. 6, a linear relationship with a slope of *ca.* 2.0 was obtained for the n-hexane and cyclohexane systems. Accordingly, the relationship shown by eqn. (4) is valid in the present systems. It may be considered that the distribution of chelating reagent and chelate are the same, because $(B-2b)$ is almost zero. Further points are that the water content of n-hexane solution[20] is very low in the presence of a metal chelate, and that the solubility of water in cyclohexane solution[21] is of the same order of magnitude as in n-hexane. However, the logarithmic plots for other systems are shifted from the correlation line. The deviations from the slope may be correlated with the interference of the interacting solvent and the amount of water in the solvents.

According to the regular solution theory, the following equations hold for the distribution coefficients of the β-diketone and its chelate[19]:

$$\log P_{HA} = \frac{V_{HA}}{2.30\,RT}(\delta_{aq} - \delta_o)(\delta_{aq} + \delta'_o - 2\delta_{HA}) \tag{5}$$

and

$$\log P_{CuA_2} = \frac{V_{CuA_2}}{2.30\,RT}(\delta_{aq} - \delta_o)(\delta_{aq} + \delta'_o - 2\delta_{CuA_2}) \tag{6}$$

where δ'_o is given by

$$\delta'_o = \delta_o + \frac{RT}{\delta_{aq} - \delta_o}\left(\frac{1}{V_o} - \frac{1}{V_{aq}}\right) \quad (7)$$

where δ_{aq}, δ_o, δ_{HA} and δ_{CuA_2} are the solubility parameters of the aqueous solution, organic solvent, β-diketone and chelate, respectively; V_{HA} and V_{CuA_2} denote the molar volumes of the β-diketone and chelate, respectively.

The right-hand side of eqns. (2) and (3) can be evaluated by the molar volume and the solubility parameter of the solute and the solvent in eqns. (5) and (6), respectively. The values of δ_{HA} and δ_{CuA_2} can be calculated by the procedure of Omori *et al.*[18] from the experimental values of log P_{HA} and log P_{CuA_2}. The results obtained are shown in Table IV. The effect of solvent polarity on the extraction behaviour of the copper chelates roughly parallels that on the β-diketones. The increase in the number of carbon atoms in the copper chelate molecule, which might be expected to decrease polarity, would seem to be compensated by the polar centre of the molecule, resulting in a chelate polarity quite like that of the β-diketone. Further, the molar volume of solute increases with increasing number of carbon atoms in β-diketone and its chelate molecule[15]. It is evident from eqns. (5) and (6) that log P_{CuA_2} is equal to 2 log P_{HA}, assuming that $V_{CuA_2} = 2\ V_{HA}$ and that $\delta_{CuA_2} = \delta_{HA}$. This is in agreement with eqn. (4).

The authors wish to thank Dr. Totaro Goto for his helpful advice.

SUMMARY

The distribution ratios of alkyl-substituted β-diketone derivatives and their copper(II) chelates between water and a number of common water-immiscible solvents were investigated, in order to establish the effect of substituents and solvents on the extraction. A plot of the logarithms of the distribution coefficients of the β-diketones and of their copper chelates as a function of the number of carbon atoms in the molecule, gave a linear relationship. The relationship between the distribution coefficients of the copper chelate (P_{CuA_2}) and those of β-diketone (P_{HA}) was shown to be log $P_{CuA_2} = 2$ log P_{HA} + const.

RÉSUMÉ

Une étude est effectuée sur les coefficients de partage de dérivés alcoylés de β-dicétones et de leurs chélates avec le cuivre(II), utilisant un certain nombre de solvants non miscibles à l'eau. Les logarithmes des coefficients de partage des β-dicétones et de leurs chélates avec le cuivre, en fonction du nombre d'atomes de carbone de la molécule correspondent à une relation linéaire. La relation entre les coefficients de partage du chélate de cuivre (P_{CuA_2}) et ceux de la β-dicétone (P_{HA}) correspond à log $P_{CuA_2} = 2$ log P_{HA} + const.

ZUSAMMENFASSUNG

Die Verteilungsverhältnisse von alkyl-substituierten β-Diketon-Derivaten und

deren Kupfer(II)-Chelaten zwischen Wasser und einer Anzahl von üblichen, mit Wasser nicht mischbaren Lösungsmitteln wurden untersucht, um den Einfluss von Substituenten und Lösungsmitteln auf die Extraktion festzustellen. Bei der Auftragung der Logarithmen der Verteilungskoeffizienten der β-Diketone und der Kupfer-Chelate als Funktion der Zahl der Kohlenstoffatome im Molekül wurde eine lineare Beziehung erhalten. Die Beziehung zwischen den Verteilungskoeffizienten des Kupfer-Chelates (P_{CuA_2}) und jenen des β-Diketons (P_{HA}) wurde wiedergegeben durch die Gleichung $\log P_{CuA_2} = 2 \log P_{HA} + \text{const.}$

REFERENCES

1 G. H. Morrison and H. Freiser, *Solvent Extraction in Analytical Chemistry*, J. Wiley, New York, 1957.
2 J. Starý, *The Solvent Extraction of Metal Chelates*, Pergamon Press, Oxford, 1964.
3 D. E. Noel and C. E. Meloan, *Sep. Sci.*, 7 (1972) 75.
4 E. M. Kuznetsova, G. M. Panchenkov and T. V. Klinovskaya, *Russ. J. Phys. Chem.*, 44 (1970) 1258.
5 H. A. Mottola and H. Freiser, *Talanta*, 13 (1966) 55.
6 I. Kojima, M. Uchida and M. Tanaka, *J. Inorg. Nucl. Chem.*, 32 (1970) 1333.
7 A. S. Kertes and Y. Marcus (Editors), *Proc. Int. Conf. Solvent Extr. Chem.*, Wiley-Interscience, New York, 1968, p. 59.
8 O. E. Zvyagintsev, Yu. G. Frolov, Ch. Chin-pang and A. V. Volkov, *Zh. Neorg. Khim.*, 10 (1965) 981.
9 B. Tremillon, *Bull. Soc. Chim. Fr.*, 10 (1964) 57.
10 H. Koshimura and T. Okubo, *Anal. Chim. Acta*, 55 (1971) 163.
11 H. Koshimura and T. Okubo, *Anal. Chim. Acta*, 49 (1970) 67.
12 J. L. Burdett and M. T. Rogers, *J. Amer. Chem. Soc.*, 86 (1964) 2105.
13 J. Powling and H. J. Bernstein, *J. Amer. Chem. Soc.*, 73 (1951) 4353.
14 H. Koshimura, J. Saito and T. Okubo, *Bull. Chem. Soc. Jap.*, 46 (1973) 632.
15 H. Koshimura, submitted to *Jap. Anal.*
16 L. W. Reeves, *Can. J. Chem.*, 35 (1957) 1351.
17 T. Sekine and D. Dyrssen, *J. Inorg. Nucl. Chem.*, 29 (1967) 1475.
18 T. Omori, T. Wakahayasi, S. Oki and N. Suzuki, *J. Inorg. Nucl. Chem.*, 26 (1964) 2265.
19 I. P. Alimarin and Y. A. Zolotov, *Talanta*, *9* (1962) 891.
20 J. R. Ferraro and T. V. Healy, *J. Inorg. Nucl. Chem.*, 24 (1962) 1463.
21 C. Black, G. G. Joris and H. S. Taylor, *J. Chem. Phys.*, 16 (1948) 537.

Analytica Chimica Acta, 67 (1973) 341–347

THE SIMULTANEOUS DETERMINATION OF THE STABILITY CONSTANTS OF PROTONATED AND UNPROTONATED COMPLEXES IN SOLUTION

H. S. DUNSMORE and D. MIDGLEY
Chemistry Department, The University, Glasgow G12 8QQ (Scotland)
(Received 7th February 1973)

The determination of stability constants in systems such as tartrate and citrate, where protonated complexes co-exist to a significant extent with unprotonated complexes, is not possible by explicit mathematical manipulation, if the data comprise only the pH and the overall composition of the solution. The constants may be obtainable by means of iterative techniques, and computer programs such as LETAGROP[1] and GAUSS G[2] can calculate stability constants, given a set of initial estimates of the true values. The need for such initial values, and for a check on the final values, justifies the existence of programs of more restricted applicability, simpler in form and quicker in operation. The program described in this paper deals with the case where the principal 1:1 complex, MA, co-exists with the most likely related species, *i.e.*, the next higher complex in the series, MA_2, and the protonated complex, MHA. Other methods of dealing with the protonation of complexes have been discussed by Rossotti and Rossotti[3] and Beck[4]; Irving and Stacey[5] and Rossotti and Whewell[6] have used computers for iterative methods of calculation.

Unlike the above-mentioned programs, the proposed program has provision for calculating activity coefficients, and thus for obtaining constants from titration data when the ionic strength is not kept constant. Copies of the program are available from the authors on request.

CALCULATION

A solution contains a salt, MY_m, and a dibasic acid, H_2A, with the addition of a strong acid, HX, and/or a strong base, BOH. The total concentrations of these components are T_M, T_A, T_S and T_B, respectively. The positive charge on the metal ion is m and the negative charge on the ligand is n. The known dissociation constants of the acid are

$$K_1 = \{H\}\{HA\}/\{H_2A\} \quad \text{and} \quad K_2 = \{H\}\{A\}/\{HA\}.$$

(For convenience, the charges have been omitted from the symbols for ionic species.) The stability constants to be determined are

$$\beta_{101} = \frac{\{MA\}}{\{M\}\{A\}}, \quad \beta_{102} = \frac{\{MA_2\}}{\{M\}\{A\}^2} \quad \text{and} \quad \beta_{111} = \frac{\{MHA\}}{\{M\}\{H\}\{A\}}$$

It is convenient to define the constant

$$\beta^{H} = \beta_{111} \cdot K_2 = \frac{\{MHA\}}{\{M\}\{HA\}}$$

The following treatment holds for titrations in constant ionic media if the activity coefficients are set equal to unity. Stoicheiometric stability constants are then obtained. The mass and charge balance equations are

$$T_M = [M] + [MA] + [MA_2] + [MHA] \quad (1)$$

$$T_A = [A] + [HA] + [H_2A] + [MA] + 2[MA_2] + [MHA] \quad (2)$$

$$m[M] + (m-n)[MA] + (m-2n)[MA_2] + (m+1-n)[MHA] + [H] + [B] = [X] + [Y] + [OH] + n[A] + (n-1)[HA] + (n-2)[H_2A] \quad (3)$$

Combination of eqns. (1)–(3) yields a function

$$Z = nT_A - T_B - [H] + [OH] + T_S = [HA] + 2[H_2A] + [MHA]$$

Hence,

$$[HA] = Z \Big/ \left(1 + \frac{2[HA]f_{HA}}{K_1 \cdot f_{H_2A}} + \beta^{H}[M]\frac{f_M \cdot f_{HA}}{f_{MHA}}\right) \quad (4)$$

Activity coefficients are calculated from the equation

$$-\log f_z = A \cdot z^2 \left(\frac{I^{\frac{1}{2}}}{1 + B \cdot a \cdot I^{\frac{1}{2}}} - b \cdot I\right) \quad (5)$$

where z is the charge on the ion, A and B are the parameters of the Debye–Hückel equation and a and b are adjustable parameters.

If eqn. (4) is to be solved for [HA], the activity coefficients, [M] and β^{H} must be known. Initially, these quantities must be approximated and then improved by iteration. β^{H} may be estimated by analogy with literature values for similar complexes, or, ignoring the species MA_2, calculated roughly by methods such as that of Nancollas[7] for simpler systems. A starting value $I = mT_M + T_B$ is taken for the ionic strength. [M] may be set to zero or any more realistic figure for which there are grounds. With the above assumptions, an approximate [HA] can be calculated, and [A] and $[H_2A]$ obtained from the acid dissociation constants.

We can now define the function

$$V = T_A - [A] - [HA] - [H_2A]$$

and set up the functions

$$y = \frac{(V - [MHA])f_{MA_2}}{[A]^2 f_A^2 f_M (2T_M - V - [MHA])}$$

and

$$x = \frac{(T_M - V)f_{MA_2}}{[A] f_A f_{HA} (2T_M - V - [MHA])}$$

which have the property that $y = \beta_{101}x + \beta_{102}$.

The functions x and y are analogous to those obtained by Gelles and Nancollas[8] for the case where no MHA complex is formed, and reduce to the Gelles and Nancollas functions when $\beta_{111}=0$. The stability constants β_{101} and β_{102} are obtained from the slope and intercept, respectively, of a plot of y against x.

The values of [A] and the stability constants are substituted in eqn. (1) and a new value of [M] is obtained, with which the above process is repeated from eqn. (4) onwards. When values of β_{101} and β_{102} are reproduced to within 0.1% in successive cycles, iteration stops. If activity coefficients are to be calculated, an improved estimate of the ionic strength is now available; the new activity coefficients are substituted in eqn. (4), and the whole process started again. This doubly cyclic procedure is repeated until consistent values of β_{101}, β_{102} and I are achieved at the end of both cycles. The process is shown diagrammatically in Fig. 1.

The accuracy of the above procedure depends on the closeness of the estimated value of β^H to the true value. A poor estimate results in a curved plot of y against x (Fig. 2), the shape of the curve depending on whether the estimate was high

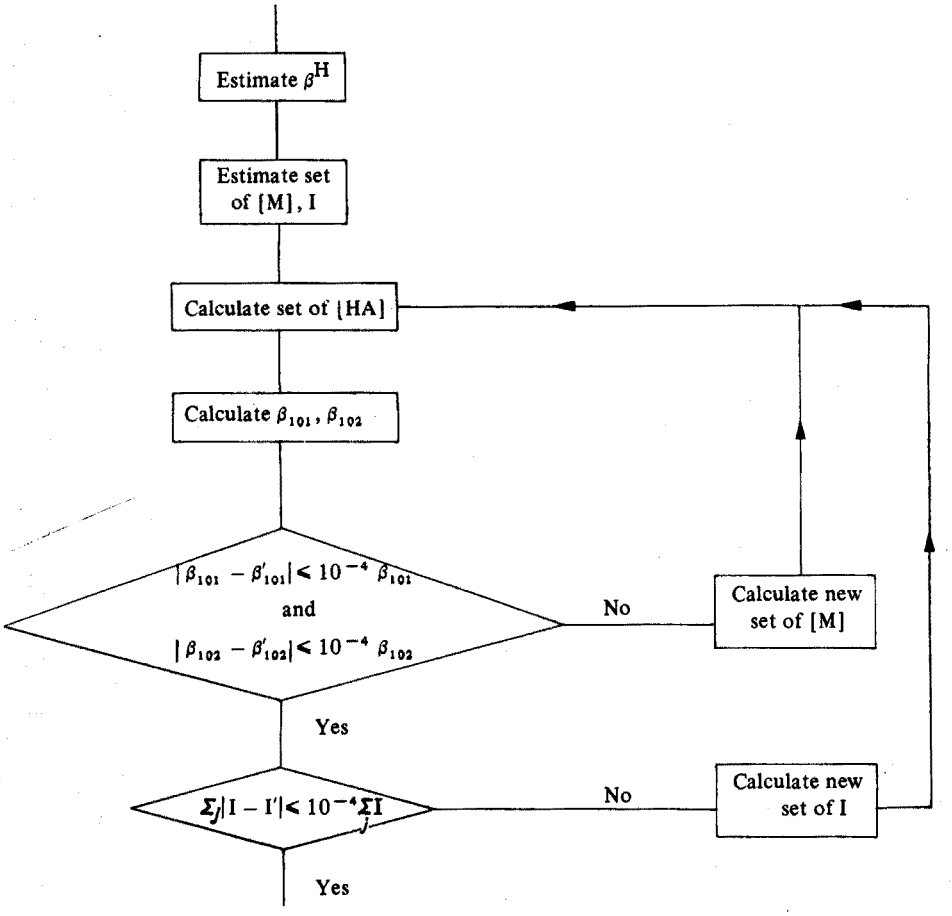

Fig. 1. Flow diagram for program.

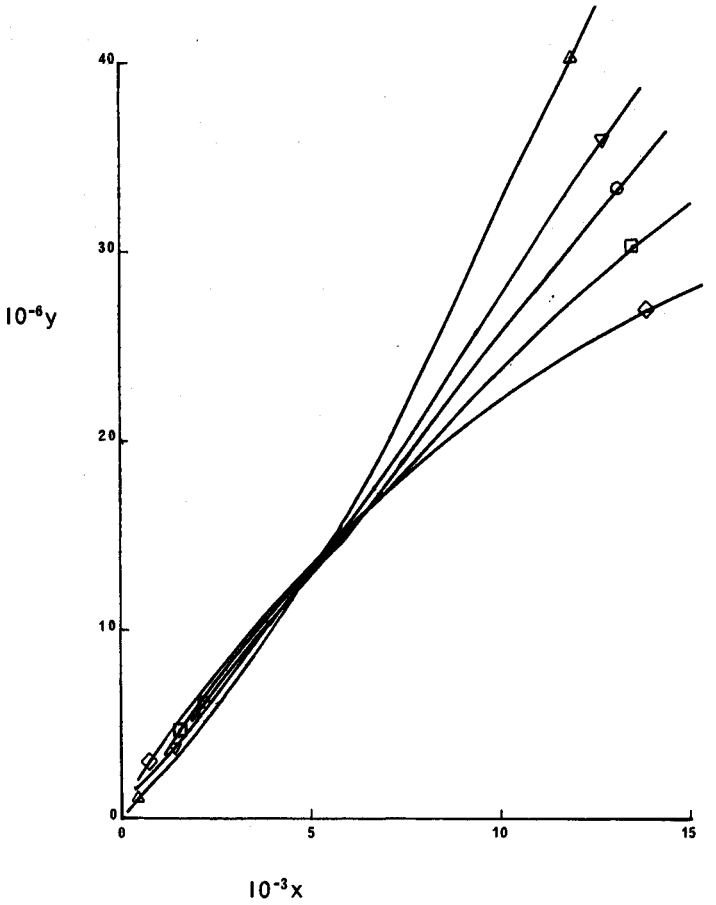

Fig. 2. Variation in x–y plot depending on initial estimate of β_H. (△) 50, (▽) 150, (○) 200, (□) 250, and (◇) 300.

or low. The extent of the curvature can be used to correct the estimate of β^H as outlined below.

As a test for curvature the points are fitted to a second-order equation

$$y = a + bx + cx^2$$

by the method of least squares. (Since the "linear" equation has already been fitted, this involves relatively little extra calculation.) Corresponding to each experimental value of y, there are two obtained by substituting for x in both the first- and second-order equations. The sums of the squares of the deviations between calculated and experimental values of y are calculated for both the first- and second-order fits. If these two quantities agree within a prescribed limit, the first-order line is taken to be a "good" one, and the value of β^H used in the calculation is assumed to be a "good" value; otherwise β^H is adjusted as follows.

The second-order curve is tested for the direction of its deviation from linearity, by comparing the area under the curve (calculated from the integral of the

second-order fit) with the area under the straight line between its extremities. The algebraic difference between these two areas is designated D_i, where

D_i = (area under curve) − (area under line) for the ith value of β^H tried. If D_i is negative, β^H is increased by a given proportion, say 10%, and conversely if it is positive. The new β^H value is substituted in eqn. (4) and values of β_{101} and β_{102} are calculated as before. This procedure is repeated until two successive differences, D_j and D_k, are of opposite sign, when a new value β^H_{k+1} is assigned by means of the equation

$$\beta^H_{k+1} = \beta^H_k \left(1 - \frac{D_k}{|D_j - D_k|}\right) \tag{6}$$

Alternatively, β^H_{k+1} may be set equal to the arithmetic or geometric mean of the jth and kth values.

The calculation is again carried through from eqn. (4) onwards, new values of β^H being determined by eqn. (6), where D_j and D_k are the least negative and least positive values (or *vice versa*) of D_i so far obtained. Iteration continues in this way until a "good" value of β^H is attained, as defined above.

The standard deviations of β_{101} and β_{102} are calculated from the least-squares fit and are printed out. The last high and low values of β^H are also printed out.

RESULTS

In a recent study[9] of lanthanum–tartrate complex formation in acidic solution, it was concluded that the data could be satisfactorily interpreted in terms of three complexes—$LaTar^+$, $La(Tar)_2^-$ and $LaHTar^{2+}$. This conclusion was reached after testing for other complexes both by specific calculation and by use of the general program GAUSS G[2]. The results obtained by this method and by GAUSS G are compared for several runs at 25° and different ionic strengths in Table I. The ionic strength was maintained with tetramethylammonium chloride. It made no

TABLE I

COMPARISON OF RESULTS BY THE PRESENT METHOD AND BY GAUSS G FOR LANTHANUM–TARTRATE COMPLEXES AT 25°

Run	*Present method*			*GAUSS G*		
	$\log \beta_{101}$	$\log \beta_{102}$	$\log \beta_{111}$	$\log \beta_{101}$	$\log \beta_{102}$	$\log \beta_{111}$
A[a]	3.72	6.47	6.56	3.73	6.38	6.53
B[a]	3.65	6.26	6.36	3.66	6.27	6.40
C[b]	3.40	5.70	6.23	3.40	5.73	6.24
D[b]	3.41	5.71	6.20	3.42	5.68	6.20
E[c]	3.08	5.58	5.88	3.09	5.49	5.85
F[c]	3.15	5.70	5.92	3.16	5.76	6.01

[a] $I = 0.1$.
[b] $I = 0.2$.
[c] $I = 0.4$.

difference whether the initial estimate of β^H was high or low, nor whether the first value of [M] was 0.0 or a more realistic estimate.

Figure 3 shows a plot of points taken from 4 runs at each of 15, 25 and 35°. The ionic strength was not kept constant in these runs, the extremes being $I=0.0045$ and $I=0.013$.

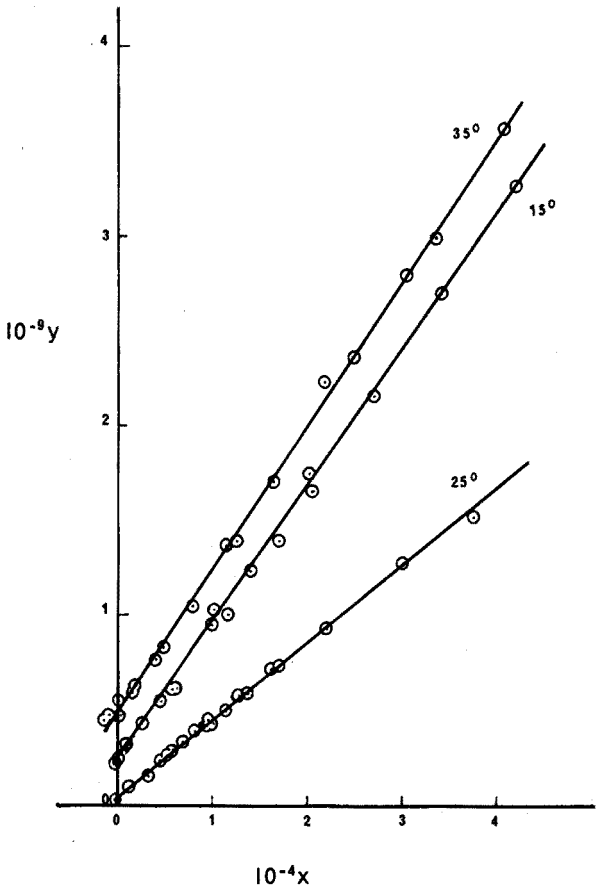

Fig. 3. x–y plots for lanthanum–tartrate complex formation. Allowance was made for ionic strength variation. Line for 15° is displaced 1 cm upwards and that for 35° 2 cm upwards.

DISCUSSION

The agreement between the results calculated by GAUSS G and those obtained by the present method shows that the simpler program can usefully be applied to systems of complexes such as that described here. Figure 3 shows that consistent results can be obtained for runs at different ionic strengths when activity coefficients are calculated by means of eqn. (5), so that the range of application of the program extends into regions not covered by established programs such as GAUSS G.

SUMMARY

A method is given for the simultaneous calculation of the stability constants of complexes of the type, MA, MA_2, MHA, given the overall composition of the solution and the pH. Iterative calculation of activity effects enables constants to be obtained when the ionic strength is not kept constant.

RÉSUMÉ

Une méthode est décrite, permettant de calculer simultanément les constantes de stabilité des complexes du type MA, MA_2 et MHA, connaissant les concentrations totales du métal et du complexant, ainsi que le pH de la solution. Un calcul itératif des coefficients d'activité permet de déterminer les constantes de stabilité, lorsque la force ionique n'est pas constante.

ZUSAMMENFASSUNG

Es wird eine Methode für die gleichzeitige Berechnung der Beständigkeitskonstanten von Komplexen des Typs MA, MA_2 und MHA angegeben, für den Fall dass die Gesamtkonzentrationen des Metalls und des Komplexbildners und der pH-Wert der Lösung bekannt sind. Durch die iterative Berechnung von Aktivitätskoeffizienten, kann man Konstanten erhalten, wenn die Ionenstärke nicht gleich bleibt.

REFERENCES

1 L. G. Sillén, *Acta Chem. Scand.*, 16 (1962) 159; 18 (1964) 1085; N. Ingri and L. G. Sillén, *Acta Chem. Scand.*, 16 (1962) 173; *Ark. Kem.*, 23 (1964) 97.
2 R. S. Tobias and M. Yasuda, *Inorg. Chem.*, 2 (1963) 1307.
3 F. J. C. Rossotti and H. Rossotti, *The Determination of Stability Constants*, McGraw-Hill, New York, 1961, p. 398.
4 M. T. Beck, *Chemistry of Complex Equilibria*, Van Nostrand Reinhold, London, 1970, p. 145.
5 H. M. N. H. Irving and M. H. Stacey, *J. Chem. Soc.*, (1961) 2019.
6 F. J. C. Rossotti and R. J. Whewell, *Proc. Third Symposium on Co-ordination Chemistry, Debrecen, 1970*, Vol. 1, Akadémiai Kiadó, Budapest, 1970, p. 233.
7 G. H. Nancollas, *Interactions in Electrolyte Solutions*, Elsevier, Amsterdam–New York–London, 1966.
8 E. Gelles and G. H. Nancollas, *Trans. Faraday Soc.*, 52 (1956) 98.
9 H. S. Dunsmore and D. Midgley, *J. Chem. Soc. (Dalton)*, (1972) 1138.

Analytica Chimica Acta, 67 (1973) 349–355

ANALYTICAL USES OF SOME N-NITROSO-N-ALKYL (OR -N-CYCLOALKYL)HYDROXYLAMINES

PART I. N-NITROSO-N-CYCLOHEXYLHYDROXYLAMINE

F. BUSCARÓNS and J. CANELA

Department of Analytical Chemistry, Faculty of Sciences, University of Barcelona, Barcelona (Spain)

(Received 21st March, 1973)

Recent studies in this Department have concentrated on the N-nitroso-N-alkylhydroxylamines or -N-cycloalkylhydroxylamines, such as N-nitroso-N-cyclohexylhydroxylamine, N-nitroso-N-cyclooctylhydroxylamine, N-nitroso-N-cyclododecylhydroxylamine and N-nitroso-N-isopropylhydroxylamine, as analytical reagents. Their reactions with different ions, their analytical uses and structural effects have been studied. The present paper reports the results obtained with the sodium salt of N-nitroso-N-cyclohexylhydroxylamine (I), which may be called "hexahydrocupferron", for it has the same reactive functional groups as cupferron (ammonium salt of N-nitroso-N-phenylhydroxylamine); this reagent forms inner complexes of type (II).

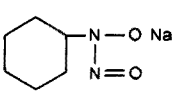

(I)

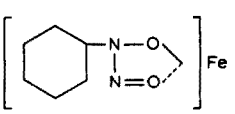

(II)

The preparation of this substance has been described[1], and its analytical properties are discussed below.

Stability of the reagent

Cupferron is stable even as a solid only if it is stored in the dark with a stabilizer such as ammonium carbonate, and its solutions, especially in acidic media, rapidly become yellow. Hexahydrocupferron, however, does not need stabilizers in the solid state (stored in the dark, it does not show the 685 cm^{-1} band of bis-nitrosocyclohexane), and its solutions do not become yellow on standing, which represents a considerable advantage in colorimetry. Solutions of the two substances (10^{-4} *M*) in 6 *M* hydrochloric acid decompose at different rates; after 65 min the concentration of cupferron decreases by 50%, whereas hexahydrocupferron reaches this value after 4 days.

Reactions with metal ions

A study of the reactions of hexahydrocupferron with 50 inorganic ions showed that, like cupferron, the reagent lacks selectivity. The difference in acidity

TABLE I

DETECTION LIMITS FOR REACTIONS OF HEXAHYDROCUPFERRON

(All reactions involve precipitation unless specified otherwise)

Ion	*NH_4OH*	*Neutral*	*NaAcO*	*HAcO*	*HCl*	*Ion*	*NH_4OH*	*Neutral*	*NaAcO*	*HAcO*	*HCl*
Ag(I)		W[a] 1:50,000	W 1:50,000			Mn(II)		W[b] 1:5,000	W[b] 1:5,000		
Pb(II)		W 1:10,000	W 1:10,000	W 1:7,000		Ti(IV)					Y[b] 1:300,000
Hg(I)		W 1:10,000	W 1:10,000	W 1:10,000	W 1:20,000	Be(II)		W[b] 1:500,000	W[b] 1:500,000	W 1:200,000	W 1:50,000
Hg(II)	W 1:20,000	W 1:20,000	W 1:20,000	W 1:5,000	W 1:5,000	V(V)				Y[b] 1:100,000	Red[b] 1:500,000
Cu(II)	V[b] 1:10,000	V[b] 1:200,000	V[b] 1:200,000	V[b] 1:200,000	V[b] 1:70,000	U(VI)		Y[e] 1:10,000	Y[e] 1:10,000	Y[e] 1:10,000	
Bi(III)	W[b] 1:10,000	W[b] 1:30,000	W[b] 1:30,000	W[b] 1:30,000	W[b] 1:20,000	Zr(IV)	W 1:10,000	W 1:30,000	W 1:30,000	W 1:50,000	W 1:50,000
Cd(II)	W 1:5,000	W 1:1,000	W 1:1,000	W 1:1,000		Ce(III)	Y[b] 1:30,000	Y[b] 1:30,000	Y[b] 1:30,000	Y[b] 1:20,000	
Sb(III)		W[b] 1:100,000	W[b] 1:100,000	W[b] 1:100,000	W[b] 1:100,000	Ce(IV)	Y[b] 1:10,000	Y[b] 1:50,000	Y[b] 1:50,000	Y[b] 1:50,000	Y[b] 1:30,000
Pd(II)		Y[b] 1:7,000	Y[b] 1:7,000	Y[b] 1:7,000	Y[b] 1:3,000	Th(IV)	W[b] 1:10,000	W[b] 1:30,000	W[b] 1:30,000	W[b] 1:10,000	W[b] 1:10,000

Sn(II)		W[b] 1:70,000	W[b] 1:70,000	W[b] 1:70,000	W[b] 1:50,000	La(III)	W 1:30,000	W 1:3,000	W 1:3,000	W 1:1,000	
Sn(IV)		W[b] 1:30,000	W[b] 1:30,000	W[b] 1:30,000	W[b] 1:30,000	In(III)	W[b] 1:2,000	W[b] 1:2,000	W[b] 1:2,000	W[b] 1:2,000	
Mo(VI)				W[b] 1:7,000	W[b] 1:100,000	W(VI)					W 1:3,000
Au(III)		Purple[c] 1:2,000	Purple[c] 1:2,000	Purple[c] 1:2,000		Nb(V)					W 1:70,000
Al(III)	W[b] 1:5,000	W[b] 1:500,000	W[b] 1:500,000	W[b] 1:500,000		Y(III)	W 1:20,000	W 1:30,000	W 1:30,000	W 1:30,000	W 1:10,000
Cr(III)		Green 1:5,000	Green 1:5,000			Ca(II)	W 1:2,000	W 1:2,000			
Fe(III)	Red[b] 1:50,000	Red[b] 1:700,000	Red[b] 1:700,000	Red[b] 1:700,000	Red[b] 1:700,000	Sr(II)	O[f] 1:1,000	O[f] 1:1,000			
Fe(II)		Y[b] 1:200,000	Y[b] 1:200,000	Y[b] 1:300,000		Ba(II)	O[f] 1:1,000	O[f] 1:1,000			
Co(II)		Pink[d] 1:10,000	Pink[d] 1:10,000	Pink[d] 1:1,000		Mg(II)		O[f] 1:1,000			

[a] W = white, V = violet, Y = yellow.
[b] Soluble in organic solvents.
[c] A purple colour is formed.
[d] A pink colour is formed.
[e] A yellow colour is formed.
[f] Opalescence.

between hexahydrocupferron and cupferron—pK 5.58 and 4.28, respectively—does not affect the reactions. Concentration limits of the reactions (Table I) are the same as for cupferron; this was checked in comparative tests. All the reactions of hexahydrocupferron with metal ions involve precipitation except for cobalt(II) and uranium(VI), which form soluble complexes. Most of the precipitates are soluble in organic solvents, such as chloroform and ethyl ether, and those of Cu(II), Pd(II), V(V), Fe(II,III), Ti(IV) and Ce(III,IV) develop a colour in the organic layer; this can be utilized in extraction spectrophotometry.

The reagent may be used for the same precipitations as cupferron with the same procedures[2]. Despite its lack of selectivity, it should be useful for the group separation of Hg(I), Cu, Bi, Sb(III), Sn, Fe and V in acidic media from elements such as Al, Pb, Zn, Cd, Ni, Co, Ag, Hg(II), Cr, Mn, Zn and alkaline earths. Like cupferron, this new reagent should be of value not only in the separation of elements which are later to be determined, but also in the removal of interferences.

The reactions with Ti(IV), V(V) and Fe(III) are selective and sensitive enough to be used for detection and colorimetric determination.

The compositions of some of these complexes were determined. Ag, Cu, Ti, Ca, and Mg compounds were studied gravimetrically and those of iron and aluminium by the Job[3] and Yoe–Jones[4] methods. If R represents the reagent, the compositions were found to be AgR, CuR_2, TiR_4, CaR_2, MgR_2, FeR_3 and AlR_3, like cupferron with the same metals[5].

The high sensitivity of the reaction with aluminium (1:500,000) allowed the development of a turbidimetric determination of this element; the accuracy and a precision were much better than the errors obtained by Schams[6] for the analogous determination with cupferron. The procedure was applied to a pharmaceutical product with good results.

EXPERIMENTAL

Preparation and solubility of hexahydrocupferron

The sodium salt of N-nitroso-N-cyclohexylhydroxylamine was prepared from N-cyclohexylhydroxylamine, as described by Metzger[7]. Recrystallized from water, it decomposes at 250°. The ammonium salt[1] melts at 140°.

The solubility, determined at 20° as described by Wittenberger[8], was found to be 11.49 g per 100 ml in water and 0.43 g per 100 ml in ethanol. The reagent is sparingly soluble in apolar solvents.

Properties of hexahydrocupferron

Determination of R_F value. The R_F value was determined by thin-layer chromatography on non-activated silica gel GF_{254} (0.25 mm, Merck). Methanol–concentrated ammonia solution (88 + 12) was used as developing solvent. The approximate R_F value of hexahydrocupferron was 0.76; that of bis-nitrosocyclohexane (its decomposition product) was 0.83.

Ultraviolet absorption spectra. Mueller and Metzger[1] have published the spectrum of N-nitroso-N-cyclohexylhydroxylamine in methanol, but not in aqueous solution. Spectra were measured in a Perkin–Elmer M 124 spectrophotometer in

0.1 *M* hydrochloric acid and 0.1 *M* sodium hydroxide solutions. In acidic medium, hexahydrocupferron shows an absorption maximum at 229–230 nm ($\varepsilon_{max} = 6{,}250$) and in alkali at 249–250 nm ($\varepsilon_{max} = 8{,}370$).

Determination of pK. The p*K* value was determined, as described by Albert and Sergeant[9], at a wavelength (260 nm) at which only the anionic form of the reagent absorbs. The p*K* value was found to be 5.58 ± 0.03.

Infrared spectra. The spectra were recorded in potassium bromide discs on a Beckman spectrophotometer Model 20 A. Hexahydrocupferron is characterized by three bands of high intensity at 1450 and 1170 cm^{-1} assigned[10] to the N=O stretching vibration in the monomeric and dimeric forms, respectively, and at 950 cm^{-1} assigned to the N–N stretching vibration.

Stability in 6 M hydrochloric acid. The decomposition of a 10^{-4} *M* solution of the reagent in 6 *M* hydrochloric acid was followed by measuring its absorbance at 224 nm. After 4 days the decomposition of the reagent reached 50%; cupferron decomposed to the same extent in only 65 min. An aqueous solution of the reagent is stable for at least 12 weeks.

Reactions with metal ions

Reagent. An aqueous 1% (w/v) solution was used.

Metal test solutions. Aqueous solutions containing 1 g Me l^{-1} were prepared.

Experimental technique. In a microtube, 0.25 ml of reagent and 0.25 ml of 2 *M* nitric acid, acetic acid, sodium acetate, ammonium or sodium hydroxide, were added to 1 ml of each metal to be tested. Very dilute metal solutions were assayed with 5 ml.

The results of the reaction study are given in Table I. Hexahydrocupferron does not react with alkali metals, As(III,V), Sb(V), Te(VI), Pt(IV), Zn, Ni or Tl(III). In sodium hydroxide solutions, the reagent did not react with any ion.

REACTIONS OF QUALITATIVE INTEREST

Detection of titanium(IV)

Titanium(IV) may be identified if the test is carried out in a hydrochloric acid solution of the hydroxides of the third group. The yellow precipitate formed is soluble in ether giving the same colour (concentration limit, 1:350,000). The only interferences are those of iron(III) and cerium(IV) (which can be avoided by reducing first with ascorbic acid) and vanadium(V).

Procedure. Treat 1 ml of the hydrochloric acid test solution with 5 drops of 1% reagent and extract with 1 ml of ether. An orange-yellow colour appears in the organic layer.

Detection of vanadium(V)

Vanadium may be identified in the precipitate of the third group of cations, by the procedure described for titanium(IV); a red-orange colour appears (concentration limit, 1:1,000,000). Interference of iron(III) and cerium(IV) can be avoided by prior reduction with ascorbic acid, but titanium(IV) interferes.

Detection of iron(III)

Iron(III) may be detected in hydrochloric acid solutions of the hydroxides

of the third group. The reagent forms an orange-red precipitate which can be extracted into ether, giving the same colour (concentration limit, 1:2,000,000). The procedure is the same as that for titanium(IV). Precipitates of V(V), Ti(IV) and Ce(IV) (to a lesser extent, for it may be reduced first with peroxide) interfere.

TURBIDIMETRIC DETERMINATION OF ALUMINIUM

Measurements were made with a Metrohm E 1009 spectrocolorimeter with 1-cm cells. The absorbance was constant between 400 and 430 nm, using water as a reference. A 1% (w/v) solution of polyvinyl alcohol was used as protective colloid. The absorbance was not affected by 1–15% of this solution.

The stability of the turbidity was studied. The absorbance reached a constant level after a developing period of 20 min and began to decrease after 40 min.

The intensity of the turbidity was dependent on pH. The absorbance was constant between pH 3.0 and 4.0; above this pH it decreased slightly, but another plateau in the absorbance–pH plot was obtained between pH 6.0 and 8.5. These results led to the development of the following method.

Procedure

Place samples containing 15–250 μg of aluminium in 25-ml volumetric flasks, and add 5 ml of a pH 3.35 buffer solution (potassium hydrogenphthalate), 1 ml of 1% polyvinyl alcohol solution and 3 ml of aqueous 3% hexahydrocupferron solution. Dilute to volume and measure the absorbances at 420 nm after 20 min, using water as a reference.

Results

Beer's law was followed within the range 0.6–10 μg Al ml^{-1}. A concentration of 0.1 *M* sodium perchlorate changed neither the slope nor the limits of Beer's law. The standard deviation for 166 μg of aluminium (21 measurements; 95% confidence limit) was less than 0.2%.

Errors of less than 1% were caused by 8000-fold amounts of sodium nitrate or ammonium chloride, 150-fold Zn, 100-fold Cd, 1,000-fold Mg, 30-fold Pb, 15-fold Sb(V), 25-fold Ni or Mn, 5-fold Co, and 100-fold phosphate.

This determination was applied to an aluminium β-glycyrrhetinate ($Al(C_{30}H_{45}O_4)_3$). Suitable samples were mineralized in concentrated sulphuric acid and analyzed turbidimetrically; the errors were less than 1.5% compared with the gravimetric aluminium oxinate method.

SUMMARY

The analytical properties of N-nitroso-N-cyclohexylhydroxylamine ("hexahydrocupferron") are described. This reagent is much more stable in acidic media than its analogue cupferron, but offers very similar reactions and sensitivities. The solubility, R_F and pK values, u.v. and i.r. spectra for the reagent are given. Very sensitive qualitative tests for iron, vanadium and titanium are reported. A turbidimetric determination of aluminium(III), suitable for 0.6–10 μg Al ml^{-1}, is evaluated.

RÉSUMÉ

Une étude est effectuée sur les propriétés analytiques de la N-nitroso-N-cyclohexylhydroxylamine ("hexahydrocupferron"). Ce réactif présente des réactions et des sensibilités tout à fait similaires à celles du cupferron; il a l'avantage d'être beaucoup plus stable en milieu acide. On indique la solubilité, les valeurs R_F et pK de ce réactif et on en donne les spectres u.v. et i.r. Il permet des tests qualitatifs très sensibles pour le fer, le vanadium et le titane. Un dosage turbidimétrique est décrit pour l'aluminium (0.6 à 10 μg Al ml^{-1}).

ZUSAMMENFASSUNG

Die analytischen Eigenschaften von N-Nitroso-N-cyclohexylhydroxylamin ("Hexahydrocupferron") werden beschrieben. Dieses Reagenz ist viel beständiger in sauren Medien als das analoge Cupferron, die Reaktionen und Empfindlichkeiten sind jedoch sehr ähnlich. Für das Reagenz werden die Löslichkeit, die R_F- und pK-Werte sowie die u.v.- und i.r.-Spektren angegeben. Es wird über einen sehr empfindlichen qualitativen Nachweis von Eisen, Vanadin und Titan berichtet. Eine turbidimetrische Bestimmung von Aluminium(III), die sich für 0.6–10 μg Al ml^{-1} eignet, wird beschrieben.

REFERENCES

1 E. Mueller and H. Metzger, *Chem. Ber.*, 89 (1956) 396.
2 F. J. Welcher, *Organic Analytical Reagents*, Vol. III, D. Van Nostrand, New York, 1948, p. 355.
3 P. Job, *Ann. Chim. (Paris)*, 9 (1928) 113; 6 (1936) 97.
4 J. H. Yoe and A. L. Jones, *Ind. Eng. Chem., Anal. Ed.*, 16 (1944) 111.
5 N. H. Furman, *Anal. Chem.*, 21 (1949) 1325.
6 O. Schams, *Mikrochem.*, 25 (1938) 16.
7 H. Metzger, *B.A.S.F. A.G., D.A.S. 1,019,657 Kl.12q from 18.8.56.*
8 W. Wittenberger, *Chemisches Laboratoriums Technik*, Springer Verlag, Wien, 1950, p. 101.
9 A. Albert and E. P. Sergeant, *Ionization Constants of Acids and Bases*, Methuen, London, 1962, p. 69.
10 R. N. Haszeldine, *J. Chem. Soc.*, (1955) 4172.

Analytica Chimica Acta, 67 (1973) 357–376

THIN-LAYER CHROMATOGRAPHY OF METAL CHELATES

PART II. AN EXTENDED THEORY AND ITS TESTING ON METAL DITHIZONATES AND METAL DIETHYLDITHIOCARBAMATES*

A. GALÍK

Lachema, N.C., 33151 Kaznějov, Pilsen North (Czechoslovakia)

(Received 30th January 1973)

The adsorption chromatography of extractable metal chelates has become a promising means of inorganic multicomponent analysis[1–4]. However, because the relationships governing the chromatographic behaviour of the chelates are not well established, progress is slow; for the conditions for optimal separation must be sought empirically. Very few papers have dealt with the problem more systematically. Hilliard and Freiser[5] and Pantony *et al.*[6,7] have studied the general adsorption characteristics of various metal chelates in relation to their thermodynamic properties and to the type of adsorbent, Busev *et al.*[1,8] compared several adsorbents for the column separation of metal dithizonates, and Galík[9], inspired by the mathematical model of the chromatographic process suggested by Soczewiński[10], tried to explain the effect of solvent composition and of air humidity on the thin-layer chromatographic (t.l.c.) behaviour of metal pyridylazonaphtholates.

The present paper deals with an extension of the latter approach so that the model would be capable of predicting more phenomena, and could form the basis of further research leading to a better understanding of the chromatography of metal chelates. It should be realized, however, that direct harnessing of the model for practical purposes requires considerable further work.

For experimental verification, the t.l.c. behaviour of metal chelates of dithizone and of diethyldithiocarbamic acid was studied. These reagents are unsuitable for quantitative analysis by means of t.l.c. and reflectance photometry, because most of their chelates change colour rapidly after development of the chromatogram. However, these reagents seemed appropriate, because their metal chelates are sufficiently well known for a realistic comparison of the chelate properties and chromatographic behaviour.

THEORETICAL CONSIDERATIONS

The mathematical model of the t.l.c. process, as described previously[9], is based on the assumption that separation of the compound being chromatographed (*i.e.* the solute) occurs between two phases as in paper chromatography. The mobile

* Part I: *Anal. Chim. Acta*, 57 (1971) 399.

phase is the solvent flowing freely through the adsorbent particles, while the stationary phase is the layer of solvent molecules and water at the surface of the adsorbent particles, the intermolecular forces of which are modified by the adjacent solid phase (the adsorbent). Any assumptions on the thickness of this stationary phase are unnecessary.

General equations

According to the above idea, Martin's equation[11] may be applied to describe the solute distribution in adsorption thin-layer chromatography:

$$R_M = \log[(1/R_F)-1] = \log \alpha + \log Q \quad (1)$$

where α represents the distribution coefficient of the solute, and Q is the ratio of the cross-sections of the stationary and mobile phases. Because the Q value may be considered almost constant over the most interesting range of $R_F=0$ to about 0.7 (supposing that the chromatogram starts well above the level of the developing solvent in the container, *cf.* ref. 12), R_M depends mainly on the distribution coefficient α. If the concentration of the solute is very small and if chromatography is performed under equilibrium conditions, this coefficient may be expressed by applying the law of mass action.

The chromatographic system considered involves the solute Z to be chromatographed, the developing solvent consisting of a number of components S_i (i=1, 2, ..., d), the molecules of water W, and the active centres A of the adsorbent. During the development of the chromatogram, the solute Z is distributed between the two phases, and its transition into the stationary phase can be attributed to the formation of adsorption complexes with the active centres of the adsorbent (*e.g.* free hydroxyl groups in silica gel). Generally, a stepwise complexation might occur via formation of complexes ZA_j, where j=1, 2, ..., m. It is, however, very likely that only one complex predominates, as in solvent extraction of metal chelates. The formation of this complex, ZA_m, may be described by a two-phase stability constant:

$$K_{ZA_m} = (X_{ZA_m})_a / [X_Z \cdot (X_A)_a^m] \quad (2)$$

where X_i denotes the molar fraction of the indexed species in either the mobile phase or the stationary phase, the latter being indicated by the suffix a. These symbols are used throughout this paper.

As well as being bound by the adsorbent, solute Z may also be solvated by components of the developing solvent, to form the solvation complexes $Z(S_i)_s$, where s=1, 2, ..., i. This solvation by component S_i may be described by consecutive solvation constants:

$$K_{Z(S_i)_s} = X_{Z(S_i)_s} / [X_Z \cdot (X_{S_i})^s] \quad (3)$$

In addition to solvation, the solvent components may also compete with solute Z during the adsorption process: each of these components might form adsorption complexes with one or more active centres A of the adsorbent. As in the case of adsorption of the solute, the predominance of only one type of adsorption complex is again assumed. The adsorption of component S_i via formation of the complex $S_i(A_{n_i})$ may then be described by the following constant:

$$K_{S_i(A_{n_i})} = (X_{S_i(A_{n_i})})_a / [X_{S_i} \cdot (X_A)_a^{n_i}] \quad (4)$$

Water must also be considered. Water is present in each t.l.c. system (*cf. e.g.* ref. 13), originating from laboratory humidity. Because of its high dielectric constant, it is strongly adsorbed by polar adsorbents[14], and so competes seriously with both solute Z and solvent components S_i for the adsorption centres A. Moreover, because the developing solvents commonly used in t.l.c. are much less polar than water, adsorption of water may be considered as essentially independent of the solvent composition. The molar ratio of water in the above-defined stationary phase, $(X_W)_a$, may be affected seriously, however, by the changes of partial pressure of water vapour in the atmosphere, P_W, and, like any adsorption process, by temperature T:

$$(X_W)_a = f(P_W, T) \quad (5)$$

(Dissolution of water in organic solvents is neglected.)

Besides of the equilibria described by eqns. (2)–(5), mass balances of all the species present must be valid in the system. In the mobile phase, it is possible to neglect the molar fractions of the solute Z and of its solvates $Z(S_i)_s$ in comparison with the molar fractions of the components of the developing solvent:

$$\sum_1^i X_{S_i} = 1 \quad (6)$$

Moreover, changes in composition of the solvent along the practically meaningful part of the chromatogram can also be neglected, because the stationary phase can be assumed to be very thin compared to the mobile one. Therefore the molar fractions X_{S_i} may be identified with their original values in the solvent container. With regard to mass balances in the stationary phase, the molar fractions of most of the species are much larger than that of the adsorption complex of the solute, $(ZA_m)_a$, so that the following equation applies:

$$(X_A)_a + \sum_1^i (X_{S_i(A_{n_i})})_a + (X_W)_a = 1 \quad (7)$$

By rearranging eqns. (2) and (3), and after substitution into the equation which defines the distribution coefficient α:

$$\alpha = \frac{\text{total concentration of the solute Z in the stationary phase}}{\text{total concentration of the solute Z in the mobile phase}} = \frac{(X_{ZA_m})_a}{X_Z + \sum_1^i \sum_1^s X_{Z(S_i)_s}} \quad (8)$$

Martin's eqn. (1) can be transformed as follows:

$$R_M = \log Q + \log K_{ZA_m} + m \log (X_A)_a - \log \left\{ 1 + \sum_1^i \sum_1^s K_{Z(S_i)_s} \cdot (X_{S_i})^s \right\} \quad (9)$$

For the purpose of discussion, the values of the constants Q, K_{ZA_m} and $K_{Z(S_i)_s}$ may be assumed to be known, similarly to the molar fractions of the solvent components X_{S_i} (see above). Equation (9) includes, however, an unknown molar fraction of free adsorption centres $(X_A)_a$; this can be eliminated by using eqn. (7). Substitution into eqn. (7) from eqns. (4) and (5) yields:

$$(X_A)_a + \sum_{1}^{i} K_{S_i(A_{n_i})} \cdot X_{S_i} \cdot (X_A)_a^{n_i} = 1 - f(P_W, T) \tag{10}$$

This equation contains, except for an unknown function f describing the adsorption of water vapours (which could be found experimentally), only assumable constants $K_{S_i(A_{n_i})}$, known values of X_{S_i}, and the desired value of the equilibrium molar fraction of free adsorption centres in the stationary phase, $(X_A)_a$. By solving eqn. (10) with respect to $(X_A)_a$, and substituting the result into eqn. (9), a general equation explicitly describing the chromatographic process on a thin layer of adsorbent would be obtained. Unfortunately, eqn. (10) is not algebraically solvable for each value of n_i. Therefore, the chromatographic process is here described implicitly, by the parametric eqns. (9) and (10). For the purposes of experimental testing of the theory and of its usage for improvements in separation of metal chelates, particular cases of these equations are discussed below.

Discussion of particular cases

One-component developing solvent. One of the simplest cases met in t.l.c. involves development with a single organic solvent S (which is here assumed to have very low dielectric constant). In this case, naturally, $X_S = 1$. Because of the low polarity of the solvent, the solvation of the non-polar solute Z (*i.e.* extractable metal chelate) may be neglected, so that $K_{Z(S_i)_s} = 0$. As a further approximation, adsorption of the solvent by the adsorbent may also be neglected. This means that $(X_{SA_n})_a \ll (X_A)_a + (X_W)_a$ may be assumed. These assumptions are needed to simplify the equations for experimental verification, and seem reasonable for the systems considered.

The solution of eqn. (10) under these assumptions gives the formula for $(X_A)_a$ which, on substitution into eqn. (9), yields:

$$R_M = \log Q + \log K_{ZA_m} + m \log [1 - f(P_W, T)] \tag{11}$$

It is obvious that the position of the spot of solute Z on the chromatogram in this simple system is determined mainly by the strength of the solute–adsorbent bonds and that this position may be affected by changes of air humidity or temperature. The differences of the R_M values of two solutes to be separated, Z and Z′ (*i.e.*, their separation factor) cannot be influenced, however, by changing P_W or T, unless the solutes differ in the numbers m, m′ of their bonds to the adsorbent.

If the single solvent S is more polar so that its adsorption cannot be neglected, eqn. (10) becomes:

$$(X_A)_a^n \cdot K_{SA_n} + (X_A)_a = 1 - f(P_W, T) \tag{12}$$

which is of n-th order with respect to $(X_A)_a$, and can be solved algebraically for, *e.g.*, n = 1, 2 and 3. More general solution of eqn. (12) is possible, however:

because of the strong adsorption of the solvent, the molar fraction of free active groups of the adsorbent, $(X_A)_a$, can be neglected in comparison with the molar fraction of the adsorption complex of the solvent, $(X_{SA_n})_a$. Then eqn. (12) simplifies and its solution gives:

$$(X_A)_a = \left(\frac{1-f(P_W, T)}{K_{SA_n}}\right)^{1/n} \tag{13}$$

Substitution of eqn. (13) into eqn. (9) gives the following equation, which describes the position of the spot of the solute Z:

$$R_M = \log Q + \log K_{ZA_m} - \log (K_{SA_n})m/n + \log [1-f(P_W, T)]m/n \tag{14}$$

Comparison of eqn. (14) with that derived for a non-polar single solvent (eqn. 11) makes it obvious that here the choice of a polar solvent can alter the effect of air humidity or temperature on the position of the spot. With regard to the separation of the two different solutes, the same conclusions as those reached above remain valid.

Two-component developing solvent. The use of a single organic solvent for development is quite rare in the case of metal chelates; mixtures of two or more organic solvents are usual. In a typical case, the developing mixture consists of a solvent of low polarity, N, and a more polar solvent S, so that $X_N + X_S = 1$. It may be assumed that both adsorption and solvation can be neglected for component N. Component S, however, can both form adsorption complex SA_n and solvate solute Z via formation of solvates ZS_1, ZS_2, ..., ZS_s. Under these assumptions, eqn. (10) transforms into:

$$(X_A)_a^n \cdot K_{SA_n} \cdot X_S + (X_A)_a = 1 - f(P_W, T) \tag{15}$$

The general algebraical solution of eqn. (15), with respect to $(X_A)_a$, for each value of n is again impossible. The equation may be solved, however, if it is assumed that the molar fraction of unoccupied adsorption centres A may be neglected in comparison with molar fractions of other components of the adsorbed–stationary phase; this seems acceptable, considering the properties of component S. Then the solution of eqn. (15) gives:

$$(X_A)_a = \left[\frac{1-f(P_W, T)}{K_{SA_n} \cdot X_S}\right]^{1/n} \tag{16}$$

After substitution of this result into eqn. (9), Martin's equation becomes:

$$R_M = \log Q + \log K_{ZA_m} + \frac{m}{n} \log [1-f(P_W, T)] - \frac{m}{n} \log K_{SA_n} \cdot X_S - \log \left(1 + \sum_1^s K_{ZS_s} \cdot X_S^s\right) \tag{17}$$

This equation can be simplified further in two cases. First, if solvation of the solute can be neglected, the last term of eqn. (17) becomes zero:

$$R_M = \log Q + \log K_{ZA_m} + \log [1-f(P_W, T)]\ m/n - \log [K_{SA_n} \cdot X_S]m/n \tag{17a}$$

Secondly, if the metal chelate—solute Z—is solvated very strongly, and among the possible solvates ZS, ZS_2, ..., ZS_r, ..., ZS_s only ZS_r predominates, then, for $K_{ZS_r} \cdot X_S^r \gg 1$, eqn. (17) becomes:

$$R_M = \log Q + \log K_{ZA_m} - \frac{m}{n} \log K_{SA_n} - \log K_{ZS_r} +$$

$$+ \frac{m}{n} \log [1 - f(P_W, T)] - \left(\frac{m}{n} + r\right) \log X_S \qquad (17b)$$

From eqns. (17), (17a) and (17b), it is clear that the position of the spot of solute Z on the chromatogram may be influenced by the choice of the polar component of the solvent mixture S (see K_{SA_n}, r, n), by the concentration of this component in the mixture (see X_S) and by air humidity and temperature; the extent of the latter effects again depends on the polar component.

When two chelates, Z and Z', are to be separated, several cases may occur. The easiest is the case when the two chelates differ in the number of their bonds, m and m', to the adsorbent: the above equations for R_M show that the separation factor, defined as $(R_M)_Z - (R_M)_{Z'} = \log \alpha - \log \alpha'$, may be increased both by change of X_S and of the water content of the adsorbent. In another case, when the solutes Z and Z' are bound to the adsorbent by the same number of bonds, m = m', improvement of the separation factor by changing the concentration of polar component S depends on the differences in solvation of Z and Z', *i.e.* on the differences between r and r' (see eqn. 7b). If this difference is small, or when r = r' = 0, the separation cannot be improved by change of X_S.

The practical utility of the above conclusions which are drawn from eqns. (17a) and (17b), is largely contingent on the validity of these equations. Subsequent parts of this paper are therefore devoted to experimental testing of the mathematical model suggested.

EXPERIMENTAL

Solutes

Solutions of metal dithizonates were prepared by extracting 10-ml portions of aqueous 10^{-4} *M* solutions of the metal salt with 5 ml of 10^{-3} *M* dithizone (Merck) in carbon tetrachloride. This dithizone solution was prepurified by extracting dithizone into dilute aqueous ammonia and re-extracting into carbon tetrachloride after acidification. Mercury was extracted at pH 3, copper at pH 4.5, zinc at pH 6, and cobalt, nickel, lead and cadmium at pH 8.5–9 (adjusted with aqueous ammonia).

Mercury, bismuth, copper, nickel, cobalt and lead diethyldithiocarbamate solutions were prepared by adding 2 ml of 20% (w/v) ammonium tartrate and 5 ml of 0.1% (w/v) sodium diethyldithiocarbamate to 10 ml of aqueous solution containing 500 μg of the cation, adjusting to pH 9–10 (aqueous ammonia), and extracting with 3 ml of chloroform for 10 min. Zinc, cadmium and indium diethyldithiocarbamates were prepared similarly, extractions being done at pH 7, 8 and 5–6, respectively. Iron diethyldithiocarbamate was prepared by adding solid sodium diethyldithiocarbamate to 15 ml of iron(II) sulphate solution con-

taining 500 μg Fe^{2+} at pH 3–4 (acetate buffer), and extracting with 3 ml of chloroform for 1 min. Antimony diethyldithiocarbamate was obtained by adding ascorbic acid to 15 ml of potassium antimony tartrate solution containing 500 μg Sb^{3+}, adjusting to pH 6, adding solid sodium diethyldithiocarbamate and shaking with 3 ml of carbon tetrachloride for 5 min.

All these solutions were filtered through paper into glass test tubes which were then closed by polyethylene stoppers and stored in the dark at room temperature. The solutions remained stable for at least one month, during which they were used continuously.

Adsorbent

Commercially available Silufol chromatographic plates (Kavalier, ČSSR) were used unless otherwise specified.

Solvent systems

In the two-component solvent systems investigated, carbon tetrachloride usually served as the apolar diluent but benzene was used occasionally. The purity and dryness of these solvents was checked from the boiling point and refractive index. All other organic solvents were of *pro analysi* grade, except for chloroform, which was purified as described earlier[9]. Solvent mixtures were prepared immediately before use.

Studies of solvent composition

Procedure A. About 1-mm wide strips of adsorbent were removed from each side of square (15 × 15 cm) Silufol plates in order to prevent side effects. Up to ten aliqots of the dithizonate (1–5 μl) or the diethyldithiocarbamate (5–10 μl) solutions were applied on the start which was positioned 2.5 cm above the bottom of the plate. Each of the aliquots formed a strip-shaped spot (5 × 15 mm). The plate was positioned in a tilted Kavalier chromatographic chamber (18 × 18 × 6.5 cm) lined with filter paper. The developing mixture (50 ml) was added, the chamber was closed, and the system was left to equilibrate for 1 h. The chamber was then set upright so that the solvent wetted the bottom end of the Silufol. Chromatography was ended when the visible solvent front had travelled 10 cm from the start.

Procedure B. In order to provide more strictly controlled humidity conditions than in Procedure A, volumetric cylinders provided with a hygrostat were used instead of the above arrangement. The apparatus used is shown in Fig. 1; this is an improved version of that described earlier[9]. Freshly supplied 20 × 20 cm Silufol sheets (with the same quality of adsorbent as above) were cut into ten 2.5 × 12 cm strips, and 1-mm strips of adsorbent were removed at the sides. Up to five different solutions of metal chelates (1–2 μl of metal dithizonates, 2–5 μl of metal diethyldithiocarbamates) were applied on the start of a single strip, 2.5 cm above the bottom. The strips were hung on wire hooks, the cylinders were closed, and the adsorbent was left to equilibrate for 3–4 h (see Fig. 2a) with the air humidity determined by the hygrostat used (calcium chloride hexahydrate, unless otherwise stated). Then 15 ml of freshly prepared developing solvent mixture was poured through the funnel into the 25-ml beaker, and the

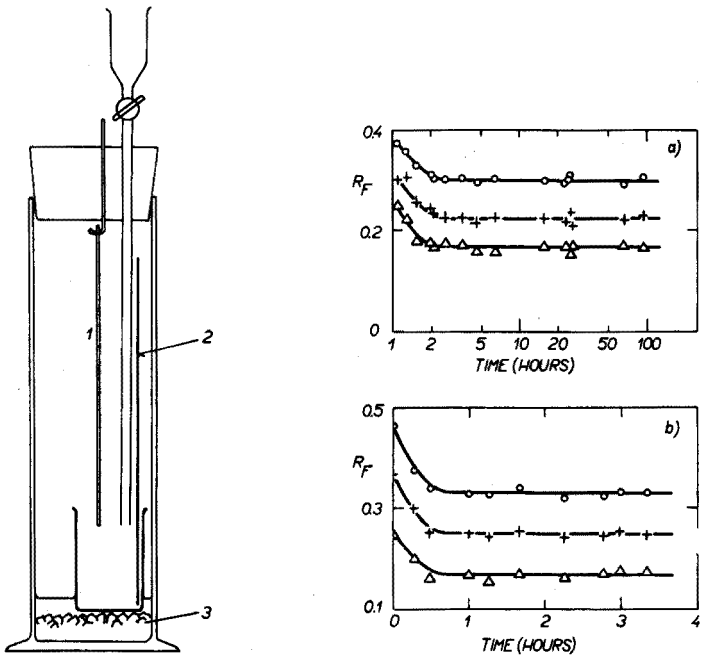

Fig. 1. Chromatographic assembly used in Procedure B. (1) Strip of Silufol, (2) filter paper, (3) crystals of inorganic salt used as a hygrostat.

Fig. 2. Saturation characteristics of chromatographic cylinder as observed during t.l.c. of mercury, copper and bismuth diethyldithiocarbamates. N = CCl_4, S = acetone (4% v/v), $CaCl_2 \cdot 6H_2O$ as hygrostat, laboratory humidity 90%. (a) Effect of time of equilibration of the adsorbent with water vapours inside the cylinder (followed by 1-h saturation with developing solvent vapours). Temperature 22°. (b) Effect of time of equilibration of the adsorbent with the vapours of the developing solvent mixture (after 3-h equilibration with air humidity). Temperature 24°. (○), Hg; (+), Cu; (△), Bi.

cylinder atmosphere was left to become saturated with solvent vapours for 1 h (see Fig. 2b). The wire hooks were then pushed down so that 1–2 mm of the chromatostrip dipped into the solvent. Chromatography was ended when the solvent reached a pencilled mark 9 cm from the start. Spots of dithizonates or coloured diethyldithiocarbamates (yellowish-brown for copper, green for nickel or cobalt, yellow for bismuth or brownish-grey for iron) were located by their characteristic colours; colourless diethyldithiocarbamates were made visible by spraying with saturated copper sulphate solution in (30+70) water–ethanol.

In order to exclude any effects of variation in individual Silufol chromatoplates, test substances were chromatographed simultaneously with the chelates. Either copper diethyldithiocarbamate or mercury dithizonate was used as test substance. However, the properties of Silufol chromatoplates proved to be remarkably homogeneous.

Studies of air humidity

In order to study the effect of humidity, Procedure B was modified. Into each of ten chromatographic cylinders, different hygrostats were placed, all other

chromatographic conditions being kept constant. The hygrostats used were saturated solutions over crystals of the following salts: sodium chloride, potassium chloride, ammonium sulphate, potassium bromide, ammonium chloride, ammonium nitrate, a mixture of ammonium chloride with potassium nitrate, magnesium nitrate hexahydrate, potassium carbonate dihydrate, calcium chloride hexahydrate, potassium acetate, or sodium acetate trihydrate. Both in Procedure B and here, the temperature was measured to within 0.2°. The temperature changes during a single run did not exceed $\pm 1°$.

Measurement of adsorption isotherms of water on Silufol at different temperatures

The chromatostrips (Procedure B) were hung into chromatographic cylinders containing the above hygrostats for 3–4 h. Then they were taken out and weighed at 30-s intervals. The total weight g_1 of the wet chromatostrip was obtained by

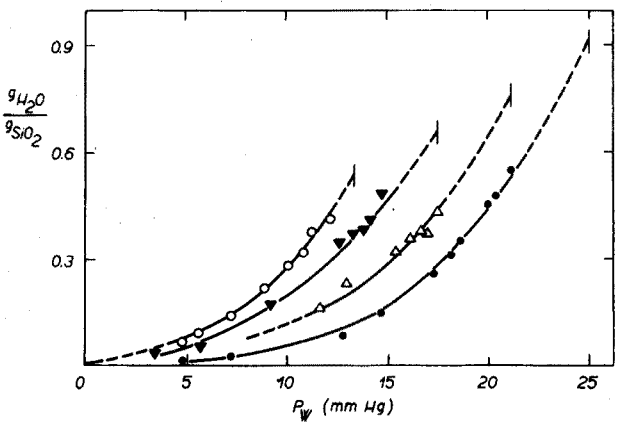

Fig. 3. Adsorption isotherms of water on Silufol at various temperatures. Curves are finished at the values of partial pressure of water vapours P_W over pure water at temperatures indicated. (○), 16.5°; (▼), 20°; (△), 23°; (●), 26°.

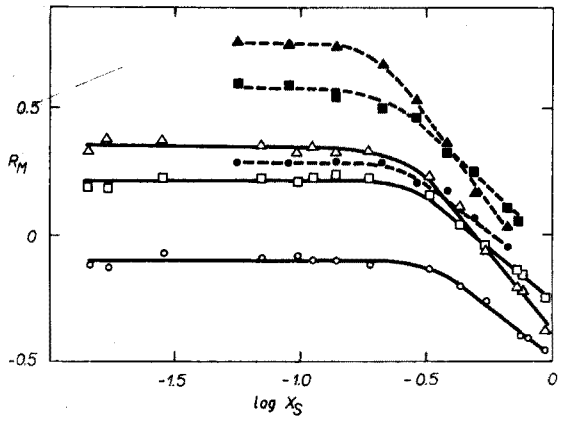

Fig. 4. Effect of the content of component S of small polarity on metal dithizonates. $N=C_6H_6$, $S=CHCl_3$. Full lines: Procedure B, $T=25°$, over $Mg(NO_3)_2 \cdot 6H_2O$ saturated solution. Broken lines: Procedure A, $T=16°$, $P/P_0=57\%$. (▲, △) Co; (■, □) Ni; (●, ○) Hg.

graphical extrapolation to the time of opening the cylinder. The strips were dried at 105–110° for 2 h and then cooled in a desiccator over freshly activated silica gel. After opening the desiccator just for the time necessary to remove one strip, the weight g_2 of a dry strip was found by weighing the strip at 30-s intervals again and by graphical extrapolation to the time of opening the desiccator. As a third step, the weight g_3 of the aluminium support of each strip was found after scraping away all the adsorbent. The weight ratio of adsorbed water to dry silica gel was calculated from:

$$g_{H_2O}/g_{SiO_2} = (g_1 - g_2)/(g_2 - g_3) \tag{18}$$

The values obtained were plotted in Fig. 3 *versus* the partial pressure of water at a given temperature, P_W, which was found in the literature[15–17] for each of the hygrostats employed.

RESULTS AND DISCUSSION

Effect of changes of developing solvent composition at constant humidity

According to the results reported earlier[9], and by considering the theoretical part of the present paper, it is obvious that a deeper insight into the chromatographic behaviour of metal chelates may be obtained by changing the composition of the developing solvent while the air humidity is kept constant. Then eqn. (17), or eqn. (17a) in the case of negligible solvation, simplifies to:

$$R_M = \text{const}_1 - \log [K_{SA_n} \cdot X_S] m/n \tag{17c}$$

Equation (17c) describes plots of R_M *vs.* log X_S, where two branches may be distinguished. First, when the product of $K_{SA} \cdot X_S$ is sufficiently high (*i.e.* the polar component S is strongly adsorbed or X_S is relatively high), the asymptote of the curve (17c) may be described by:

$$R_M = \text{const}_1 - \log (K_{SA_n}) m/n - \log (X_S) m/n = \\ = \text{const}_2 - \log (X_S) m/n \tag{17d}$$

which is the equation of a straight line in the coordinates R_M, log X_S, with a slope of m/n. The second branch of the curve may be found when the product of $K_{SA_n} \cdot X_S$ is so small that its contribution may be neglected. Then the equation of the asymptote is

$$R_M = \text{const}_1 \tag{17e}$$

i.e. R_F values of the metal chelates become independent of changes in composition of the developing solvent mixture in the range of changes considered. (This case is similar to development by a single organic solvent.) An experimental proof of the case considered (and described by eqn. 17e) was observed when metal dithizonates were developed by various chloroform–benzene solvent mixtures (Fig. 4).

For experimental proof of the first of above-mentioned branches (described by eqn. 17d), 1,2-dichloroethane, ethyl methyl ketone, acetone, n-propanol, and in the case of metal diethyldithiocarbamates also chloroform, were used as relatively polar components, with carbon tetrachloride as the essentially apolar unadsorbed

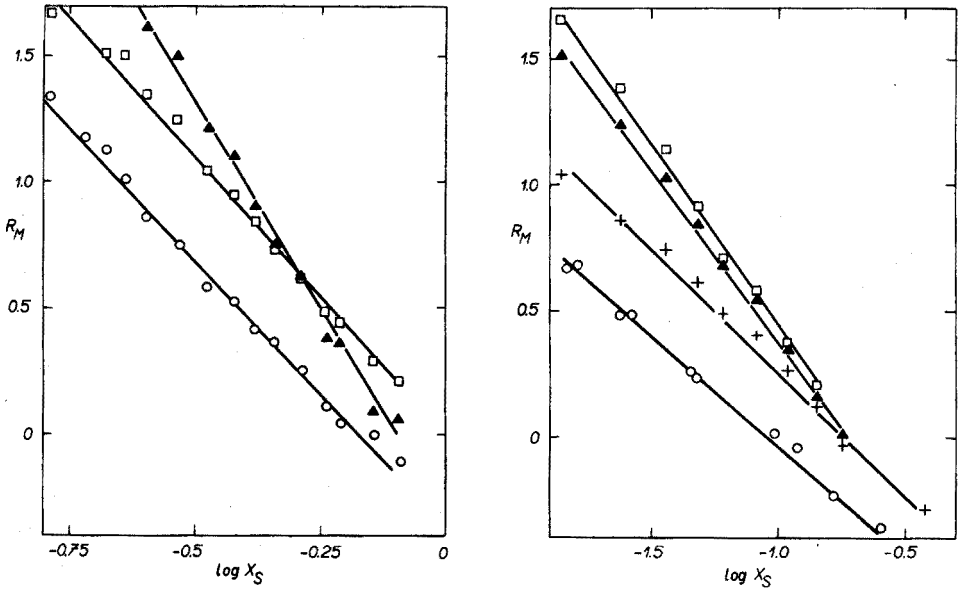

Fig. 5. The R_M *vs.* log X_S relationships for mercury, nickel and cobalt dithizonates. N = CCl_4, S = $C_2H_4Cl_2$. Runs no. 1, 7 and 8 of Table I. (▲), Co; (□), Ni; (○), Hg.

Fig. 6. The R_M *vs.* log X_S relationships for bismuth, cobalt, copper and mercury diethyldithiocarbamates. N = CCl_4, S = acetone. Runs no. 33, 36, 42 and 44 of Table II. (□), Bi; (▲), Co; (+), Cu; (○), Hg.

TABLE I

STRAIGHT LINES $R_M = a + b \log X_S$ OF METAL DITHIZONATES

Run no.	*Solute*	*Slope b* ($\pm s$)[a]	*Abscissa a* ($\pm s$)	n^b	*Procedure*	*Remarks*
S = 1,2-dichloroethane						
1	$Hg(HDz)_2$	−2.10 (0.056)	−0.35 (0.027)	15	A	$P/P_0 = 60\%$
2	$Hg(HDz)_2$	−1.97 (0.068)	−0.12 (0.023)	18	B	$T = 19°$
3	$Cu(HDz)_2$	−2.08 (0.045)	−0.24 (0.024)	16	A	$P/P_0 = 60\%$
4	$Cd(HDz)_2$	−1.87 (0.050)	−0.19 (0.030)	14	A	$P/P_0 = 60\%$
5	$Zn(HDz)_2$	−1.96 (0.050)	−0.25 (0.027)	16	A	$P/P_0 = 60\%$
6	$Pb(HDz)_2$	−1.92 (0.026)	−0.18 (0.014)	16	A	$P/P_0 = 60\%$
7	$Ni(HDz)_2$	−2.11 (0.012)	+0.03 (0.064)	15	A	$P/P_0 = 60\%$
8	$Co(HDz)_2$	−3.35 (0.123)	−0.34 (0.055)	14	A	$P/P_0 = 60\%$
S = acetone						
9	$Hg(HDz)_2$	−0.85 (0.022)	−0.77 (0.027)	20	B	$T = 20°$
10	$Hg(HDz)_2$	−0.91 (0.042)	−0.92 (0.057)	10	B	$T = 22°$
11	$Hg(HDz)_2$	−0.83 (0.029)	−0.93 (0.035)	10	B	$T = 24°$
12	$Cu(HDz)_2$	−0.84 (0.035)	−0.61 (0.039)	17	B	$T = 19°$
13	$Cu(HDz)_2$	−0.78 (0.037)	−0.71 (0.042)	9	B	$T = 23°$
14	$Zn(HDz)_2$	−0.83 (0.055)	−0.95 (0.059)	20	B	$T = 22°$
15	$Pb(HDz)_2$	−0.80 (0.058)	−0.72 (0.062)	10	B	$T = 22°$
16	$Ni(HDz)_2$	−1.02 (0.063)	−0.82 (0.064)	18	B	$T = 18°$
17	$Co(HDz)_2$	−1.40 (0.071)	−1.04 (0.076)	19	B	$T = 18°$

[a] The standard deviations ($\pm s$) were evaluated as normally done in full least-squares treatment: see, *e.g.* K. Eckschlager, *Errors in Chemical Analysis*, SNTL, Prague, 1961, pp. 147–149.

[b] Number of chromatograms included in the calculation of a and b.

TABLE II

STRAIGHT LINES $R_M = a + b \log X_S$ OF METAL DIETHYLDITHIOCARBAMATES

Run no.	Solute	Slope b ($\pm s$)[a]	Abscissa a ($\pm s$)	n[a]	Procedure	Remarks
S = 1,2-dichloroethane						
1	$Hg(DDTC)_2$	−1.75 (0.069)	−0.24 (0.038)	8	B	$T = 20°$
2	$Hg(DDTC)_2$	−1.79 (0.109)	−0.31 (0.067)	8	B	$T = 18°$
3	$Cu(DDTC)_2$	−1.74 (0.060)	−0.34 (0.026)	12	A	$P/P_0 = 57\%$
4	$Cu(DDTC)_2$	−1.97 (0.055)	−0.37 (0.023)	29	B	$T = 19°$
5	$Zn(DDTC)_2$	−1.67 (0.068)	−0.36 (0.042)	10	B	$T = 19°$
6	$Cd(DDTC)_2$	−1.90 (0.100)	−0.02 (0.044)	11	A	$P/P_0 = 57\%$
7	$Cd(DDTC)_2$	−2.01 (0.080)	−0.07 (0.030)	9	B	$T = 18°$
8	$Cd(DDTC)_2$	−1.96 (0.085)	−0.05 (0.032)	10	B	$T = 20°$
9	$Pb(DDTC)_2$	−1.79 (0.016)	−0.06 (0.004)	11	A	$P/P_0 = 57\%$
10	$Ni(DDTC)_2$	−1.99 (0.027)	−0.26 (0.012)	10	A	$P/P_0 = 57\%$
11	$Co(DDTC)_2$	−2.17 (0.118)	+0.02 (0.039)	10	A	$P/P_0 = 57\%$
12	$Co(DDTC)_2$	−2.53 (0.133)	+0.05 (0.053)	15	B	$T = 19°$
13	$Bi(DDTC)_3$	−2.68 (0.258)	+0.28 (0.086)	15	B	$T = 19°$
14	$In(DDTC)_3$	−2.42 (0.086)	−0.20 (0.023)	16	B	$T = 19°$
15	$Sb(DDTC)_3$	−2.38 (0.100)	+0.05 (0.037)	16	B	$T = 19°$
S = chloroform						
16	$Hg(DDTC)_2$	−2.02 (0.141)	−0.47 (0.063)	14	A	$P/P_0 = 55\%$
17	$Cu(DDTC)_2$	−1.92 (0.080)	−0.31 (0.035)	8	A	$P/P_0 = 55\%$
18	$Zn(DDTC)_2$	−1.99 (0.118)	−0.52 (0.058)	14	A	$P/P_0 = 55\%$
19	$Cd(DDTC)_2$	−1.79 (0.171)	+0.11 (0.081)	12	A	$P/P_0 = 55\%$
20	$Pb(DDTC)_2$	−2.02 (0.121)	−0.21 (0.057)	12	A	$P/P_0 = 55\%$
21	$Ni(DDTC)_2$	−2.00 (0.116)	−0.12 (0.054)	12	A	$P/P_0 = 55\%$
22	$Co(DDTC)_3$	−2.94 (0.216)	−0.24 (0.090)	12	A	$P/P_0 = 55\%$
23	$Bi(DDTC)_3$	−3.04 (0.261)	−0.29 (0.107)	10	A	$P/P_0 = 55\%$
S = n-propanol						
24	$Hg(DDTC)_2$	−1.20 (0.044)	−1.60 (0.070)	30	B	$T = 20°$
25	$Cu(DDTC)_2$	−1.07 (0.049)	−1.35 (0.080)	27	B	$T = 20°$
26	$Ni(DDTC)_2$	−1.27 (0.039)	−1.56 (0.060)	27	B	$T = 20°$
27	$Co(DDTC)_3$	−1.79 (0.090)	−2.30 (0.151)	14	B	$T = 20°$
28	$Bi(DDTC)_3$	−1.89 (0.067)	−2.32 (0.110)	15	B	$T = 20°$
S = methyl ethyl ketone						
29	$Hg(DDTC)_2$	−0.83 (0.076)	−0.69 (0.029)	20	B	$T = 19°$
30	$Cu(DDTC)_2$	−1.00 (0.036)	−0.73 (0.052)	20	B	$T = 19°$
31	$Co(DDTC)_3$	−1.54 (0.048)	−1.35 (0.075)	16	B	$T = 19°$
32	$Bi(DDTC)_3$	−1.32 (0.024)	−0.71 (0.036)	19	B	$T = 19°$
S = acetone						
33	$Hg(DDTC)_2$	−0.91 (0.037)	−0.94 (0.061)	10	A	$P/P_0 = 57\%$
34	$Cu(DDTC)_2$	−0.84 (0.085)	−0.61 (0.125)	13	A	$P/P_0 = 57\%$
35	$Cu(DDTC)_2$	−0.94 (0.091)	−0.79 (0.125)	10	B	Over $Mg(NO_3)_2 \cdot 6H_2O$, $T = 27°$

(continued)

TABLE II (*contd.*)

Run no.	*Solute*	*Slope b* ($\pm s$)[a]	*Abscissa a* ($\pm s$)	*n*[a]	*Procedure*	*Remarks*
36	$Cu(DDTC)_2$	−0.96 (0.050)	−0.69 (0.056)	10	B	$T=20.5°$
37	$Zn(DDTC)_2$	−0.92 (0.072)	−0.88 (0.095)	12	A	$P/P_0=57\%$
38	$Cd(DDTC)_2$	−0.96 (0.051)	−0.78 (0.072)	14	A	$P/P_0=57\%$
39	$Pb(DDTC)_2$	−0.88 (0.077)	−1.04 (0.110)	11	A	$P/P_0=57\%$
40	$Ni(DDTC)_2$	−0.95 (0.052)	−0.60 (0.073)	13	A	$P/P_0=57\%$
41	$Co(DDTC)_2$	−1.14 (0.052)	−0.93 (0.068)	12	A	$P/P_0=57\%$
42	$Co(DDTC)_3$	−1.49 (0.047)	−1.10 (0.057)	10	B	$T=20.5°$
43	$Bi(DDTC)_3$	−1.52 (0.043)	−1.38 (0.065)	12	A	$P/P_0=57\%$
44	$Bi(DDTC)_3$	−1.46 (0.052)	−1.03 (0.058)	10	B	$T=20.5°$
45	$In(DDTC)_3$	−1.29 (0.049)	−0.82 (0.063)	10	B	$T=20.5°$
46	$Sb(DDTC)_3$[b]	−1.29 (0.049)	−0.95 (0.060)	10	B	$T=20.5°$
47	$Fe(DDTC)_3$	−1.50 (0.047)	−1.17 (0.065)	14	A	$P/P_0=57\%$

[a] See Table I.
[b] Composition assumed.

diluent. The results obtained with metal dithizonates and diethyldithiocarbamates confirm the theoretical predictions outlined, as is obvious from Figs. 5 and 6 which are given as examples. Since the results plotted in R_M *vs.* log X_S co-ordinates gave straight lines in all cases, they could be treated by the least-squares method. The results of this treatment for metal dithizonates are listed in Table I. The data listed show a considerable correlation of the slopes b of R_M *vs.* log X_S plots with the stoichiometric composition of metal dithizonates, the only exception being cobalt dithizonate. This deviation might be caused by oxidation of cobalt during equilibration time, when the solid chelate on the strip is exposed to air. In addition to the dithizonates mentioned in Table I, palladium, silver and bismuth dithizonates were also investigated. With palladium dithizonate, two spots appeared during chromatography: a greyish-green one, which tailed back to the start so that its R_F could not be measured precisely, and a pink one, which moved faster than mercury dithizonate. Both silver and bismuth dithizonates were not evaluated because of tailing. Free dithizone decomposes during the equilibration time.

The results obtained with metal diethyldithiocarbamates are listed in Table II. As with metal dithizonates, a considerable correlation between the stoichiometric composition of the solutes and the slopes of their R_M *vs.* log X_S plots can be observed. Deviations were found, especially for the cobalt, indium and antimony chelates. With regard to the cobalt chelate, the most probable explanation is the tendency of cobalt(II) diethyldithiocarbamate to oxidize to the cobalt(III) chelate even in solution[18,19]. This view is supported by comparing results 11 and 41 of Table II, where a freshly prepared extract of cobalt chelate was chromatographed, with results 12, 22, 27 and 42, where the extracts had aged for up to 4 weeks before use. Indium and antimony diethyldithiocarbamates exhibited even more unusual behaviour than cobalt, as regards their R_M *vs.* log X_S slopes. While the ratio of the slopes of most diethyldithiocarbamates of divalent metals to those of tervalent ones is about 2:3 (irrespective of the solvent used,

cf. Table II), these ratios were about 2:2.5 for the indium and antimony chelates. Unfortunately, there are no literature data on the stoichiometry of these chelates, and so these cases are not discussed further.

In addition to the correlations of the slopes of the R_M *vs.* log X_S plots with the stoichiometry of the metal dithizonates and diethyldithiocarbamates, another remarkable phenomenon may be noted when the data listed in Tables I and II are compared. The slopes of the R_M *vs.* log X_S lines in solvent systems where S is 1,2-dichloroethane or chloroform, are about twice as high as those found in systems containing acetone, ethyl methyl ketone, or n-propanol. Furthermore, this finding is common for such different solutes as dithizonates and diethyldithiocarbamates. This becomes explicable if the equations derived in the theoretical part are considered: the slopes of the R_M *vs.* log X_S plots depend on the properties of component S of the developing mixture, as well as on the properties of the solutes (see *e.g.*, eqns. 17a, c, d). The phenomenon mentioned may therefore be considered as further experimental evidence of the adequacy of the equations derived, even though any direct information on the real stoichiometry of the adsorption complexes SA_n is not available at present.

Changes of humidity at constant composition of developing solvent

In order to confirm the conclusions made above, and to support the earlier far-reaching generalizations[9], it was considered very important to prove experimentally the validity of that part of eqns. (17) and (17a, b), which deals with the effect of the water content of the adsorbent on the chromatographic behaviour of metal chelates, *i.e.* the term $\log[1-f(P_W, T)]m/n$. In attempts to obtain proof, the mobility of solute spots was observed for a series of chromatostrips with the same solvent mixture, but in atmospheres of varied (controlled) humidity. Evaluation of the experimental results obtained was hampered by the same obstacle as earlier[9], *viz.* uncertainty in the value of the molar fraction of water in the layer adjacent to the surface of adsorbent particles, *i.e.* lack of knowledge of function $f(P_W, T)$. Previously[9], the relative humidity P/P_0 was employed to approximate this function, but in the present work, the adsorption isotherms of water (Fig. 3) were utilized. In this new approach, the R_M values of metal chelates were plotted against $\log(1-g_{H_2O}/g_{SiO_2})$, taking the temperature into account, of course. As can be seen in Figs. 7 and 8, almost linear relationships were found, at least for low contents of the polar component of the solvent mixture where its competition with molecules of water may be neglected. The predictions of eqn. (17) are obviously confirmed by these experimental findings, at least partially.

Further qualitative proof of the validity of eqn. (17) is obvious by comparing the slopes of the lines depicted in Figs. 7 and 8 with those given in Figs. 5 and 6: while the lines are mutually parallel for chelates of divalent metals in both R_M *vs.* log X_S and R_M *vs.* $\log(1-g_{H_2O}/g_{SiO_2})$ coordinates, the slopes for chelates such as cobalt dithizonate and cobalt diethyldithiocarbamate are higher in both coordinates. This observation is in agreement with eqn. (17), where both the term concerning the solvent composition and that expressing the effect of humidity are multiplied by m/n.

The limitations of the approximation of the function $f(P_W, T)$ used became

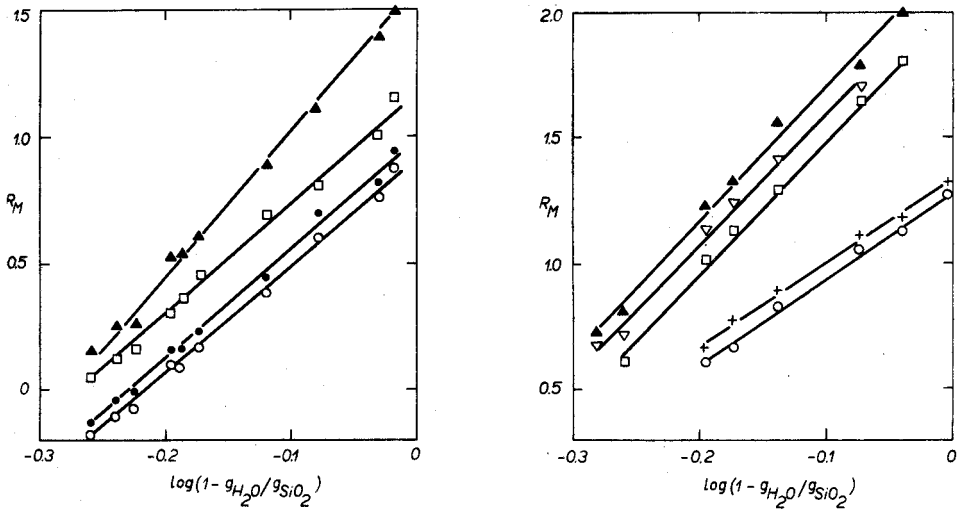

Fig. 7. The R_M *vs.* $\log(1-g_{H_2O}/g_{SiO_2})$ relationships for metal dithizonates at $T=22°$. N=CCl_4, S=$C_2H_4Cl_2$, log $X_S=-0.462$. (▲), Co; (□), Ni; (●), Zn; (○), Hg.

Fig. 8. The R_M *vs.* $\log(1-g_{H_2O}/g_{SiO_2})$ relationships for metal diethyldithiocarbamates at $T=26°$. N=CCl_4, S=acetone, log $X_S=-2.947$. (▲), Co; (▽), Fe; (□), In; (+), Cu; (○), Hg.

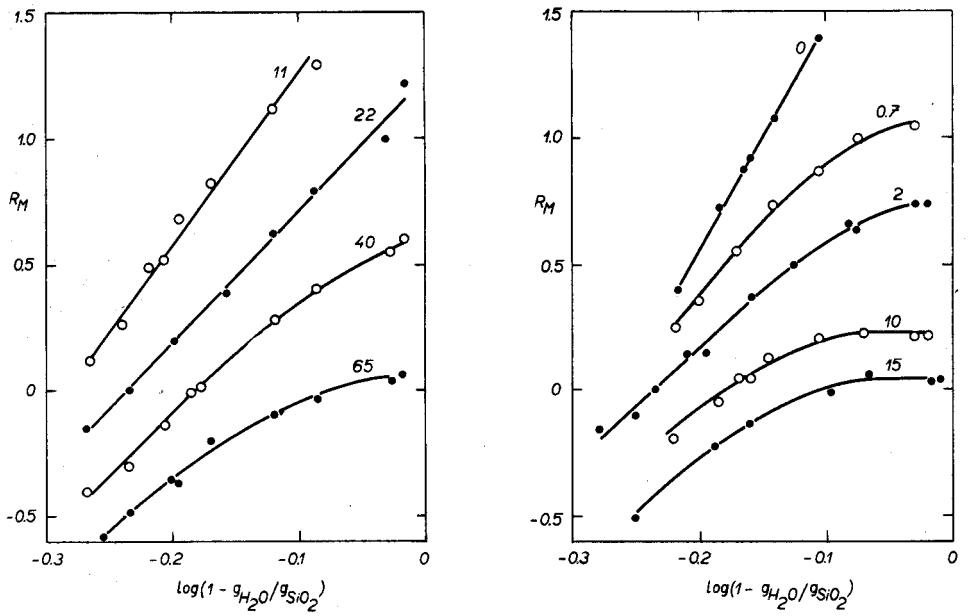

Fig. 9. Competition of water and of 1,2-dichloroethane during t.l.c. of mercury dithizonate. N=CCl_4, S=$C_2H_4Cl_2$; numbers on the curves indicate % (v/v) of $C_2H_4Cl_2$.

Fig. 10. Competition of water and of acetone during t.l.c. of copper diethyldithiocarbamate, N=CCl_4, S=acetone; numbers on the curves indicate % (v/v) of acetone.

obvious when the proportion of the polar component in the solvent was increased, so that competition with water was more probable. Then the R_W *vs.* $\log(1-g_{H_2O}/g_{SiO_2})$ plots deviated progressively from linearity. Figures 9 and 10 show the results obtained with mercury dithizonate and copper diethyldithiocarbamate; similar results were obtained with zinc, nickel and cobalt dithizonate, and with mercury, iron, indium and cobalt diethyldithiocarbamate. These deviations might be avoided by direct measurement of $(X_W)_a$ in the adsorbed layer; unfortunately, this is not possible with the available equipment.

Correlation between the extraction constants of the metal chelates and their adsorption constants on silica gel

The above theoretical conclusions about solvent composition and air humidity, supported by the experimental results, are of obvious practical importance in seeking optimal conditions for the separation of metal chelates. They can serve as a guide to changing either the solvent composition or the air humidity in order to improve separations. This is simple if the two metal chelates differ in the number of their bonds m to the adsorbent, but not if the two chelates are bound by the same number of bonds. In the latter case, eqn. (17) shows that neither the choice of solvent composition, nor a change of humidity conditions can improve the separation factor. The remaining possibility offered by eqn. (17) is to change the adsorption constant of the metal chelates, K_{ZA_m}, which may be achieved, as indicated earlier[1,4,8], by the choice of adsorbent; this possibility could be tested in future work. Here, another approach to the problem is discussed: the possibility of predicting—at least roughly—successful separations on the basis of prior general knowledge of the metal chelates.

There is a large literature on the extraction properties of metal chelates from aqueous solutions into organic solvents. Correlation of this knowledge with the chromatographic behaviour of metal chelates would allow at least qualitative estimates of the mobility order of the chelates. Adsorbents of the silica gel type, the adsorbing centres of which are hydroxyl groups, bind the metal chelate via hydrogen bridge formation; accordingly, the stronger the metal chelate, *i.e.* the lower the electron density in the outer parts of the chelate molecule, the higher its mobility during chromatography. To investigate the validity of this assumption, the value of the extraction constant was chosen as an approximate measure of the strength of a metal chelate. Obviously, formation constants would be more appropriate, but these are not so widely available as extraction constants. As a measure of the mobility of the metal chelates, the R_M values are most suitable, as can be seen from eqn. (17): the R_M values depend mainly on the value of the adsorption constant K_{ZA_m} of the chelate Z, other conditions, *e.g.* S, X_S, P_W, T, being constant.

For experimental testing, both the literature data on the chromatography of metal chelates and the data listed in Tables I and II were used. These data were plotted in Fig. 11 which includes: (*a*) the R_M values of metal benzoylacetonates[20] chromatographed on silica gel G (Merck) with an ammoniacal cyclohexane–butanol–benzoylacetone solvent plotted against the extraction constants for the benzoylacetonates into benzene[21]; (*b*) the R_M values of metal salicylaldoximates[22] chromatographed on silica gel D with 75:25 benzene–chloro-

form, against the extraction constants calculated from the extraction data of Dahl[23]; (*c*) the R_M values of metal 8-hydroxyquinolinates obtained on Siluten (silica gel sheets like Silufol but with a polyethylene support instead of aluminium) by development with chloroform–acetone mixtures as in Procedure A at air humidity $P/P_0 = 58\%$ (Table III), plotted against the extraction constants for these chelates into chloroform[21]; and (*d*) the R_M values of metal dithizonates calculated for average log X_S from the data of Table I (in order to avoid the risk of extrapolation to log $X_S = 0$), against the extraction constants for these chelates into carbon tetrachloride[24]. The value of the extraction constant of nickel dithizonate was estimated by simple recalculation of the value reported recently for a chloroform–water[25] system into a carbon tetrachloride–water system.

As can be observed in Fig. 11, the conclusion outlined above was proved to be valid for cobalt, copper and nickel benzoylacetonates and for salicylaldoximates of the same metals. Agreement is also obvious for metal 8-hydroxyquinolinates when it is realised that only chelates with the same slopes in the R_M *vs.* log X_S plots can be compared (*cf.* eqn. 17). With regard to the metal dithizonates, the correlation between the extraction constants and R_M values seems to be valid only separately for either the nickel, copper and mercury chelates or for the lead, cadmium and zinc chelates, even though both these groups exhibit the same number of bonds to silica gel (Table I). The break observed can be understood by scrutinizing the metal ion properties: lead, cadmium and zinc are known to have the coordination number 6, but nickel, copper and mercury have lower coordination numbers, frequently 4; because metal chelates are adsorbed at the silica gel surface, steric effects are obviously important.

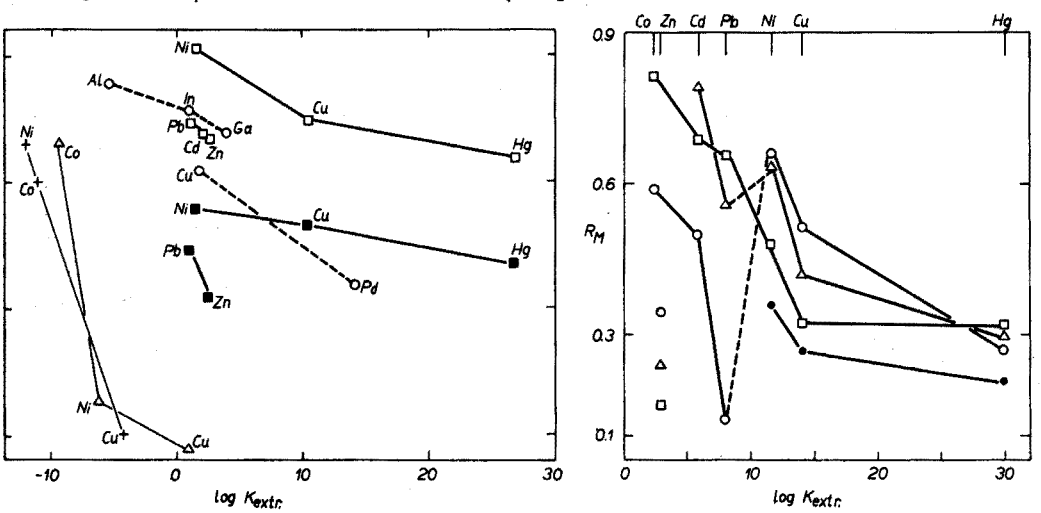

Fig. 11. Correlation of R_M with log K_{extr} of metal benzoylacetonates (+), metal salicylaldoximates (△), metal 8-hydroxyquinolinates (○), and of metal dithizonates developed either by CCl_4–$C_2H_4Cl_2$ mixture with log $X_S = -0.475$ (□) or by CCl_4–acetone mixture with log $X_S = -1.20$ (■).

Fig. 12. Correlation of R_M with log K_{extr} of metal diethyldithiocarbamates developed by $N = CCl_4$ and $S = CHCl_3$, log $X_S = -0.38$ (△); S = acetone, log $X_S = -1.33$ (○); S = n-propanol, log $X_S = -1.51$ (●); and $S = C_2H_4Cl_2$, log $X_S = -0.37$ or -0.31 (□). *Cf.* text.

TABLE III

CHROMATOGRAPHY OF METAL 8-HYDROXYQUINOLINATES ON SILUTEN

Run no.	*Solute*	*Graphical estimate of slope b*	n^a	R_M *at* $\log X_S = -0.5^b$	$\log K_{extr/CHCl_3}$ *(cf. ref. 21)*[c]
1	$Al(Ox)_3$	−1	4	0.90	−5.22
2	$In(Ox)_3$	−1	4	0.79	0.89
3	$Ga(Ox)_3$	−1	4	0.70	3.72
4	$Cu(Ox)_2$	−0.5	5	0.55	1.77
5	$Pd(Ox)_2$	−0.5	5	0.10	15

[a] Number of chromatograms.
[b] −0.5 is an average value of log X_S employed. N = $CHCl_3$, S = acetone.
[c] $K_{extr} = ([ML_q]_{org}\,[H^+]^q)/([M^{q+}][HL]^q_{org})$, where chelate ML_q is formed between metal ion M^{q+} and HL, subscript org denotes the organic phase.

In order to investigate these effects further, the correlation between R_M and $\log K_{extr}$ was studied on a larger set of experimental data obtained during the t.l.c. of metal diethyldithiocarbamates (Table II). Only results obtained under comparable conditions could be used. Thus, with chloroform as the active solvent component runs 16–22 may be compared (Procedure A at constant humidity and temperature); with acetone as the active component runs 33, 34, 37–41, are comparable; and with n-propanol (Procedure B) runs 24–26 are comparable. The data on slopes b and abscissae a from these runs were used to calculate the R_M values at the average values of $\log X_S$ and the R_M values were compared with the extraction constants found in the literature[18,24]. The results are shown in Fig. 12, which also includes the results obtained when the chromatograms were developed with mixtures of 1,2-dichloroethane and carbon tetrachloride. So that the data obtained by Procedure A (runs 3, 6, 9, 10 and 11) could be joined with those obtained by Procedure B (runs 2, 4, 5, 7 and 8) under different humidity and temperature conditions, the difference between the R_M values of copper diethyldithiocarbamate found in Procedures A and B, was added to the R_M values of all other diethyldithiocarbamates. Whenever two or more values of a and b are listed in Table II for the same solute, a weighted average of R_M values was calculated and used for Fig. 12.

As can be observed in Fig. 12, the hypothesis about a decrease in the R_M value of a metal chelate (*i.e.* increase in R_F and mobility) corresponding to an increase in its extraction constant was confirmed clearly for nickel, copper and mercury diethyldithiocarbamates, irrespective of the developing solvent used. This result is similar to that reported above for dithizonates of these metals. With regard to the diethyldithiocarbamates of metals with higher coordination numbers (*i.e.* lead, cadmium, zinc and divalent cobalt), the picture seems more complicated until it is recognized that the behaviour of zinc diethyldithiocarbamate is anomalous. The reason of this deviation of the zinc chelate is not clear.

In general, however, the correlation between the mobility of metal chelates on a thin layer of silica gel and the values of their extraction constants seems to be confirmed also for metal diethyldithiocarbamates. Even though more experi-

mental evidence of such a correlation is necessary, it seems useful as a practical guide for a preliminary estimate of the probable mobility order of metal chelates on the basis of extraction data, if used with care.

The author wishes to express his deep gratitude for encouraging interest to Professor L. Sommer of J. E. Purkyně University, Brno, to Professor E. Soczewiński, Akademia Medyczna, Lublin, and to Dr. I. Dahl of National Institute of Public Health, Oslo, who kindly provided the numerical data on the extraction of metal salicylaldoximates.

SUMMARY

The model of thin-layer chromatography suggested earlier has been developed so that it describes solute behaviour more thoroughly. Equations have been derived which describe particular cases such as development by a single solvent, or by a mixture of two solvents of different polarity, or by a mixed solvent of constant composition at varying humidity. Experimental verification was provided by a study of the t.l.c. behaviour of metal dithizonates and diethyldithiocarbamates on Silufol. A comparison of the mobilities of these metal chelates, as well as of those of 8-hydroxyquinoline, salicylaldoxime and benzoylacetone, with their extraction constants showed a mutual correlation between these properties.

RÉSUMÉ

On propose une modification de la chromatographie sur couche mince, permettant d'arriver à des équations décrivant des cas particuliers tels que développement par un solvant unique ou par un mélange de deux solvants de polarité différente, ou par un solvant mixte de composition constante, à diverses humidités. Une étude expérimentale est effectuée au moyen de dithizonates métalliques et de diéthyldithiocarbamates sur Silufol. Une comparaison des mobilités de ces chélates métalliques, de mème que ceux de l'hydroxy-8-quinoléine, de la salicylaldoxime et de la benzoylacétone, avec leurs constantes d'extraction montre une corrélation mutuelle entre ces propriétés.

ZUSAMMENFASSUNG

Das seinerzeit vorgeschlagene Modell der Dünnschichtchromatographie wurde weiter entwickelt, so dass es das Verhalten des Gelösten gründlicher beschreibt. Es wurden Gleichungen abgeleitet, welche besondere Fälle wie die Entwicklung des Chromatogramms durch ein einzelnes Lösungsmittel oder durch ein Gemisch zweier Lösungsmittel verschiedener Polarität oder durch ein gemischtes Lösungsmittel konstanter Zusammensetzung, aber bei verschiedenen Feuchtigkeiten beschreiben. Diese Gleichungen wurden durch Untersuchung des dünnschichtchromatographischen Verhaltens der Metall-Dithizonate und -Diäthyldithiocarbamate auf Silufol geprüft. Der Vergleich der Beweglichkeit dieser Metall-Chelate eben so jener des 8-Hydroxychinolins, des Salicylaldoxims und des

Benzoylacetons mit ihren Extraktionskonstanten zeigte eine Wechselbeziehung zwischen diesen Eigenschaften.

REFERENCES

1 A. I. Busev, I. P. Kharlamov and O. V. Smirnova, *Zavod. Lab.*, 35 (1969) 1301; *Zh. Anal. Khim.*, 25 (1970) 2541.
2 J. Rai and V. P. Kukreja, *Chromatographia*, 3 (1970) 41.
3 M. Kiboku, *Jap. Anal.*, 17 (1968) 722.
4 A. Galík and A. Vincourová, *Anal. Chim. Acta*, 46 (1969) 129.
5 L. B. Hilliard and H. Freiser, *Anal. Chem.*, 24 (1952) 752.
6 A. J. Blair and D. A. Pantony, *Anal. Chim. Acta*, 14 (1956) 545; 16 (1957) 121.
7 M. P. T. Bradley and D. A. Pantony, *Anal. Chim. Acta*, 38 (1967) 113; *Talanta*, 16 (1969) 473.
8 A. I. Busev, I. P. Kharlamov and O. V. Smirnova, *Anal. Lett.*, 3 (1970) 177.
9 A. Galík, *Anal. Chim. Acta*, 57 (1971) 399.
10 E. Soczewiński, *Anal. Chem.*, 41 (1969) 179.
11 Through A. Tockstein, in I. M. Hais and K. Macek, *Paper Chromatography* (in Czech), NČSAV, Prague, 1954, pp. 45 to 70.
12 G. H. Stewart and T. D. Gierke, *J. Chromatogr. Sci.*, 8 (1970) 129.
13 E. V. Kuznetsova and E. O. Turgel', *Zh. Anal. Khim.*, 26 (1971) 2311.
14 S. Sandroni and F. Geiss, *Chromatographia*, 2 (1969) 165.
15 Yu. Yu. Lurye, *Spravochnik po Anal. Khim.*, Khimiya, Moscow, 1965.
16 V. I. Perelman, *Little Chemical Handbook* (in Czech), SNTL, Prague, 1954, pp. 257–265.
17 *Tables on Physical Chemistry Data* (in Czech), SNTL, Prague, 1953, pp. 497 to 498.
18 J. Starý and K. Kratzer, *Anal. Chim. Acta*, 40 (1968) 93.
19 J. Starý and J. Růžička, *Talanta*, 15 (1969) 505.
20 J. C. Trehan, *Chromatographia*, 2 (1969) 17.
21 J. Starý, *The Extraction of Metal Chelates* (in Russian), Mir, Moscow, 1966.
22 H.-J. Senf, *Mikrochim. Acta*, (1969) 522.
23 I. Dahl, *Anal. Chim. Acta*, 41 (1968) 9.
24 J. Starý and R. Burcl, *Radiochim. Radioanal. Lett.*, 7 (1971) 235.
25 B. E. McClellan and P. Sabel, *Anal. Chem.*, 41 (1969) 1077.

Analytica Chimica Acta, 67 (1973) 377–385

THE APPLICATION OF PHOTO-OXIDATION TO THE DETERMINATION OF STABLE COBALT IN SEA WATER

B. R. HARVEY and J. W. R. DUTTON

Ministry of Agriculture, Fisheries and Food, Fisheries Radiobiological Laboratory, Hamilton Dock, Lowestoft, Suffolk (England)

(Received 12th April 1973)

Cobalt is an element of considerable importance in biogeochemical systems. The presence of artificial radioactive isotopes of cobalt in the sea as a result of nuclear waste disposal now makes it even more desirable to acquire an accurate knowledge of the distribution and behaviour of stable cobalt in the marine environment. Only in this way is it possible to make accurate assessments of the behaviour and fate of the radionuclides discharged.

Many of the methods that have been proposed for the determination of cobalt in sea water are unable to provide reliable data below a few hundred ng l^{-1}, either because of lack of instrumental sensitivity or of interference in the form of very large blank readings.

Robertson[1] and other workers, using neutron activation analysis of the dried salt residue, have shown that the concentration of cobalt in sea water is frequently less than 0.05 μg l^{-1}, but such techniques are not widely available for routine work.

The use of photo-oxidation to assist in the determination of trace elements in sea water was first envisaged by Armstrong *et al.*[2], who showed that complex organic molecules are broken down under the influence of ultraviolet light. During an assessment of the procedure at this laboratory, with a Hanovia 1-l photochemical reactor[3], it was found that, at the natural pH of sea water, manganese was deposited—presumably as a hydrated form of manganese dioxide—on the quartz jacket surrounding the u.v. lamp.

Manganese dioxide has previously been used to scavenge trace elements from sea water[4]. In particular, cobalt in sea water has been scavenged in this way[5], and it therefore seemed worthwhile to investigate the scavenging properties of the deposit in the u.v. irradiator. It was found that small quantities of several trace metals, including cobalt, were co-precipitated if the manganese content of the original sea-water sample was increased to about 100 μg l^{-1} before irradiation.

The present paper describes the development of a procedure, based on the precipitation of manganese dioxide in the photochemical reactor, which permits the determination of cobalt in sea water down to a few nanograms per litre with minimal contamination. Pulse polarography is used for the cobalt measurement.

EXPERIMENTAL

Apparatus

A standard 1-l Hanovia photochemical reactor was used, fitted with a 2-W

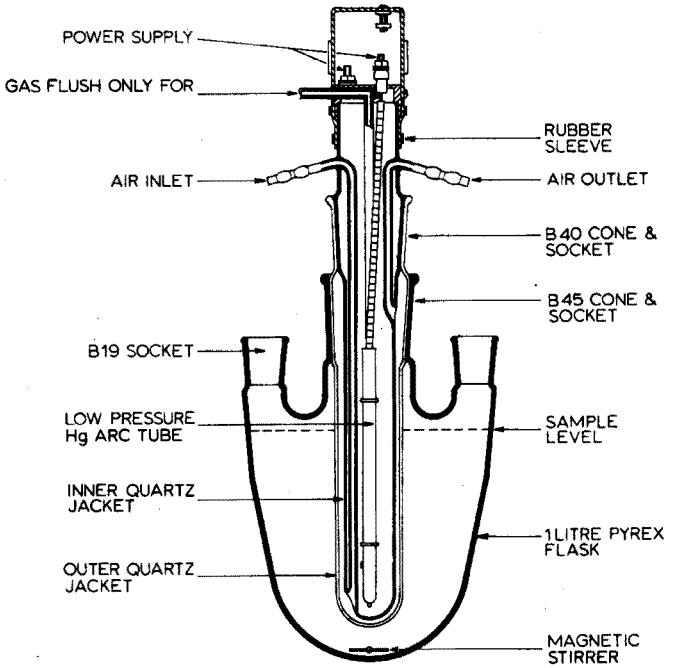

Fig. 1. Hanovia photochemical reactor used for sample irradiation. The gas flush inlet/outlet and the outer quartz jacket were not used during irradiation.

low-pressure mercury vapour discharge lamp radiating mainly at 254 and 185 nm. The apparatus normally consists of a 1-l Pyrex flask, with the lamp mounted vertically and enclosed in an inner and an outer quartz jacket (Fig. 1). The outer jacket was not used during the irradiation.

When radioactive tracers were used, assay was carried out with standard γ-counting equipment: a 3×3 in. NaI(Tl) crystal coupled to a simple scaling device, gated to measure the count-rate under the total absorption peaks area of the spectra. The photon energies used were 0.122 MeV for ^{57}Co ($t_{\frac{1}{2}}$ 270 days), 1.17 and 1.33 MeV for ^{60}Co ($t_{\frac{1}{2}}$ 5.26 years), and 0.84 MeV for ^{54}Mn ($t_{\frac{1}{2}}$ 314 days). The radioactive tracers were obtained from the Radiochemical Centre, Amersham.

Polarographic measurements were made with a Shandon-Southern A3100 pulse polarograph. All polarograms were obtained in the derivative mode, with a 50-mV pulse height and a 1-s mercury drop-life. The glass polarographic cells were maintained at 25° in a thermostatically controlled water bath.

Reagents

Manganese solution (100 μg ml^{-1}). Dissolve 0.18 g of analytical-grade manganese(II) chloride tetrahydrate in distilled water and dilute to 500 ml.

Sulphurous acid solution. Dilute 13 ml of Aristar (BDH Ltd.) hydrochloric acid (d. 1.18) to 1 l with distilled water, and pass a slow stream of sulphur dioxide through the solution from a cylinder of the compressed gas for 1 min.

Aristar reagents were used in the preparation of dilute acid and ammonia solutions with twice-distilled water. Analar dimethylglyoxime was used.

Standard cobalt solutions. A 1000 μg ml^{-1} stock solution was kept in 1 *M* hydrochloric acid. Dilutions of 100, 10, 1 and 0.1 μg ml^{-1} were prepared in 0.1 *M* hydrochloric acid as required. Standard additions were made by dropwise addition of the appropriate standard from 10-ml polythene bottles drawn out at the neck to provide dropping facilities. The amount of standard added to the sample (usually 0.02–0.1 μg) was determined by weighing the polythene bottle, containing the standard solution, on a balance (to an accuracy of 0.1 mg) before and after making the addition.

Note. All reagents, especially the hydrochloric acid, should be tested for cobalt content by evaporating 50 ml to dryness and then measuring the cobalt content by pulse polarography; batch selection may be necessary to secure a low cobalt blank. Impurities in the ammonia solution cause special problems which are discussed below.

The co-precipitation of cobalt with manganese dioxide

The photo-oxidation of manganese and its deposition as manganese dioxide on to the quartz jacket surrounding the u.v. lamp in the photochemical reactor was first demonstrated by an experiment in which 500 μg of manganese (labelled with ^{54}Mn) was dissolved in 1 l of distilled water and irradiated. When the irradiated solution was filtered, none of the ^{54}Mn activity was found on the filter paper; about 50% was present in the filtrate and the rest was recovered from the quartz thimble by washing with dilute hydrochloric acid.

A series of experiments was then carried out in which varying amounts of manganese (labelled with ^{54}Mn) were added to filtered sea water and irradiated for several hours. The deposition of manganese on to the central thimble was followed by removing aliquots of sea water from the reactor at intervals and measuring the radioactivity. At the end of the experiment, the thimble was washed with dilute hydrochloric acid to recover the manganese; this solution was counted to provide a final check on the recovery figure. A quantitative collection of manganese at concentrations between about 1 and 100 μg l^{-1} was achieved by irradiation for 7–8 h.

The rate of deposition of ionic cobalt on to manganese dioxide formed by photo-oxidation was studied by the addition of cobalt (labelled with ^{60}Co) as cobalt(II) chloride to sea water in the photochemical reactor, to which varying amounts of stable manganese had been added. Figure 2 shows that quantitative deposition of ^{60}Co occurred in about 8 h with initial stable manganese levels of 50–100 μg l^{-1}, and very little deposition with no addition of manganese.

The experiments were then continued with 100 μg l^{-1} of stable manganese with various complexes of cobalt: as an ethylenediaminetetraacetic acid complex, as cobalticyanide and, because a small percentage of cobalt in sea water is present as the vitamin B_{12} complex[6], as cyanocobalamin. This last complex was obtained from the Radiochemical Centre, Amersham, labelled with ^{57}Co; the other forms were labelled at the laboratory by adding ^{60}Co. The level of stable cobalt added in these tracer experiments was in all cases less than 0.5 μg l^{-1} of sea water. Examples of the way in which cobalt is scavenged from

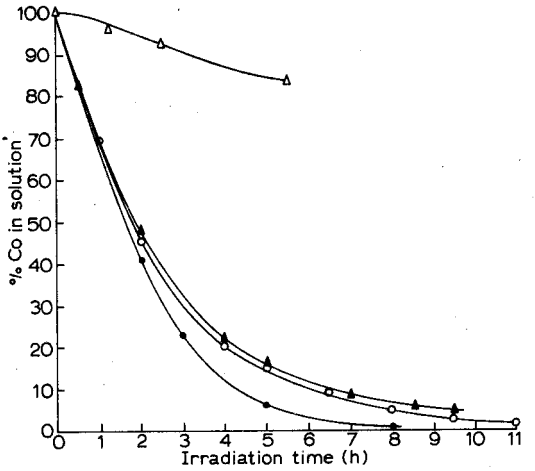

Fig. 2. Co-precipitation of cobalt(II) with varying amounts of manganese carrier in the photochemical reactor. (△) No carrier; (▲) 50 μg Mn carrier; (○) 80 μg Mn carrier; (●) 100 μg Mn carrier.

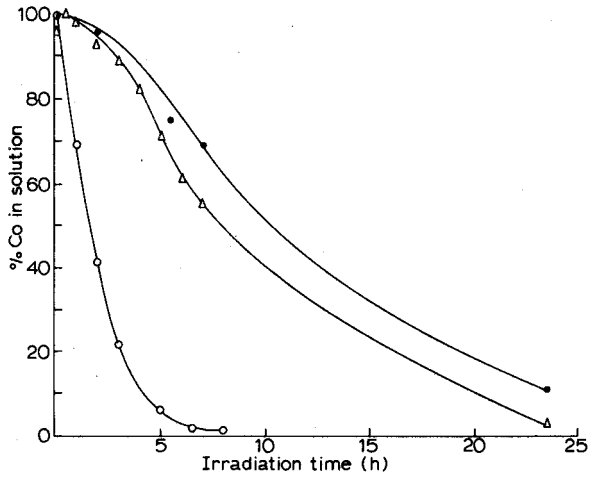

Fig. 3. Co-precipitation of cobalt in various forms with 100 μg of manganese as scavenger. (●) ^{57}Co from cyanocobalamin; (△) ^{60}Co from cobalticyanide; (○) ^{60}Co from cobalt chloride.

complexes and from the ionic state are shown in Fig. 3. It can be seen that virtually complete removal of cobalt from the complexed condition is achieved after irradiation for *ca.* 24 h. These experiments do not provide absolute proof that the complexes are actually being broken down before the cobalt is scavenged; this seems to be the most likely mechanism, however, because extended periods of irradiation were needed to complete the deposition of this initially complexed cobalt, and there was no indication that manganese was acting as a slow scavenger for such complexes.

Determination of cobalt by pulse polarography

One of the most sensitive methods available for the determination of cobalt

in solution depends on the polarographic measurement of the reduction wave (at −1.10 V) of the cobalt–dimethylglyoxime complex in ammoniacal solution[7]. This method is very convenient for measuring cobalt scavenged with the manganese dioxide in the photochemical reactor, because no interference is experienced from the reduction of manganese(II) at −1.45 V. Some nickel and zinc are co-precipitated along with cobalt in the scavenge, but the cobalt reduction peak at −1.10 V is again well separated from that of nickel–DMG at −0.95 V and the zinc(II) peak at −1.24 V.

Procedure. To determine cobalt in the manganese dioxide scavenge, the deposit adhering to the quartz jacket of the photochemical reactor was first dissolved in hydrochloric acid solution—0.15 *M* containing a trace of sulphur dioxide; the outer quartz jacket provided with the equipment but not used in the irradiation, was used for this dissolution. The sulphur dioxide assists the dissolution and permits a lower hydrochloric acid concentration to be used, thus minimizing contamination. The solution was then transferred to a 50-ml beaker and evaporated to dryness under an infrared lamp. The residue was dissolved in 4 ml of 0.625 *M* hydrochloric acid, 1 ml of 5 *M* ammonia solution was added to bring the final base electrolyte concentration to 0.5 *M* ammonium chloride–0.5 *M* ammonia, and 0.1 ml of an ethanolic 1% solution of DMG was added to complex the cobalt. The mixture was then transferred to a polarographic cell and de-oxygenated for 5 min with oxygen-free nitrogen, and a derivative polarogram was plotted starting at −1.0 V. A second polarogram was plotted after making a standard addition of a suitable quantity of cobalt. A further addition of cobalt can be made if required.

Blank readings

Great efforts were made to minimize the blank reading by careful selection of chemicals, particularly the hydrochloric acid. This eventually led to difficulties at the lower end of the calibration, where a negative bias arose, and no positive reading could be obtained for less than a few nanograms of cobalt added to the base electrolyte (Fig. 4, line A). This apparent threshold level of cobalt was only slightly affected by changes in the DMG concentration but appeared to be directly proportional to the amount of ammonia solution added. The ammonia

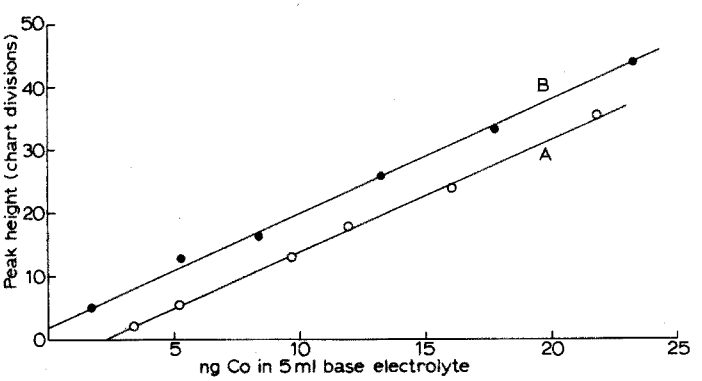

Fig. 4. Calibration of pulse polarograph for cobalt as the DMG complex. (A) Base electrolyte; (B) base electrolyte doped with 3.3 ng of cobalt.

concentration does not itself affect the cobalt–DMG reduction peak height between *ca.* 0.3 *M* and 2 *M* ammonia solution and it was therefore concluded that trace impurities, probably organic bases, in the ammonia solution were forming complexes with the cobalt which were stronger than the cobalt–DMG complex. The problem is at present being overcome by "doping" the ammonia solution with sufficient cobalt (2–3 ng) to produce a small positive blank reading, and the resultant calibration graph is shown in Fig. 4, line B.

RESULTS AND DISCUSSION

Figure 3 shows that well over 90% of the radioactive cobalt added to sea water in various chemical forms can be scavenged by irradiation for a period of up to 24 h in the photochemical reactor, if 100 μg of manganese is used as a carrier. In some of the experiments, the level of stable cobalt carrier was as high as 0.5 μg l^{-1}; it was considered essential therefore to evaluate the procedure as a method for determining cobalt in sea water over the whole range of concentrations likely to be encountered in samples.

Ten separate 1-l aliquots of a 20-l sample of Millipore-filtered sea water were irradiated for 16 h (overnight) at pH 8.0–8.5 in the presence of 100 μg of manganese. The manganese dioxide deposit was then dissolved from the quartz thimble and cobalt determined by pulse polarography as described above. A second 16-h scavenge was then carried out on each sample after adding a further 100 μg of manganese and re-adjusting the pH with a drop of ammonia solution. The samples were then spiked with different amounts of stable cobalt and a third scavenge was performed with added manganese. Table I shows the results obtained in these experiments; the ten replicate determinations on the 20-l sample are given in column 1 and indicate that cobalt can be measured with a precision

TABLE I

DETERMINATIONS AND RECOVERY OF COBALT FROM SEA WATER

Aliquot number	*1st scavenge (ng Co l^{-1})*[a,b]	*Co added before 3rd scavenge (ng)*	*Co found at 3rd scavenge (ng)*	*% Recovery of spike*
1	16.1	3.4	3.3	97
2	16.8	9.8	9.5	97
3	16.6	24	23	96
4	15.6	43	40	93
5	15.8	76	73	96
6	16.5	161	154	96
7	16.1	267	255	96
8	17.2	490	465	95
9	15.9	1003	894	89
10	16.5	2076	1690	81
Mean	16.3 ± 0.5 (σ one result)			

[a] The polarogram chart was read to the nearest ½ division (fsd = 100 divisions), corresponding to about 0.6 ng Co.

[b] In the second scavenge, the results were 0.6 ng Co l^{-1} in all cases (see text).

(σ) of $\pm 3\%$ at the 16 ng l^{-1} level. The sensitivity of the polarographic measurement was limited by the sloping base line (caused by the presence of DMG) and this limited the accuracy with which the chart could be read to about ± 1 division (*ca.* 0.6 ng of cobalt). The amount of cobalt found in the second scavenge was very close to the detection limit, the results being 0.6 (± 0.6) ng Co l^{-1} for all 10 scavenges. It can be seen from column 5 that recovery of added cobalt was substantially constant up to about 0.5 μg l^{-1} (average 95.7%). As the cobalt concentration increased beyond this level, recovery gradually diminished but was still more than 80% at 2 μg l^{-1}.

The cobalt concentration is unlikely to exceed the working limits of the method in the vast majority of sea-water samples. However, samples taken close inshore often show considerably higher concentrations of cobalt as well as other heavy metals, and in such cases a second scavenge may be necessary to achieve complete recovery.

The method has now been incorporated into a programme of analysis for selected trace metals in sea water and certain indicator organisms; this is part of the research supporting the control of radioactive waste disposal to the marine environment around the British Isles for which the Fisheries Radiobiological Laboratory is responsible. An extensive network of sampling points has been established, centred mainly on the Irish Sea but including also the North Sea and north-east Atlantic Ocean. Data are being obtained for both radioactive and

TABLE II

CONCENTRATION OF COBALT IN BRITISH COASTAL WATERS (SURFACE SAMPLES)

Sampling date	*Location*		*Concentration (ng l^{-1})*		
	Latitude	*Longitude*	*Filtrate*	*Particulate*	*Total*
28 Sept. 1971	53°41′00″N	00°31′00″E	18	3	21
	55 05 00	00 50 00 W	25	3	28
	56 12 00	01 45 00	7	3	10
29 Sept. 1971	56 56 00	01 14 00	7	≈0.6	8
	57 40 00	00 40 00	13	5	18
	58 08 00	01 35 00	8	3	11
	58 34 00	02 28 00	9	8	17
	58 38 30	03 41 00	10	4	14
	58 40 00	05 01 30	10	1	11
30 Sept. 1971	58 20 00	05 45 00	9	2	11
	58 45 00	07 10 00	11	1	12
	59 00 00	08 30 00	9	1	10
	59 15 00	10 00 00	8	2	10
1 Oct. 1971	58 30 00	10 50 00	9	3	12
	57 40 00	11 40 00	8	3	11
	57 22 00	10 10 00	8	2	10
	57 00 00	08 30 00	7	6	13
	56 45 00	07 14 00	8	2	10
	56 00 00	07 00 00	9	≈0.6	10

stable isotopes for a number of trace heavy metals[8] and other elements of radiological importance.

Table II shows some typical results for cobalt in surface waters for samples collected during a research cruise in the North Sea and north-east Atlantic. Immediately after collection, the sample was filtered through a 142-mm, 0.22-μm Millipore filter membrane supported in a Teflon filter press. The first 3 l of filtrate served to wash the filter paper and were discarded; the fourth litre was retained for cobalt analysis by rapidly freezing and storing at $-20°$ until the determination could be completed. The filter membrane containing the particulate fraction was stored dry in a polystyrene petri dish. Analysis of this fraction was completed by leaching the filter membrane with a mixture of hydrochloric acid and hydrogen peroxide, followed by the destruction of organic matter with nitric and perchloric acids and subsequent pulse polarographic determination of cobalt.

The authors wish to thank Mr. J. H. Clark who carried out much of the photochemical investigation[3] at this laboratory during the second-year industrial training period of his integrated applied chemistry course at the University of Salford (Lancashire).

SUMMARY

A method is described for the determination of nanogram quantities of cobalt in a 1-l sample of sea water after preconcentration with sub-milligram quantities of manganese dioxide formed by the oxidation of manganese(II) in a photochemical reactor. The cobalt is measured by pulse polarography as the dimethylglyoximate after dissolving the manganese dioxide deposit adhering to the quartz jacket surrounding the ultraviolet lamp. The detection limit of the method is *ca.* 0.6 ng Co l^{-1}.

RÉSUMÉ

Une méthode est décrite pour le dosage du cobalt, en quantité de l'ordre du nanogramme, dans 1 l d'eau de mer. On procède à une préconcentration au moyen de dioxyde de manganèse obtenu par oxydation du manganèse(II) dans un réacteur photochimique. Le cobalt est dosé par polarographie à pulsation, sous forme de diméthylglyoximate, après dissolution du dioxyde de manganèse déposé sur la lampe. La limite de détection de cette méthode est d'environ 0.6 ng Co l^{-1}.

ZUSAMMENFASSUNG

Es wird eine Methode für die Bestimmung von Nanogramm-Mengen Kobalt in einer Probe von 1 l Meerwasser beschrieben. Das Kobalt wird mit Hilfe von Submilligramm-Mengen Mangandioxid angereichert, das durch photochemische Oxidation von Mangan(II) gebildet wird. Der Mangandioxid-Niederschlag, der an dem die Ultraviolett-Lampe umgebenden Quarzmantel haftet, wird aufgelöst und das Kobalt als Dimethylglyoximat durch Pulse-Polarographie bestimmt. Die Nachweisgrenze der Methode ist *ca.* 0.6 ng Co l^{-1}.

REFERENCES

1 D. E. Robertson, *Geochim. Cosmochim. Acta*, 34 (1970) 553.
2 F. Armstrong, P. M. Williams and J. D. H. Strickland, *Nature*, 211 (1966) 481.
3 B. R. Harvey and J. H. Clark, *M.A.F.F. Fish. Radiobiol. Lab., Lowestoft, Tech. Memo. 1*, 1970.
4 N. Yamagata and K. Iwashima, *Nature*, 200 (1963) 52.
5 R. Fukai, *J. Oceanogr. Soc. Jap.*, 24 (1968) 265.
6 L. Provasoli, in *The Sea*, Vol. 2, Wiley, 1964, pp. 162–219.
7 P. Nangniot, *J. Electroanal. Chem.*, 7 (1964) 50.
8 A. Preston, D. F. Jefferies, J. W. R. Dutton, B. R. Harvey and A. K. Steele, *Environ. Pollut.*, 3 (1972) 69.

Analytica Chimica Acta, 67 (1973) 387–393

SURFACTANT-SELECTIVE ELECTRODES

PART I. AN IMPROVED LIQUID ION-EXCHANGER

B. J. BIRCH and D. E. CLARKE

Unilever Research Port Sunlight Laboratory, Unilever Limited, Port Sunlight, Wirral, Cheshire L62 4XN (England)

(Received 17th May 1973)

A previous communication[1] discussed the limitations of a liquid ion-exchanger membrane electrode, selective to the dodecylsulphate anion, which utilized nitrobenzene as the carrier liquid. This electrode was satisfactory in the absence of micellar material but, at the electrode–solution interface, interaction between nitrobenzene and surfactant gave a low value for the critical micelle concentration (c.m.c.).

An exhaustive search for an alternative water-immiscible liquid led to *o*-dichlorobenzene. This liquid has no apparent effect upon the c.m.c. of sodium dodecylsulphate within experimental error, as shown by pNa and conductance measurements. This implies that the liquid does not alter the micellar properties, even though u.v. measurements indicate that some solubilization does occur. It was found, however, that at temperatures below 32°, the solubility of the original ion-association complex ($C_{12}H_{25}SO_4^- \cdot C_{16}H_{33}(CH_3)_3N^+$) in this solvent was too small for the electrode to function satisfactorily. This was overcome by addition of small amounts of water-insoluble hydrogen-bonding solutes. The most satisfactory "solvent" for the 10^{-3} *M* ion-association complex was found to be 0.17 *M* hexachlorobenzene plus 0.017 *M* bromoacetanilide in *o*-dichlorobenzene, for which the critical solution temperature was 18°.

A variety of carrier complexes of dodecylsulphate with large organic cations were synthesized, which were soluble in *o*-dichlorobenzene without addition of further solutes. These cations were: hexadecylpyridinium, hyamine 1622, tetrazolium violet, tetrazolium blue, crystal violet, phenazine methosulphate and 1,10-phenanthroline. With the exception of the hexadecylpyridinium cation, electrodes based upon these complexes in *o*-dichlorobenzene gave unstable and rapidly increasing potential values above about $4 \cdot 10^{-3}$ *M* sodium dodecylsulphate (SDS). This is ascribed to solubilization of the complex by the SDS solution immediately adjacent to the electrode sensing surface.

When the dodecylsulphate electrode, based on the original complex plus added solutes, or on the hexadecylpyridinium complex in *o*-dichlorobenzene, was used in sodium dodecylsulphate solutions, with the experimental set-up described previously[1], results identical to those for the electrode with nitrobenzene as exchanger liquid were obtained for the electrode stability and drift, the limit of detection (10^{-6} *M*), for the premicellar slope of the *E vs.* log a_{DS} plot, and for the degree of micellar dissociation (α). However, the c.m.c. value for sodium dodecylsulphate

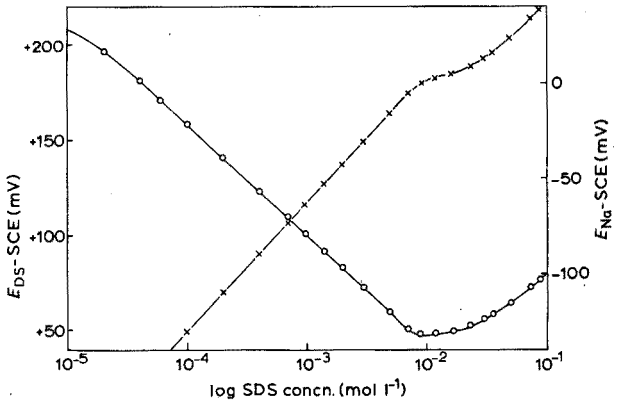

Fig. 1. Response of dodecylsulphate and sodium electrodes in SDS solutions. (○) DS^-; (×) Na^+.

was increased to $8.0 \cdot 10^{-3}$ *M*. This value was identical with that obtained by simultaneous use of a sodium-selective electrode (Fig. 1), and is completely consistent with the accepted range of values[2].

The electrode was also used as a sensor for cationic surfactants. For tetradecyltrimethylammonium bromide, for example, the electrode gave near-Nernstian response, with a c.m.c. value of $2.6 \cdot 10^{-3}$ *M*. This value agreed well with that found by simultaneous use of a bromide-selective electrode. The ion-exchanger used was 10^{-3} *M* tetradecyltrimethylammoniumdodecyl sulphate plus hydrogen-bonding solutes in *o*-dichlorobenzene, with an internal reference solution of tetradecyltrimethylammonium bromide.

Occasionally, the production of a calibration curve for SDS resulted in a sudden increase in electrode potential from about 0.006 *M* SDS to the c.m.c., after which the potential fell in the usual manner. The deviation from the "correct" value at the c.m.c. was about 15 mV. This effect could also be obtained when micellar solutions were diluted to below the c.m.c. The cause of this phenomenon, the appearance of which seems random from electrode to electrode, has not been investigated in any detail. It can however be prevented by use of an internal reference electrode system consisting of a silver wire dipping into SDS solution, (*i.e.* without sodium chloride present) which implies that the effect may be due to transport of chloride ions across the membrane/internal reference solution interface. The solubility of silver dodecylsulphate in water ($5 \cdot 10^{-3}$ mol l^{-1}) is however too high for this internal reference electrode to be used with confidence. A satisfactory system (with no potential increase) has been obtained by replacing the silver wire by one of aluminium (solubility of aluminium dodecylsulphate is *ca.* 10^{-4} mol l^{-1}).

EFFECT OF INTERFERING IONS

Inorganic salts

Calibration curves were obtained for sodium dodecylsulphate in solutions of sodium chloride, sodium sulphate and sodium phosphate, up to concentrations of $2 \cdot 10^{-2}$ *M* added salt. No significant change in electrode potential or limit of

detection was found from 10^{-6} *M* to the reduced c.m.c. value. These findings have been confirmed by the S.I.R.A. Institute, Chislehurst, Kent, who also find no significant potential change in solutions ranging from pH 4 to 10.

Alkyl sulphates

The electrode behaviour was examined in varying concentrations of sodium n-alkyl sulphates and in solutions in which the concentration of sodium dodecylsulphate was varied, whilst the concentration of a second alkyl sulphate was kept constant.

For solutions containing a single component, the plots of *E vs.* log (surfactant concentration) were linear, with slopes ranging from near zero (sodium hexylsulphate) to near-Nernstian (sodium dodecylsulphate and sodium tetradecylsulphate).

For the two-component case, the electrode potential remained practically constant at low sodium dodecylsulphate concentrations. At higher concentrations, the electrode responded to dodecylsulphate only (Figs. 2, 3 and 4). It should be

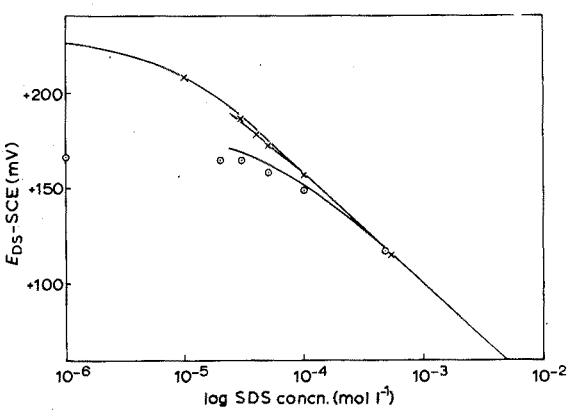

Fig. 2. Addition of $5 \cdot 10^{-4}$ *M* alkylsulphate to SDS solutions. (×) C_8; (○) C_{10}.

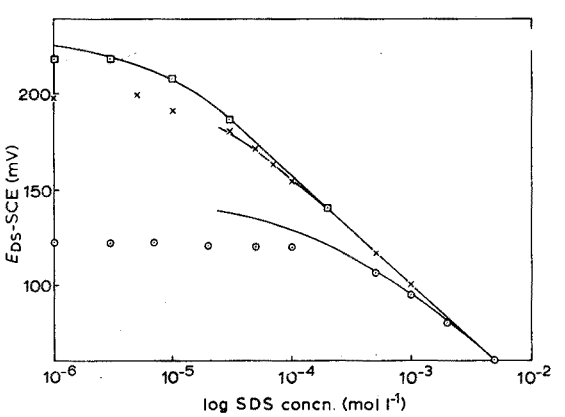

Fig. 3. Addition of $5 \cdot 10^{-3}$ *M* alkylsulphate to SDS solutions. (○) C_{10}; (×) C_8; (□) C_6. (———) Calculated from eqn. (1).

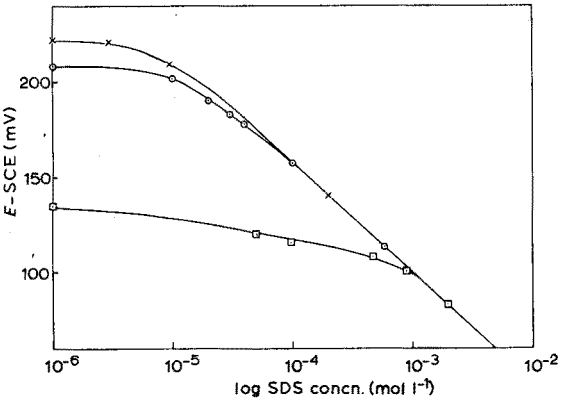

Fig. 4. Addition of Na C_{14} SO_4 to SDS solutions. (×) 10^{-6} *M*; (○) 10^{-5} *M*; (□) 10^{-4} *M*.

noted that, at the small concentrations used, activity and concentration may be taken as equal.

The data from both sets of experiments can be represented by the Nicolsky equation[3], over the linearity range of the electrode for dodecylsulphate.

$$E = E_0 - \frac{2.303\,RT}{F}\,[\log a_A + K a_B^N] \qquad (1)$$

where a_A is the activity of dodecylsulphate, a_B is the activity of another alkyl sulphate of different chain length, K is a selectivity constant, and N gives a measure of the nonideality of species B within the liquid ion-exchanger[4].

Values of log K and N obtained from the data for single-component solutions ($a_A = 0$) are given in Fig. 5, as functions of alkyl chain length. Use of these values together with data for the two-component systems leads to the solid lines in Figs. 2 and 3, which show excellent agreement with the experimental points. For the case of sodium tetradecylsulphate in sodium dodecylsulphate solutions, the value of E calculated from eqn. (1) is very sensitive to small changes in N. For

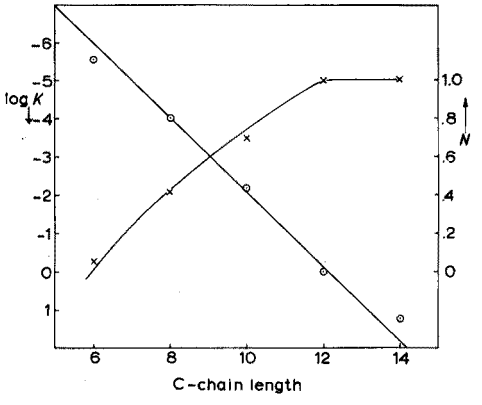

Fig. 5. Values of log K (○) and N (×) for different chain lengths.

example, a change in N from 1.0 to 1.1 results in an alteration in E of 15 mV, for a solution containing 10^{-4} M sodium tetradecylsulphate plus $5 \cdot 10^{-4}$ M sodium dodecylsulphate. Accordingly, calculated lines are not shown for these systems.

Now, when dissolved in *o*-dichlorobenzene (dielectric constant 9.9) the carrier complex will be associated to a considerable extent. Also, as A and B are similar ions in this case, it is likely that the properties of their neutral salts with $C_{16}(CH_3)_3N^+$ will be very close, in particular their mobility values and association constants within the *o*-dichlorobenzene phase. With these assumptions, eqn. (1) can be cast into the form derived by Sandblom *et al.*[5] for the selectivity of a liquid ion-exchanger membrane electrode, for the special case of $\tau = 0$, with inclusion of the "N" factor. When this is done, K can be approximately identified with the relative partition coefficient, $C_nSO_4^-/C_{12}SO_4^-$, for the process $C_nSO_4^-$ (water)$\rightleftarrows C_nSO_4^-$ (ion-exchanger). The decrease in both K and N values with decrease in alkylsulphate chain length follows directly from the increasing hydrophilic character of these materials, in comparison of properties in a hydrophobic solvent such as *o*-dichlorobenzene.

PREPARATION OF ELECTRODES FOR OTHER SURFACTANTS

That the dodecylsulphate electrode can determine dodecylsulphate ion only, in the presence of excesses of material of shorter chain length (and in the presence of comparable concentrations of $C_{14}SO_4^-$), makes possible the development of electrodes selective to single alkyl chain surfactants in commercial mixtures. Work is now proceeding to make such electrodes for a variety of surfactant systems.

As a first step, electrodes reponsive to the common anionic surfactant types have been prepared from carrier complexes synthesized from the $C_{16}(CH_3)_3N^+$ salt. The anionic surfactants used were: sodium n-alkylsulphates with alkyl chain lengths from C_6 to C_{14}, sodium dodecylbenzenesulphonate, sodium dodecylsulphonate, sodium dodecenylsulphonate, sodium dodecylethersulphate and sodium dodecanoate. Each of the electrodes gave near-Nernstian behaviour when placed in solutions of the pure corresponding surfactants.

These electrodes are being used for the determination of some thermodynamic parameters of micellization; in effluent and pollution monitoring; in surfactant adsorption studies; and to investigate the interactions between surfactants and co-solutes in solution.

A further application is to the study of the precipitation process between anionic surfactants and alkaline earth ions. Electrodes selective to two commercial sodium alkylbenzenesulphonates, Marlon A and Alkylate 230 sulphonate, were used to measure the solubility products of their calcium and magnesium salts at 25° and 50°. Electrode bodies manufactured by Corning were used for these experiments, with the original sealed internal reference system opened and refilled with a solution of 10^{-3} M surfactant + 10^{-2} M sodium chloride. The liquid ion-exchangers were 10^{-2} M solutions of the (benzyldimethyl-n-hexadecylammonium) salts of the surfactants, dissolved in *o*-dichlorobenzene. These electrodes gave more stable potential values at 50° than those based on Orion electrode bodies. This is probably due to the less robust construction of the former, which allows a more

rapid attainment of thermal equilibrium. The temperatures of the surfactant selective electrode, the reference electrode (Radiometer K401) and the test solution were held constant to $\pm 0.5°$ by means of individual water jackets. When the temperature was raised from 25° to 50°, electrode potentials stable to ± 0.2 mV were obtained within 1.5 h, with a Radiometer pHM 52 millivoltmeter. Known amounts of calcium chloride or magnesium chloride were added to a solution of surfactant, and the fall in surfactant activity was found from calibration graphs.

Results obtained are given in Table I. Within the accuracy of the method, no increase in solubility of any salt can be detected from 25° to 50°. The difference in solubility products between the salts of Marlon A and Alkylate 230 is explained by the distribution of surfactant alkyl chain lengths in these materials (Table II). The Alkylate 230 sample contains predominantly C_{13}–C_{14} alkyl chain lengths, thus conferring greater insolubility on the calcium and magnesium salts compared with Marlon A (predominantly C_{11}–C_{12}).

TABLE I

DETERMINATION OF SOLUBILITY PRODUCTS

Species		*Solubility product* $(mol\ l^{-1})^3$		*Reproducibility*
		25°	*50°*	
Marlon A	Ca	$6 \cdot 10^{-12}$	$4 \cdot 10^{-12}$	$2 \cdot 10^{-12}$
	Mg	$10 \cdot 10^{-12}$	$8 \cdot 10^{-12}$	
Alkylate 230	Ca	$2 \cdot 10^{-13}$	$3 \cdot 10^{-13}$	$2 \cdot 10^{-13}$
	Mg	$5 \cdot 10^{-13}$	$9 \cdot 10^{-13}$	

TABLE II

ALKYL CHAIN LENGTH DISTRIBUTION OF SURFACTANTS

Species	%				
	C_{10}	C_{11}	C_{12}	C_{13}	C_{14}
Marlon A	7	50	35	8	
Alkylate 230		1	10	59	28

It may be noted that the simultaneous use of a calcium (or divalent ion) selective electrode was not possible in these systems, owing to serious interference by surfactant ion. For example, in the absence of calcium ion, the electrode responds to addition of surfactant ion, the calibration plot having a slope factor of about -20 mV. Such interference does not seem to have been previously reported and may constitute a serious limitation to calcium activity measurements in, for example, industrial waste discharge or *in vivo* studies in the pulmonary area. The

reason for this behaviour probably lies in the structural similarity of long-chain surfactants to the phosphate esters used as site-ions in the calcium ion-exchanger which allows exchange of these surfactant ions to take place.

We thank Mrs. J. M. Burgess and Mr. R. S. Lee for carrying out some of the determinations.

SUMMARY

An improved electrode selective to the dodecylsulphate anion is described, which has no apparent effect on micellar properties. Electrodes selective to a variety of surfactant types have been prepared and the manufacture of electrodes specific to single alkyl chain length surfactants is discussed. An example is given of their use in the study of the precipitation of commercial surfactants.

RÉSUMÉ

On décrit une électrode sélective à l'anion dodécylsulfate, qui n'a pas d'effet apparent sur les propriétés micellaires. On a préparé des électrodes sélectives pour divers types de surfactants. Un exemple est donné de leur emploi dans l'étude de la précipitation de surfactants du commerce.

ZUSAMMENFASSUNG

Es wird eine verbesserte für das Dodecylsulfat-Anion selektive Elektrode beschrieben, die keinen augenscheinlichen Einfluss auf die micellaren Eigenschaften hat. Elektroden, die für verschiedene Arten von Tensiden selektiv sind, wurden hergestellt. Die Herstellung von Elektroden, die spezifisch für Tenside mit einer einzigen Alkylkettenlänge sind, wird diskutiert. Es wird ein Beispiel für deren Verwendung bei der Untersuchung der Fällung handelsüblicher Tenside angegeben.

REFERENCES

1 B. J. Birch and D. E. Clarke, *Anal. Chim. Acta*, 61 (1972) 159.
2 P. Mukerjee and K. J. Mysels, *C.m.c.'s of Aqueous Surfactant Systems*, N.B.S. Publication NSRDS/NBS 36, 1971.
3 B. P. Nicolsky, *Acta Physicochim. URSS*, 7 (1937) 597.
4 G. Karreman and G. Eisenman, *Bull. Math. Biophys.*, 24 (1962) 413.
5 J. P. Sandblom, G. Eisenman and J. L. Walker, Jr., *J. Phys. Chem.*, 71 (1967) 3862.

Analytica Chimica Acta, 67 (1973) 395–402

GOLD TWIN-ELECTRODES IN THIN-LAYER ELECTROCHEMISTRY

JOHN W. MACKAY and ANNEKE S. ALLEN
Department of Chemistry, Wichita State University, Wichita, Kan. 67208 (U.S.A.)
(Received 24th April 1973)

The theory and technique of studying small solution thickness by chronopotentiometry and linear potential-sweep voltammetry was introduced by Anson *et al.*[1,2] and has recently been reviewed[3]. Various electrode materials, including gold, have been suggested[3,4] for use in thin-layer cells, but generally polished platinum is used. Gold electrodes offer the advantage of a high hydrogen overpotential and a low hydrogen adsorption. The lack of acceptance of the gold electrodes is possibly due to the fact that the electrode reactions are not as yet completely established[5–20].

The thin-layer electrochemical technique is employed in this study of the behavior of gold electrodes in perchloric acid and sodium perchlorate solutions containing chloride ions. One of the attractive features of this technique is its high sensitivity, so that the cyclic voltammetric curves show peaks, where only general adsorption areas were observed with conventional techniques. Additionally, adequate separation was obtained for the peaks, because of the reduction of a gold(III) chloride species and the adsorbed oxygen layer, so that these could be identified correctly.

EXPERIMENTAL

The thin-layer electrode system used was similar to that outlined by Oglesby *et al.*[5]. The gold electrodes were made by casting gold foil into rods, which were mechanically attached to the micrometer spindles, and turned down to the same diameter (0.3166 cm^2). A glass H-cell, as designed by Hubbard and Anson[2], was constructed and proved most satisfactory. A ground-glass fitting was added on the sample side of the sintered glass to aid in rapid cleaning and washing.

All chemicals were of reagent grade and were used without further purification. Boiled, distilled water was used in the preparation of all solutions. Nitrogen gas was bubbled through the test solutions after preparation, and flowed over, but not through, the test sample in the teflon cup.

Cyclic voltammetry curves were obtained with a Beckman Electroscan 30[6]. The potential difference between the working and auxiliary electrodes used throughout this investigation was less than 0.01 V. Pretreatment of the electrode consisted of continued potential cycling between 0.0 and 1.2 V in a 0.1 *M* perchloric acid solution until 2 or 3 successive voltammograms showed no significant changes. Solution thicknesses of about $2.54 \cdot 10^{-3}$ cm were used (not calibrated). The potentials

recorded were measured *versus* a Beckman saturated single-shielded calomel electrode, model 39005, and all potentials are given with respect to this electrode. Unless otherwise noted, the traces displayed in Figs. 1–6 are at least duplicates, and the number of prior cycles necessary to obtain this duplication varied from 1 to 10.

RESULTS AND DISCUSSION

Figure 1 shows triangular sweep voltammetric curves on a 0.1 *M* perchloric acid electrolyte, demonstrating the effect of increasing turn-around potentials. The cathodic peak potential for the reduction of the adsorbed oxygen layer, which initially appears at 0.88 V, moves to less anodic potentials as the turn-around potential is increased. When the turn-around potential is boosted to 2.0 V, the cathodic peak shifts downward to *ca.* 0.65 V. This shift in the cathodic peak potential for the reduction of the adsorbed oxygen layer indicates that the layer formed at higher potentials is more difficult to remove than the layer arising from lower potentials[7–16]. This layer approaches a 1:1 stoichiometry of adsorbed oxygen atoms[18]. For turn-around potentials beyond 2.0 V, the gold "phase-oxide" is formed[18], which is reduced at yet less anodic potentials, and results in a reduction peak (Fig. 1d) which is considerably asymmetric, but which could not

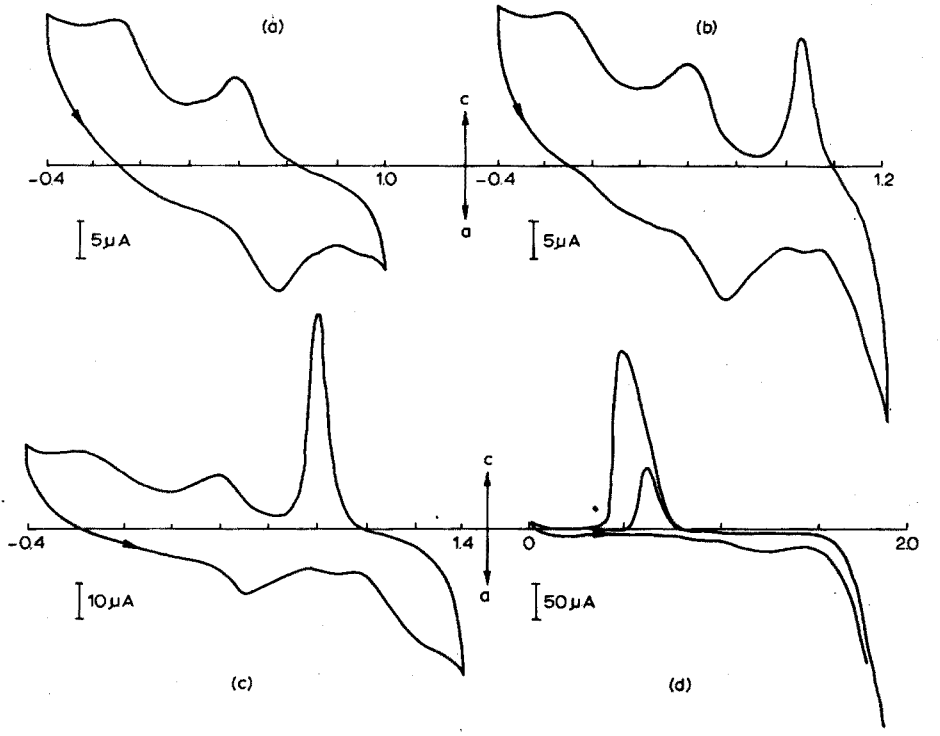

Fig. 1. Triangular sweep voltammetry curves for gold in 0.1 *M* $HClO_4$. Sweeprate, 40 mV s^{-1}; turn-around potentials: (a) 1.0 V, (b) 1.2 V, (c) 1.4 V, (d) 3.0 V.

be separated into two peaks. This peak also shifts toward lower potentials, as the turn-around potential is increased.

In the lower potential region, a distinct anodic peak appears at 0.5 V, and on the cathodic sweep two peaks are observed, at 0.4 V and −0.1 V respectively. This region has recently been identified as a platinum contamination of the working electrode, owing to the dissolution of an auxiliary platinum electrode[13]. On addition of some platinum to the present system, a platinum reduction peak was observed at 0.4 V, with a corresponding anodic peak at 0.9 V. A platinum black deposit could be visually observed at 0.4 V, which disappeared on the anodic scan at 0.9 V. No increase in the anodic peak current at 0.5 V was evident. Ellipsometric studies[19] indicate significant oxygen coverage at these lower potentials; however, a platinum counter electrode was again used in these experiments. Specular reflectance studies[20], with a gold electrode as the counter electrode, failed to provide strong evidence for or against this oxygen chemisorption. In the present study, a long period of cycling between 0 V and 1.2 V was necessary for the proper development of these peaks in the lower potential region. It would appear that the oxygen chemisorption is largely a function of the surface condition of the gold electrode.

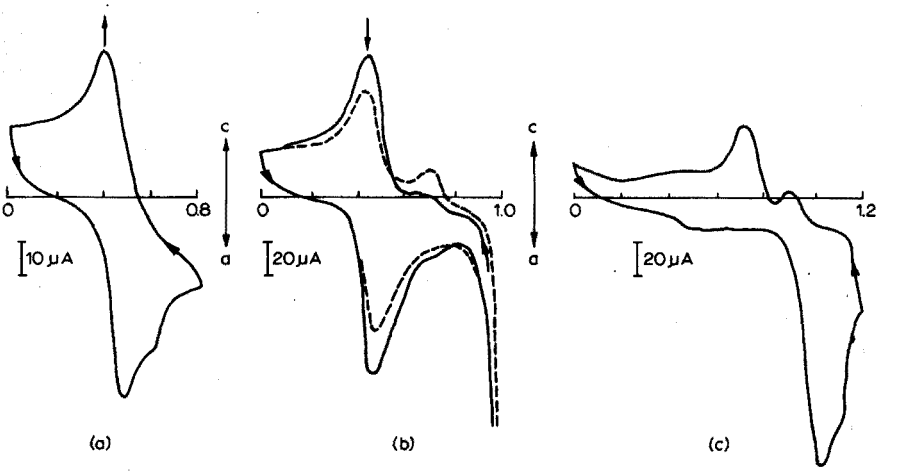

Fig. 2. Triangular sweep voltammetry curves for gold in 0.1 *M* $HClO_4$ and $2.4 \cdot 10^{-3}$ *M* NaCl. Sweeprate, 40 mV s^{-1}; turn-around potentials: (a) 0.8 V, (b) −0.98 V–1.02 V, (c) 1.2 V.

The effect of chloride is apparent in Fig. 2a where the anodic peak is observed with a shoulder on the anodic side at 0.6 V. After passage through the turn-around potential of 0.8 V, chloride adsorption continues on the cathodic scan until the desorption of both the chloride and the oxygen takes place at 0.4 V. In Fig. 2b, the solid line refers to a turn-around potential of −0.98 V and the dashed line to 1.02 V. New peaks appear on both sweeps, the cathodic peak is located at 0.7 V, and a new anodic peak appears at 1.0 V. These new peaks cannot be due to the formation and reduction of gold oxide, because the latter does not noticeably form until the potential is above 1.0 V, and its reduction takes place at 0.88 V for a turn-around potential of 1.02 V.

Dissolution of the gold electrode into a gold(III) chloride species will account for the 1.0-V anodic peak[12–17] with the reduction of the gold(III) chloride ion appearing at 0.7 V. As this reduction peak appears at 0.7 V, the amplitude of the cathodic desorption peak at 0.4 V is measurably lowered. On the anodic sweep, the amplitude of the 0.5-V adsorption peak has decreased also. Figure 2c shows the effect of a turn-around potential of 1.2 V. Here it is noted that the peaks formerly observed at 0.4 V and at 0.5 V have disappeared but a region of adsorption remains in that potential range. Apparently, the electrode surface which initially results from the reduction of tetrachloroaurate at the surface does not allow the formation of a distinct chemisorption layer. On continued cycling of the electrodes at turn-around potentials of less than 1.0 V, the peaks reappear and increase in amplitude with repetitive cycling.

The deterioration of the peaks at 0.4 V cathodic and 0.5 V anodic with increase in the turn-around potential (Fig. 2) does not take place in a chloride-free system (Fig. 1). The chloride ion values permit an alternative competitive reaction path of gold⇌gold(III) chloride over gold⇌gold oxide. In the chloride-free system, the gold electrode forms an adsorbed oxygen layer which approaches a monolayer; in such perchloric acid solutions, the metal surface appears to be essentially unchanged after potential cyclings. In the chloride-containing perchloric acid electrolyte (Fig. 2b and c), reduction of the gold(III) chloride species on the electrode produces a fresh metal coating. Repeated cycling of the freshly coated electrode at turn-around potentials of less than 1.0 V restores the original adsorption characteristics of the electrode. Figure 2c shows a sweep for a turn-around potential of 1.2 V. In this Figure the electrode dissolution peak of 1.05 V appears, accompanied by an anodic shoulder at 1.1 V. The 1.1-V anodic shoulder is the region of the formation of the adsorbed oxygen layer. This adsorbed oxygen layer then prevents any further dissolution of the gold to gold(III) chloride[12].

These findings generally concur with those reported by Gaur and Schmid[12] except that here a 1.0-V value is assigned to the anodic peak for formation of a gold(III) chloride ion and the anodic shoulder of the peak at 1.1 V to the formation

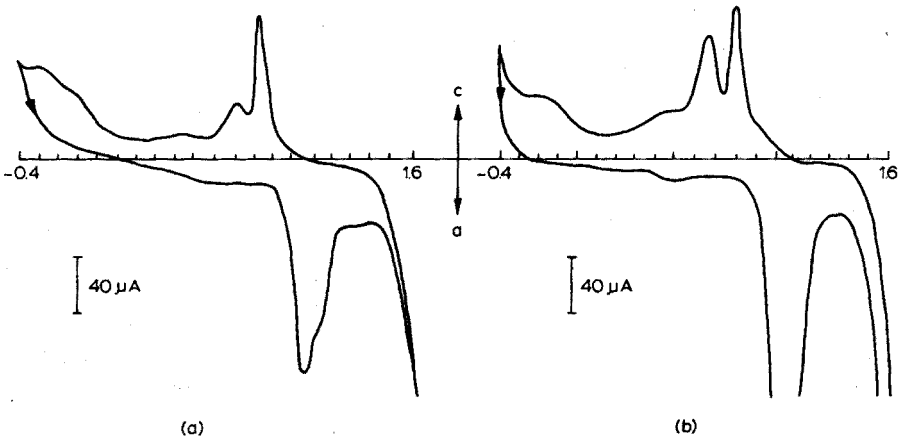

Fig. 3. Triangular sweep voltammetry curves for gold in 0.1 *M* $HClO_4$. Sweeprate, 40 mV s^{-1}; turn-around potential, 1.6 V; (a) $2.4 \cdot 10^{-3}$ *M* NaCl; (b) $6.3 \cdot 10^{-3}$ *M* NaCl.

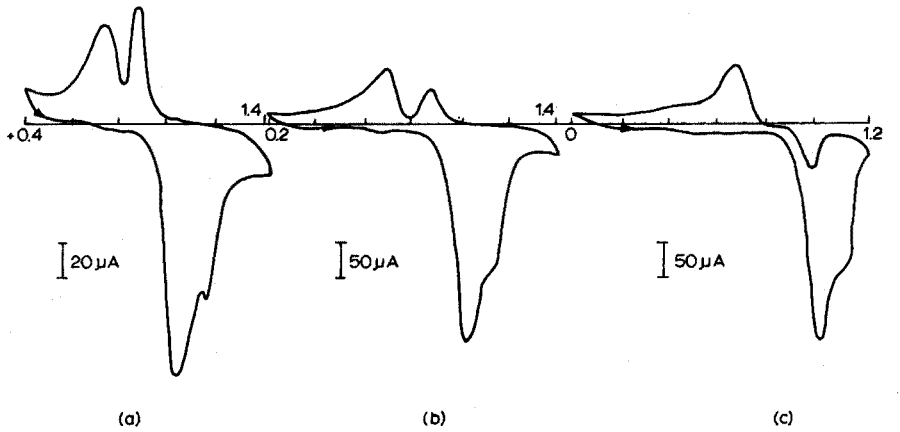

Fig. 4. Triangular sweep voltammetry curves for gold in 0.1 *M* $HClO_4$. Sweeprate, 40 mV s^{-1}. (a) $2.4 \cdot 10^{-3}$ *M* NaCl, turn-around potentials +0.4 V and 1.4 V; (b) $6.3 \cdot 10^{-3}$ *M* NaCl, turn-around potentials 0.2 V and 1.4 V; (c) $6.3 \cdot 10^{-3}$ *M* NaCl, turn-around potentials 0.0 V and 1.2 V.

of an adsorbed oxygen layer. Assignment of the 0.7-V cathodic peak to gold(III) chloride reduction is supported by Figs. 3 and 4, where the 0.7-V peak height is shown to be dependent on the chloride ion concentration.

It is again noted that the locations of the adsorbed oxygen reduction peak can be changed with changes of turn-around potential. This property of the adsorbed oxygen peak allows clear distinction to be made between it and the gold(III) chloride ion reduction peak. In Fig. 4c, the sweep produced a small but observable amount of gold(III) oxide which was readily removed during the cathodic scan, and tetrachloroaurate was still formed.

Figure 5 shows the behavior of gold electrodes in a 0.1 *M* sodium perchlorate solution. In this electrolyte, there are no sharp peaks for turn-around potentials less than 1.3 V. Three adsorption areas are visible in the anodic scans, from 0.2 to 0.4 V, from 0.4 to 0.7 V, and from 0.7 to 1.1 V. A cathodic desorption area is observed below 0.5 V (Fig. 5a). Above 1.3 V on the anodic scan, an adsorbed oxygen layer is formed, but this is reduced at 0.7 V during the cathodic sweep (Fig. 5b). Continued potential cycling in this 0.1 *M* sodium perchlorate electrolyte with a turn-around potential of 1.4 V causes the cathodic peak at 0.25 V to diminish gradually and eventually disappear. In place of the broad peak, a region of desorption remains (Fig. 5c).

The dashed line in Fig. 6a shows a sweep in 0.1 *M* sodium perchlorate where the electrodes had not yet developed any particular adsorbed oxygen layer. A drop of a tetrachloroaurate solution was added to the sample cup and after some of this had diffused into the thin layer, the solid line sweep was obtained. The oxidation and reduction of the tetrachloroaurate(III) occur at 1.1 V and 0.8 V, respectively.

Figure 6b shows a starting potential of 1.4 V for a cathodic sweep, which produces an asymmetric peak at about 0.75 V. This peak separates into two peaks on a second pass, and the electrode surface rapidly deteriorates on succeeding sweeps, which do not show any well defined peaks. The broken line represents the

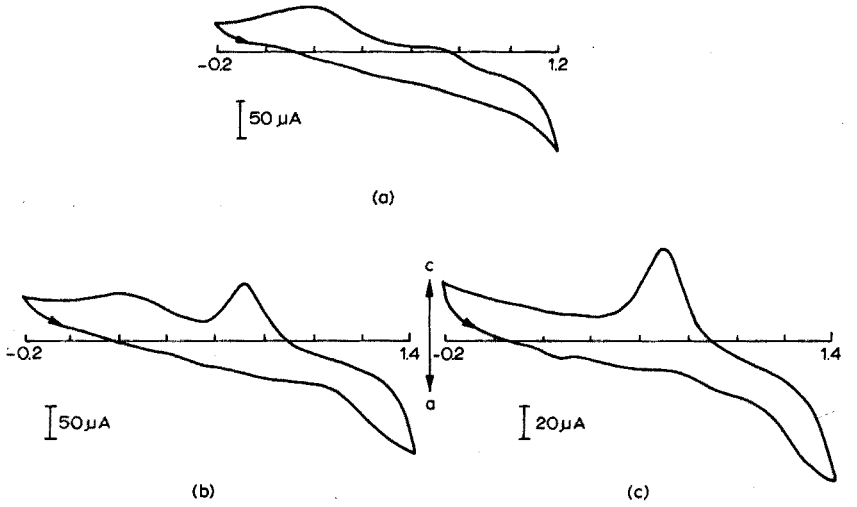

Fig. 5. Triangular sweep voltammetry curves for gold in 0.1 *M* $NaClO_4$. Sweeprate, 100 mV s^{-1}; turn-around potentials: (a) 1.2 V, (b) 1.4 V, (c) 1.4 V.

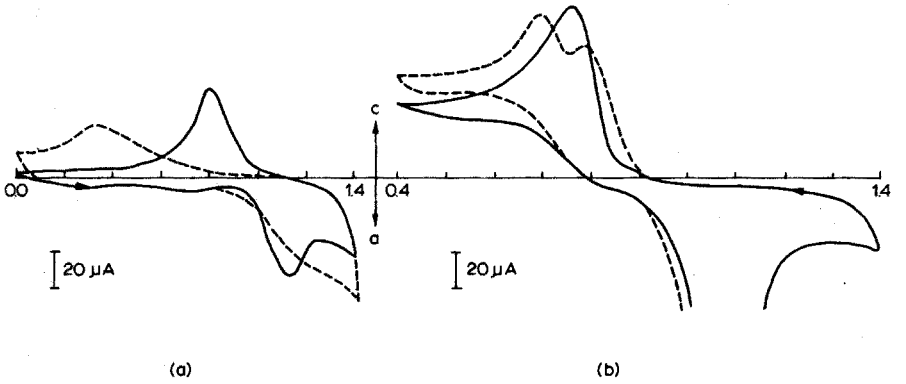

Fig. 6. Triangular sweep voltammetry curves for gold in 0.1 *M* $NaClO_4$. Sweeprate, 40 mV s^{-1}; turn-around potential, 1.4 V. (a) (---) No chloride present; (——) trace of $AuCl_4$ added; (b) 0.001 *M* $AuCl_4^-$: (———) start at 1.4 V, (-----) 7th cycle.

seventh cycle. It was not possible to separate the gold(III) chloride reduction peak from the "adsorbed oxygen layer" reduction peak as was done in the perchloric acid solution.

SUMMARY

The characteristics of a gold twin-electrode system in a thin-layer cell containing 0.1 *M* perchloric acid, and varying amounts of sodium chloride, were investigated by triangular sweep voltammetry. The "adsorbed oxygen" layer starts to form above 1 V, and the peak from reduction of this layer shifts from 0.88 V to 0.65 V on changing the turn-around potential from 1.02 to 2.0 V. A distinct adsorption peak appears at 0.5 V, with cathodic peaks at 0.4 V and −0.1 V.

Chloride adsorption is observed at 0.6 V, with desorption at 0.4 V. The dissolution of the gold electrode to gold(III) chloride occurs at 1.1 V; but this reaction is blocked above 1.2 V by the formation of the "adsorbed oxygen" layer. The peak from the reduction of the gold(III) chloride is located at 0.7 V and is separable from the "adsorbed oxygen" reduction peak. The electrode surface obtained from the reduction of gold(III) chloride shows characteristics different from those obtained by the reduction of the "adsorbed oxygen" layer.

RÉSUMÉ

Les caractéristiques d'un système d'électrode d'or combinée, dans une cellule à couche mince, contenant de l'acide perchlorique 0.1 *M* et des quantités variables de chlorure de sodium, sont examinées à l'aide de la voltammétrie à balayage triangulaire. La couche d'oxygène adsorbé commence à se former au-dessus de 1 V; le pic obtenu par réduction de cette couche se situe entre 0.88 et 0.65 V. Un pic d'adsorption distinct apparaît à 0.5 V, avec des pics cathodiques à 0.4 V et −0.1 V. Une adsorption de chlorure est observée à 0.6 V, avec désorption à 0.4 V. La dissolution de l'électrode d'or en chlorure d'or(III) se produit à 1.1 V; cette réaction est bloquée-au-dessus de 1.2 V par formation de la couche d'oxygène adsorbé. La surface de l'électrode obtenue par réduction de l'or(III) présente des caractéristiques différentes de celles obtenues par réduction de la couche d'oxygène adsorbé.

ZUSAMMENFASSUNG

Die charakteristischen Eigenschaften eines Gold-Doppelelektrodensystems in einer Dünnschichtzelle, die 0.1 *M* Perchlorsäure und variierende Mengen an Natriumchlorid enthält, wurden mittels Dreieck-Sweep-Voltammetrie untersucht. Die Schicht des "adsorbierten Sauerstoffs" beginnt sich oberhalb 1 V auszubilden, und der von der Reduktion dieser Schicht herrührende Peak verschiebt sich von 0.88 V zu 0.65 V, wenn das durchlaufene Potential von 1.02 auf 2.0 V erhöht wird. Ein getrennter Adsorptionspeak erscheint bei 0.5 V mit kathodischen Peaks bei 0.4 V und −0.1 V. Die Adsorption von Chlorid wird bei 0.6 V beobachtet, die Desorption bei 0.4 V. Die Auflösung der Goldelektrode zu Gold(III)-chlorid tritt bei 1.1 V auf; jedoch wird diese Reaktion oberhalb 1.2 V durch die Ausbildung der Schicht von "adsorbiertem Sauerstoff" blockiert. Der durch die Reduktion von Gold(III)-chlorid hervorgerufene Peak liegt bei 0.7 V und ist vom Reduktionspeak des "adsorbierten Sauerstoffs" zu trennen. Die durch die Reduktion von Gold(III)-chlorid erhaltene Elektrodenoberfläche zeigt Eigenschaften, die sich von denen unterscheiden, die bei der Reduktion der Schicht von "adsorbiertem Sauerstoff" auftreten.

REFERENCES

1 C. R. Christensen and F. C. Anson, *Anal. Chem.*, 35 (1963) 205; 36 (1964) 495.
2 A. T. Hubbard and F. C. Anson, *Anal. Chem.*, 36 (1964) 723; 38 (1966) 58; *J. Electroanal. Chem.*, 9 (1965) 163.

3 C. N. Reilley, *Pure Appl. Chem.*, 18 (1968) 137; A. T. Hubbard and F. C. Anson, in A. J. Bard, *Electroanalytical Chemistry, A Series of Advances, 4*, Marcel Dekker, New York, pp. 129–214.
4 L. B. Anderson and C. N. Reilley, *J. Electroanal. Chem.*, 10 (1965) 538.
5 D. M. Oglesby, S. H. Omang and C. N. Reilley, *Anal. Chem.*, 37 (1965) 1312.
6 Beckman Instruments, Inc., Fullerton, Calif. 92634, *Bull. 1303-A.*
7 H. A. Laitinen and M. S. Chao, *J. Electrochem. Soc.*, 108 (1961) 726.
8 F. Bauman and I. Shain, *Anal. Chem.*, 29 (1957) 303.
9 J. K. Lee, R. N. Adams and C. E. Bricker, *Anal. Chim. Acta*, 17 (1957) 321.
10 G. M. Schmid and N. Hackerman, *J. Electrochem. Soc.*, 109 (1962) 243; 110 (1963) 440.
11 G. M. Schmid and R. N. O'Brien, *J. Electrochem. Soc.*, 111 (1964) 832; G. M. Schmid, *Electrochim. Acta*, 12 (1967) 449.
12 J. N. Gaur and G. M. Schmid, *J. Electroanal. Chem.*, 24 (1970) 279.
13 R. A. Bonewitz and G. M. Schmid, *J. Electrochem. Soc.*, 117 (1970) 1367.
14 D. D. Bode, T. N. Andersen and H. Eyring, *J. Phys. Chem.*, 71 (1967) 792.
15 R. A. Bonewitz, *J. Electrochem. Soc.*, 116 (1969) 78C.
16 S. B. Brummer and A. C. Makrides, *J. Electrochem. Soc.*, 111 (1964) 1122.
17 T. Heumann and H. S. Panesar, *Z. Phys. Chem.*, 229 (1965) 84.
18 D. A. J. Rand and R. Woods, *J. Electroanal. Chem.*, 31 (1971) 29.
19 R. S. Sirohi and M. A. Genshaw, *J. Electrochem. Soc.*, 116 (1969) 910.
20 T. Takamura, K. Takamura, W. Nippe and E. Yeager, *J. Electrochem. Soc.*, 117 (1970) 626.

Analytica Chimica Acta, 67 (1973) 403–413

NOUVELLE MÉTHODE DE DOSAGE AUTOMATIQUE DE SUBSTANCES OXYDANTES OU RÉDUCTRICES PAR POTENTIOMÉTRIE DIFFÉRENTIELLE

PARTIE I. ÉTUDE THÉORIQUE†

J. O. BOSSET et B. BLANC

Station Fédérale de Recherches Laitières. CH-3097 Liebefeld-Berne (Suisse)

E. PLATTNER

Institut de Génie Chimique, Ecole Polytechnique Fédérale, CH-1025 Lausanne (Suisse)

(Reçu le 28 février 1973)

INTRODUCTION ET DÉVELOPPEMENT THÉORIQUE DE LA MÉTHODE DE SCHIERJOTT

Dans sa publication sur la détermination de systèmes rédox en flux continu, Schierjott[1] propose une méthode qui consiste à mesurer la différence des potentiels $E_{\text{rédox } i} - E_{\text{rédox } j} = \Delta E_{\text{rédox } j}^{\ i}$ que montre une solution titrante à deux instants consécutifs donnés i et j d'une même réaction d'oxydo–réduction. L'auteur propose pour un "Auto-Analyzer" de Technicon un "flow diagram" dans lequel i est le début de la réaction et j la fin de la réaction. La seconde condition est implicite mais non impérative. La solution titrante est composée d'un oxydant (respectivement d'un réducteur) réversible, dont le couple (forme oxydée/forme réduite) suit la loi de Nernst:

$$E_{\text{rédox}} = E^0_{\text{rédox}} + \frac{RT}{nF} \ln \frac{o}{r} \tag{1}$$

où o = activité* de la forme oxydée et r = activité de la forme réduite de la solution "titrante". On désignera par o^* et r^* les activités correspondantes de la solution "titrée".

L'auteur considère le cas de solutions suffisamment diluées pour que les coefficients d'activité deviennent unitaires (activités = concentrations) et celui de $n = 1$. Il est alors possible de formuler la base théorique de sa méthode de la manière suivante:

$$\Delta E_{\text{rédox}\ j}^{\ i} = \frac{RT}{F} \left[\ln \frac{o_i}{r_i} - \ln \frac{o_j}{r_j} \right] \tag{2}$$

Vu que Schierjott choisit, aussi bien pour i que pour j, des conditions de

† Extrait d'une thèse de doctorat publiée prochainement.

* L'invariabilité de tous les volumes permet de substituer systématiquement la dimension "activité" ou "concentration" à celle de "quantité".

travail proches de $E^0_{\text{rédox}}$, à savoir:

$$\frac{o_i}{r_i} \cong \frac{o_j}{r_j} \cong 1 \tag{3}$$

il est possible pour i comme pour j de procéder au développement en série suivant:

$$\ln \frac{o}{r} = \ln u = \sum_{n=1}^{n=\infty} (-1)^{n+1} \cdot n^{-1} \cdot (u-1)^n \tag{4}$$

à condition que $0<u<2$, condition vérifiée puisque:

$$u_i \cong u_j \cong 1 \tag{3a}$$

En ne gardant que le terme du développement correspondant à $n=1$, on obtient après substitution pour i et pour j la nouvelle expression:

$$\Delta E_{\text{rédox}}{}^i_j = \frac{RT}{F} (\ln u_i - \ln u_j) \cong \frac{RT}{F} (u_i - u_j) \tag{5}$$

La nouvelle expression ne comporte plus de logarithme. Elle est donc partiellement linéarisée.

Dans le cas du dosage d'un réducteur de concentration r^* par un oxydant de concentration o, on peut écrire stoechiométriquement que:

$$o_i - o_j = +\Delta o^i_j = -(r_i - r_j) = -\Delta r^i_j = +\Delta r^*{}^i_j \tag{6}$$

où $\Delta r^*{}^i_j$ est la variation de la concentration de la forme réduite du réducteur entre i et j (par analogie, $\Delta o^*{}^i_j$ serait celle de la forme oxydée de ce dernier). Si la réaction est complète, on a alors:

$$\Delta r^*{}^i_j = r^* \tag{7}$$

Après introduction des égalités (4) et (6) dans l'expression (5), on peut récrire cette dernière sous la forme:

$$\Delta E_{\text{rédox}}{}^i_j = \frac{RT}{F}\left[\frac{o_i}{r_i} - \frac{o_i - \Delta o^i_j}{r_i - \Delta r^i_j}\right] = \frac{RT}{F}\left[\frac{o_i}{r_i} - \frac{o_i - \Delta r^*{}^i_j}{r_i + \Delta r^*{}^i_j}\right] =$$

$$= \frac{RT}{F}\left[\frac{o_i + r_i}{r_i (r_i + \Delta r^*{}^i_j)}\right] \Delta r^*{}^i_j \tag{8}$$

L'hypothèse de travail définie sous (3) permet de tirer l'inégalité:

$$\Delta r^*{}^i_j \ll r_i \tag{9}$$

Cette dernière inégalité permet de simplifier une seconde fois par approximation l'expression de la différence de potentiel rédox qui devient:

$$\Delta E_{\text{rédox}}{}^i_j \cong \frac{RT}{F} \cdot \frac{o_i + r_i}{r_i^2} \cdot \Delta r^*{}^i_j \tag{10}$$

En définitive, la relation (10) indique que la différence de potentiel d'oxydo–réduction du couple réversible o/r entre les instants i et j de la même réaction est directement proportionnelle à la concentration du réducteur consommé pendant

ce laps de temps, à condition de travailler dans le voisinage de $E^0_{\text{rédox}}$ (concentration égale des formes oxydée et réduite). Cette relation peut donc être condensée sous la forme:

$$\Delta E_{\text{rédox}}{}^{i}_{j} \cong K^{\text{I}} \cdot \Delta r^{*}{}^{i}_{j} \tag{10a}$$

où $\Delta E_{\text{rédox}} = K^{\text{I}} \cdot r^{*}$ (réaction complète).

CRITIQUE DE LA MÉTHODE ET PROPOSITION D'UNE VARIANTE

Si la méthode de Schierjott est intéressante pour les réactions d'oxydo–réduction rapides et réversibles, elle n'est pas idéale pour les réactions lentes, comme par exemple l'oxydation de certaines substances organiques. Dans de tels cas, il faut non seulement opérer à haute température pour augmenter la vitesse de la réaction, mais encore engager un excès suffisant de réactif pour influencer la cinétique rédox. Il en résulte que l'hypothèse définie sous (3) ($\Delta r^{*}{}^{i}_{j} \ll o_i \cong r_i$) est peu favorable à cet égard puisqu'elle oblige à travailler dans le domaine où la solution "titrante" offre sont pouvoir tampon maximum, donc une assez faible sensibilité analytique. D'autre part, la présence dans le réactif d'une concentration r_i, respectivement r_j (forme inactive pour l'oxydation) pratiquement aussi élevée que o_i, respectivement o_j, peut même nuire dans certains cas à la solubilité de la forme active (particulièrement pour le $Ce(SO_4)_2$). Sur le plan économique finalement, le coût du réactif pour une analyse donnée est le double de celui calculé pour o_i seul.

Tenant compte des remarques précédentes, la variante proposée dans ce travail est basée sur des conditions expérimentales très différentes ($\Delta r^{*}{}^{i}_{j} \ll o_i \neq r_i$). Elle peut être formulée de la manière suivante, à partir de la relation différentielle (2):

$$\Delta E_{\text{rédox}}{}^{i}_{j} = \frac{RT}{F} \ln \frac{o_i \cdot r_j}{r_i \cdot o_j} = \frac{RT}{F} \ln \frac{o_i(r_i - \Delta r^{i}_{j})}{r_i(o_i - \Delta o^{i}_{j})} \tag{11}$$

En substituant les égalités de (6) dans la relation (11), on obtient:

$$\Delta E_{\text{rédox}}{}^{i}_{j} = \frac{RT}{F} \ln \frac{o_i(r_i + \Delta r^{*}{}^{i}_{j})}{r_i(o_i - \Delta r^{*}{}^{i}_{j})} \tag{12}$$

puis après simplification:

$$\Delta E_{\text{rédox}}{}^{i}_{j} = \frac{RT}{F} \ln \frac{(\Delta r^{*}{}^{i}_{j})^{-1} + (r_i)^{-1}}{(\Delta r^{*}{}^{i}_{j})^{-1} - (o_i)^{-1}} \tag{13}$$

Comme $\Delta r^{*}{}^{i}_{j}$ est une fraction de r^{*} (total), $\Delta E_{\text{rédox}}{}^{i}_{j}$—à T, o_i, r_i et j donnés—est une nouvelle fonction bijective de la concentration initiale en réducteur. Réciproquement, il est possible de déterminer la teneur en réducteur d'une solution inconnue en mesurant le $\Delta E_{\text{rédox}}$ qui lui est associé.

Néanmoins, sous sa forme générale, la relation (13) ne se prête guère, vu sa complexité, à une application à des analyses de routine. En effet, l'exponentielle $[F \cdot (RT)^{-1} \cdot \Delta E_{\text{rédox}}{}^{i}_{j}]$ varie hyperboliquement avec la consommation du réducteur.

En choisissant les conditions expérimentales initiales telles que:

$$r_i \ll \Delta r^{*}{}^{i}_{j} \ll o_i \tag{14}$$

il devient possible de simplifier par approximation la relation (13):

$$\Delta E_{\text{rédox}}{}^{i}_{j} \cong \frac{RT}{F} \ln \frac{\Delta r^{*}{}^{i}_{j}}{r_i} = \frac{RT}{F} \ln \Delta r^{*}{}^{i}_{j} - \frac{RT}{F} \ln r_i \tag{15}$$

Pour une température maintenue constante au cours de la réaction, il est possible de regrouper toutes les constantes dans la nouvelle expression:

$$\Delta E_{\text{rédox}}{}^{i}_{j} \cong K^{\text{II}} \ln \Delta r^{*}{}^{i}_{j} + K^{\text{III}} \tag{15a}$$

c'est à dire:

$$\Delta r^{*}{}^{i}_{j} \cong \exp \frac{\Delta E_{\text{rédox}}{}^{i}_{j} - K^{\text{III}}}{K^{\text{II}}} \tag{15b}$$

Lorsque les hypothèses de travail définies par la relation (14) sont respectées, l'argument de la fonction logarithmique devient linéaire. La différence des potentiels rédox du couple réversible *o/r* à deux instants donnés *i* et *j* est proportionnelle* au logarithme de la concentration du réducteur consommé entre ces mêmes instants. Les relations (15a) et (15b) sont à la base de la variante proposée.

Si de surcroît la teneur en réducteur (respectivement en oxydant) à doser ne varie que faiblement d'un échantillon à l'autre, on peut assimiler le segment de la courbe logarithmique considéré (*cf.* relation 15) à un segment de droite. Cette seconde simplification par approximation se justifie à nouveau par un développement en série. Dans ce cas, on retrouve une relation de simple proportionnalité entre la teneur en réducteur et la différence de potentiel rédox mesurée (*cf.* relation 10a) à une constante additive près, du type:

$$\Delta E_{\text{rédox}}{}^{i}_{j} \cong K^{\text{IV}} \cdot \Delta r^{*}{}^{i}_{j} + K^{\text{V}} \tag{16}$$

Si la précision demandée ne permet cette dernière approximation en raison de l'écart existant entre le logarithme et son développement en série, l'exploitation des données analytiques peut se faire par l'emploi d'une petite calculatrice, d'un papier semi-logarithmique ou d'une table de conversion.

COMPARAISON DES DEUX MÉTHODES

Les deux méthodes décrites se distinguent essentiellement par leurs conditions expérimentales. S'il faut dans les deux cas engager un excès d'oxydant par rapport au réducteur ($\Delta r^{*}{}^{i}_{j} \ll o_i$), Schierjott indique $\Delta r^{*}{}^{i}_{j} \ll r_i$, alors que la variante proposée préconise $\Delta r^{*}{}^{i}_{j} \gg r_i$. Cette dernière solution est plus adéquate que la précédente lorsque la réaction rédox est lente même avec un oxydant (respectivement un réducteur) puissant, puisqu'elle offre—au dessus d'un certain seuil—une meilleure sensibilité pour un même excès:

$$Q = o_i / \Delta r^{*}{}^{i}_{j} \tag{17}$$

A titre d'exemple, il est possible de calculer les $\Delta E_{\text{rédox}}{}^{i}_{j}$ obtenus par l'une et l'autre méthode pour une concentration égale en oxydant ($o_i = 1$) et une même température T.

---

* A une constante additive près (fonction affine).

Calcul de $\Delta E_{\text{rédox}}{}^{i}_{j}$ *selon Schierjott*

$\Delta E_{\text{rédox}}{}^{i}_{j}$ dépend évidemment du domaine de travail considéré. Plus on le choisit grand, c'est à dire plus on s'écarte des conditions définies sous chiffre (3a) ($u_i \cong 1$), moins bonne est l'approximation supposée par la relation (10a), comme le montre le Tableau I.

TABLEAU I

ESTIMATION DE L'ERREUR COMMISE SUR $\Delta E_{\text{rédox}}{}^{i}_{j}$ DUE AU DÉVELOPPEMENT EN SÉRIE DÉFINI SOUS CHIFFRE (4)

$u_i = o_i/r_i$ *(fraction ordinaire)*	$u_i - 1$ *(approximation)*	$\ln u_i$ *(Nernst)*	$(u_i-1)-(\ln u_i)$ *(erreur absolue)*	$\{[(u_i-1)-(\ln u_i)]/\ln u_i\}100$ *{erreur relative (%)}*
50/50	0.0000	0.0000	0.0000	0.00
55/45	0.2222	0.2007	0.0215	+10.71
60/40	0.5000	0.4055	0.0945	+23.30
65/35	0.8571	0.6190	0.2381	+38.47
70/30	1.3333	0.8473	0.4860	+57.36

L'auteur indique qu'il est possible de choisir le rapport initial $u_i = o_i/r_i = r_i^{-1}$ entre 2.3 et 1.0 approximativement, le rapport final $u_j = o_j/r_j$ étant choisi aussi voisin que possible de 1. Pour les conditions extrêmes de validité de l'approximation, à savoir $u_i = 2.33$ (70% de forme oxydée/30% de forme réduite), on peut écrire en fonction de Q:

$$\Delta E_{\text{A}} \cong \Delta E_{\text{rédox}}{}^{i}_{j} \frac{F}{RT} = \frac{o_i + r_i}{r_i^2} \Delta r^{*}{}^{i}_{j} = \frac{1 + u_i^{-1}}{u_i^{-2}} Q^{-1} = \frac{u_i + u_i^2}{Q} = \frac{7.77}{Q} \qquad (18)$$

Calcul de $\Delta E_{\text{rédox}}{}^{i}_{j}$ *selon la variante proposée*

L'hypothèse de travail définie sous chiffre (14) indique que $r_i << o_i$, ce qui revient à considérer r_i comme une "impureté" (forme réduite de l'oxydant) dans le réactif (forme oxydée de ce dernier). Si l'on définit par K la teneur du réactif en cette impureté, c'est à dire:

$$K = r_i/o_i = u_i^{-1} \qquad (19)$$

il devient possible de calculer le $\Delta E_{\text{rédox}}{}^{i}_{j}$ obtenu en fonction de K (paramètre) et de Q (variable):

$$\Delta E_{\text{B}} \cong \Delta E_{\text{rédox}}{}^{i}_{j} \frac{F}{RT} = \ln \frac{\Delta r^{*}{}^{i}_{j}}{r_i} = \ln (Q^{-1} K^{-1}) = -\ln KQ = \ln u_i/Q \qquad (20)$$

On déduit de la relation (20) que la sensibilité de la méthode proposée dépend de la pureté du réactif utilisé. A $Q > 0$, elle décroît lorsque K croît. Pour $K = 7 \cdot 10^{-3}$*, le calcul donne:

$$\Delta E_{\text{B}} \cong -\ln (0.007\ Q) \qquad (20a)$$

* *Cf.* les résultats expérimentaux (Partie II) (ref. 2).

Calcul du seuil d'"équisensibilité" des méthodes

Comparer la sensibilité des deux méthodes revient à comparer leur $\Delta E_{\text{rédox}\,j}$. En résolvant l'équation:

$$\Delta E_A = \Delta E_B \tag{21}$$

on détermine la valeur de Q, désignée par Q_s, pour laquelle les deux méthodes sont équivalentes.

Dans le cas particulier envisagé où $K = 7 \cdot 10^{-3}$ et $u_i = 2.33$, la résolution graphique de cette équation conduit à la valeur $Q_s = 1.77$. Pour tout excès de réactif Q supérieur à l'excès équivalent Q_s défini précédemment, ce qui est généralement le cas en pratique, la méthode proposée est nettement plus sensible que celle de Schierjott (*cf.* Tableau II).

TABLEAU II

COMPARAISON DE LA SENSIBILITÉ DES DEUX MÉTHODES POUR QUELQUES VALEURS DE Q

$Q = o_i/\Delta r^{*i}_j$	$\Delta E_A \cdot (RT/F) =$ $RT\ 7.77/(F \cdot Q)$[a]	$\Delta E_B \cdot (RT/F) =$ $(-RT/F) \cdot \ln(0.007\ Q)$[b]
1.00	200.0 mV	127.6 mV
1.77[c]	112.9 mV	112.9 mV
2.00	100.0 mV	109.8 mV
5.00	40.0 mV	86.2 mV
10.00	20.0 mV	68.4 mV

[a] Méthode de Schierjott, pour $u_i = 2.77$ (à 25°) (*cf.* éqn. 18).
[b] Variante proposée, pour $K = 7 \cdot 10^{-3}$ (à 25°) (*cf.* éqn. 20a).
[c] $Q = Q_s$ (équisensibilité).

Jusqu'ici tous les calculs ont été effectués sur la base de $K = 7 \cdot 10^{-3}$. Si l'on parvient à abaisser le taux d'impureté par exemple jusqu'à $K = 1 \cdot 10^{-3}$ (purification, choix d'un produit plus pur, etc.), on abaisse encore la valeur de Q_s à 1.15, même pour les conditions de validité extrêmes envisagées, à savoir $u_i = 2.33$ (70%/30%).

OPTIMISATION DES DIVERS PARAMÈTRES

Une analyse de la relation fondamentale (13) permet de caractériser le rôle des principaux paramètres qui y interviennent, à savoir la concentration du réactif, la température et le temps de réaction.

Influence de la concentration du réactif: étude de $\Delta E_{\text{rédox}\,j}^{\,i}$ en fonction de Q ($o_i = 1$)

L'étude de la concentration du réactif revient à optimiser le rapport $Q = o_i/\Delta r^{*i}_j$. Après substitution de r_i par $K \cdot o_i$ (*cf.* éqn. 19) et amplification de la fraction par Δr^{*i}_j, l'argument du logarithme de l'éqn. (13) devient, pour $Q \neq 0$:

$$\exp\left[\Delta E_{\text{rédox}\,j}^{\,i} \cdot F/RT\right] = \frac{1 + (KQ)^{-1}}{1 - Q^{-1}} = \frac{KQ + 1}{K(Q - 1)} \tag{22}$$

De cette dernière expression, on peut tirer quelques informations importantes concernant le comportement du logarithme pour certaines valeurs de Q:

pour $Q \rightleftarrows 1$ (stoechiométrie oxydant/réducteur), $\Delta E_{\text{rédox}} \to \infty$: la fonction croît indéfiniment. La valeur $Q=1$ est un pôle de la fonction.

pour $Q \to \infty$ ("très grand"), $\Delta E_{\text{rédox}} \to 0$: on perd toute sensibilité.

pour $Q<1$, $\Delta E_{\text{rédox}}$ n'est plus défini (réaction incomplète par manque de réactif): logarithme d'une valeur négative.

D'autre part, on remarque que, pour avoir en début de réaction un $E_{\text{rédox}\,i}$ défini, il est nécessaire de disposer d'un $r_i \neq 0$, si minime soit-il, c'est à dire un $K \neq 0$.

L'inégalité (14) renseigne de manière plus précise sur le choix de Q, puisqu'elle lui impose une borne supérieure et une borne inférieure:

$$r_i = K o_i \ll \Delta r^{*\,i}_j \ll o_i \Rightarrow K \ll \frac{\Delta r^{*\,i}_j}{o_i} \ll 1 \Rightarrow 1 \ll Q \ll K^{-1} \tag{23}$$

$$\text{Pour } K = 7 \cdot 10^{-3}, \text{ cela implique: } 1 \ll Q \ll 140 \tag{24}$$

Dans le domaine d'existence de Q défini par la double inégalité (23), on peut chercher la valeur de Q (optimisation) qui rende minimale la différence absolue D existant entre les formes exacte (*cf.* relations 13 et 22) et approchée de la fonction $\Delta E_{\text{rédox}}{}^{i}_{j} = \mathrm{f}(Q)$ (*cf.* relations 15 et 20), pour $K \neq 0$:

$$D = \frac{RT}{F} \cdot \left[\ln \frac{KQ+1}{K(Q-1)} - \ln \frac{1}{KQ} \right] = \frac{RT}{F} \cdot \ln \frac{(KQ+1)Q}{Q-1} \tag{25}$$

Les valeurs pour lesquelles la dérivée première par rapport à Q de cette nouvelle fonction de Q s'annule, donnent les extrema de cette dernière:

$$\frac{\mathrm{d}D}{\mathrm{d}Q} = \frac{KQ^2 - 2KQ - 1}{(KQ+1)Q(Q-1)} = 0 \tag{26}$$

à savoir:

$$Q_1 = \frac{K + (K^2+K)^{\frac{1}{2}}}{K} = 1 + \frac{(K^2+K)^{\frac{1}{2}}}{K} \tag{27}$$

$$Q_2 = \frac{K - (K^2+K)^{\frac{1}{2}}}{K}$$

Seule la solution Q_1 est admissible. La seconde, négative, n'a pas de signification physique, puisque pour $K>0$, $\Rightarrow K^2 < K^2 + K$.

$$\text{Si } K \ll 1 \Rightarrow K^2 \ll K \Rightarrow Q_1 \cong 1 + K^{-\frac{1}{2}} \text{ (première approximation)} \tag{27a}$$

$$\text{Si } K << 1 \Rightarrow Q_1 \cong K^{-\frac{1}{2}} \text{ (seconde approximation)} \tag{27b}$$

Pour $K = 7 \cdot 10^{-3}$, le calcul exact donne 13.0. Pour les valeurs de K égales à $1 \cdot 10^{-2}$ et $1 \cdot 10^{-3}$, on trouve pour Q_1 respectivement 10.0 et 30.0.

Le signe du coefficient du terme dominant étant positif, l'extremum obtenu est bien le minimum recherché, le dénominateur étant toujours positif si $Q>1$.

Le Tableau III donne en fonction de Q les différences absolues $D \cdot F/RT$, définies par la relation (25), et relatives $[D \cdot F/RT] \cdot \{\ln[(KQ+1)(KQ-K)^{-1}]\}^{-1}$

TABLEAU III

COMPARAISON DES FORMES EXACTE ET APPROCHÉE (VARIANTE PROPOSÉE) DE LA FONCT $\Delta E_{\text{rédox}}^{j} \cdot (F/RT) = f(Q)$

Q	$(KQ+1)/(KQ-1)$	$(KQ)^{-1}$	$\ln[(KQ+1)/(KQ-K)]$	$\ln(KQ)^{-1}$	$D(F/RT)$	$[D(F/RT)\cdot 100]/\{\ln[(KQ+1)/(KQ-K$
1.00	∞	142.857	∞	2.155	∞	—
1.77	187.827	80.710	5.236	4.391	0.845	16.14%
2.00	144.857	71.429	4.976	4.269	0.707	14.21%
3.00	72.929	47.619	4.290	3.864	0.426	9.33%
4.00	48.952	35.714	3.891	3.576	0.315	8.10%
5.00	36.964	28.571	3.610	3.353	0.257	7.12%
10.00	16.984	14.286	2.832	2.059	0.173	6.11%
13.00	12.988	10.989	2.565	2.397	0.168	6.55%
15.00	11.276	9.524	2.422	2.254	0.168	6.94%
20.00	8.571	7.143	2.148	1.966	0.182	8.47%

calculées pour $K = 7 \cdot 10^{-3}$. Il confirme l'existence d'une différence absolue minimale pour $Q \cong 13.0$ et relative pour $Q = 10$. Il montre encore que les valeurs de la fonction exacte $\ln[(KQ+1)(KQ-K)^{-1}]$ sont toujours plus élevées que celles de la fonction approchée $\ln(1/QK)$. Cette constatation permet de diminuer encore l'écart existant entre ces deux fonctions puisqu'il est possible d'ajouter aux valeurs déduites de la fonction approchée une valeur constante (par exemple 0.168 ou 6.55% respectivement).

Par analogie, le Tableau IV donne l'écart $D' \cdot F/RT$, absolu et relatif, existant entre la fonction exacte $\ln[(KQ+1)(KQ-K)^{-1}]$ et l'approximation proposée par Schierjott $[(KQ+1)(KQ-K)^{-1}]-1$, pour la valeur extrême $K = u_i^{-1} = 1/2.33 = 0.4286$.

La qualité de l'approximation de Schierjott décroît lorsque la sensibilité croît. L'optimisation de Q, qui rend minimale la différence D' existant entre les deux expressions considérées (*cf.* Tableau IV) conduit à $Q = \infty$, donc à une sensibilité nulle. D'autre part, on ne peut réduire la différence existant entre la fonction

TABLEAU IV

COMPARAISON DES FORMES EXACTE ET APPROCHÉE (SELON SCHIERJOTT) DE LA FONCT $\Delta E_{\text{rédox}}^{j} \cdot (F/RT) = f(Q)$

Q	$(KQ+1)/(KQ-K)$	$\ln[(KQ+1)/(KQ-K)]$	$[(KQ+1)/(KQ-K)]-1$	$D'(F/RT)$	$[D'(F/RT)\cdot 100]/\{\ln[(KQ+1)/(KQ-$
1.00	∞	∞	∞	—	—
2.00	4.333	1.467	3.333	−1.866	−127.20%
3.00	2.667	0.981	1.667	−0.686	− 69.93%
4.00	2.111	0.747	1.111	−0.364	− 48.73%
5.00	1.833	0.606	0.833	−0.227	− 37.46%
10.00	1.370	0.315	0.370	−0.055	− 17.46%
13.00	1.278	0.245	0.278	−0.033	− 13.47%
15.00	1.238	0.214	0.238	−0.024	− 11.21%
20.00	1.175	0.162	0.175	−0.013	− 8.02%
∞	1.000	0.000	0.000	−0.000	− 0.00%

approchée et la fonction exacte, puisque cette différence ne présente pas de composante constante.

Influence des températures de réaction et de mesure

La température intervient dans l'expression même du potentiel rédox (*cf.* formules 1, 2, 10 et 15) et dans la cinétique proprement dite de la réaction. Dans un cas comme dans l'autre, une augmentation de T est intéressante, puisqu'elle augmente d'une part le signal électrique $\Delta E_{\text{rédox}}$ et diminue de l'autre le temps de réaction. On recherchera donc la température la plus élevée et la plus constante possible.

Influence du temps de réaction

Théoriquement il faut choisir un temps j (pour effectuer la mesure) aussi proche que possible de la fin de la réaction, puisque le signal électrique obtenu croît au cours de la réaction. L'expérience montre que la vitesse de réaction est plus grande en début qu'en fin de réaction, l'équilibre étant atteint de façon asymptotique. Pourtant, si la réaction est très ou trop lente, il peut être néanmoins indiqué de choisir j avant la fin effective de la réaction, spécialement dans un analyseur automatique à flux continu, afin de garder pour la bobine de réaction des dimensions acceptables (perte de charge pour la pompe, dimension du bain marie, séparation des pics, etc.).

CONCLUSION

Il ressort de cette étude que la variante proposée s'avère plus avantageuse que celle de Schierjott lorsqu'il est nécessaire de travailler avec un certain excès de réactif dans le but d'augmenter la cinétique. Cette variante permet encore d'utiliser le réactif de façon beaucoup plus rationnelle (coût, solubilité, préparation, etc.) puisque ce dernier n'est composé pratiquement que de sa forme active (forme oxydée pour un oxydant, forme réduite pour un réducteur).

A condition de doser un constituant dont la concentration ne varie que faiblement d'un échantillon à l'autre, ce qui est souvent le cas par exemple des produits biologiques dont la synthèse est contrôlée génétiquement, on peut encore considérer avec une bonne approximation que le signal $\Delta E_{\text{rédox}}\,\overset{j}{}$ obtenu sur l'enregistreur varie proportionnellement* avec la teneur en oxydant ou en réducteur à déterminer. Même dans le cas général, où cette condition quelque peu restrictive ne peut être observée, la méthode reste valable; le calcul est alors effectué en utilisant la relation (15b).

Finalement, la variante proposée présente encore un avantage: l'approximation proposée pour la fonction théorique exacte est meilleure que celle de Schierjott. Cette constatation doit être néanmoins assortie des quelques réserves suggérées par la remarque qui suit.

Remarque

L'analyse des valeurs obtenues lors du calcul des différences tant absolues que

*A une constante additive près.

relatives existant entre la fonction exacte et la fonction approchée (*cf.* Tableaux I et IV) suggère deux autres possibilités d'interprétation de la proportionnalité indiquée par Schierjott. En effet, si ces valeurs ne présentent aucune composante constante, elles sont néanmoins toutes munies du même signe algébrique et monotones croissantes avec u_i (respectivement décroissantes avec Q). Ce comportement des différences s'explique par le fait que le développement en série proposé sous chiffre (4) est effectué pour $u_i = 1$, c'est à dire à l'une des frontières du domaine de travail considéré. On peut donc en déduire les deux nouvelles méthodes d'approximation suivantes, valables aussi bien pour la méthode de Schierjott que celle proposée dans ce travail.

Considérer comme droite "de proportionnalité" la tangente à la courbe théorique en un point judicieusement choisi, situé à l'intérieur du domaine de travail. Les différences absolues et relatives seront toujours munies du même signe algébrique, mais plus faibles comparativement aux écarts précédents.

Considérer la droite de régression obtenue à partir d'un certain nombre de points de la courbe théorique (assimilée à une droite sur un certain segment) situés dans le domaine de travail considéré. Cette solution pratique est intéressante puisqu'elle donne par définition la fonction linéaire qui approche le mieux la fonction théorique. Cette opération permet de diminuer notablement la valeur absolue des écarts observés—tant absolus que relatifs—puisqu'elle les distribue bilatéralement de part et d'autre de la droite de proportionnalité sous forme de déviations positives et négatives. Les deux points d'intersection de cette droite avec la courbe théorique déterminent les deux valeurs pour lesquelles l'approximation est idéale (différences absolue et relative nulle).

RÉSUMÉ

Le travail a pour objet l'étude d'une nouvelle méthode destinée aux déterminations quantitatives de routine de substances oxydables ou réductibles. Après un développement mathématique et une critique de la méthode de Schierjott, les auteurs proposent une modification fondamentale des conditions expérimentales indiquées par Schierjott, afin d'acroître considérablement la sensibilité de la méthode. Cette amélioration se révèle particulièrement avantageuse lors du dosage de substances peu réactives, tels les glucides. Elle permet une diminution de la quantité, donc du prix du réactif utilisé par analyse et minimise le risque de précipitation de l'un des composés formés ou engagés. Le développement mathématique de cette variante permet une comparaison théorique rigoureuse des deux méthodes. Les auteurs proposent encore une évaluation de la qualité des approximations introduites dans l'une et l'autre méthode. La dernière partie du travail est consacrée à l'optimisation des divers paramètres principaux qui y interviennent, à savoir la concentration du réactif, la température et le temps de réaction.

SUMMARY

A new method is proposed for routine determinations of oxidizable and reducible substances. A mathematical development and criticism of the method of Schierjott has led to a fundamental modification of the earlier experimental

conditions (ratio of the oxidized/reduced forms of the reagent at the start and end of the redox reaction). This improvement allows a considerable increase in the sensitivity of the method and is particularly advantageous for the determination of substances of low reactivity, *e.g.* carbohydrates. Other advantages are a reduction in the quantity and thus cost of the necessary reagent, and a decreased risk of precipitation of the substances involved. The mathematical treatment of the proposed version allows a rigorous theoretical comparison of the two methods. An evaluation of the quality of the approximations introduced into both methods is also proposed, based on the calculation of the deviation (absolute and relative differences) of approximated values from theoretical values. The final part of the work deals with optimization of the different principal parameters, *i.e.* concentration of the reagent, temperature and reaction time.

ZUSAMMENFASSUNG

Es wird eine neue Methode für die routinemässige, quantitative Analyse oxidier- oder reduzierbarer Substanzen beschrieben. Ausgehend von einer mathematischen Entwicklung und einer Kritik der Schierjott Methode werden experimentelle Bedingungen vorgeschlagen (Verhältnis oxidierte/reduzierte Form des Reagenzes zu Beginn und am Ende der Reaktion), die gegenüber derjenigen der Methode des genannten Autors eine beträchtliche Erhöhung der Empfindlichkeit erwarten lassen. Die vorgeschlagenen Konzentrationsverhältnisse wirken sich besonders günstig bei denjenigen Substanzen aus die normalerweise schwach oder langsam reagieren (z.B. Kohlhydrate). Die neue Methodik erlaubt den Einsatz geringerer Reagenzmengen—und erniedrigt somit auch den Reagenzpreis pro Analyse—und vermindert die Gefahr des Fällens der Ausgangs- oder Reaktionsprodukte. Die mathematischen Formulierungen der Redoxvorgänge in den beiden Methoden erlauben einen exakten Vergleich und eine genaue Interpretation der Resultate. Dabei werden die Genauigkeiten der in beiden Verfahren eingeführten mathematischen Approximationen in Form von Differenzen zwischen angenäherten und theoretischen Werten angegeben. Im letzten Teil der vorliegenden Arbeit werden die optimalen Reaktionsparameter (Konzentrationen, Temperatur, Reaktionszeit) der neuen Methode festgelegt.

BIBLIOGRAPHIE

1 G. Schierjott, *Z. Anal. Chem.*, 255 (1971) 350.
2 J. O. Bosset, B. Blanc et E. Plattner, *Anal. Chim. Acta*, sous presse.

Analytica Chimica Acta, 67 (1973) 415–426

MECHANISM OF ELECTROCHEMICAL REDUCTION OF OXAMIDE ANALYTICAL APPLICATIONS

DAVID L. McALLISTER, JEAN P. PINSON and GLENN DRYHURST
Department of Chemistry, University of Oklahoma, Norman, Okla. 73069 (U.S.A.)
(Received 11th May 1973)

During an investigation of the electrochemical oxidation of some pteridines in this laboratory, it became necessary to detect and determine oxamide, an oxidation product. Very few methods have been described for the determination of oxamide. The reported methods generally involve alkaline hydrolysis of oxamide to oxalic acid and ammonia, followed by titration of the acid[1] or titration of the liberated ammonia[2]. These methods were unsatisfactory for analysis of our mixtures, which contained ureas, amides and other species that are hydrolyzed to ammonia, other volatile bases or organic acids. Investigation showed that oxamide gives a very well-defined polarographic wave in neutral and alkaline solutions which could be used for its analytical determination.

This paper describes a detailed examination of the mechanism of the electrochemical reduction of oxamide and the use of the d.c. polarographic wave for its determination.

EXPERIMENTAL

Chemicals

Oxamide (Matheson, Coleman and Bell), glycolamide (Pfalz and Bauer) and acetonitrile (Mallinckrodt) were used.

Buffer solutions were prepared from analytical reagent-grade chemicals. Water-saturated nitrogen was used for deoxygenation of aqueous solutions. Dried argon saturated with acetonitrile was used for deoxygenation of acetonitrile solutions.

Apparatus

Polarograms and voltammograms were obtained with an instrument of conventional operational amplifier design, and were recorded on a Hewlett-Packard Model 7001A X-Y recorder. Fast-sweep voltammograms were recorded on a Tektronix Model 5031 Dual-Beam Storage Oscilloscope and photographed with a Tektronix Model C-70 camera. A three-compartment cell maintained at $25 \pm 0.1°$ containing a saturated calomel reference electrode (S.C.E.) and platinum gauze counter electrode was used. All potentials are referred to the S.C.E. at 25°.

The drop time of the D.M.E. was mechanically controlled at 2.00 s except for mercury column height dependence experiments when natural drop times were employed.

The hanging mercury drop electrode (H.M.D.E.) was a Metrohm Model E 410.

Controlled potential electrolysis and coulometry was performed with a Wenking Model 66TA1 Potentiostat. A Koslow Scientific Model 541 Coulometer was employed for current integration.

The three-compartment cell used for controlled potential electrolysis employed a mercury pool working electrode (area ≈ 16.6 cm^2), an S.C.E. reference electrode and platinum gauze counter electrode.

Mass spectra were recorded on a Hitachi RMU-6E mass spectrometer. N.m.r. spectra were obtained on a Varian T-60 spectrometer. Infrared spectra were recorded on a Beckman IR-8 spectrometer.

Polarographic and voltammetric procedures

Test solutions were prepared by diluting a known volume of stock solution with an appropriate buffer to give a final ionic strength of 0.5 *M*. The solution was then deaerated for about 5 min and the polarogram or voltammogram was recorded.

Coulometric and macroscale electrolysis procedure

For controlled-potential coulometry, 80 ml of a 1.0 m*M* solution of oxamide in the appropriate buffer was placed in the working electrode compartment of the coulometric cell. The solution was deaerated for *ca.* 10 min, and the nitrogen flow was continued during the electrolysis. When the current decreased to a low constant value, the counts per unit time produced by the coulometer was noted, and the electrolysis was stopped. The procedure for macroscale electrolysis was essentially the same, except that about 200 mg of oxamide in 80 ml solution was used. At the beginning of the electrolysis only a small portion of this oxamide was in solution, but as the reduction proceeded the remainder dissolved. Macroscale electrolyses of this nature usually required 36–48 h.

Determination of ammonia

The working electrode compartment of the cell was sealed with a large rubber stopper through which passed a glass tube. This glass tube was connected via Tygon tubing to a gas bubbling tower containing 80 ml of 0.05 *M* sulfuric acid, in which any ammonia flushed out of the electrolysis solution was trapped. After electrolysis, ammonia was determined spectrophotometrically in both the sulfuric acid and in the electrolysis solution with Nessler's reagent[3].

Isolation and identification of electrolysis product

To facilitate isolation of electrolysis products other than ammonia, macroscale electrolyses were carried out in carbonate buffer pH 10. After completion of the electrolysis, the solution was passed through a column of Dowex 50W-X8 ion-exchange resin (H^+ form) and eluted with 0.1 *M* acetic acid. The eluent was freeze-dried and a white solid was obtained, and recrystallized from ethyl acetate. This material (m.p. 114.5°) was identified as glycolamide by comparison of its mass, n.m.r. and infrared spectra and melting point with those of the authentic material. Analysis showed that the yield of glycolamide was 90% or better based on the amount of oxamide electrolyzed.

RESULTS AND DISCUSSION

D.c. polarography.

Between pH 5.6 and 11.6, oxamide exhibits a single well formed polarographic wave. The half-wave potential of this wave is independent of pH, $E_{\frac{1}{2}} = -1.59 \pm 0.01$ V. Between pH 5.6 and 8.0, the polarographic diffusion current constant ($I = i_l/Cm^{\frac{2}{3}}t^{\frac{1}{6}}$) is constant, but at higher pH it systematically decreases with increasing pH (Fig. 1). At pH values above 11.6 the hydrolysis of oxamide becomes rapid[4]. Below pH 5.6 the wave is obscured by background discharge. Relatively small but definite changes were noted in the dependence of the limiting current on the mercury column height and temperature at different pH values. Thus, at pH 8.1 the ratio of the limiting current to the square root of the corrected mercury height was constant, while at pH 11.1 there was a small but definite decrease (Table I). Coupled with the fact that the temperature coefficient of the limiting current at pH 8.1 is 0.4% per ° but 2.0% per ° at pH 11.1, it was concluded that above pH 8.1 the decrease in the limiting current was due to some homogeneous kinetic process. There are only two probable processes of this kind: the first is a chemical reaction preceding the electron transfer reaction, and the

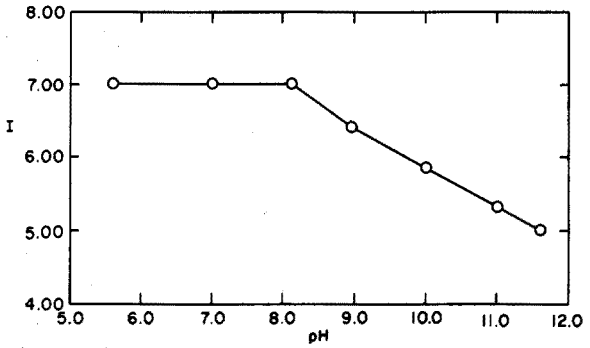

Fig. 1. Variation of the diffusion current constant with pH for oxamide.

TABLE I

EFFECT OF CORRECTED MERCURY COLUMN HEIGHT AND TEMPERATURE ON THE LIMITING CURRENT FOR OXAMIDE

h^a_{corr} (cm)	$i_l/h^{\frac{1}{2}}_{corr}$ ($\mu A\ cm^{-\frac{1}{2}}$)		*Temperature coefficient of* i_l[b]	
	pH 8.1	*pH 11.1*	*pH 8.1*	*pH 11.1*
41.7	0.794	0.665		
51.7	0.797	0.642		
61.7	0.787	0.624	0.4% per °	2.0% per °
71.7	0.804	0.622		
81.7	0.803	0.612		

[a] $h_{corr} = h_{mea} - 3.1\ (mt)^{-\frac{1}{2}}$.

[b] $TC = 2.303/(T_2 - T_1) \log_{10}[(i_2/i_1)]$, where i_2 is the limiting current at T_2 (40°) and i_1 the current at T_1 (25°).

second a chemical reaction or reactions interposed between two electrochemical reactions, *i.e.*, an e.c.e. mechanism. Before attempting to elucidate the details of the electrode mechanism, it was necessary to decide which of the two homogeneous chemical steps was involved in the overall electrode process. The only reasonable preceding chemical reactions would involve dissociation or hydration of oxamide. Spectrophotometrically, no evidence for dissociation of oxamide up to pH 11.6 could be obtained. Indeed, compounds similar to oxamide (*e.g.*, acetamide) have acidic pk_a values of around 30[5].

In order to investigate the possibility of a hydration–dehydration reaction involving oxamide, the variation of the molar absorptivity of oxamide as a function of pH was investigated. Oxamide exhibits two absorption bands in the u.v. region, at *ca.* 280 nm ($\varepsilon \approx 50$) and at *ca.* 205 nm ($\varepsilon \approx 10^4$). The former peak is probably due to a $n \rightarrow \pi^*$ transition, and the latter to a $\pi \rightarrow \pi^*$ transition, both associated with the carbonyl groups. The peak at 205 nm could only be satisfactorily observed below pH 8 because of solvent absorption. The peak at *ca.* 280 nm was essentially independent of pH with respect to both λ_{max} and ε_{max}. Addition of dioxan to aqueous buffered solutions of oxamide at pH 8–11 caused no significant spectral changes except for minor shifts of λ_{max}. A temperature change of *ca.* 40° also caused no appreciable spectral changes. Bell[6] has indicated that if a carbonyl compound shows an absorption band around 280 nm in aqueous solution which is unaffected by addition of dioxan or change of temperature, then hydration probably does not occur.

In view of these findings, it was concluded that oxamide is reduced in a process where one or more chemical reactions are interposed between two electron-transfer reactions. This conclusion was borne out by further electrochemical studies described below.

Controlled potential electrolysis and coulometry

Coulometry of oxamide at pH 8–11 indicated that 4 ± 0.2 electrons per molecule were transferred at all pH values (Table II). Analysis for ammonia liberated during the reduction (see Experimental) showed that 1 ± 0.2 mole of ammonia per mole of oxamide electrolyzed was liberated. After larger scale electrolyses at controlled potential, glycolamide was found to be the only other product in essentially quantitative yield (see Experimental).

TABLE II

COULOMETRIC *n*-VALUES FOR THE ELECTROCHEMICAL REDUCTION OF OXAMIDE AT A MERCURY ELECTRODE

(Borax buffers were used for pH 8.1 and 9.8, and carbonate buffer for pH 10.0. The potential was controlled at −1.65 V *vs.* S.C.E.)

pH	8.1	9.8	10.0
n	3.82	3.95	4.15
	3.92	3.77	3.90

Voltammetry at the H.M.D.E.

Linear and cyclic sweep voltammograms of oxamide were run at the H.M.D.E. in aqueous solutions of pH 5.6–11.6. At sweep rates of 5 mV s^{-1}, oxamide

shows a single peak (peak I_c), the peak potential (E_p) of which is independent of pH, $E_p = -1.63 \pm 0.02$ V. As the potential sweep rate is increased, the peak shifts to more negative potentials, *e.g.*, at 200 V s^{-1} in pH 10.0 carbonate buffer, $E_p = -1.90$ V. Such behavior is expected of an irreversible electrochemical reaction.

At sweep rates below 20 V s^{-1} in aqueous solution cyclic voltammetry gave no indication of any anodic peaks after the cathodic peak had been scanned (Fig. 2A). However, at sweep rates above 50 V s^{-1}, a small anodic peak (peak I_a) was observed after cathodic peak I_c had been scanned (Fig. 2B). Anodic peak I_a was always much smaller than the cathodic peak I_c, and its E_p was about 200 mV more positive than peak I_c.

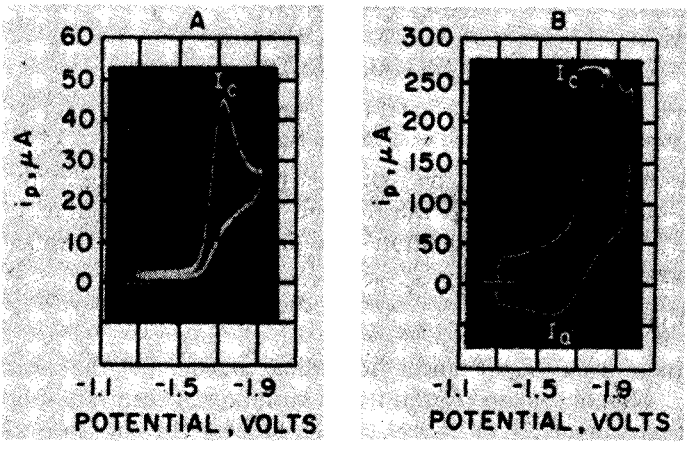

Fig. 2. Cyclic voltammograms of 0.5 m*M* oxamide at the H.M.D.E. in pH 10.0 carbonate buffer. Sweep rate (A) 2 V s^{-1}, (B) 100 V s^{-1}.

In an attempt to observe this anodic peak I_a more clearly, some studies were carried out in acetonitrile solution. Unfortunately, oxamide is extremely insoluble in pure acetonitrile and other aprotic solvents, and useful data could not be obtained. However, in 50% aqueous buffered solutions–50% acetonitrile, peak I_a appears at a sweep rate as low as 2 V s^{-1}. At very rapid sweep rates in the latter medium, a new cathodic peak (peak II_c) appears at more positive potentials than peak I_c (Fig. 3A). As the concentration of oxamide is decreased, peak I_c decreases in height, but the height of peak II_c remains constant (Fig. 3B) until very low concentrations are reached. The peak current function for peak II_c increases greatly with increasing scan rate. This evidence supports the view that peak II_c is an adsorption prepeak, corresponding to reduction of oxamide to an adsorbed product[7].

The fact that peak I_a could be observed at considerably lower can rates in partially non-aqueous medium suggests that the stability of the species being oxidized in the peak I_a process is considerably less in totally aqueous solution.

The shift of the peak potential for peak I_c with sweep rate, the failure to detect anodic peak I_a except at very fast sweep rates, and the separation of peak potentials for peaks I_c and I_a when both can be observed, are all consistent with an overall irreversible electrode reaction.

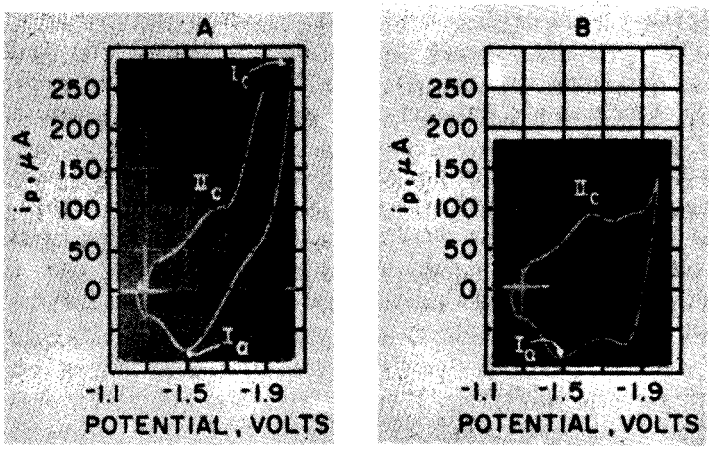

Fig. 3. Cyclic voltammograms of oxamide at the H.M.D.E. in 50% acetonitrile–50% pH 10.0 carbonate buffer. (A) 0.5 m*M* oxamide; (B) 0.05 m*M* oxamide. Sweep rates 100 V s^{-1}.

In order to define more completely the reduction process occurring at the electrode, the effect of the potential sweep rate on the peak voltammogram of oxamide was examined. The theoretical equation of a linear diffusion-controlled irreversible peak voltammogram is[8]:

$$(i_p)_{irrev} = 2.98 \cdot 10^5 n(\alpha n_a)^{\frac{1}{2}} AD^{\frac{1}{2}} v^{\frac{1}{2}} C \quad (1)$$

where all terms have their usual significance. According to eqn. (1) the peak current function, $i_p/ACv^{\frac{1}{2}}$, should remain constant with variation in scan rate if no chemical complications are involved in the electrode process. In the case of oxamide, the peak current function decreases with increasing scan rate (Fig. 4) at all pH values. The onset of the decrease shifts to lower sweep rates with increase in pH.

By computing a value of αn_a from the equation[9]:

$$(E_{p/2})_2 - (E_{p/2})_1 = (0.0128/\alpha n_a) \log_e (v_2/v_1) \quad (2)$$

where $(E_{p/2})_2$ and $(E_{p/2})_1$ are the half-peak potentials in volts for oxamide peak I_c at sweep rates v_2 and v_1 (V s^{-1}), it is possible to compute theoretical peak current functions for uncomplicated irreversible electrode reactions. For an αn_a value of 1.0 (the measured values of αn_a between pH 7 and 11.6 ranged from 1.04 to 0.80), theoretical peak current functions for $n=4$ and $n=2$ were computed (Fig. 4). It is clear that at slow sweep rates the peak current function of oxamide peak I_c is close to that expected for a 4*e* reaction while at fast sweep rates it approaches the theoretical value for a 2*e* reaction. This behavior indicates an electrode process in which the initial electron-transfer reaction is followed by one or more chemical reactions which in turn are followed by a further electron-transfer process, *i.e.*, an e.c.e. process[8], or an electrode process preceded by a chemical reaction. However, in view of the spectrophotometric studies of oxamide, the probability of the latter process was considered remote and an e.c.e. mechanism was presumed to occur.

The theory of stationary electrode voltammetry for the e.c.e. mechanism has

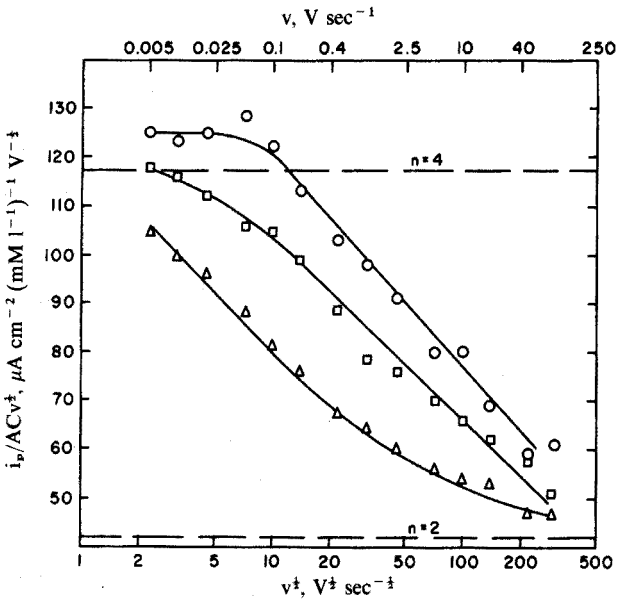

Fig. 4. Variation of the peak current function of oxamide peak I_c at the H.M.D.E. with he square root of scan rate in various buffer systems. (○—○) pH 7, McIlvaine; (□—□) pH 10, carbonate; and (△—△) pH 11.8, hydroxide–chloride buffer. (---) Theoretical peak current functions for $n=4$ and $n=2$ when no chemical complications occur.

been treated by Nicholson and Shain[10]. According to this treatment the observed current can be calculated for a process in which both electron-transfer steps are reversible from the expression

$$i = 0.602\, n^{\frac{3}{2}}\, AD^{\frac{1}{2}}\, Cv^{\frac{1}{2}}[\pi^{\frac{1}{2}}\chi(at)+\pi^{\frac{1}{2}}\phi(at)] \qquad (3)$$

where $a=nFv/RT$, $\pi^{\frac{1}{2}}\chi(at)$ is the current function for the first charge transfer, and $\pi^{\frac{1}{2}}\phi(at)$ is the current function for the second charge transfer. Values for the functions $\pi^{\frac{1}{2}}\chi(at)$ and $\pi^{\frac{1}{2}}\phi(at)$ are tabulated for various values of $k_{f/a}$, where k_f is the homogeneous rate constant for the chemical step(s) interposed between the two charge-transfer reactions. In order to adapt this theory to the reduction of oxamide in which both electron-transfer reactions are irreversible, eqn. (3) was rewritten in a form that probably approximates this process, but still allows the use of theoretical current functions tabulated by Nicholson and Shain[8,10], as follows:

$$i = 0.602\, n\,(\alpha n_a)^{\frac{1}{2}}\, AD^{\frac{1}{2}}\, Cv^{\frac{1}{2}}[\pi^{\frac{1}{2}}\chi(bt)+\pi^{\frac{1}{2}}\phi(at)] \qquad (4)$$

where $\pi^{\frac{1}{2}}\chi(bt)$ is the current function for an irreversible charge transfer[8]. Theoretical current functions for the second irreversible electron-transfer step have never been derived, and accordingly the function $\pi^{\frac{1}{2}}\phi\ (at)$ was employed. From eqn. (4), theoretical peak current functions, $i_p/ACv^{\frac{1}{2}}$, were calculated for e.c.e. processes where the rate constant k_f ranged from 1–200 s^{-1}. The values of $\pi^{\frac{1}{2}}\chi(bt)$ and $\pi^{\frac{1}{2}}\phi(at)$ were obtained from refs. 8 and 10, respectively, and are the maximal values. When these theoretical peak current functions *vs.* square root of sweep rate curves were

compared to the experimental curves it was possible to obtain approximate values of k_f (Table III). The value of αn_a used in the calculations was unity (*vide supra*). The diffusion coefficient was determined at pH 7 from current–time curves by the method of Shain and Martin[11] and had a value of $9.73 \cdot 10^{-6}$ cm^2 s^{-1}. The values of k_f calculated here are of course only approximate because of the lack of rigour in the use of eqn. (4). Nevertheless, when the values were compared to those determined by alternative methods, the error involved was not excessive, and this method could probably be applied to other systems.

TABLE III

VALUES OF THE HOMOGENEOUS RATE CONSTANT, k_f, FOR THE CHEMICAL STEP IN THE ELECTROCHEMICAL REDUCTION OF OXAMIDE AT A MERCURY ELECTRODE

Buffer system	*pH*	$k_f(s^{-1})$ *from*		
		Peak voltammetry	*Potentiostatic*	*Polarographic*
McIlvaine	7.0	50	30	—
Borax	10.0	10	13	6.5
Chloride/hydroxide	11.6	1	2	1

Potentiostatic studies

In an attempt to verify the above values of k_f, the potentiostatic method of Alberts and Shain[12] as applied to the e.c.e. mechanism was employed. In this method the potential of a stationary microelectrode (*e.g.*, the H.M.D.E.) is stepped to a value corresponding to the plateau of a polarographic wave and the resultant current is monitored as a function of time. At short times the observed current corresponds to the first charge-transfer step, but at longer times there is a transition to a current corresponding to both charge-transfer steps. The time at which the transition occurs depends on the rate of the intervening chemical reaction. The equation relating current to time for an e.c.e. process is [12]

$$i_t = \frac{FAD^{\frac{1}{2}}C[n_1 + n_2(1 - e^{-k_f t})]}{t^{\frac{1}{2}}\pi^{\frac{1}{2}}} \qquad (5)$$

where i_t is the instantaneous current at time t (s) in μA; n_1, the number of electrons involved in the first electron-transfer step; n_2, the number of electrons involved in the second electron-transfer step, and t the time (s) elapsed since application of the potential step. The remaining terms have their usual significance. Theoretical current–time curves were calculated for $n=4$ (*i.e.*, where k_f is infinite) and for $n=2$ (*i.e.*, where k_f is zero) from the Cottrell equation and the value of D computed previously. Experimental current–time curves showed that at very short times the current was close to that expected for a 2*e* reaction (Fig. 5A, B), and then at longer times the curve deviated and ultimately coincided with the theoretical 4*e* curve. The transition from the 2*e* to 4*e* reaction took considerably longer at high pH (*e.g.*, pH 11.6, Fig. 5A) than at lower pH (*e.g.*, pH 7.0, Fig. 5B), *i.e.* k_f decreases as the pH increases. The value of k_f at each pH can be obtained from data of the type shown in Fig. 5 by use of the working curves prepared by Alberts and Shain[12]. Theoretical curves can then be constructed

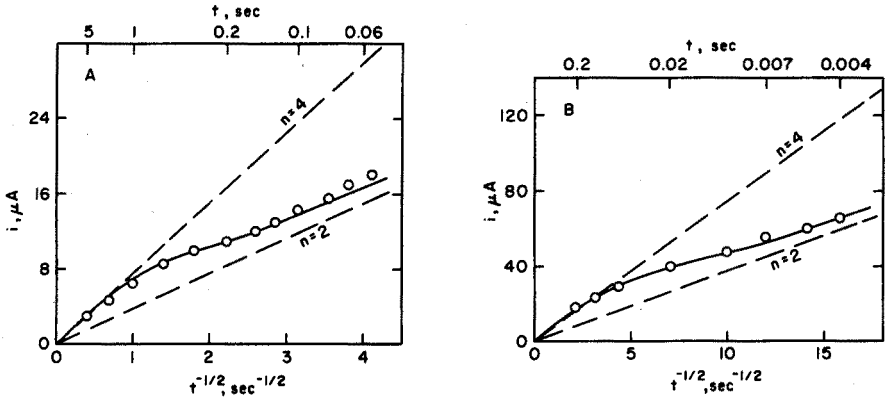

Fig. 5. Comparison of experimental and theoretical current–time curves for the electrochemical reduction at the H.M.D.E. (A) pH 11.8, $k_f = 2\ s^{-1}$; (B) pH 7, $k_f = 30\ s^{-1}$. (○) Experimental values; (—) theoretical curves for the given rate constants calculated from eqn. (5); (– – –) theoretical curves for uncomplicated 2*e* and 4*e* transfer processes.

by means of eqn. (5). The agreement between theoretical and experimental current *vs.* time curves was excellent. Typical values of k_f computed at representative pH values are shown in Table III; the agreement between the values determined potentiostatically and by peak voltammetry is quite good.

Further polarographic studies

The effect of an e.c.e. mechanism on a d.c. polarographic wave has been examined by Nicholson *et al.*[13]. Their approach allows an estimate of the rate constants of rather slow chemical reactions interposed between two charge-transfer reactions. In the present study, the value of k_f at pH values above *ca.* 8–9 is sufficiently low to cause a measurable decrease of the polarographic limiting current below the 4*e* value. From the working tables of Nicholson *et al.*[13], values of k_f were calculated and compared to those obtained by the potentiostatic and peak voltammetric methods. The value of i_d (the diffusion current for the first electrochemical step) was taken as one-half of the value of the limiting current at the end of the drop life at pH 5.6–7, *i.e.*, where k_f is large and does not affect the polarographic limiting current. The value of i_k was then the measured limiting current above pH 9, *i.e.*, where k_f is so small that the limiting current decreases below the diffusion-limited value. Typical values of k_f so calculated are presented in Table III. This polarographic method is probably the least satisfactory method for calculation of k_f. The range of values which can be determined is limited, and small errors in measurement of i_d and i_k lead to large errors in the value of k_f.

Mechanism

From the experimental data, it is clear that oxamide is electrochemically reduced between pH 5.6 and 11.6 in a pH-independent, overall 4*e* process to give glycolamide as the ultimate product. The pH independence of the voltammetric peak potential and polarographic half-wave potential in this pH range implies that protons are not involved in the rate-determining process. The total

electron-transfer process is electrochemically irreversible. The effect of increasing potential sweep rate in peak voltammetric studies, and the variation of current with time in potentiostatic studies, support the view that the overall electrode process follows an e.c.e. type mechanism with both the initial and final charge-transfer steps involving 2*e*. D.c. polarography also supports the e.c.e. mechanism.

The only reasonable reaction for the initial 2*e* charge-transfer reaction of oxamide (I) is formation of a dianion (II). The following chemical processes probably involve protonation of the dianion to an enediol (III) followed by rearrangement to compound IV and loss of ammonia to compound V. Similar reduction mechanisms have been proposed for benzil and other 1,2-diketones[13–15].

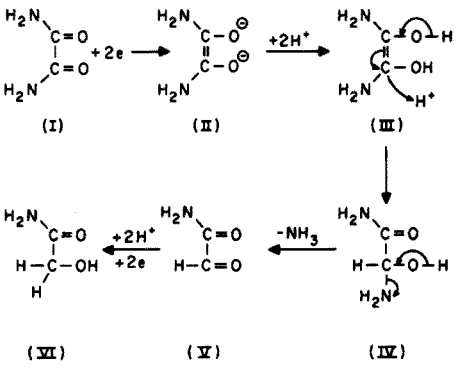

The anodic peak I_a observed on cyclic voltammetry of oxamide may correspond either to the oxidation of the dianion or the enediol. The fact that the anodic peak can be observed at lower sweep rates in a more aprotic solvent (50% acetonitrile) suggests that the dianion is oxidized. In any event the enediolate (II) or the enediol (III) would both be expected to be readily oxidized species as are many enediols both chemically[16] and electrochemically[17].

The chemical reactions describing transformation of II–V may occur quite separately or proceed via a concerted reaction. Nevertheless, the effect of pH on the overall rate constant of the reaction is obvious, *i.e.*, the rate of the chemical reaction decreases with increasing pH. However, the measured rate constant (k_f) may have a value corresponding to any of the individual reactions or may simply reflect a value for the overall rate. The compound formed by the chemical reactions characterized by k_f is glyoxylamide (V). There are no electrochemical data on this compound, and efforts to prepare it by the method of Tits and Bruylants[18] were unsuccessful. However, it has been reported that glyoxylic acid is easily reduced electrochemically to glycolic acid[19]. Also, phenylglyoxylamide is reduced electrochemically to phenylglycolamide[20]. It seems reasonable, therefore, that glyoxylamide is similarly reduced to glycolamide.

Analytical utility of d.c. polarography

Linear limiting current *versus* concentration curves were obtained for oxamide in solutions of pH 5.6–11. However, the polarographic reduction wave is best defined in borax buffer pH 8.1 or carbonate buffer pH 10.0, *i.e.*, the wave

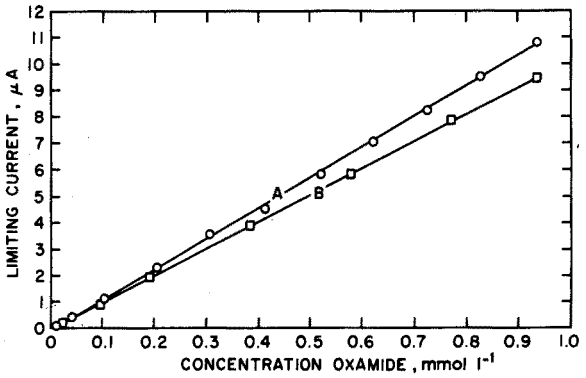

Fig. 6. Linear variation of the limiting current *vs.* concentration of oxamide in (A) borax buffer pH 8.1 and (B) carbonate buffer pH 10.

exhibits its best separation from background reduction. Linear concentration curves in these buffers could be obtained between 10^{-5} to $>10^{-3}$ *M* oxamide (Fig. 6). From the viewpoint of quantitative analysis, oxamide can be satisfactorily determined by preparation of a calibration curve at the desired pH and over the concentration range of interest. The pH employed would be selected where the wave of oxamide does not fall in the same potential region as waves of other electroactive components in the sample. It was found that neither oxalic acid nor oxamic acid (the monoamide of oxalic acid) are electrochemically reducible in weakly acidic or basic media, hence these two compounds do not interfere with the determination of oxamide.

This work was supported by the National Science Foundation and the Faculty Research Committee of the University of Oklahoma. Their support is greatly appreciated.

SUMMARY

Oxamide is electrochemically reduced at mercury electrodes between pH 5.6 and 11.6. The overall mechanism proceeds by an initial 2*e* reduction of the 1,2-carbonyl groups of oxamide to give a dianion. This then protonates, rearranges, and loses ammonia to glyoxylamide, which is reduced in a further $2e/2H^+$ reaction giving glycolamide as the ultimate product. The reaction thus proceeds by a typical e.c.e. mechanism. The overall homogeneous rate contant for the chemical reaction(s) interposed between the two charge-transfer steps was measured by peak voltammetric, potentiostatic and d.c. polarographic methods. The d.c. polarographic wave of oxamide between pH 5.6 and 11 provides the basis for a very simple analytical method for the determination of oxamide.

RÉSUMÉ

L'oxamide est réduite électrochimiquement aux électrodes de mercure entre le pH 5.6 et le pH 11.6. La réaction se fait en deux stades: d'abord réduction (2*e*)

des groupes 1,2-carbonyle de l'oxamide pour donner un dianion. Après réarrangement et départ d'ammoniac, on arrive à la glyoxylamide qui se réduit à son tour ($2e/2H^+$) pour donner la glycolamide, le produit final. Des mesures voltammétriques, potentiostatiques et polarographiques à courant continu, ont été faites. Une méthode d'analyse très simple est proposée pour le dosage de l'oxamide, par polarographie à courant continu, entre le pH 5.6 et le pH 11.0.

ZUSAMMENFASSUNG

Oxamid wird an Quecksilberelektroden zwischen pH 5.6 und 11.6 elektrochemisch reduziert. Zu Beginn des gesamten Vorganges findet eine 2*e*-Reduktion der 1,2-Carbonyl-Gruppen von Oxamid unter Bildung eines Dianions statt. Nach Protonierung und Neuordnung gibt dieses dann Ammoniak unter Bildung von Glyoxylamid ab, welches in einer weiteren $2e/2H^+$-Reaktion zu Glykolamid als Endprodukt reduziert wird. Die Reaktion verläuft also nach einem typischen e.c.e. Mechanismus. Die gesamte homogene Geschwindigkeitskonstante der zwischen den beiden Ladungsübertragungsstufen ablaufenden chemischen Reaktion(en) wurde mittels peak-voltammetrischer, potentiostatischer und gleichstrompolarographischer Methoden gemessen. Die gleichstrompolarographische Welle von Oxamid zwischen pH 5.6 und 11 bildet die Grundlage für eine sehr einfache analytische Methode für die Bestimmung von Oxamid.

REFERENCES

1 R. D. Tiwari, J. P. Sharma and I. C. Shulka, *Ind. J. Chem.*, 4 (1966) 221.
2 J. B. Apatoff, J. Cohen and G. Norwitz, *Anal. Chem.*, 35 (1963) 800.
3 G. Dryhurst and P. J. Elving, *J. Electrochem. Soc.*, 115 (1968) 1014.
4 X. V. Voortam, P. Crooy, A. Bruylants and L. Baczynsky, *Bull. Soc. Chim. Belg.*, 73 (1964) 753.
5 D. J. Cram, *Chem. Eng. News*, 41, No. 33 (1963) 94.
6 R. P. Bell, in V. Gold, *Advances in Physical Organic Chemistry*, Vol. 4, Academic Press, New York, 1966, pp. 1–29.
7 R. H. Wopschall and I. Shain, *Anal. Chem.*, 39 (1967) 1514.
8 R. S. Nicholson and I. Shain, *Anal. Chem.*, 36 (1964) 706.
9 R. N. Adams, *Electrochemistry at Solid Electrodes*, Marcel Dekker, New York, 1969, p. 137.
10 R. S. Nicholson and I. Shain, *Anal. Chem.*, 37 (1965) 178.
11 I. Shain and K. J. Martin, *J. Phys. Chem.*, 65 (1961) 254.
12 G. S. Alberts and I. Shain, *Anal. Chem.*, 35 (1963) 1859.
13 R. S. Nicholson, J. M. Wilson and M. L. Olmstead, *Anal. Chem.*, 38 (1966) 542.
14 R. H. Philip, R. L. Flurry and R. A. Day, *J. Electrochem. Soc.*, 111 (1964) 328.
15 J. Holubek and J. Volke, *Collect Czech. Chem. Commun.*, 25 (1960) 3292.
16 L. F. Fieser and M. Fieser, *Reagents for Organic Synthesis*, Wiley, New York, 1967, pp. 159–160.
17 G. Dryhurst, *J. Electrochem. Soc.*, 119 (1972) 1559.
18 M. Tits and A. Bruylants, *Bull. Soc. Chim. Belg.*, 57 (1948) 50.
19 V. D. Bezuglyi, V. N. Dmitrieva, T. S. Tarasyuk and N. A. Izmailov, *Zh. Obshch. Khim.*, 30 (1960) 2415; *Chem. Abstr.*, 55 (1961) 8120.
20 J. Armand, P. Souchay and F. Valentini, *C. R., Ser. C*, 265 (1967) 1267.

Analytica Chimica Acta, 67 (1973) 427–436

AN ANALYTICALLY USEFUL COULOMETRIC GENERATION OF MICRO AMOUNTS OF METAL IONS

PART I. ELECTROGENERATION OF BISMUTH(III)

TH. J. M. POUW, G. DEN BOEF and U. HANNEMA

Laboratory for Analytical Chemistry, University of Amsterdam, Nieuwe Achtergracht 125, Amsterdam (The Netherlands)

(Received 6th April 1973)

The electrogeneration of a great number of analytical reagents has become a well-established technique in titrimetric analysis. However, there are few reports on the electrogeneration of metal ions, despite their importance as analytical reagents, especially in complexometry. Only the electrolytic preparation of silver and mercury ions from the corresponding metals has been investigated extensively[1–19], and electrogenerated silver and mercury ions are now widely used in many precipitation titrations. Reports on the electrogeneration of other metal ions are scarce: Su[20] has described the electrolytic preparation of Bi(III), Zr(IV), Hf(IV), Ni(II), Pb(II), In(III), Al(III), Co(II) and Th(IV) from their metals; and Tutundzic and Stojkovic[21] have reported a phosphate determination with electrogenerated bismuth(III).

Instead of the pure metals, amalgams may be used as the electrode material from which metal ions can be generated. The most important advantage of amalgams over the pure metals is the fact that their electrochemical behaviour is generally less complicated. There is also the minor advantage that it is possible to vary the concentration of amalgams, thus providing an extra means of controlling the experimental conditions. A study of the electrogeneration of Cd(II), Bi(III), In(III), Co(II) and Ni(II) from the corresponding amalgams has been made by Wells[22], but he did not try to generate micro amounts of these metal ions.

This paper deals with the electrogeneration of micro amounts of bismuth(III) ions from dilute bismuth amalgam. In order to measure the current efficiency, an accurately known amount of EDTA was added to the solution in the electrolysis cell so that the bismuth ions released immediately yielded the bismuth–EDTA complex. Because of the very high u.v. absorbance of this complex, the reaction between EDTA and bismuth(III) could be followed spectrophotometrically[23]. The bismuth–EDTA complex shows maximal absorbance at 263 nm with a molar absorptivity of about 10000. The general shape of a plot of absorbance *vs.* total time of electrolysis is shown in Fig. 1.

The main problem encountered in the preparation of bismuth ions by electrolytic oxidation of bismuth amalgam is that oxygen present in the solution contacting the amalgam can also oxidize the amalgam. Therefore, the generation of bismuth ions proceeds even if the generation current is switched off, so that

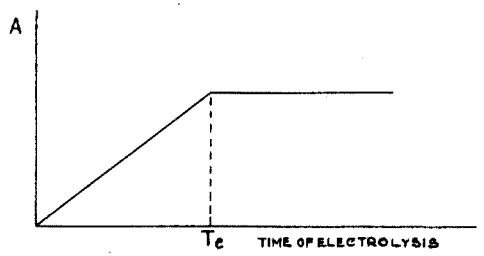

Fig. 1. Coulometric titration of EDTA with bismuth(III) with photometric end-point detection.

the current efficiency is always above 100%. Substantial deviations from 100% current efficiency occur especially if the total amount of bismuth ions generated is in the micromole range. Even prolonged passage of nitrogen is then insufficient to render the interference of oxygen negligible. However, this interference can be largely eliminated by using an experimental set-up which allows the application of a negative potential on the amalgam electrode whenever the generation current is interrupted. By such a procedure trace quantities of bismuth(III) can be generated with 100% current efficiency. Although the stability of the bismuth–EDTA complex is large enough to allow accurate determinations of concentrations of EDTA smaller than 10^{-6} *M*, the lower limit of determination is 10^{-6} *M* because the total change in absorbance at lower concentrations becomes too small for the accurate measurement of an absorbance *vs.* time of generation plot.

EXPERIMENTAL

Equipment and chemicals

A top view of the electrolysis cell used for generation of bismuth(III) is shown in Fig. 2. The volume of the measuring compartment (anode compartment) was 30 ml. Air was excluded from this compartment by means of a cover containing two holes, one for a nitrogen inlet tube and the other one for the introduction and removal of solutions. The optical length of the cell was 5.3 cm. The walls through which light enters and leaves the cell were made of quartz to allow measurements in the u.v. region. The cell was placed in a Zeiss PMQ II spectrophotometer. Electrical wires and the nitrogen inlet tube were connected to the electrolysis cell through a hole in the back of the cell compartment of the spectrophotometer.

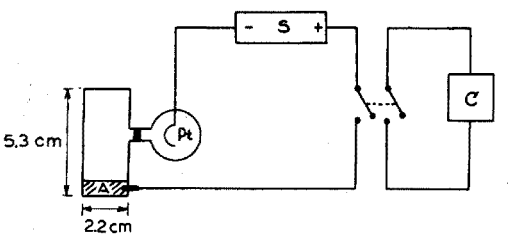

Fig. 2. Circuit for electrolytic generation of bismuth(III). (A) Amalgam electrode (1 cm wide, 0.5 cm high); (Pt) platinum spiral electrode; (S) current supply; (C) clock. The amalgam layer is held in position with a glass strip at a height of 0.5 cm.

Constant currents were supplied by an Ultra-stable current supply, model UCS6-2F (Laboratorium voor Instrumentele Electronica, Amsterdam). This instrument is capable of supplying currents in the range 1 μA–125 mA.

A Jaquet electromagnetic stopclock was used as the current timer.

The potentiostat which was used for the elimination of the interference of oxygen was the "Beckman Electroscan 30" employed in its potentiostat mode of operation. The saturated calomel reference electrode (type K100, Radiometer), which is necessary for the proper operation of the potentiostat, was connected to the electrolysis cell by polyethylene capillary tubing, filled with saturated potassium chloride solution.

Polarograms of a dropping bismuth amalgam electrode were recorded with a Radiometer PO4 polarograph.

All chemicals used were of reagent grade.

The influence of oxygen

A series of electrogenerations of bismuth(III) was carried out with the simple circuit shown in Fig. 2. The amalgam electrode had a concentration of about 0.2 *M*. The experimental procedure was as follows.

A stock solution of perchloric acid (pH 1.3) was kept free of oxygen by passing nitrogen through it. About 30 ml of this solution was pumped from the stock vessel into the electrolysis cell by means of the nitrogen pressure. Nitrogen was also passed through the solution in the cell, by means of a tube placed close to the amalgam surface. The bubbling nitrogen caused a vibration of the amalgam, which enhanced the rate of transport of bismuth(III) from inside the amalgam to the surface; this was important for reducing the chance that during the generation the limiting current of the oxidation of the amalgam would fall below the generation current.

Subsequently, a small volume (0.025–0.125 ml) of 0.01 *M* EDTA solution was added to the perchloric acid solution in the electrolysis cell from a micro burette (Metrohm E.374). The EDTA was titrated with electrogenerated bismuth(III), the generating current being 5 mA. The generating current was interrupted several times; at each interruption, the absorbance of the solution in the cell was measured at 263 nm after homogenization of the solution by bubbling nitrogen through it.

Finally, absorbance was plotted against total generation time. The current efficiency of the generation was calculated as C.E. $= T_t/T_f \cdot 100\%$, where T_f was the experimental generation time needed to convert all the EDTA present, and T_t was the theoretical generation time according to Faraday's first law.

Figure 3 summarizes the results of all of the titrations performed; each point is the average of five different titrations. The deviations of the current efficiency from 100% which occurred when the total amount of bismuth(III) generated was less than 1 μmole must be ascribed to traces of oxygen which remained in the solution despite of the passage of nitrogen. During the interruptions of the current, these traces of oxygen caused a spontaneous oxidation of the amalgam.

More evidence for the interfering influence of oxygen was obtained from polarization curves of a dropping bismuth amalgam electrode. An experimental polarization curve of a dropping bismuth amalgam electrode in a perchloric acid

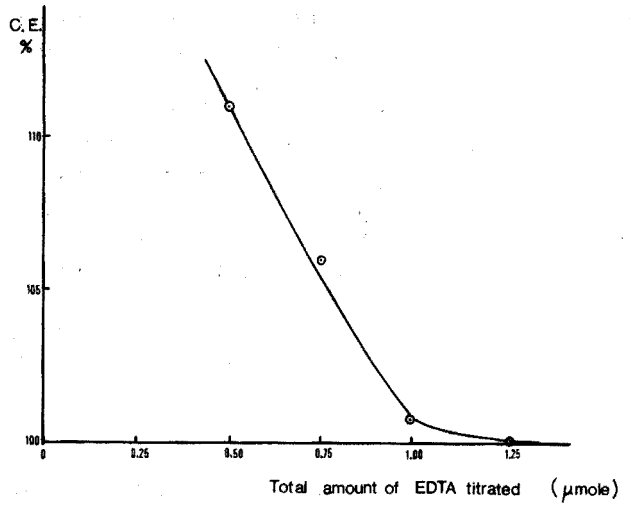

Fig. 3. Current efficiency of electrogeneration of bismuth(III).

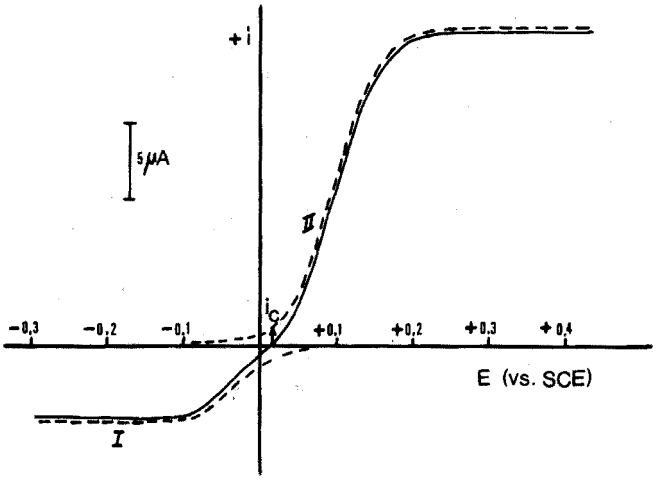

Fig. 4. Influence of oxygen on the polarization curve of a dropping bismuth electrode.

solution (0.003% in triton X-100) of pH 1.3 from which oxygen had not been removed is given in Fig. 4. The concentration of the amalgam was about 0.001 *M*. The curve is a summation of the reduction curve of oxygen (I) and the oxidation curve of bismuth amalgam (II). The electrochemical processes associated with I and II are:

$$O_2 + 2H_3O^+ + 2e \rightarrow H_2O_2 + 2H_2O \qquad \text{(I)}$$

$$Bi(Hg) \rightarrow Bi^{3+} + 3e + (Hg) \qquad \text{(II)}$$

In the absence of a polarizing potential the amalgam assumes the potential E_c and will be oxidized spontaneously, at a rate given by the corrosion current, i_c. The reaction according to which the corrosion occurs can be found by combining

the separate electrode processes (I) and (II):

$$3O_2 + 6H_3O^+ + 2Bi(Hg) \rightarrow 2Bi^{3+} + 3H_2O_2 + 6H_2O + 2(Hg)$$

Elimination of the interference of oxygen by cathodic protection of the amalgam electrode

Tests were made to establish whether spontaneous oxidation of the amalgam electrode could be prevented to a sufficient extent by applying a negative potential. The electrolysis cell, equipped with an amalgam electrode of concentration 0.2 *M*, was filled with 30 ml of an oxygen-free perchloric acid solution of pH 1.3, and 0.1 ml of 0.01 *M* EDTA was added. The rate of spontaneous oxidation was then determined by measuring the absorbance of the solution in the electrolysis cell at 263 nm every 5 min. Different values of the negative potential were applied to the amalgam electrode. Nitrogen was passed through the solution except during the few seconds required to measure the absorbance. Figure 5 summarizes the results. It can be seen that a potential of −0.6 V *vs.* S.C.E. reduces the rate of spontaneous oxidation of the bismuth amalgam electrode virtually to zero.

The use of cathodic protection in the electrogeneration of trace amounts of bismuth(III)

The cathodic protection was achieved by the experimental arrangement given in Fig. 6. According to Fig. 5, the potential supplied by the potentiostat should be −0.6 V *vs.* S.C.E. Under the given experimental conditions, the bismuth–EDTA complex, formed during the generation, was not reduced at this potential. This was proved by measuring the absorbance of a bismuth–EDTA solution over a prolonged period of time, with the amalgam electrode at −0.6 V *vs.* S.C.E.; the absorbance remained constant, indicating that no reduction occurred.

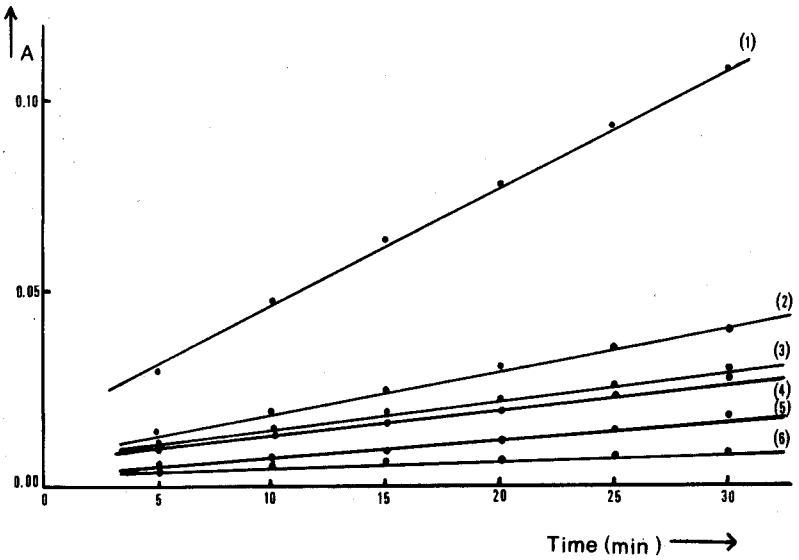

Fig. 5. Oxidation of bismuth amalgam at various potentials. (1) No cathodic protection; (2) −0.2 V; (3) −0.3 V; (4) −0.4 V; (5) −0.5 V; (6) −0.6 V *vs.* S.C.E.

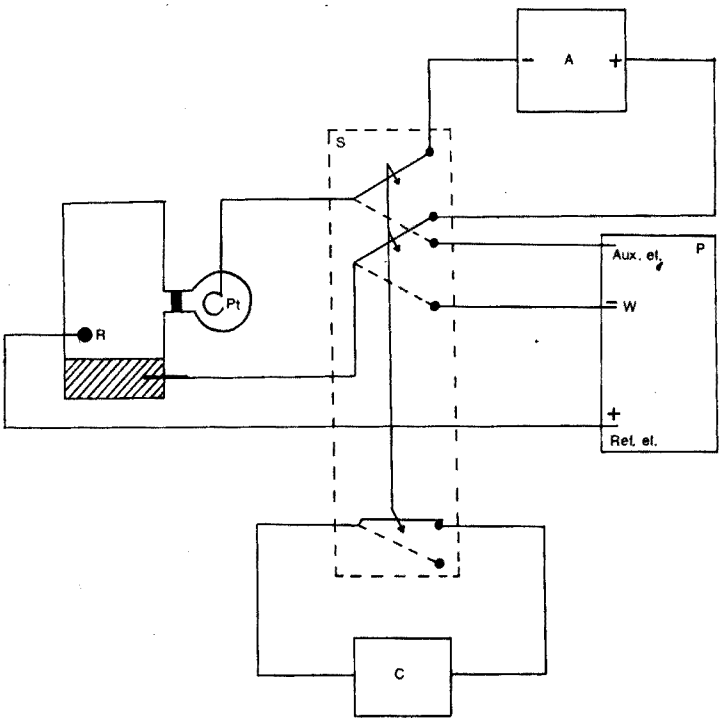

Fig. 6. Coulometric circuit for the generation of trace quantities of bismuth(III) from bismuth amalgam. (A) Amperostat; (P) three-electrode potentiostat; (R) reference electrode; (C) clock; (S) switching device.

RESULTS

Table I presents the results of titrations of small amounts of EDTA with electrogenerated bismuth(III), obtained as described above. As the amount of EDTA to be titrated decreased, the generation current was made smaller in order to obtain titration times sufficiently long for accurate measurement. Therefore, the concentration of the amalgam could also be lowered.

TABLE I

ELECTROGENERATION OF SMALL AMOUNTS OF BISMUTH(III)

Amount of EDTA titrated (moles)	*I (mA)*	*Conc. of the amalgam (M)*	T_t *(s)*	T_c *(s)*	*C.E.(%)*	s_r[a] *(%)*
$5.15 \cdot 10^{-7}$	2.5	0.2	59.6	59.3	100.5	0.5
$1.038 \cdot 10^{-7}$	1.0	0.1	30.0	29.6	101.3	0.6
$5.19 \cdot 10^{-8}$	0.25	0.05	60.0	59.3	101.2	0.5

[a] $n = 10$.

A typical curve for the titration of $5.19 \cdot 10^{-8}$ moles of EDTA with electro generated bismuth(III) is shown in Fig. 7. This curve indicates that the total ob

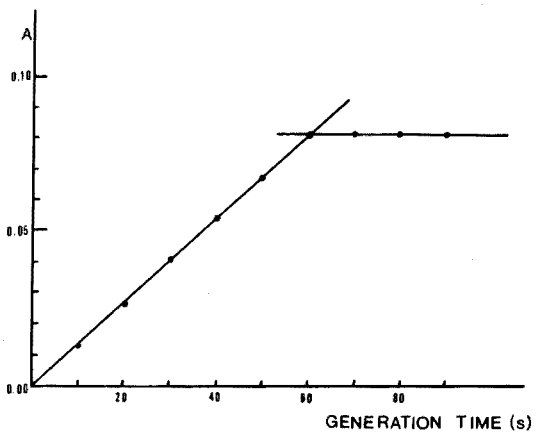

Fig. 7. Titration curve of $5.19 \cdot 10^{-8}$ moles of EDTA with bismuth(III).

served change in absorbance would not allow the determination of amounts of EDTA much smaller than $5 \cdot 10^{-8}$ moles, which corresponds to an EDTA concentration in the cell of $1.5 \cdot 10^{-6}$ *M*.

Influence of the generation current

The influence of the value of the generating current on the current efficiency was investigated by titrating $5.19 \cdot 10^{-8}$ moles of EDTA at different generation currents. Table II summarizes the results.

TABLE II

TITRATIONS OF $5.19 \cdot 10^{-8}$ MOLES OF EDTA WITH ELECTROGENERATED BISMUTH-(III)

I (mA)	T_t *(s)*	T_f *(s)*	*C.E.* = $T_t/T_f \cdot 100\%$	s_r
0.10	150.0	132.1	113.6	1.06(n=3)
0.15	100.0	95.1	105.2	1.84(n=3)
0.20	75.0	72.2	103.9	0.37(n=3)
0.25	60.0	59.3	101.1	0.45(n=4)
0.30	50.0	49.8	100.4	0.26(n=4)
0.35	42.9	42.9	100.0	0.90(n=4)
0.40	37.5	38.3	98.1	2.52(n=4)
0.45	33.3	35.6	93.6	1.84(n=4)
0.50	30.3	33.3	89.9	0.65(n=4)

DISCUSSION

The dependence of the current efficiency upon the generation current as shown in Table II can be explained theoretically by considering the polarization curves in Fig. 8. The solid curve on the right-hand side of Fig. 8 representing the polarization curve of the bismuth amalgam electrode actually used during the

generation of bismuth(III) is a summation of the two dotted curves representing the oxidation of bismuth amalgam and the reduction of oxygen, respectively.

It is clear that if the value of the generation current is chosen smaller than A, the amalgam assumes a potential at which the oxidation is still partially caused by the small amount of oxygen which remains in the solution even after passage of nitrogen. Consequently the current efficiency is above 100%.

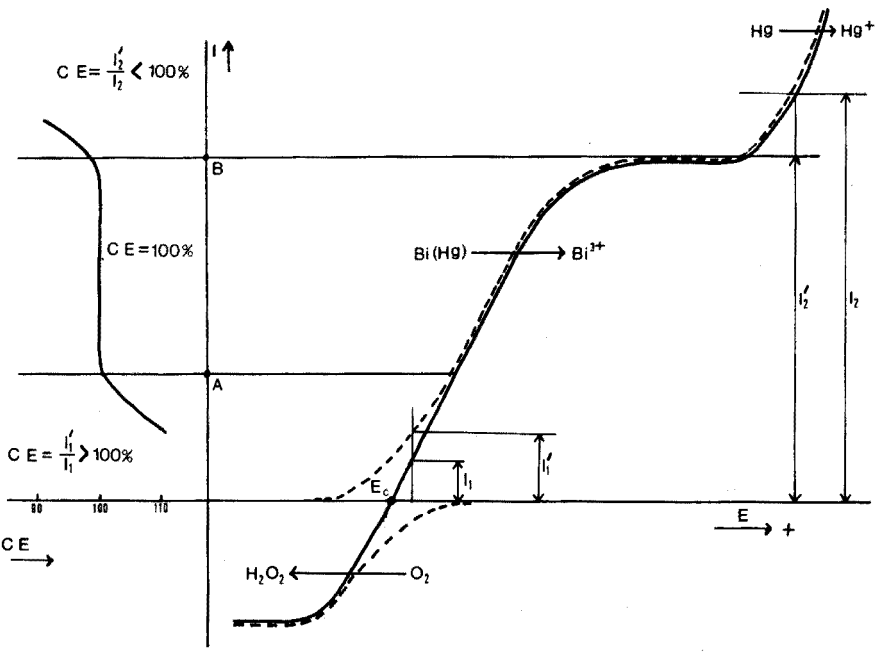

Fig. 8. Theoretical explanation of the relation between current efficiency and generating current.

At currents larger than B, the amalgam is polarized to such an extent that bismuth atoms cannot be transported from inside the amalgam to the surface as quickly as should correspond with the applied current. Thus oxidation of mercury partially contributes to the total current. This results in a current efficiency less than 100%.

If the generation current is chosen between A and B the current efficiency will be 100%. The behaviour of the current efficiency as experimentally determined (Table II) confirms the above treatment. The position of the point B in Fig. 8 depends on the conditions which govern the mass transport within the amalgam. This mass transport is mainly controlled by the vibration of the amalgam electrode caused by bubbling of nitrogen near the surface of the amalgam electrode.

Because the spectrophotometric indication of the reaction between bismuth(III) and EDTA appears to determine the lower limit of determination, it might be advantageous for a further lowering of this limit, to try another indication method, *e.g.* amperometry by means of the anodic EDTA wave at a rotating mercury electrode.

SUMMARY

Bismuth(III) can be generated in a solution by electrolytically oxidizing dilute bismuth amalgam. Oxygen present in the solution contacting the amalgam also oxidizes the amalgam. Therefore normal coulometric circuits are not suitable for the generation of trace quantities of bismuth(III), even after prolonged passage of nitrogen. A procedure is described by which the interference of oxygen is eliminated so that amounts of bismuth(III) down to $5 \cdot 10^{-8}$ moles (in 30 ml) can be generated with 100% current efficiency.

RÉSUMÉ

Le bismuth(III) est produit par oxydation électrolytique de son amalgame. L'amalgame de bismuth est également oxydé par l'oxygène présent dans la solution. Il n'est par conséquent pas possible d'appliquer un circuit coulométrique normal. Une méthode est décrite, évitant l'interférence de l'oxygène, et permettant de produire des quantités de bismuth de l'ordre de $5 \cdot 10^{-8}$ mol (dans 30 ml) ou davantage avec un rendement de courant de 100%.

ZUSAMMENFASSUNG

Wismut(III) wurde durch elektrolytische Oxidation von Wismutamalgam erzeugt. In der Lösung vorhandener Sauerstoff oxidiert das Amalgam ebenfalls, so dass eine normale coulometrische Schaltung nicht angewendet werden kann. Es wird eine Methode zur Beseitigung der Störung durch Sauerstoff beschrieben. $5 \cdot 10^{-8}$ Mol Bi(III) können (in 30 ml) mit einer Stromausbeute von 100% erzeugt werden.

REFERENCES

1 M. Nakanishi and H. Kobayashi, *Bull. Chem. Soc. Jap.*, 26 (1953) 394.
2 J. Badoz-Lambling, *Anal. Chim. Acta*, 7 (1952) 585.
3 J. J. Lingane, *Anal. Chem.*, 26 (1954) 622.
4 R. L. Kowalkowski, J. H. Kennedy and P. S. Farrington, *Anal. Chem.*, 26 (1954) 626.
5 P. S. Tutundzic, J. Doroslovacki and O. Tatic, *Anal. Chim. Acta*, 12 (1955) 481.
6 O. E. Sundberg, H. C. Craig and J. S. Parsons, *Anal. Chem.*, 30 (1958) 1842.
7 E. Bishop and R. G. Dhaneshwar, *Anal. Chem.*, 36 (1964) 726.
8 D. F. Ketchum and H. E. Pragle Johnson, *Microchem. J.*, 11 (1966) 139.
9 J. Cadersky, *Mikrochim. Acta*, (1966) 401.
10 G. G. Christian, E. C. Knoblock and W. C. Purdy, *Anal. Chem.*, 35 (1963) 1869.
11 J. Cadersky and M. Pribyl, *Z. Anal. Chem.*, 217 (1966) 252, 259.
12 W. Lädrach, F. v.d. Craats and P. Gouverneur, *Anal. Chim. Acta*, 50 (1970) 219.
13 W. R. Carroll, *Anal. Chem.*, 42 (1972) 144.
14 J. H. Ladenson and W. C. Purdy, *Anal. Chim. Acta*, 57 (1971) 465.
15 D. D. Deford and H. Horn, *Anal. Chem.*, 28 (1956) 797.
16 E. P. Przybylowicz and L. B. Rogers, *Anal. Chem.*, 28 (1956) 799; 30 (1958) 65, 1064.
17 E. P. Przybylowicz and L. B. Rogers, *Anal. Chim. Acta*, 18 (1958) 596.
18 H. L. Kies and G. J. van Weezel, *Z. Anal. Chem.*, 161 (1958) 348.
19 H. L. Kies, *Z. Anal. Chem.*, 183 (1961) 194.
20 Yao-Sin Su, *Dissertation*, Pittsburgh, 1963.

21 P. S. Tutundzic and D. J. Stojkovic, *Mikrochim. Acta*, (1966) 666.
22 J. R. Wells, *Dissertation*, Pittsburgh, 1967.
23 G. den Boef, W. E. van der Linden and S. Beyer, *Mikrochim. Acta*, (1971) 761.

Analytica Chimica Acta, 67 (1973) 437–443

SIMULTANEOUS THERMOGRAVIMETRIC AND THERMO-GAS-TITRIMETRIC INVESTIGATIONS UNDER QUASI-ISOTHERMAL AND QUASI-ISOBARIC CONDITIONS

F. PAULIK and J. PAULIK

Institute for General and Analytical Chemistry, Technical University, Budapest (Hungary)

(Received 2nd April 1973)

Recently, a new measuring technique has been developed[1–5] in which thermogravimetric measurements can be carried out under quasi-isothermal and quasi-isobaric conditions by means of the derivatograph[6,7]. However, the interpretation of the specially shaped curves obtained by using the new technique, has caused difficulties, similar to those found with conventional thermogravimetric curves, in cases when the resulting curves represent more or less overlapping partial reactions. In order to overcome these problems, the new technique has now been combined with the earlier thermo-gas-titrimetric method[7–9], and a complex method has been developed for the simultaneous determination of the weight change of the sample and the amount of the evolving gases (CO_2, NH_3, SO_2, SO_3, H_2O, Cl_2, NH_4Cl, etc.).

EXPERIMENTAL

Figure 1 shows the design and operation of the derivatograph modified for these investigations. In the new measuring technique, the temperature of the furnace (3) is raised by the program regulator (24) in the conventional way at a constant speed (3–10° min^{-1}) until the sample begins to decompose. Even a minute variation in the rate of the weight change causes the light signal of the DTG galvanometer (15) to deflect. This signal falls on to a photo-transistor (16) connected to a relay system (23) which cuts out the voltage of the heating current. Owing to the decrease in temperature, the rate of the reaction is reduced, and accordingly the light signal moves away from the photo-transistor, whereupon the relay system switches on the heating current again. The process described lasts only a few seconds and is repeated regularly during innumerable cycles until the end of the reaction[1,4,5]. In the method described, it can be ensured that thermal decomposition reactions, leading to an equilibrium, take place extremely slowly, under quasi-equilibrium conditions and at a given constant temperature value. However, this can be realized only on two conditions. First, constant experimental conditions must be maintained, because there is a close correlation between experimental circumstances (*e.g.*, partial pressure of the decomposition product) and the equilibrium established or the decomposition temperature relevant to particular reaction. Secondly, during the experiment, no other process (*e.g.*, nucleus growth, recrystallization) should take over from the heat transfer the role of the slowest reaction

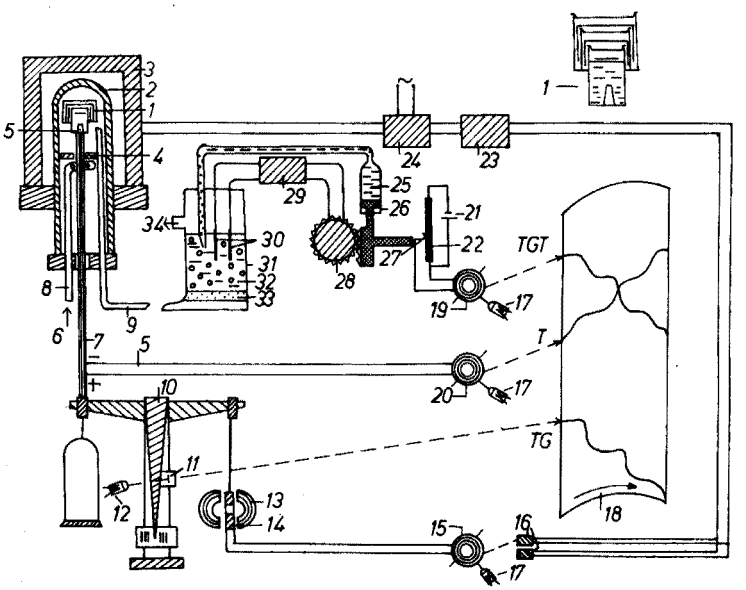

Fig. 1. Structure of the derivatograph modified for the simultaneous performance of thermogravimetric and thermo-gas-titrimetric investigations under quasi-isothermal and quasi-isobaric conditions. (1) Crucible, (2) silica bell, (3) furnace, (4) gas deflecting silica plate, (5) thermocouple, (6) inlet of the carrier gas, (7) corundum tube, (8) gas inlet tube, (9) gas outlet tube, (10) balance, (11) optical slit, (12) lamp, (13) permanent magnet, (14) coil, (15) galvanometer, (16) photo-transistor, (17) lamps, (18) photographic paper, (19, 20) galvanometers, (21) direct-current supply, (22) potentiometer, (23) amplifier and relay-system, (24) heating regulator, (25) reagent, (26) automatic burette, (27) potentiometer-slide, (28) servo-motor, (29) amplifier and relay-system, (30) electrodes, (31) absorption vessel, (32) absorption liquid, (33) porous glass plate, (34) junction to the gas suction pump.

governing the reaction rate[5]. An example of a change of role of this nature will be demonstrated later in the case of potassium hydrogencarbonate.

In order to maintain constant experimental conditions, the use of the so-called labyrinth sample holder[3–5] also proved to be indispensable. The lids of the specially shaped labyrinth sample holder (1; Fig. 1) can be placed in such a way on the crucible that a long and narrow channel system is formed. The gaseous decomposition products, streaming outwards from the sample through this labyrinth, impede the diffusion of air from the opposite direction. Accordingly, the construction of the sample holder makes it possible for the decomposition reactions always to occur in a self-generated atmosphere and under quasi-isobaric conditions.

The device simultaneously records not only the temperature (T) and weight (TG) changes of the sample, but also the course of one of the partial reactions leading to the formation of various gaseous decomposition products[7–9]. The gaseous decomposition products are collected quantitatively in the quartz tube system (2, 4, 8, 9), whence they are transported with the help of a carrier gas into the absorption vessel (31) in which they are absorbed by water (32). Between the electrodes (30) dipping into the solution, a potential difference is formed which actuates an automatic burette (25–27). By means of this automatic burette, one of the absorbed components is continuously titrated with an appropriate and selective reagent. In the so-called thermo-gas-titrimetric (TGT) curve the changes in the volume of the consumed

titrant are recorded, and the curve shows the course of the partial reaction in question either against time (CO_2 curve in Figs. 2 and 4) or against temperature (CO_2' curve in Figs. 2 and 4).

RESULTS AND DISCUSSION

The application of the new measuring technique will be demonstrated in practice for two examples.

Thermal decomposition of potassium hydrogencarbonate

The thermal decomposition of potassium hydrogencarbonate has been investigated by many researchers[10–14] by means of classical thermoanalytical methods, and has also been examined earlier[1] by means of the derivatograph, partly under conventional (Fig. 2, TG″ curve) and partly under quasi-isothermal and quasi-isobaric conditions (TG′ curve). The shapes of the thermogravimetric curves obtained under different experimental conditions differed significantly from one another. The TG″ curve showed the thermal decomposition of potassium hydrogencarbonate as a one-step process, while the TG′ curve indicated that the

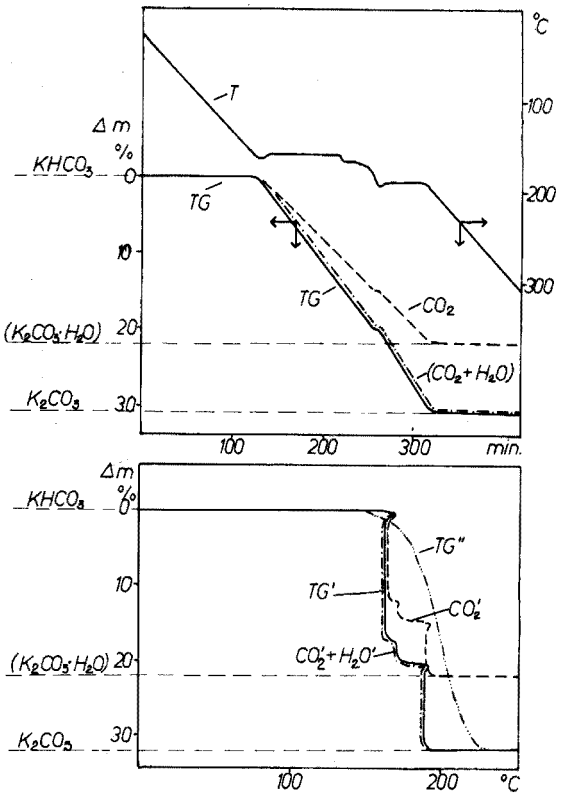

Fig. 2. Thermal decomposition of potassium hydrogencarbonate. The curves were recorded partly with the new technique as a function of time: T, TG, CO_2, CO_2+H_2O; and as a function of temperature: TG′, CO_2', $CO_2'+H_2O'$; and partly by using the dynamic heating program (10° min^{-1}): TG″.

decomposition reaction occurred in two steps. Since the latter curve showed a sharp break-like change at the weight ratio corresponding nearly to the composition of potassium carbonate monohydrate, it was assumed that under the changed experimental conditions (self-generated atmosphere), the one-step decomposition reaction separated into two consecutive partial reactions; potassium carbonate monohydrate was formed as an intermediate product, which proved to be stable up to 188°. This assumption seemed to be supported by the fact that, except for the small step at 170°, the temperature became spontaneously constant in both phases of the decomposition. Accordingly, at the two temperature values corresponding to the two different compositions, *i.e.* to the two different reactions supposed, the system attained, at least apparently, an equilibrium.

The special combination of measuring techniques described in this paper made it possible to examine the correctness of the earlier suppositions. As will be seen, the results of the present examination unanimously contradicted these earlier assumptions. According to the CO'_2 curve in Fig. 2, carbon dioxide was being developed not only during the first period of the reaction, *i.e.* not only at 162°, but during the whole course of the thermal decomposition at a uniform rate, which was similar to the weight change represented by the TG curve. Furthermore, since the curves for CO_2+H_2O, and CO'_2 and H_2O' (constructed by calculation from the amount of carbon dioxide measured) can be brought into an exact concordance with the TG and TG′ curves, respectively, there is no doubt that carbon dioxide and water were liberated strictly in parallel, and that no potassium carbonate monohydrate was formed in any measurable amount. Consequently, the question why the sample showed a stepwise decomposition, cannot be explained.

This phenomenon was reproducible but only under the given quasi-isothermal and quasi-isobaric conditions, as can be seen from the course of the decomposition curves in Fig. 3. Curves 1–4 of this Figure were all recorded by using a quasi-isothermal heating program but the applied sample holders were different; the labyrinth sample holder, the covered and uncovered conventional

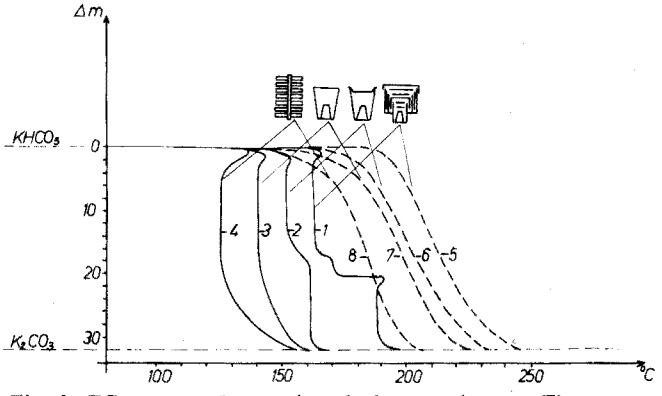

Fig. 3. TG curves of potassium hydrogencarbonate. The curves were recorded partly with the quasi-isothermal technique (curves 1–4), and partly with the dynamic (10° min^{-1}) heating program (curves 5–8), by using the labyrinth sample holder (curves 1, 5), the conventional crucible of the derivatograph with cover (2, 6), without cover (3, 7) and the polyplate sample holder (4, 8).

crucible of the derivatograph, and the polyplate sample holder[7] were all used. In this way the influence of the partial pressure of the gaseous decomposition products on the reaction equilibrium, could be studied; for, in the four cases, the concentration of the gaseous decomposition products in the vicinity of the solid phase, was very different. This difference was also indicated by the variety of the decomposition temperatures. As can be seen from curves 5–8, the course of the thermal decomposition changed to a significant extent when a dynamic heating program of 10° min^{-1} was applied.

A further remarkable phenomenon can be observed in curves 1–4: at the start of the thermal decomposition, the sample took up temporarily a temperature value higher by 5–10° than the constant equilibrium temperature established later spontaneously. This may be explained by assuming that under the given experimental conditions, formation of nuclei can begin only at higher energy levels; after the formation of a certain amount of nuclei, there is no further obstacle to the occurrence of the reaction with the given speed, even at lower temperatures.

Thermal decomposition of sodium hydrogencarbonate

The thermal decomposition of sodium hydrogencarbonate, which has often

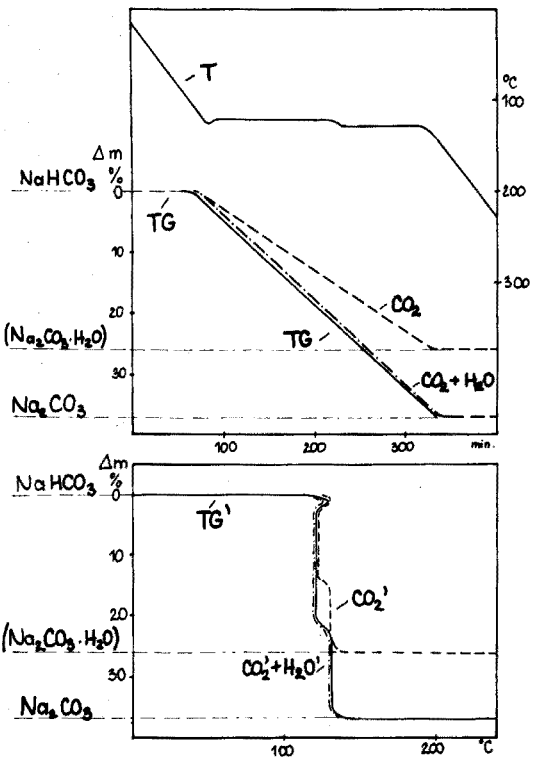

Fig. 4. Thermal decomposition of sodium hydrogencarbonate. The curves were recorded with the new technique as a function of time: T, TG, CO_2, CO_2+H_2O; and as a function of temperature: TG', CO_2', $CO_2'+H_2O'$.

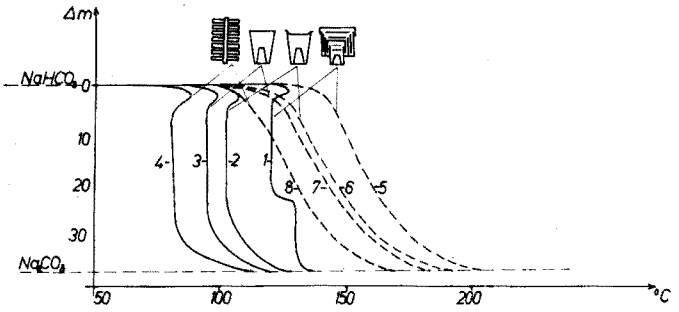

Fig. 5. TG curves of sodium hydrogencarbonate. The experimental conditions for the recording of the curves were the same as for Fig. 3.

been investigated by classical methods[15–19], was examined by the new technique in an analogous manner. The results were similar to those obtained in the investigation of potassium hydrogencarbonate (Figs. 4 and 5).

The authors wish to thank Prof. E. Pungor for valuable discussions.

SUMMARY

The derivatograph has been modified to provide a new technique with the help of which the weight change of a sample and the amount of the evolving gases can be determined as a function of the temperature of the sample under quasi-isothermal and quasi-isobaric conditions. The thermal decompositions of potassium and sodium hydrogencarbonate were investigated; it was established that under special conditions the otherwise one-step thermal decomposition of the two materials becomes a two-step process. The phenomenon involves a change only from the point of view of kinetics, for the decomposition itself does not split into two consecutive processes.

RÉSUMÉ

On propose un dérivatographe modifié, permettant une nouvelle technique pour déterminer le changement de poids d'un échantillon et la quantité de gaz dégagés, en fonction de la température, dans des conditions quasi-isothermiques et quasi-isobariques. Les décompositions thermiques des hydrogénates de potassium et de sodium ont été examinées. On constate, que dans des conditions spéciales, la décomposition se fait en deux stades, du point de vue cinétique.

ZUSAMMENFASSUNG

Unter Abwandlung des Derivatographen wurde ein neues Verfahren entwickelt, mit dessen Hilfe die Gewichtsänderung einer Probe und die Menge der sich entwickelnden Gase als Funktion der Temperatur der Probe unter quasi-isothermen und quasi-isobaren Bedingungen bestimmt werden können. Die thermische Zersetzung von Kalium- und Natriumhydrogencarbonat wurde unter-

sucht. Es wurde festgestellt, dass unter besonderen Bedingungen die sonst in einer Stufe ablaufende thermische Zersetzung der beiden Stoffe zu einem Zweistufen-Prozess wird. Dieser Wechsel tritt nur in kinetischer Hinsicht auf, die Zersetzung selbst erfolgt nicht in zwei aufeinanderfolgenden Stufen.

REFERENCES

1 J. Paulik and F. Paulik, *Anal. Chim. Acta*, 56 (1971) 328.
2 F. Paulik and J. Paulik, in A. G. Wiedemann, *Proc. 3rd. Int. Conf. Thermal Anal., Davos, 1971*, Vol. I, Verlag Birkhäuser, Basel, 1972, p. 161.
3 J. Paulik and F. Paulik, *Anal. Chim. Acta*, 60 (1972) 127.
4 F. Paulik and J. Paulik, *Thermochim. Acta*, 4 (1972) 189.
5 F. Paulik and J. Paulik, *J. Thermal Anal.*, 5 (1973) 253.
6 F. Paulik, J. Paulik and L. Erdey, *Z. Anal. Chem.*, 160 (1958) 241.
7 F. Paulik, J. Paulik and L. Erdey, *Talanta*, 13 (1966) 1405.
8 J. Paulik, F. Paulik and L. Erdey, *Mikrochim. Acta*, (1966) 886.
9 J. Paulik and F. Paulik, *Thermochim. Acta*, 3 (1971) 13.
10 R. M. Caven and H. S. Sand, *J. Chem. Soc.*, 105 (1914) 2754.
11 R. L. Bohon, *Anal. Chem.*, 35 (1963) 1845.
12 T. P. Firsova, A. N. Molodkina, T. G. Morozova and I. V. Aksenova, *Zh. Neorg. Khim.*, 9 (1964) 1066.
13 A. Kh. Melkinov, T. P. Firsova and A. N. Molodkina, *Zh. Neorg. Khim.*, 7 (1962) 1237.
14 C. Duval, *Mikrochim. Acta*, (1963) 348.
15 W. Smykatz-Kloss, *Beitr. Mineral. Petrogr.*, 9 (1964) 481.
16 T. P. Firsova, A. N. Molodkina, T. G. Morozova and I. V. Aksenova, *Zh. Neorg. Khim.*, 8 (1963) 278.
17 W. W. Wendlandt, *J. Chem. Educ.*, 38 (1961) 571.
18 M. G. McAdie, *Anal. Chem.*, 35 (1963) 1843.
19 T. Czarnota and W. Celler, *Przem. Chem.*, 42 (1963) 439.

Analytica Chimica Acta, 67 (1973) 444–447

SHORT COMMUNICATION

Neutron irradiation of mercury in polyethylene containers

H. V. WEISS
Naval Undersea Center, San Diego, Calif. 92132 (U.S.A.)
K. CHEW
Department of Chemistry, California State University at San Diego, Calif. 92115 (U.S.A.)
(Received 13th April 1973)

This note reports the behavior of mercury on neutron irradiation in polyethylene containers. The work was precipitated by Bate[1] reporting the loss of substantial quantities of radioactive mercury from such containers when mercury was bombarded in a flux of $1 \cdot 10^{12}$ n cm^{-2} s^{-1} for 12–65 h. Moreover, he recommended that mercury be contained in quartz for periods of irradiation in excess of a few minutes.

In the development of procedures and in sample analyses, we previously had performed numerous 1-h irradiations of acidified solutions of mercury contained in snap-top polyethylene vessels. Neither the data from the mercury flux monitors nor the proof of procedures[2] suggested any error attributable to this factor, and the method was therefore regarded as valid. Irradiation by this method is preferred since the sample preparation is simple and the cost of the container economic. Accordingly, it was essential to look more closely at the basis for the contradictory results.

In procedural development, inconsistencies were encountered with aqueous samples that were unacidified; it was therefore considered that this factor could be responsible for the discordancy. The following gives data on the effect of acid concentration and irradiation time on the amount of radio-induced ^{197}Hg recoverable from solution and the conditions for the reliable neutron bombardment of this element in polyethylene.

Experimental

Solutions. Solutions of mercury and cadmium were prepared at a concentration of 1 p.p.m. either in water or in 1.6, 2.5, or 16 *M* nitric acid; 10 ml of each were transferred to a 15-ml polyethylene vial, of which the lid was simply snapped shut.

Irradiations. Samples were irradiated for a specified interval in a specimen rack that rotated about the core of the reactor (1 r.p.m.). The TRIGA nuclear reactor of Gulf Energy and Environmental Systems, La Jolla, Calif., provided the neutrons at a flux of $2 \cdot 10^{12}$ n cm^{-2} s^{-1}. In one irradiation, the mercury solutions were neutron-bombarded for 10 or 60 min, then processed as described below. In

another irradiation, cadmium and mercury solutions were irradiated for 30 min and the induced activity was measured without further treatment.

Sample processing. Samples from the first irradiation were transferred to another vessel and the volume was raised to 100 ml with water that contained mercury carrier. To the solutions of 2.5 and 16 *M* nitric acid were added 1.5 and 9 ml of concentrated ammonia liquor, respectively. Hydrogen sulfide was bubbled through the solutions, and the resultant sulfide was collected and transferred to counting vials.

Carrier yield determination. After several weeks of radioactive decay, the processed mercury samples as well as the mercury carrier standards were re-irradiated for 10 s. Through comparison of the activity level of the samples and the standards, the carrier yield was computed and the counting rate in the original irradiation was corrected for this factor.

Measurement. The radioactive measurements were made with a sodium iodide detector coupled to a 400-channel pulse-height analyzer. The counts attributable to the 77 and 340-keV radiations of ^{197}Hg and ^{115}Cd–^{115}In, respectively, were integrated by the method of Covell[3].

Results

The results of irradiating mercury for 10 and 60 min in solutions of different nitric acid concentration appear in Table I. For each of the irradiation time periods, the unacidified solutions contained less ^{197}Hg than their acidified counterparts; this difference was more pronounced for the 60-min irradiated samples. Further, the degree of activity was related to the concentration of the nitric acid. Comparison of activity levels for solutions irradiated for the two time intervals indicate the counting rates scale by a factor of six for the acidified solutions but not for water.

Table II gives the counting data for irradiation vials directly counted several days after neutron activation of cadmium and mercury solutions of varying acidity. With cadmium the counting rate decreased regularly as a function of nitric acid concentration, while with mercury the activity level in the unacidified sample was substantially less than for the samples in nitric acid solution. The relationship between the comparable nitric acid solutions of mercury parallels that of cadmium.

TABLE I

^{197}Hg ACTIVITY ISOLATED FROM SOLUTIONS OF VARYING ACIDITY AND FOR TWO IRRADIATION TIMES

Nitric acid concentration (M)	*^{197}Hg activity (c.p.m.)*	
	10 min irrad. time	*60 min irrad. time*
0	10077	46836
1.6	11182	65454
2.5	10916	66183
16.0	10262	60182

TABLE II

^{197}Hg AND ^{115}Cd–^{115}In INDUCED IN SOLUTIONS OF VARYING ACIDITY AND MEASUREMENT IN THE IRRADIATED CONTAINERS

Nitric acid concentration (M)	*Activity (c.p.m.)*	
	^{197}Hg	^{115}Cd–^{115}In
0	20788	5006
1.6	25480	4960
2.5		4918
16.0	22892	4326

Discussion

From these results the conclusion is drawn that mercury in acidified solution is not lost during irradiation, at least not over the interval 10–60 min. But in the absence of acid, substantial loss is encountered. The loss appears to occur by two routes: adsorption and volatilization.

In the case of the unacidified solution bombarded for 60 min, only about 70% of the anticipated induced activity is accountable. About 12% of the total activity is associated with the walls of the irradiation vial. Moreover, this fraction cannot be leached upon treatment with warm nitric acid washings. This bound fraction may be the manifestation of a recoil mechanism in a situation where a disproportionate fraction of the mercury is situated in juxtaposition to the polyethylene through adsorption on active exchange sites. The affinity for these sites is apparently neutralized by the action of hydrogen ion. (We had previously observed that hydrochloric acid is also an effective agent in the prevention of adsorption that would occur if, for example, sea water containing mercury were stored in polyethylene[2].)

About 18% of the unaccounted-for induced activity in the 60-min irradiation is lost through volatilization. Perhaps sufficient reducing substances exist within the unacidified solutions which allow for the transformation of the small quantities of mercury to the volatilizable metal, which then vaporizes as the irradiated solution attains the ambient waterpool temperature of the nuclear reactor (usually about 30° in the TRIGA Reactor).

The reduction in the quantity of induced activity with elevation in the nitric acid concentration is not the result of losses. The relation of cadmium activity (cadmium is an element whose volatility is not in question) as a function of nitric acid concentration (Table II) points to the fast-neutron thermalizing effect of the hydrogen atom. Obviously the greater the degree of thermalization, the greater the degree of neutron activation. Accordingly, as hydrogen is substituted by the less thermalizing nitrate ion, the degree of induction is diminished.

The reliability of irradiating mercury with neutrons in polyethylene under appropriate conditions has been established for bombardments of 1-h duration. Conceivably these conditions may also apply for considerably longer irradiation periods.

REFERENCES

1 L. C. Bate, *Radiochem. Radioanal. Lett.*, 6 (1971) 139.
2 H. V. Weiss and T. E. Crozier, *Anal. Chim. Acta*, 58 (1972) 231.
3 D. F. Covell, *Anal. Chem.*, 31 (1959) 1785.

Analytica Chimica Acta, 67 (1973) 448–452

SHORT COMMUNICATION

Ultraviolet absorption studies and analytical applications of the ether complexes of boron trifluoride and phosphorus pentafluoride

HARVEY POBINER

American Can Company, Princeton Laboratory, P.O. Box 50, Princeton, N.J. 08540 (U.S.A.)

(Received 9th March 1973)

It has been observed in this laboratory that a new ultraviolet absorption spectrum accompanies complexation between ethers and certain volatile Lewis acids, such as boron trifluoride and phosphorus pentafluoride. This new ultraviolet spectrum, not shown by the individual reactants, is useful as a confirmatory test for these two Lewis acids. It has also been developed into a rapid quantitative analysis for the boron trifluoride, which may be used as a polymerization catalyst.

Boron trifluoride and phosphorus pentafluoride readily form complexes with oxygen compounds, such as ethers, which have unshared electron pairs to donate to available orbitals of the boron and phosphorus atoms[1]. For example, composition studies of the addition compounds of phosphorus pentafluoride with different ethers[2] and of boron trifluoride with simple ethers[3] have been reported. In the analytical study discussed here, a spectrally pure ether, such as *p*-dioxane, can act both as the electron donor for the complex with the Lewis acid fluoride, and, in excess, as the solvent in which to measure the ultraviolet spectrum.

Experimental

Sources of the Lewis acid halides were commercial boron trifluoride–ether complexes, pure anhydrous gases, and certain commercial compounds[4] which act as *in situ* generators of phosphorus pentafluoride on thermal decomposition, such as Phosfluorogen A (*p*-chlorobenzenediazonium hexafluorophosphate) and potassium hexafluorophosphate.

Calibration with boron trifluoride. The following procedure permits the catalyst composition of a boron trifluoride–etherate stock solution used in polymerization to be monitored. In a nitrogen-purged glove box, prepare a solution containing 5 ml of boron trifluoride ethyl ether (Eastman, purified, $BF_3 \cdot O(C_2H_5)_2$, No. 4272) made up to volume in a 250-ml volumetric flask with *p*-dioxane (Matheson, Coleman and Bell, Spectroquality, No. DX 2095). Prepare a series of dilutions, containing aliquots from 1 ml to 20 ml of the master solution, in a series of 25-ml volumetric flasks, made up to volume with *p*-dioxane. The *p*-dioxane stabilizes the BF_3–etherate so that these dilutions can be made outside the glove box. Record the ultraviolet absorption spectrum of each dilution *vs.* *p*-dioxane in a 1-cm cell in a double-beam spectrophotometer (*e.g.* Beckman DK-2A). Determine the absorp-

tion at the maximum, 275 nm, relative to a zero reading at 335 nm. Use density and chemical conversion factors to calculate the BF_3 concentration in each dilution and prepare a calibration curve. Beer's law is obeyed in the range 0–10 g BF_3 l^{-1}.

Complexation with phosphorus pentafluoride gas. The following procedure is used for determining the ultraviolet spectrum of the phosphorus pentafluoride–*p*-dioxane complex, followed by hydrolysis and determination of the fluoride ion as a measure of the PF_5 in the system. In a nitrogen-purged glove box, connect a lecture bottle of phosphorus pentafluoride (Matheson Company, East Rutherford, N.J.) via polyethylene tubing to a 500-ml gas washing bottle (Kontes No. K-65700) containing about 180 ml of dioxane. Bubble in the phosphorus pentafluoride gas until the solution turns red-brown. Then filter, in the glove box, into a 250-ml volumetric flask and dilute to the mark with dioxane. Dilute as necessary in the glove box with dioxane to obtain an u.v. absorption maximum at 312 nm.

Into another gas washing bottle in the glove box, bubble phosphorus pentafluoride into the dioxane until red brown. At this point, add 5 ml of distilled water and dilute to 250 ml with dioxane. This hydrolyzed solution is stable and can be diluted for the spectral measurement. Dilute as necessary to obtain the absorbance of the band at 225 nm relative to a zero reading at 360 nm. Remove an aliquot, dilute in distilled water and determine fluoride ion colorimetrically[5]. Use the appropriate conversion factor to calculate the PF_5 originally in the sample.

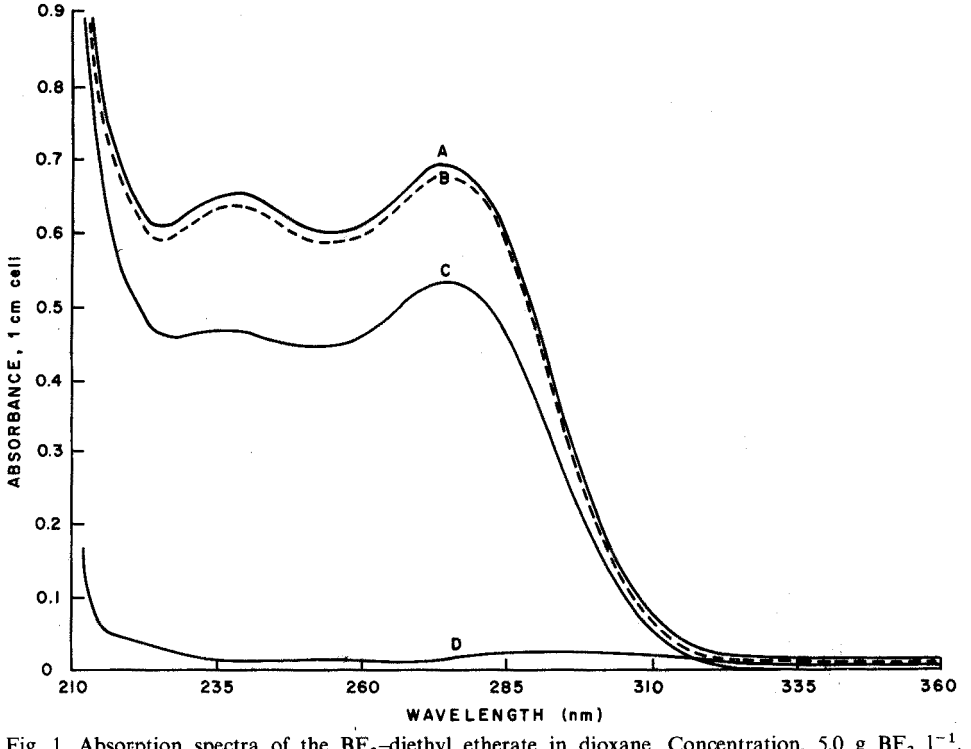

Fig. 1. Absorption spectra of the BF_3–diethyl etherate in dioxane. Concentration, 5.0 g BF_3 l^{-1}. (A) In dioxane, spectroquality, run immediately. (B) Same as A, after 16 h. (C) In dioxane containing 2% water, run immediately. (D) Same as C, after 16 h.

Discussion

The spectrophotometric measurement of the Lewis acid–etherate complex is particularly useful as a quick monitor of the available catalyst (*e.g.* BF_3) level in stock solutions of the etherate used in polymerization work. It is also useful as a confirmatory test for the detection of BF_3 or PF_5 that is liberated into a reaction vessel by the radiation of an adduct or compound containing the bound catalyst. For example, the PF_5 generated from thermal decomposition of the hexafluorophosphates, such as $NaPF_6$, and the diazonium compounds, $RN{=}NPF_6$[4], can be detected by the u.v. measurement of the complex formed with ethers.

Effect of moisture on the boron trifluoride–etherate u.v. spectrum. The dioxane has an apparent stabilizing effect on the boron trifluoride–diethylether commercial reagent. The latter reagent normally undergoes instantaneous hydrolysis, marked by strong fuming, outside a nitrogen-purged glove box, but in the presence of dioxane, as in the calibration procedure, the visible evidence of hydrolysis is eliminated. The ultraviolet spectra in Fig. 1 demonstrate this stability. Curves A and B show that the boron trifluoride–diethyl etherate is reasonably stable after 16 h in dioxane, the flask being opened under normal conditions for periodic sampling. Curve C shows the decreased absorbance caused by instability in the presence of 2% water. Curve D shows complete disappearance of the absorption maximum, after 16 h, in the presence of 2% water, probably because of complete decomposition of the complex.

Use of other solvents for complexation with boron trifluoride. It must be emphasized that the absorption maximum at 275 nm is specifically a function of the boron trifluoride–diethyl etherate. This maximum will be observed if the dilution is in a non-ether solvent, such as isopropanol, but the stabilizing property of dioxane as the solvent should be noted. One can bubble anhydrous boron trifluoride gas, exclusive of its diethylether complex, into other ether solvents, and obtain different ultraviolet spectra. For example, the complex between boron trifluoride gas and tetrahydrofuran, as a cyclic ether donor-solvent, shows a u.v. maximum at 283 nm, and that between boron trifluoride gas and dioxane, will absorb at 298 nm. The latter two complexations have been used only qualitatively here.

Analytical recovery and precision data. Table I shows that a 1.6% average

TABLE I

ANALYSES OF SYNTHETIC BLENDS OF *p*-DIOXANE CONTAINING BF_3–ETHERATE

Sample	*BF_3 ($g\ l^{-1}$)*		*% Deviation from theory*
	Theory	*Found*	
1	1.25	1.25	0.0
2	2.13	2.18	+2.3
3	2.61	2.54	−2.8
4	4.27	4.25	−0.5
5	5.10	5.23	+2.5
6	10.46	10.30	−1.6
		Average	1.6

deviation from theory is to be expected when analyzing for the boron trifluoride–diethyl etherate, corresponding to concentrations of 1–10 g BF_3 l^{-1}, in dioxane. In a series of ten determinations at a concentration level of 5.0 g BF_3 l^{-1}, the relative standard deviation for the variance from the mean was 0.7%.

Effect of moisture on the phosphorus pentafluoride–etherate u.v. spectrum. The absorbance band produced by the complexation of phosphorus pentafluoride with dioxane is a broad band with a maximum at 310–312 nm. The complex is susceptible to hydrolysis while in the absorption cell, and should only be used qualitatively to detect phosphorus pentafluoride liberated from catalysts. This hydrolytic instability is in agreement with the literature[1,4] which indicates that the organic complexes of PF_5 are less stable than those of BF_3 and are rapidly decomposed by water. In the presence of 2% moisture, the absorption maximum at 312 nm is eliminated, and a new broad maximum appears at 223 nm. The phosphorus pentafluoride–dioxane solutions containing 2% moisture are spectrally stable for at least 2 h, do not exhibit any hydrolysis in the air, and can be quantitatively diluted. Synthetic mixtures of possible hydrolysis products, such as orthophosphoric acid with hydrofluoric acid in dioxane, do not produce this spectrum. This absorption at 225 nm is possibly due to some intermediate hydrolysis product of the phosphorus pentafluoride–etherate. These spectra are shown in Fig. 2.

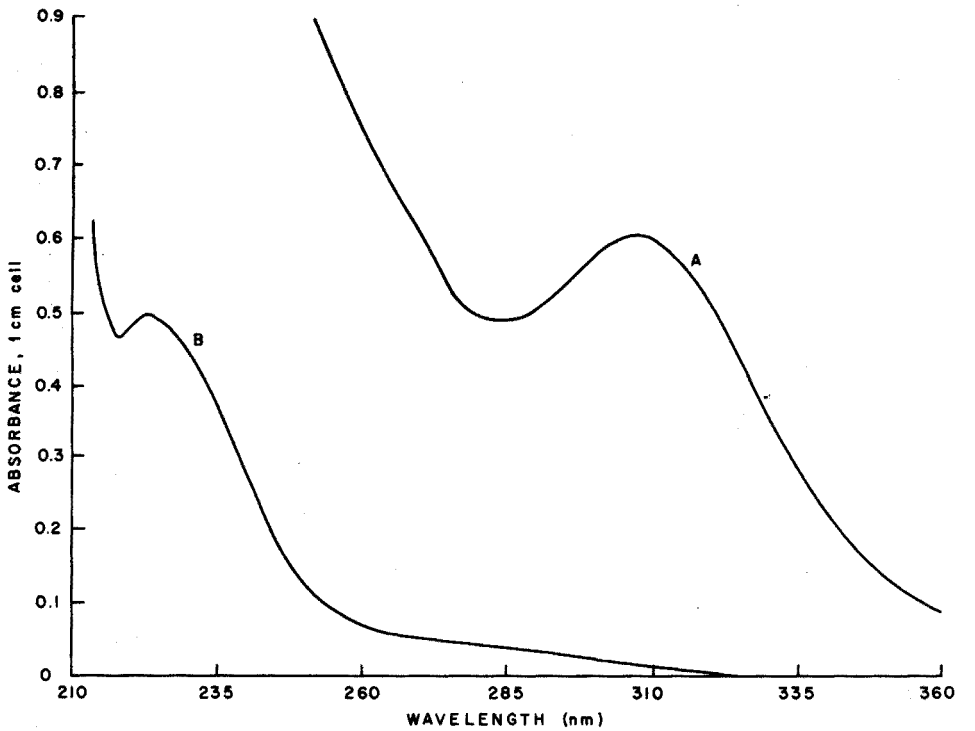

Fig. 2. Absorption spectra of the PF_5–dioxane complex. (A) In dioxane, spectroquality. (B) In dioxane containing 2% water.

Interferences. Interferences are not a major consideration because the analytical samples generally contain only one Lewis acid, either boron trifluoride or phosphorus pentafluoride, in the form of a compound or adduct. Phosphorus pentabromide and phosphorus pentachloride did not produce a new u.v. absorption spectrum in dioxane, nor did phosphorus trichloride and phosphorus oxychloride.

REFERENCES

1 F. A. Cotton and G. Wilkinson, *Advanced Inorganic Chemistry*, Wiley, New York, 1962, pp. 155, 381.
2 I. K. Gregor, *Aust. J. Chem.*, 20 (1967) 775.
3 T. A. Shchegoleva, V. D. Sheludyakov and B. M. Mikhailov, *Dokl. Akad. Nauk SSSR*, 152 (1963) 888; *Chem. Abstr.*, 60 (1964) 6455c.
4 R. E. Kirk and D. F. Othmer, *Encyclopedia of Chemical Technology*, Vol. 9, Interscience–Wiley, New York, 2nd Ed., 1966, pp. 635, 644.
5 J. M. Icken and B. M. Blank, *Anal. Chem.*, 25 (1953) 1741.

Analytica Chimica Acta, 67 (1973) 453–456

SHORT COMMUNICATION

The behavior of metal atoms in a microwave-excited plasma torch

KUNIYUKI KITAGAWA and TSUGIO TAKEUCHI

Department of Synthetic Chemistry, Faculty of Engineering, Nagoya University, Chikusaku, Nagoya (Japan)

(Received 28th March 1973)

The microwave-excited plasma torch is of considerable interest in the determination of elements with high excitation energies. This technique, however, appears to suffer from interference phenomena caused by cations and free electrons resulting from elements which have ionization potentials lower than those of the elements of interest. These phenomena might tend to increase in a gas matrix which lacks vibrational and rotational energies such as monoatomic argon; buffering effects for the interferences seem to be efficient in a diatomic gas like nitrogen.

In a previous study[1], the excitation temperature and the degree of ionization of manganese atoms, and the effects of the presence of other cations on these quantities, were estimated by means of a "three-lines method", in which the excitation temperature of ions was assumed to be similar to that of atoms. In the present work, these quantities were estimated by a "four-lines method", with elimination of the assumption. Alkaline earth metals were made to coexist as interfering elements, the excitation temperatures of which were also measured to yield their degrees of ionization by the "three-lines method".

Calculation

The excitation temperature was calculated by means of the well-known "two-lines method" based on the Boltzmann's law:

$$T = E_2 - E_1/k\left(\ln\frac{R_1}{R_2} + \ln\frac{g_1 f_1 \lambda_2^3}{g_2 f_2 \lambda_1^3} p_{1,2}\right)$$

where E and g are the energy and the statistical weight, respectively, of the upper state, k is the Boltzmann constant, R the response observed, f the oscillator strength, $p_{1,2}$ the response factor of the photomultiplier tube and the grating, and the subscripts 1 and 2 indicate the two lines observed.

The degree of ionization was estimated by the following equation, for which no assumption of reaction equilibrium is necessary, only local thermal equilibrium in the observed region in the plasma being required:

$$\chi = 1 - 1/1 + F(T_a, T_i) p_{i,a} R_i/R_a$$

and

$$F(T_a, T_i) = \frac{g_a f_a \lambda_i^3 Q_i(T_i)}{g_i f_i \lambda_a^3 Q_a(T_a)} \exp\left(\frac{E_i}{kT_i} - \frac{E_a}{kT_a}\right)$$

where $Q(T)$ is the partition function[2] and the subscripts a and i mean the atoms and the ions, respectively.

Experimental

A Hitachi 300 UHF Plasma Scan[3] was fitted with a Hitachi QPD-54 recorder as in the previous work[1].

The elements and the lines measured are listed in Table I[4,5].

TABLE I

LINES OBSERVED

Element	*Wavelength (nm)*	*Upper energy (cm^{-1})*	*gf-value*
Mn I	403.1	24,802	0.33
I	279.5	35,770	3.4
II	257.6	38.807	7.9
II	294.9	43.370	8.6
Mg I	383.8	47,957	8.6
I	285.2	35,051	1.1
II	279.6	35,761	1.1
II	280.3	35,669	0.62
Ca I	445.5	37,757	2.2
I	422.7	23,625	0.28
II	396.9	25,192	0.11
II	393.3	25,414	0.21
Sr I	460.7	21,698	0.27
I	487.6	35,400	0.47
II	407.8	24,517	0.17
II	421.6	23,715	0.10
Ba I	553.6	18,060	0.9
II	493.4	20,262	0.068
II	413.1	46,155	4.6

A standard solution of manganese was prepared by dissolving the metal in hydrochloric acid. Alkaline earth solutions were made by dissolving the carbonates (analytical grade) in hydrochloric acid; the solutions were diluted just before use, the final acidity being 0.1 *M*. The total molar concentration of manganese and alkaline earth metal was 10 mmole l^{-1} in all tests.

Observations were made through a rectangular slit (30 μm × 2 mm) 11 mm above the microwave electrode. The supporting gas was argon in which notable cationic interferences were found, rather than in nitrogen plasma. The other conditions were the same as described previously[1].

Results and discussion

Manganese atoms provide two strong lines, and the ions also provide two strong lines; these are of different energies so that the four-lines method can be applied. The alkaline earth elements emitted three lines (two atomic lines and an ionic one), which were strong enough for the three-lines method to be used. The results calculated are shown in Fig. 1 for the excitation temperature and Fig. 2 for the degree of ionization.

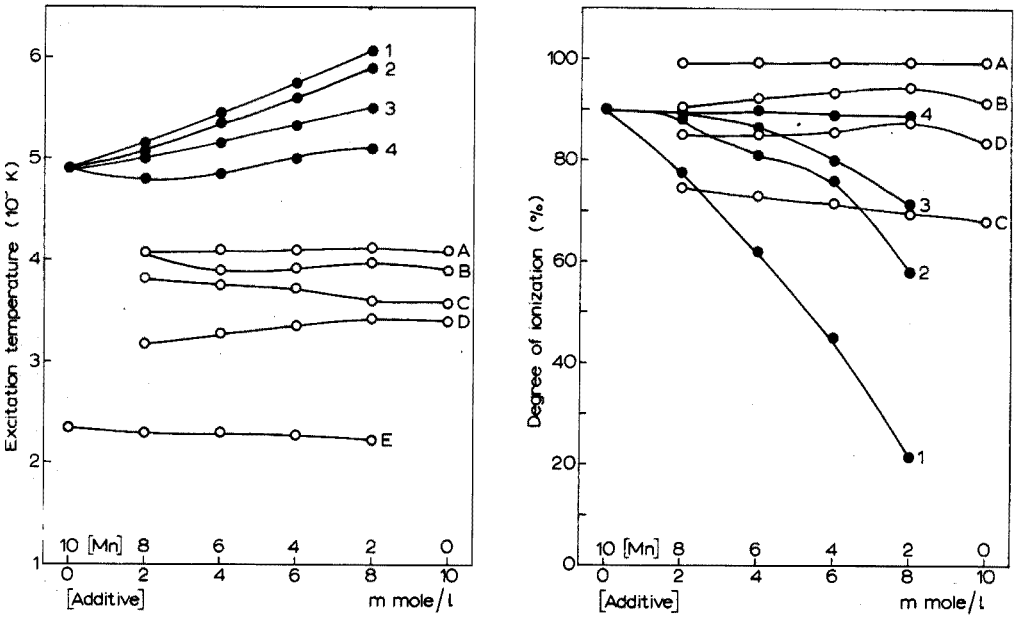

Fig. 1. Excitation temperature observed. (●) Manganese atoms: (1) barium added, (2) calcium added, (3) strontium added, (4) magnesium added, (A) Barium ions, (B) strontium atoms, (C) calcium atoms, (D) magnesium atoms, (E) manganese ions (for each additive).

Fig. 2. Degree of ionization observed. (●) Manganese atoms: (1) barium added, (2) strontium added, (3) calcium added, (4) magnesium added. (A) Barium atoms, (B) strontium atoms, (C) magnesium atoms, (D) calcium atoms.

The degree of ionization of manganese atoms was reduced in the presence of alkaline earth atoms, the effects of which followed the same sequence as the ionization potentials.

In the previous study[1], enhancement was observed when an excess of alkaline earth metal was present in the manganese solution (10 mmole l^{-1}). The results of the studies suggest that the free electrons resulting from ionization of the alkaline earth atoms, bombard the manganese atoms to enhance the degree of ionization. With lower total cationic concentrations, the degree of ionization may be reduced by charge-transfer reactions or by a tendency of the ionic equilibria (eqns. 1 and 2) to move to the left:

$$Mn \rightleftarrows Mn^+ + e^- \quad (1)$$

$$Ba^+ + e^- \rightleftarrows Ba \quad (2)$$

$$Mn^+ + Ba \rightleftarrows Mn + Ba^+ \quad (3)$$

$$Mn + e^- \rightarrow Mn^+ + 2e^- \quad (4)$$

The relationship between manganese and magnesium, which has a higher ionization potential than manganese, is different from that between manganese and the other alkaline earth metals; the degree of ionization of magnesium was reduced by manganese whilst that of the other metals was enhanced.

Despite its higher ionization potential, the degree of ionization of manganese atoms, estimated by the four-lines method, was larger than that of strontium measured by the three-lines method; this can be interpreted from the difference between the excitation temperatures of atoms and ions, as shown in Fig. 1. Thus, the degree of ionization of alkaline earth atoms may be somewhat higher than indicated, because of thermal nonequilibrium between the atomic and ionic systems. The degree of ionization of barium was found to be *ca.* 99.4%; only a weak atomic line was observed, and the excitation temperature was measured by means of the two ionic lines.

The variation in the excitation temperature of manganese atoms was found to decrease in presence of alkaline earth atoms in the previous work[1] and to increase in the present work. This suggests that the excitation transfer reaction exceeds excitation by the electron impact reaction in the presence of excess of alkaline earth atoms.

REFERENCES

1 K. Kitagawa and T. Takeuchi, *Anal. Chim. Acta*, 60 (1972) 309.
2 L. De Galan, R. Smith and J. D. Winefordner, *Spectrochim. Acta*, 23B (1968) 521.
3 S. Murayama, H. Matsumoto and M. Yamamoto, *Spectrochim. Acta*, 23B (1968) 513.
4 C. H. Corliss and W. R. Bozman, *NBS Monograph 53*, 1962.
5 R. Mavrodineanu and H. Boiteux, *Flame Spectroscopy*, Wiley, New York, 1965.

Analytica Chimica Acta, 67 (1973) 457–459

SHORT COMMUNICATION

Application of atomic absorption spectrometry with a glassy carbon tube atomizer to determination of atomic diffusion coefficients

KUNIYUKI KITAGAWA and TSUGIO TAKEUCHI

Department of Synthetic Chemistry, Faculty of Engineering, Nagoya University, Chikusaku, Nagoya (Japan)

(Received 28th March 1973)

Flameless atomic absorption spectrometry has become of increasing analytical importance, and several different systems have been described[1–5]. However, this technique has rarely been applied to studies of atomic properties, compared with the flame methods. A method of determining the diffusion coefficient of atomic vapor with an inert gas at high temperature is discussed in this communication.

A glassy carbon tube[6] was used as an atomizer; the glassy carbon reduced permeability so that no lining was necessary.

Calculation

The well known solution of the diffusion equation and the equation $\ln t^{-1} \simeq t^{-1} - 1$, were used:

$t^{-1} \simeq t^{-1} - 1$, were used:

$$p = c(t)/c_0 = (4\pi Dt)^{-\frac{1}{2}} e^{(-x^2/4Dt)}$$

and

$$\ln p = \text{const.} + (\tfrac{1}{2} - x^2/4D)t^{-1}$$

where $c(t)$ and c_0 are the atomic concentrations at time $t = t$ and $t = 0$, respectively, x the diffusion pathlength and D the diffusion coefficient. Since p is proportional to the absorbance to be measured, $\ln(A(t)/A_{max})$ was plotted against t^{-1}, and the slope corresponded to the diffusion coefficient.

Experimental

Apparatus. A Nippon Jarrell-Ash AA-780 atomic-absorption and flame-emission spectrophotometer was fitted with a tube atomizer heated electrically. Light from a Hitachi hollow-cathode lamp was modulated at 60 Hz and all responses were displayed on a Hitachi QPD 54 recorder.

The atom reservoir used in the present work is illustrated in Fig. 1. A glassy carbon tube (Tokai Electrode Manufacturing Co., Ltd.; 150 mm length, 4.0 mm i.d., 6.3 mm o.d.) sintered at 2,000° was fixed at electrodes with graphite cavities (1.0 mm i.d., 6.15 mm o.d., Hitachi Spectroscopic Graphite Electrode). The sample injection port consisted of a tapered graphite tube with a cavity (0.5 mm i.d.)

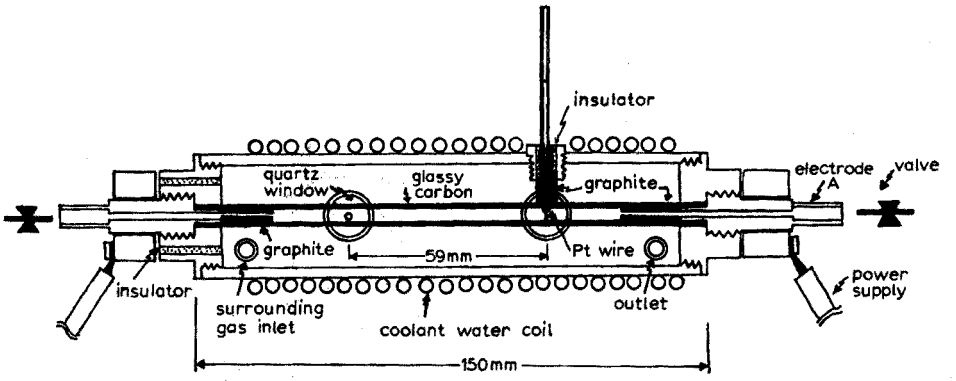

Fig. 1. Atom reservoir for measurement of atomic diffusion coefficient.

inserted into a hole in the glassy carbon tube. A platinum wire of 0.5 mm diameter, on to which the sample solution was placed by a microsyringe (Hamilton Co., Inc.) could be inserted into the tube through the cavity. The glassy carbon tube had other apertures of 1.5 mm diameter at a distance of 59 mm from the injection port; light from the hollow-cathode lamp passed through these to be absorbed by atoms diffusing from the injection port.

Reagents. Cadmium and zinc chloride stock solutions (1000 μg ml^{-1}) were prepared from the pure metals in the usual way.

Procedure. After the purging gas had been introduced into the glassy carbon tube through the electrode A, and the surrounding gas had been introduced into the chamber (see Fig. 1), the glassy carbon tube was heated electrically, and gas feeds were stopped.

A 1.0-μl aliquot of sample solution (40 μg ml^{-1} for cadmium and 25 μg ml^{-1} for zinc) was syringed on to the platinum wire, dried by infrared irradiation,

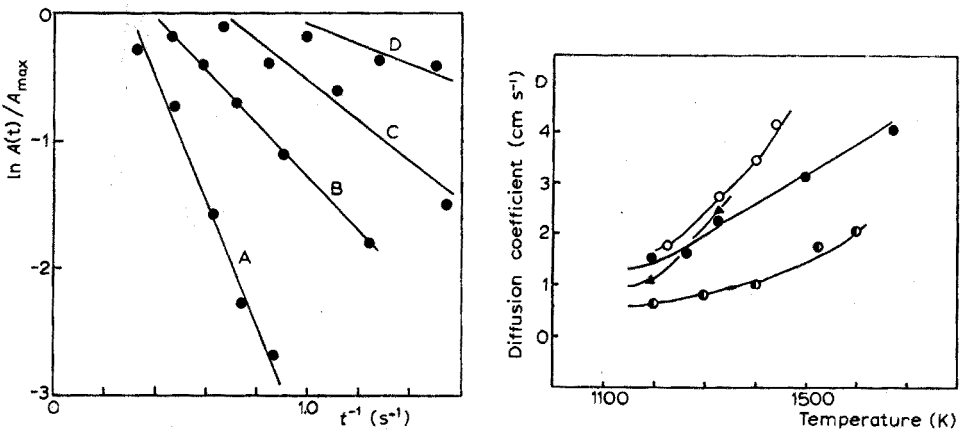

Fig. 2. Plot of ln $A(t)/A_{max}$ *vs.* t^{-1} for Zn–N_2 diffusion. (A) At 1225°K; (B) at 1325°K; (C) at 1400°K; (D) at 1440°K.

Fig. 3. Results for diffusion coefficient. (◐) Cadmium–argon, (●) cadmium–nitrogen, (▲) zinc–argon, (○) zinc–nitrogen.

and injected into the glassy carbon tube after the system had been in thermal equilibrium (for *ca.* 4 min).

The temperature was measured on the surface of the glassy carbon by an optical pyrometer.

The atomic lines used were 228.8 nm for cadmium and 213.9 for zinc, which provided the most sensitive absorptions.

Results and discussion

When a graphite tube was employed as the atomizer in preliminary experiments, atoms were adsorbed on its inner surface, and response times were delayed. When a quartz tube was used as lining in the graphite tube to reduce the adsorption, the results were consistent with those obtained by the glassy carbon. Atomization was found to be rapid (< 0.1 s) compared with diffusion time.

A plot of $\ln(A/A_{max})$ *versus* t^{-1} is shown in Fig. 2 and the results for the diffusion coefficients are shown in Fig. 3. The experiment was performed for interdiffusion coefficients between cadmium and argon, cadmium and nitrogen, zinc and argon, and zinc and nitrogen. The values for D_{Zn-Ar} found were similar to the value determined by Nikolaev and Aleksovskii[7]. The other values, when compared with values computed from the equation of Hirschfelder *et al.*[8] were found to be somewhat larger at high temperatures.

REFERENCES

1 B. V. L'Vov, *Spectrochim. Acta*, 17 (1961) 761.
2 H. Massmann, *Spectrochim. Acta*, 23B (1968) 215.
3 R. Woodriff, R. W. Stone and A. M. Held, *Appl. Spectrosc.*, 22 (1968) 408.
4 T. S. West and X. T. Williams, *Anal. Chim. Acta*, 45 (1969) 27.
5 T. Takeuchi, M. Yanagisawa and M. Suzuki, *Talanta*, 19 (1972) 465.'
6 G. Baudin, M. Chaput and L. Feve, *Spectrochim. Acta*, 26B (1971) 425.
7 G. I. Nikolaev and V. B. Aleksovskii, *Sov. Phys. Tech. Phys. (English Transl.)*, 9 (1964) 575.
8 J. O. Hirschfelder, R. B. Bird and E. L. Spotz, *Chem. Rev.*, 44 (1949) 205.

Analytica Chimica Acta, 67 (1973) 460–464

SHORT COMMUNICATION

Atomic absorption spectrometric determination of lead and cadmium in silicon, ferrosilicon and ferromanganese by direct atomization from the solid state

F. J. LANGMYHR, Y. THOMASSEN and A. MASSOUMI*
Department of Chemistry, University of Oslo, Blindern, Oslo 3 (Norway)
(Received 18th May 1973)

The realization of the importance of the trace elements has initiated studies of their occurrence, distribution and effects in industrial raw materials, intermediate and final products.

For the determination of trace components present in concentrations below 1 p.p.m., many of the conventional methods, such as emission spectrography and spectrophotometry, are not very suitable for routine application. However, the low detection limits, the small sample amounts required, the simplicity and the short time of measurement make the furnace techniques of atomic absorption spectrometry very useful in trace analysis; the method also has the advantage of permitting elements to be atomized directly from the solid state.

The present communication describes the use of the direct-atomization technique to the determination of lead and cadmium in silicon, ferrosilicon and ferromanganese; zinc was determined in the same materials by the conventional flame technique. Attempts were also made to determine bismuth, antimony and silver. The present equipment and methods have been applied previously to the determination of rubidium, cesium, cadmium, zinc and silver in silicate rocks[1,2].

Apparatus

The measurements were made with a Perkin-Elmer 303 atomic absorption spectrophotometer equipped with a deuterium lamp for background correction. The construction of the graphite furnace (heated by a high-frequency induction generator) has been described elsewhere[1]. The signals from the photometric detector were registered with a 2-channel recorder; one of the channels plotted the peak (in percent absorption), and the other transformed the detector signals into absorbance and gave the integrated peak area.

Weighings were made with semi-micro or micro balances.

Reagents and standard solutions

Standard solutions of lead, cadmium and zinc were prepared from high-purity metals, the acids were of "Suprapur" quality from E. Merck, and all other

* On leave from Department of Chemistry, Pahlavi University, Shiraz, Iran.

chemicals were of reagent-grade quality. The furnace was purged with argon (purity 99.99% by volume).

Separate primary standard solutions (1000 p.p.m.) of cadmium and zinc were prepared by dissolving the metals in a small excess of sulfuric acid. A lead solution of the same concentration was prepared by dissolving the metal in nitric acid; in the preparation of secondary diluted solutions a small excess of sulfuric acid was added, so that the element would be present as the sulfate before atomization in the furnace.

Preparation and decomposition of the samples

In order to avoid serious sampling errors, all samples were ground manually in an agate mortar to pass a 300-mesh sieve.

Silicon. Five 2-g portions of silicon were transferred to platinum dishes, and 20 ml of water, 10 ml of hydrofluoric acid and 5 ml of nitric acid were added. After the dissolution, 2.5 ml of sulfuric acid were added, and the mixtures were evaporated to dryness on the water bath and on the hot plate. The evaporations were repeated. The residues were moistened with 0.5 ml of sulfuric acid, water was added and the solutions were diluted to 50 ml with water. A blank was prepared.

Ferrosilicon. Five 1-g portions of each of the two ferrosilicon samples were dissolved as described above, the volumes of the reagents added being reduced proportionally. The solutions were diluted to 50 ml with water. A blank was prepared.

Ferromanganese. Five 1-g portions of ferromanganese were first attacked in beakers with 15 ml of nitric acid (1+2). The contents were then transferred to platinum dishes, 3 ml of hydrofluoric acid and 1.5 ml of sulfuric acid were added, and the mixtures were evaporated twice to dryness as described above. The treatment leaves most of the carbon unattacked. The final solutions were diluted to 50 ml with water. A blank was prepared.

Measurement procedures

Atomization from the solid state. Lead and cadmium were determined in silicon, ferrosilicon and ferromanganese. The solid standard for lead was the British Chemical Standard No. 305, Ferrosilicon (the content of lead in this sample was found, as discussed below, to be 7.6 p.p.m.). From previous studies it was known that cadmium in the present materials could be determined by measurements against cadmium standard solutions. The relatively high contents of zinc in the samples prevented the use of the very sensitive zinc line at 213.8 nm; but the 307.6-nm line was not sufficiently sensitive, and zinc was therefore not determined by the furnace technique.

Atomization from the liquid phase. Lead was determined in silicon and the two samples of ferrosilicon by the standard addition technique. The copious fumes developed during the atomization of ferromanganese prevented a determination of lead.

Atomization in the air/acetylene flame. Zinc was determined in silicon, the two samples of ferrosilicon and ferromanganese by the standard addition technique. The content of lead in the two ferrosilicon samples was determined by measurements

against lead standard solutions. In these determinations of zinc and lead the signals from the sample solutions were corrected for light scattering by measurements at suitable non-absorbing lines.

Procedures. The various settings of the spectrophotometer were adjusted according to the instrument manual. The wavelengths employed were: for lead 217.0 nm and 283.3 nm, for zinc 213.8 nm, and for cadmium 228.8 nm. The deuterium background corrector was used only during atomizations in the furnace. The flow of argon was adjusted to 360 ml min^{-1}. A 1–25 mg portion of the solid sample was weighed out in a small tantalum scoop (produced by Perkin-Elmer) and placed in the middle of the graphite tube by means of a home-made adjustable inserting device. The scoop was reweighed and the furnace was moved into its preadjusted position.

For lead, the drying and atomization conditions were: (*a*) atomizations from the solid state: 60-s drying at 60 V (175°), 15-s atomization at 210 V (1270°), and 60-s cleaning of the tube at 260 V (1900°); (*b*) for atomizations from the liquid state: 60-s evaporation (of water) at 40 V (80°), followed by the steps given under (*a*).

For cadmium the same procedure was followed, except that atomizations were done at 200 V (1200° after 15 s).

On the basis of the signal obtained from a suitable portion of the solid

TABLE I

ANALYTICAL RESULTS FOR LEAD

(Unless otherwise stated, 5 analyses of each sample were made)

Sample	*Content of lead in p.p.m. (as Pb)*								
	Atomizing solid sample in furnace (λ=217.0 nm)			*Atomizing sample solution in furnace (λ=283.3 nm)*			*Atomizing sample soluti in flame (λ=217.0 nm)*		
	$\bar{x}$[a]	s	s_r	$\bar{x}$	s	s_r	$\bar{x}$	s	s_r
Ferrosilicon, BCS No. 305	Standard			7.6	0.3	4.0	10	6	60
Ferrosilicon, standard sample No. 2 (Elkem-Spigerverket)	2.1	0.5	24	2.3	0.5	22	—	—	—
Silicon, standard sample 1964 (Elkem-Spigerverket)	2.0	0.5	25	2.4	0.8	33	—	—	—
Ferromanganese, high carbon (Electric Furnace Products Co., Ltd.)	3.1	0.8	26	—	—	—	—	—	—

[a] $\bar{x}$=average; s=standard deviation; s_r=relative standard deviation.

sample, two portions of the solid standard were weighed out and atomized, one to give a slightly higher, and the other a somewhat lower, signal than the sample. From a run of the empty furnace the blank signal was found.

Results

The results obtained by the present methods are given in Tables I and II. There were no previous data for the materials analyzed*.

TABLE II

ANALYTICAL RESULTS FOR CADMIUM AND ZINC

(Unless otherwise stated, 5 analyses of each sample were made)

Sample	*Content of cadmium in p.p.b. (as Cd) by atomizing solid sample in furnace*			*Content of zinc in p.p.m. (as Zn) by atomizing sample solution in flame*		
	$\bar{x}$	s	s_r	$\bar{x}$	s	s_r
Ferrosilicon, BCS No. 305	10	2	20	6.6[a]	1.6	24
Ferrosilicon, Standard sample No. 2 (Elkem-Spigerverket)	2	1	50	5.1	0.6	12
Silicon, standard sample 1964 (Elkem-Spigerverket)	4	1	25	4.4	1.0	23
Ferromanganese, high carbon (Electric Furnace Products Co., Ltd.)	7	2	29	4.3	0.6	14

[a] 4 determinations.

From Table I it appears that the measurements of lead in the flame have a poor precision. The better precision of the measurements made at 283.3 nm probably results from a lower noise level and a reduced effect of smoke.

As stated above attempts were made to determine bismuth and antimony by atomization from the solid state in the furnace; however, no signals were obtained from the above materials, which indicates contents below about 0.1 p.p.m. of bismuth and 1 p.p.m. of antimony. The samples were found to contain detectable amounts of silver, but this element is probably of little industrial interest.

The results show that lead and cadmium can be determined in silicon, ferrosilicon and ferromanganese by atomization from the solid state. However, the

* In an earlier paper[3] the content of lead in the BCS No. 305 Ferrosilicon was found to be 0.018%. This result is obviously too high and resulted from incomplete knowledge of the interferences involved.

most convenient method for zinc at the present concentration levels was the conventional flame technique.

The authors gratefully acknowledge the receipt of samples from Elkem-Spigerverket A/S, Fiskaa Verk, and from Electric Furnace Products Co., Ltd., Sauda.

REFERENCES

1 F. J. Langmyhr and Y. Thomassen, *Z. Anal. Chem.*, 264 (1973) 122.
2 F. J. Langmyhr, Y. Thomassen, J. E. Hanssen and J. Doležal, *Z. Anal. Chem.*, in press.
3 F. J. Langmyhr and P. E. Paus, *Anal. Chim. Acta*, 45 (1969) 173.

Analytica Chimica Acta, 67 (1973) 465–468

SHORT COMMUNICATION

A simultaneous determination of zinc and cadmium

RICHARD E. JENSEN and MARIAN KAEHLER
Department of Chemistry, Gustavus Adolphus College, St. Peter, Minn. 56082 (U.S.A.)
(Received 8th April 1973)

Non-selective, but highly sensitive, organic analytical reagents have been reported for many years. Picolinealdehyde-2-quinolylhydrazone (PAQH) may be regarded as belonging to this category and has been reported as a colorimetric reagent for the determination of palladium and as a sensitive fluorimetric reagent for the microdetermination of zinc[1,2]. These studies, however, demonstrated that even though the reagent is very sensitive in many of its applications, it certainly is not selective. The true value of such inselective reagents can be found only when a selective method of measurement is applied.

This communication reports the simultaneous determination of zinc and cadmium with picolinealdehyde-2-quinolylhydrazone as the complexing agent, extracting from aqueous solution into chloroform, and completing the measurement by atomic absorption spectrometry. Variables associated with metal ion complexation, with extraction of the zinc and cadmium complexes, and with atomic absorption spectrophotometric measurement of the zinc and cadmium complexes are discussed.

Experimental

Apparatus and reagents. All absorption measurements were made with a Varian Techtron Model 1000 atomic absorption spectrophotometer and an air–acetylene flame. Optimal conditions for each metal system are as follows:

	Zinc	*Cadmium*
Wavelength (nm)	213.5	228.8
Tube current (mA)	5.0	4.0
Bandpass (nm)	0.5	0.5
Flow ratio (acetylene–air)	1:2.4	1:2.7

A Beckman Zeromatic II pH meter with a Sargent S-30072-15 combination electrode was used for all pH measurements.

Picolinealdehyde-2-quinolylhydrazone (PAQH) was prepared as described by Jensen and Pflaum[2]. Stock solutions of $4.00 \cdot 10^{-3}$ *M* were prepared by heating the solid ligand in a minimum of dilute hydrochloric acid.

A buffer solution, 1.0 *M* in tris(hydroxymethyl)aminomethane, was prepared

by dissolving 122 g of tris(hydroxymethyl)aminomethane in distilled water and adding concentrated hydrochloric acid until a pH of 8.50 was attained; the final volume was 1 l.

A zinc stock solution (100 p.p.m.) was prepared by dissolving reagent-grade granular zinc in a minimum of concentrated hydrochloric acid.

A cadmium stock solution (113 p.p.m.) was prepared by dissolving reagent-grade cadmium shavings in a minimum of concentrated hydrochloric acid.

Water-equilibrated chloroform, analytical-reagent grade, was used for all extraction studies.

Procedure. Dissolve the sample containing zinc and/or cadmium by appropriate means. To a 5-ml aliquot containing 0.07–2.00 p.p.m. of zinc(II) and 0.11–2.80 p.p.m. of cadmium(II) in a 125-ml separatory funnel, add at least a twenty-fold excess of PAQH and 5 ml of pH 8.50 buffer, and dilute to *ca.* 75 ml with distilled water. Extract the aqueous solution with three 5-ml portions of chloroform, and pass the extracts through cotton to remove water. Dilute the extracts to volume in a 100-ml volumetric flask with chloroform and measure the absorbances of zinc and cadmium under the conditions described above. From previously prepared calibration curves determine the amounts of zinc and cadmium in the sample.

Results and discussion

The effects of pH on the complex were ascertained. The most efficient complexation and extraction were obtained at pH 8.50. Tris(hydroxymethyl)-aminomethane (Tris)–hydrochloric acid was found to be a satisfactory buffer when prepared at a pH of 8.50.

A study of excess of reagent on the zinc(II)–PAQH system showed that a fifteen-fold excess of ligand was sufficient for maximal complex formation. A twenty-fold excess of PAQH was necessary for maximal cadmium(II)–PAQH complex formation. Excess of ligand up to ratios of 200:1 showed no detectable adverse effects in either system.

The efficiency of the extraction of the zinc(II)–PAQH and the cadmium(II)–PAQH complexes from aqueous solution into chloroform was studied. Three 5-ml aliquots provided the greatest efficiency. Solutions of both complexes were stable for at least one week.

The zinc(II)–PAQH complex was found to obey Beer's law over a concentration range of $1.00 \cdot 10^{-6}$ *M*–$20.0 \cdot 10^{-6}$ *M* (0.065–1.30 p.p.m.) zinc(II). The sensitivity of measurement was calculated as 17.7 p.p.b., and the detection limit 3.13 p.p.b. A similar study of the zinc(II) complex absorbance over the same concentration range in aqueous solution gave the comparable sensitivity and detection limit as 27.8 p.p.b. and 9.34 p.p.b., respectively.

The cadmium(II)–PAQH complex obeyed Beer's law over the same concentration range ($1.0 \cdot 10^{-6}$ *M*–$20.0 \cdot 10^{-6}$ *M* (0.113–2.26 p.p.m.) cadmium(II)). The sensitivity level was determined as 22.6 p.p.b., and the detection limit was 1.7 p.p.b. In comparable aqueous solutions, the sensitivity was 60.3 p.p.b., and the detection limit 10.5 p.p.b.

When the expanded-scale capability of the atomic absorption spectrometer was used, the sensitivity level of the zinc(II)–PAQH system was enhanced to 7.21 p.p.b., and the detection limit to 2.28 p.p.b. The analogous cadmium(II) values

were, respectively, 14.9 p.p.b. and 1.35 p.p.b. The sensitivity of either system can be enhanced by roughly a factor of six if the three 5-ml extracts are not further diluted.

The simultaneous determination studies involved the preparation of four series of five solutions each. Within each series the concentration of one ion was kept constant and the concentration of the second ion was varied. The absorbances within each series were compared by means of the slopes and y-intercepts of the corresponding plots. The presence of cadmium(II) ion showed no effect on the extraction, formation, and absorbance of the zinc(II)–PAQH complex; nor did zinc(II) affect the treatment of the cadmium(II)–PAQH complex (Table I). Provided that a sufficient excess of ligand was present with respect to the total metal ion concentration, zinc(II) and cadmium(II) could be simultaneously determined without mutual interference.

The above procedure has been designed with the following considerations: ease of technique, use of common reagents, practical instrumentation, and applicable range of sensitivity. Although it has been shown that there is no mutual interference between the zinc and cadmium complex systems, there are interferences from other cations. These interfering ions consume the reagent and must be removed before the analysis for zinc and cadmium[1]. The use of chloroform as an

TABLE I

EFFECT OF CADMIUM ON ZINC EXTRACTION AND VICE VERSA

Concentration of Zn taken (p.p.m.)	*Absorbance for Zn*		*Concentration of Cd taken (p.p.m.)*	*Absorbance for Cd*	
0 p.p.m. Cd			*0 p.p.m. Zn*		
0.1	13.2	Slope: 81.92	0.113	5.4	Slope: 36.4
0.3	30.4	y-Intercept: 5.921	0.339	14.2	y-Intercept: 1.5
0.5	47.5		0.565	21.9	
0.7	65.3		1.130	42.6	
1.0	86.3		1.695	63.2	
0.565 p.p.m. Cd			*1.0 p.p.m. Zn*		
0.1	19.5	Slope: 77.11	0.113	6.3	Slope: 32.4
0.3	33.4	y-Intercept: 11.20	0.339	14.4	y-Intercept: 3.6
0.5	50.6		0.565	22.8	
0.7	64.2		1.130	41.2	
1.0	88.8		1.695	57.5	
1.130 p.p.m. Cd			*5.0 p.p.m. Zn*		
0.1	16.3	Slope: 79.82	0.113	5.0	Slope: 35.8
0.3	33.6	y-Intercept: 9.174	0.339	13.8	y-Intercept: 1.7
0.5	49.5		0.565	22.6	
0.7	65.8		1.130	43.3	
1.0	88.2		1.695	61.5	
1.695 p.p.m. Cd			*10.0 p.p.m. Zn*		
0.1	16.0	Slope: 80.11	0.113	4.7	Slope: 36.9
0.3	34.3	y-Intercept: 9.325	0.339	13.6	y-Intercept: 0.73
0.5	50.4		0.565	21.4	
0.7	65.5		1.130	42.4	
1.0	88.7		1.695	88.7	

extracting solvent presents a problem when introduced into the flame; the formation of hydrogen chloride and chlorine gas requires that the burner ventilation system operates efficiently.

Further studies will be initiated concerning the application of this organic analytical reagent to the complexation, extraction and atomic absorption spectrometry of a wide variety of metal ions.

The authors wish to thank the Gustavus Research Fund for the financial support of this investigation.

REFERENCES

1 R. E. Jensen and R. T. Pflaum, *Anal. Chim. Acta*, 37 (1967) 397.
2 R. E. Jensen and R. T. Pflaum, *Anal. Chem.*, 38 (1967) 1269.

Analytica Chimica Acta, 67 (1973) 469–472

SHORT COMMUNICATION

Photometric determination of diphenylamine with cerium(IV) sulphate

MURALIKRISHNA GANDIKOTA and G. GOPALA RAO
Department of Chemistry, Andhra University, Waltair (India)
(Received 18th May 1973)

Diphenylamine finds various industrial uses in the manufacture of rubber, plastics, dyes, pharmaceuticals, pesticides, and lubricating oils[1]. It is frequently added to high explosives, propellants and smokeless gun powder as a stabilizer, and is used as a fungicide in storage of apples. Adamsite (diphenylamine chlorarsine) a highly irritant poison for the mucous membranes of the throat and nose (effective in a concentration of 1 part of the dust in 30,000,000 parts of air) is derived from diphenylamine and can be decomposed by heating with an aqueous solution of hydroiodic acid. The determination of diphenylamine is therefore of great importance in view of the wide variety and number of its uses in the laboratory and industry.

Cook's[2] gravimetric method depends on the formation of an insoluble tetrabromo derivative on treatment of diphenylamine with bromine. Indirect titrimetric methods[3–6] based on bromination with an excess of bromate–bromide mixture have been extensively used. In both types of procedure, aniline and similar materials interfere. A photometric method[7] depends on coupling of diphenylamine in 50% sulphuric acid with diazosulphanilic acid to give a violet colour. In this communication are reported the conditions established for the quantitative oxidation of diphenylamine with cerium(IV) sulphate to diphenylamine blue and its photometric determination. Compared with the available procedures this has the advantages of speed, fewer reagents and freedom from interference from aniline and similar compounds.

Experimental

Reagents. A stock *ca.* 0.01 *M* solution of diphenylamine (Merck p.a.) in AnalaR sulphuric acid (free from even traces of nitric acid) was prepared. Experimental solutions of the order of *ca.* $2 \cdot 10^{-4}$ *M* were made from the stock solution by successive dilutions, the concentration of the sulphuric acid in the final solutions being kept at 5 *M*.

A stock solution of 0.1 *M* cerium(IV) sulphate in 0.5 *M* sulphuric acid was prepared and standardized against standard arsenic(III) by the methods of Willard and Young[8] and Muralikrishna and Gopala Rao[9]. From this a 0.001 *M* solution was prepared by successive dilutions, the sulphuric acid concentration being kept at 0.5 *M*.

Study of the effect of cerium(IV) concentration. A number of experiments were made where each mixture of 50 ml contained 4.25 ml of $2 \cdot 10^{-4}$ *M* diphenylamine and sulphuric acid at an overall concentration of 1 *M*, but the molar proportion of cerium(IV) sulphate was varied. The cerium(IV) sulphate solution was always added last. The mixture was shaken well, and poured quickly into the absorbance cell of a Klett-Summerson photoelectric colorimeter, and the absorbance was measured with a green filter transmitting light in the region 500–570 nm. All the operations involved were arranged so speedily as to record the dial reading within a minute of mixing the cerium(IV) sulphate solution. Similar sets of experiments were set up in 2 *M* and 5 *M* sulphuric acid.

The results obtained with molar ratios of diphenylamine to cerium(IV) varying from 1:2.5 to 1:8.0 showed that diphenylamine blue is not destroyed even by a large excess of the oxidant over and above that required for the formation of the blue colour. Experiments showed that the oxidation is complete even when the diphenylamine:oxidant ratio is 1:2.

Effect of sulphuric acid concentration on the stability of diphenylamine blue. A number of experiments were made, where each mixture of 50 ml contained 6.0 ml of $2 \cdot 10^{-4}$ *M* diphenylamine solution and 3.6 ml of 0.001 *M* cerium(IV) sulphate but with varying concentration of sulphuric acid. For each mixture the dial reading was measured at different times. The observations (Table I) showed that the stability of the blue colour increases with increasing concentration of sulphuric acid, being about 5–6 min in 4 *M* sulphuric acid, about 6–7 min in 5 *M* sulphuric acid and about 9–10 min in 6 *M* sulphuric acid. The instability of the blue colour has been reported to be due to disproportionation, by Bishop and Hartshorn[10].

Procedure for the photometric determination of diphenylamine. Treat 0.5–8.0 ml of diphenylamine solution (*ca.* $2 \cdot 10^{-4}$ *M*) in 5–6 *M* sulphuric acid, in a 50-ml glass-stoppered volumetric flask, with 0.5–8.0 ml of 0.001 *M* cerium(IV) sulphate in 5 *M* sulphuric acid, and dilute with 5 *M* sulphuric acid to the mark. Mix thoroughly, transfer to the absorbance cell of the Klett-Summerson colorimeter and measure the absorbance using a green filter.

TABLE I

EFFECT OF SULPHURIC ACID CONCENTRATION ON THE STABILITY OF DIPHENYLAMINE BLUE

Concentration of sulphuric acid (M)	*Dial reading*									
	Time (min)									
	1	*2*	*3*	*4*	*5*	*6*	*7*	*8*	*9*	*10*
0.5	385	368	363	360	355	350	340	330	325	320
1.0	385	385	380	375	365	355	350	345	340	—
2.0	385	385	385	382	380	375	370	365	360	—
3.0	385	385	385	385	385	378	375	372	370	365
4.0	385	385	385	385	385	380	378	375	375	—
5.0	385	385	385	385	385	385	382	380	378	375
6.0	385	385	385	385	385	385	385	385	385	380

TABLE II

PHOTOMETRIC DETERMINATION OF DIPHENYLAMINE

Amount taken (μmoles)	*Amount found (μmoles)*	*Relative error (%)*
0.1009	0.1009	Nil
0.2018	0.2018	Nil
0.4036	0.3935	−2.5
0.6054	0.6160	+1.8
0.9081	0.920	−1.3
1.009	1.009	Nil
1.211	1.176	−2.8
1.413	1.392	−1.5

The linearity of the plot of dial readings against mmoles of diphenylamine showed that Beer's law is obeyed in the range $8–152 \cdot 10^{-5}$ mmoles. A number of samples were assayed with the results presented in Table II. The error is quite low in view of the small quantities involved. Attempts were made to assay diphenylamine at higher concentrations with a red filter transmitting in the region 640–700 nm without success.

The accuracy of the determination is not affected by adding diphenylamine last instead of cerium(IV).

Interferences. Methanol (59 mmoles), ethanol (17 mmoles) and aniline (0.08 mmoles) do not interfere. The amounts mentioned in the brackets are the maximum tried.

Rapid spectrophotometric assay of diphenylamine. By rapid scanning of the absorption spectrum of diphenylamine blue in 5–6 *M* sulphuric acid, the absorption maximum was found to lie at 570 nm. A number of mixtures of diphenylamine and cerium(IV) sulphate were prepared and their absorbances were quickly measured in a Hilger Uvispek spectrophotometer at 570 nm in a 1-cm cell. The molar absorptivity of the diphenylamine blue was then calculated. The average of six determinations gave a value of 45000 l $mole^{-1}$ cm^{-1}, which agrees with the value reported earlier[10]. Rapid assays of unknown test solutions of diphenylamine based on calculation from the molar absorptivity then became possible; each test solution was treated with double the quantity of cerium(IV) sulphate required for oxidation to the blue in 5 *M* sulphuric acid, and diluted to known volume with 5 *M* sulphuric acid and its absorbance *E* was measured quickly at 570 nm using a cell of known thickness *t* cm. The concentration, *C*, was then calculated from the formula $Ct = E/\varepsilon$. The results obtained for diphenylamine in the concentration range 0.8–1.4 μmole showed relative errors varying from +0.8% to −2.0%.

One of us (M.K.G.) is grateful to Andhra University for the award of a U.G.C. Junior Research Fellowship.

REFERENCES

1 A. Rose and E. Rose, *The Condensed Chemical Dictionary*, Reinhold, New York, 1966, p. 344.

2 S. G. Cook, *Ind. Eng. Chem., Anal. Ed.*, 7 (1935) 250.
3 D. Craig, *Ind. Eng. Chem., Anal. Ed.*, 9 (1937) 56.
4 T. D. Waugh, G. Harbottle and R. M. Noyes, *Ind. Eng. Chem., Anal. Ed.*, 18 (1946) 636.
5 F. Ellington, *Analyst*, 71 (1946) 305.
6 W. D. Tullis and M. Roth, *U.S. Dept. Commer. Off. Tech. Serv. P.B. Rep.*, 130 (1957) 196.
7 B. V. Ponomarenko, *Zavodk. Lab.*, 13 (1947) 937.
8 H. H. Willard and P. Young, *J. Amer. Chem. Soc.*, 50 (1928) 1322.
9 Muralikrishna Gandikota and G. Copala Rao, *Anal. Chim. Acta*, in press.
10 E. Bishop and L. G. Hartshorn, *Analyst*, 96 (1971) 26, 36.

Analytica Chimica Acta, 67 (1973) 473–476

SHORT COMMUNICATION

Solvent extraction and spectrophotometric determination of molybdenum in iron

S. P. PATIL and V. M. SHINDE
Department of Chemistry, Shivaji University, Kolhapur-416004 (India)
(Received 26th March 1973)

4-Methyl-2-pentanol has been used for the extraction of vanadium[1]. This paper describes systematic studies on the solvent extraction of molybdenum(VI) with 4-methyl-2-pentanol (methyl isobutyl carbinol). The studies showed that molybdenum(VI) can be quantitatively extracted with 50% 4-methyl-2-pentanol in benzene from 1 *M* hydrochloric acid containing 10 *M* lithium chloride. The metal ion in the organic phase can be determined spectrophotometrically as the orange-red thiocyanate complex at 465 nm.

Several methods for the extraction of molybdenum are known. Solvents such as ether[2–5], and various esters[6–10], alcohols[11–14], ketones[15–18] and alkyl phosphates[19,20] have been used. However, with ether[2–5], multiple extraction is required; with esters[6–10] temperature control is critical, and reducing agents are needed to eliminate interferences; with MIBK[15–18], extraction of the thiocyanate complex is quantitative only if large volumes of extractants were used. The alkyl phosphate methods suffer from many interferences.

The solvent extraction of molybdenum(VI) with methyl isobutyl carbinol eliminates most of these drawbacks. The method is rapid and extremely simple, and the tolerance limit for foreign ions is high.

Experimental

Apparatus and reagents. A Zeiss spectrophotometer (Jena) with matched 1-cm quartz cells was used.

A stock solution of molybdenum(VI) was prepared by dissolving 0.184 g of ammonium molybdate (AnalaR) in 1 l of distilled water. Standardization showed the solution to contain 14.8 μg Mo ml^{-1}.

General procedure. Transfer an aliquot of the molybdenum(VI) solution to a separatory funnel, and add hydrochloric acid and lithium chloride, to give concentrations of 1 *M* and 10 *M*, respectively, in a volume of 10 ml. Shake for 5–10 s with 10 ml of 50% 4-methyl-2-pentanol (Merck; b.p. 131.4–134.0°) in benzene. Allow the phases to separate and withdraw the aqueous phase. To the organic phase, add 1 ml of concentrated hydrochloric acid, 1 ml of iron(II) solution (1% iron(II) ammonium sulphate in 0.1 *M* sulphuric acid), 3 ml of aqueous 10% potassium thiocyanate solution and 3 ml of 10% tin(II) chloride solution in 1 *M* hydrochloric acid. Shake well, allow the two phases to separate and measure the

absorbance of the orange-red thiocyanate complex of molybdenum in the organic phase at 465 nm against a reagent blank.

Effect of variable conditions

The concentration of hydrochloric acid was varied from 0.25 to 2.0 *M* in the presence of 10 *M* lithium chloride and that of 4-methyl-2-pentanol from 10–100% by dilution with benzene. The results (Table I) showed that quantitative extraction was achieved with 50% of the extractant from solutions containing 0.25–1.0 *M* hydrochloric acid and 10 *M* lithium chloride as the salting-out agent. In the absence of salting-out agent, extraction of molybdenum(VI) from 1–6 *M* hydrochloric acid solution was incomplete. From sulphuric acid solution (1–3 *M*) only 15% extraction was obtained. A plot of log *D* *vs.* log *C* (carbinol concentration) for 0.5 *M* hydrochloric acid solution gave a slope of 1.88, which indicates that the probable composition of the extracted species is $[MoO_2Cl_2 \cdot 2\ MIC]$.

TABLE I

DISTRIBUTION RATIO AS THE FUNCTION OF ACIDITY AND EXTRACTANT CONCENTRATION

(Mo(VI) = 14.8 μg; 10 *M* LiCl as salting-out agent)

Carbinol conc. (%)	*HCl conc. (M)*	*Extraction (%)*	*Distribution ratio (D)*
10	0.25	53.84	1.16
	0.50	57.69	1.36
	1.00	65.37	1.88
	2.00	61.53	1.60
15	0.25	69.23	2.25
	0.50	73.08	2.71
	1.00	73.08	2.71
	2.00	69.23	2.25
25	0.25	84.61	5.49
	0.50	88.45	7.65
	1.00	88.45	7.65
	2.00	84.61	5.49
50	0.25–1.00	100.00	∞
	2.00	96.14	24.90
75–100	0.25–1.00	100.00	∞

Varying concentrations of chlorides of lithium and magnesium were used as the salting-out agent. For quantitative extraction of molybdenum(VI) from 0.5–1 *M* hydrochloric acid, it was necessary to use 10 *M* lithium chloride. The use of 8 *M* lithium chloride gave about 96% extraction. Magnesium chloride had no appreciable effect on the extraction process.

Variation of shaking time from 5 s to 60 s showed that even 5 s was enough for complete extraction.

Effect of diverse ions

Table II shows the effect of various ions on the extraction. The tolerance

TABLE II

EFFECT OF DIVERSE IONS

Mo(VI) = 14.8 μg; 1 *M* HCl + 10 *M* LiCl; 50% carbinol in benzene)

Foreign ion	*Added as*	*Tolerance limit (μg)*	*Foreign ion*	*Added as*	*Tolerance limit (μg)*
Fe^{3+}	$FeCl_3 \cdot 6H_2O$	5,000	U^{6+}	$UO_2(NO_3)_2 \cdot 6H_2O$	1,000
Mn^{2+}	$MnCl_2 \cdot 4H_2O$	1,000	V^{5+}	$NaVO_3 \cdot H_2O$	1,000
Ni^{2+}	$NiCl_2 \cdot 6H_2O$	1,000	In^{3+}	$InCl_3 \cdot 4H_2O$	1,000
Cr^{3+}	$CrCl_3$	1,000	Ga^{3+}	$GaCl_3$	1,000
Cu^{2+}	$CuCl_2 \cdot H_2O$	1,000	WO_4^{2-}	$Na_2Wo_4 \cdot 2H_2O$	250[a]
Cd^{2+}	$CdCl_2$	5,000	F^-	NaF	25,000
Zn^{2+}	$ZnSO_4 \cdot 7H_2O$	5,000	PO_4^{3-}	NaH_2PO_4	5,000
Bi^{3+}	$Bi(NO_3)_3 \cdot 5H_2O$	5,000	Cit.$^{3-}$	Citric acid	5,000
Ti^{2+}	$TiCl_2$	None	Tart.$^{3-}$	Tartaric acid	5,000
Zr^{4+}	$ZrSO_4 \cdot 4H_2O$	1,000	Oxalate	Oxalic acid	5,000
Co^{2+}	$CoCl_2 \cdot 6H_2O$	5,000	Ascorbate	Ascorbic acid	5,000
Sb^{3+}	$SbCl_3$	5,000	EDTA (disodium salt)		5,000
Sn^{2+}	$SnCl_2 \cdot 2H_2O$	None			

[a] Tungstate masked with 5 mg of oxalic acid.

limit was set at the amount required to cause a ±1.0% error in the molybdenum recovery. Cations, *viz.* Cd, Sb, Fe, Cr, Ni, Mn, Cu, Zn, V and U, commonly associated with molybdenum (VI) did not interfere in the extraction and determination, even when present in ratios exceeding 1:100. Tungstate (250 μg) could be masked with 5 mg of oxalic acid. Titanium and tin however, interfered.

Application to cast iron

Two samples of alloy cast iron (No. 33b and 33d, Bureau of Analysed Samples Ltd., U.K.) were analyzed. The results are given in Table III.

TABLE III

ANALYSIS OF ALLOY CAST IRON

Alloy	*Composition of alloy (%)*	*Mo present (%)*	*Mo found (%)*
33b	C 2.24, Si 2.00, P 0.11, Mn 0.64, Ni 2.24, Cr 0.61	0.40	0.390, 0.410, 0.400
33d	C 2.30, Si 1.63, Mn 0.63, Ni 2.38, Cr 0.52, Cu 1.54	0.48	0.465, 0.470, 0.475

A known weight of alloy steel was dissolved in 9 ml of concentrated sulphuric acid and 50 ml of water. After the initial reaction was over, the solution was heated with nitric acid (5 ml) and evaporated to fumes. The extract was boiled to dissolve soluble matter, filtered to remove silica and finally diluted to 100 ml in a volumetric flask. An aliquot of this solution was extracted and analyzed by the general procedure.

The method is very selective and permits a rapid separation and determination of molybdenum. The average recovery of molybdenum(VI) was $99.0 \pm 1.0\%$. Each determination took a total of 15–20 min.

Thanks are due to U.G.C. for the award of fellowship to one of us (S.P.P.) and the University authorities for laboratory facilities.

REFERENCES

1 E. Gagliardi and P. Tummler, *Mikrochim. Acta*, (1970) 42.
2 C. E. Crouthamel and C. E. Johnson, *Anal. Chem.*, 26 (1954) 1284.
3 V.M. Tarayan and L. G. Mushegyan, *Zh. Khim.*, 34 (1959) 574.
4 I. P. Alimarin and V. N. Polyansky, *J. Anal. Chem. USSR*, 8 (1953) 266.
5 F. G. Zherovskii, *Zh. Khim.*, 46 (1958) 365.
6 S. F. Marsh, *Anal. Chem.*, 39 (1967) 696.
7 Y. Morimoto and T. Ashizawa, *Jap. Anal.*, 10 (1961) 532.
8 S. Yamamoto, *J. Chem. Soc. Jap.*, 77 (1956) 713; 76 (1955) 417.
9 R. Prosad and V. Yatirajam, *Ind. J. Chem.*, 2 (1964) 250; 2 (1969) 249; 3 (1965) 345, 544.
10 S. M. Jogdeo and L. M. Mahajan, *Ind. J. Chem.*, 3 (1965) 468.
11 F. Martinez and A. P. Bouza, *Chem. Anal.*, 46 (1957) 66.
12 S. Ambujavalli, *Chem. Anal.*, 56 (1967) 79.
13 G. A. Bauer, *Anal. Chem.*, 37 (1965) 155.
14 B. V. S. Sarma, D. Satynarayan and V. Pandu Ranga Rao, *Chem. Anal.*, 56 (1967) 78.
15 J. O. Habbits, W. F. Davis, M. R. Menke and S. Kallman, *Talanta*, 4 (1960) 104.
16 Y. Kekita and H. Goto, *J. Chem. Soc. Jap.*, 79 (1958) 1520.
17 G. R. Waterbury and C. E. Bricker, *Anal. Chem.*, 29 (1957) 129.
18 S. Kallman, E. W. Hobart and H. K. Oberthin, *Anal. Chim. Acta*, 41 (1968) 29.
19 A. Kiss, *Magy. Kem. Foly.*, 69 (1963) 131 and 272.
20 S. C. Dhara and S. M. Khopkar, *Ind. J. Chem.*, 5 (1967) 12.

Analytica Chimica Acta, 67 (1973) 477–479

SHORT COMMUNICATION

The reaction of iron(III) and 2,3-dihydroxypyridine in phosphoric acid solutions

K. E. CURTIS* and G. F. ATKINSON
Department of Chemistry, University of Waterloo, Ont. (Canada)
(Received 9th March 1973)

In an earlier report[1] on complexes of iron(III) with 2,3-dihydroxypyridine in various media which were all nominally 1 *M* in hydrogen ion, phosphoric acid was found to produce anomalous effects. Further investigations of such solutions are reported here.

In phosphoric acid media, iron(III) and 2,3-dihydroxypyridine reacted to give a blue-violet solution, unlike the clear blue produced in other mineral acids; further acidification caused fading of the colour without any significant change toward blue. With the other mineral acids, it was practical to prepare all solutions in the desired final acid concentration as solvent, but the low solubility of iron(III) and the reagent in phosphoric acid made it necessary to use perchloric acid also. Stock solutions of iron(III) perchlorate and of 2,3-dihydroxypyridine were prepared so that the final solutions for measurements were 0.2 *M* in phosphoric acid and 0.4 *M* in perchloric acid. The preparation of samples containing the two reactants at total molarities of $9.824 \cdot 10^{-3}$ and $5.044 \cdot 10^{-3}$, the preparation of similar series lacking one or the other reactant, the measurements of spectra with the Cary 14 spectrophotometer, and the treatment of the digitized data by the method of Varga and Veatch[2], were all carried out as before[1]. The computer program RANK indicated the presence of one absorbing complex (estimated absorbance error, 0.010) and the program CONTOUR displayed a pattern supporting this result. However, the contour map indicated a mole ratio of Fe: 2,3-dihydroxypyridine = 2:3 in the complex (Fig. 1). Replotting the mapped data as conventional Job curves at four selected wavelengths showed no peculiarities, and the agreement in shape of Job curves at the two working concentrations suggested that the apparent 2:3 single species was unlikely to be a mixture.

A conventional mole-ratio experiment, with up to 200 moles of reagent per mole of iron(III) being added, gave a very rounded curve (Fig. 2a). Since it was impractical to increase the reagent:metal ratio further, in order to establish the maximal absorbance obtainable from a given amount of iron(III), the data already obtained were replotted to estimate the maximal sensitivity of the system; the value found, by extrapolation to an infinite excess of reagent, was 0.025_9 μg of iron. From this value, by calculation from the iron(III) concentration in the mole-ratio

* Present address: Ontario Hydro Research Laboratories, Kipling Avenue, Toronto, Canada.

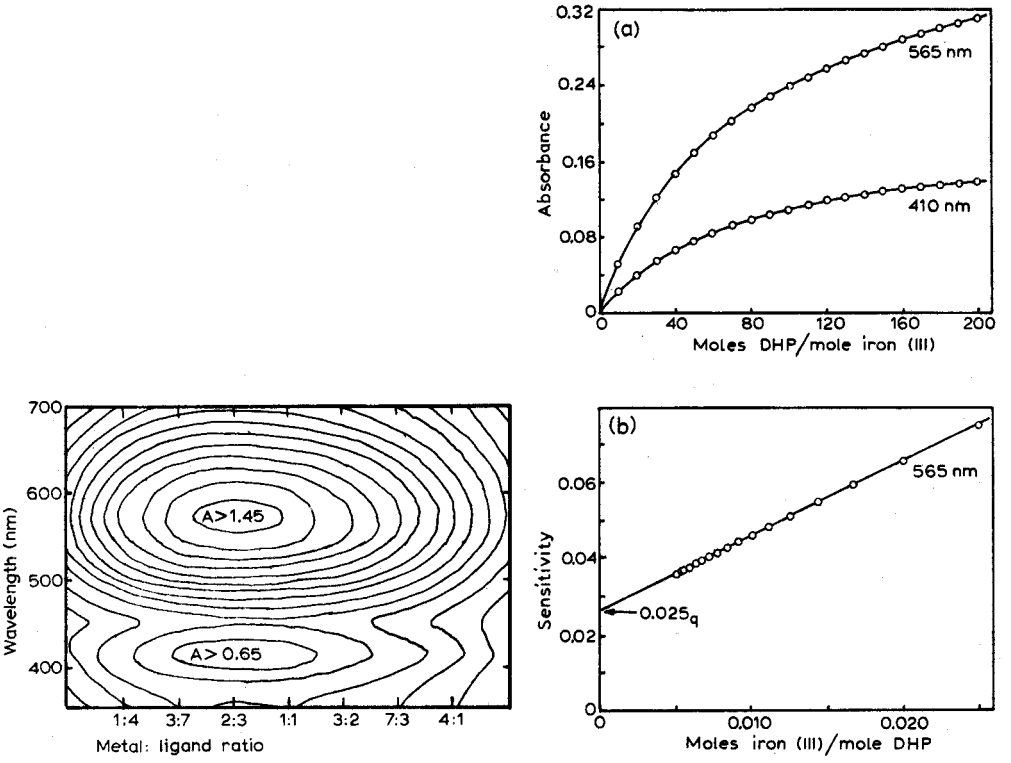

Fig. 1. Absorbance map for complex in phosphate–perchlorate medium. Contour intervals *ca.* 0.05 absorbance unit.

Fig. 2. Mole-ratio curve (a) and maximum sensitivity extrapolation (b). Sensitivity is expressed as μg Fe cm^{-3} for $A = 0.001$. 10-mm cells were used.

experiment, the ultimate maximal absorbance at the inaccessible end of the curve was estimated to be 0.429, and the method of Momoki *et al.*[3] for dealing with curved mole-ratio plots was applied. The constraints of experimental conditions placed the data available outside the recommended working range of the method, but the results suggested that the stoichiometry of the iron–2,3-dihydroxypyridine complex was 1:1.

The modified terminal tangent method proposed by Likussar and Boltz[4] was then applied, and agreement to better than 1% was found between the results and the model $Fe_2(DHP)_3$. The application of the method of Holme and Langmyhr[5] as modified by Thomson and Atkinson[6], however, indicated that the model Fe(DHP) was correct. A calculated maximal absorbance for a mole-ratio type experiment derived from the results of the Holme and Langmyhr method gave 0.432, which agrees within 1% with the estimate from the sensitivity plot.

Despite the conflict of evidence outlined above, it can be reported that in solutions 0.2 *M* in phosphoric acid and 0.4 *M* in perchloric acid, the iron(III) –2,3-dihydroxypyridine system obeys Beer's law with respect to iron(III) up to 40 μg cm^{-3} at 565 nm with a molar absorptivity of *ca.* 2156.

REFERENCES

1 K. E. Curtis, J. A. Thomson and G. F. Atkinson, *Anal. Chim. Acta*, 49 (1970) 351.
2 L. P. Varga and F. C. Veatch, *Anal. Chem.*, 39 (1967) 1101.
3 K. Momoki, J. Sekino, H. Sato and N. Yamaguchi, *Anal. Chem.*, 41 (1969) 1286.
4 W. Likussar and D. F. Boltz, *Anal. Chem.*, 43 (1971) 1265.
5 A. Holme and F. J. Langmyhr, *Anal. Chim. Acta*, 36 (1966) 383.
6 J. A. Thomson and G. F. Atkinson, *Anal. Chim. Acta*, 47 (1969) 380.

Analytica Chimica Acta, 67 (1973) 480–485

SHORT COMMUNICATION

Anionic electrophoretic pattern of five ruthenium salts in fresh and sea water: effects of ageing and dilution*

J. VOS, S. VAN PUYMBROECK and O. VAN DER BORGHT
Mineral Metabolism Laboratory, Radiobiology Department, Belgian Nuclear Centre S.C.K./C.E.N., B-2400 Mol (Belgium)
and
H. PEPERSTRAETE** and M. D'HONT**
Laboratories of Radiochemistry, K. Univ., Leuven (Belgium)
(Received 11th May 1973)

The presence of ruthenium species in the wastes of nuclear fuel reprocessing plants has led to considerable interest in the very complex behaviour of ruthenium. Most chemical studies have been concerned with its forms and reactions in acidic media[1–4], and the biological experiments have been aimed at predicting ruthenium uptake by living organisms under complex conditions. The chemistry of ruthenium under conditions such as those encountered in fresh or sea water at about neutral pH, has been less studied. Several workers[5–10] have stressed the important role that the salts and their physicochemical forms could have on their biological accumulation and their evolution under various environmental conditions. These forms were determined by electro-osmosis[7], paper chromatography[5,11] and ion exchangers[8]. High-voltage electrophoresis has yielded a considerable amount of information, owing to the large number of species that could be separated, not only in chemical studies in acidic media[12] but also in neutral and more dilute solutions[13,14]. This study aimed to relate the physico-chemical characteristics of different ruthenium salts to their differences in fixation by aquatic organisms, differences that we observed under laboratory conditions[9,10,16]. Therefore, five ruthenium salts were studied for influence of dilution and ageing, by means of high-voltage electrophoresis: (*a*) in concentrated aqueous solutions; (*b*) after further dilution with fresh water; (*c*) after further dilution with sea water.

Experimental

The following five ruthenium salts labelled with ^{106}Ru, were studied in neutral aqueous solution:

* Presented in part at the I.A.E.A. Symposium on Interaction of Radioactive Contaminants with the Constituents of the Marine Environment, Seattle, Wash., U.S.A., July 1972.

** Under a research grant of Interuniversitair Instituut Kernwetenschappen (Brussels).
grant of Interuniversitair Instituut Kernwetenschappen (Brussels).

(*a*) nitrosylhydroxynitrite*, $Na_2RuNO(NO_2)_4OH \cdot 2\,H_2O$, specific activity 300 mCi g^{-1};

(*b*) nitrosylchloride*, $RuNOCl_3 \cdot (H_2O)_2$, specific activity 300 mCi g^{-1};

(*c*) chloride, $RuCl_3 \cdot x\,H_2O$, carrier-free;

(*d*) nitrosylnitrate complexes $RuNO(NO_3)_x \cdot (H_2O)_{5-x}$, carrier-free;

(*e*) nitrosylhydroxide* $RuNO(OH)_3 \cdot (H_2O)_2$, specific activity 300 mCi g^{-1}.

All the stock solutions had an activity of 0.1 mCi ml^{-1}, except for the chloride (*c*) which was 0.02 mCi ml^{-1}. The three asterisked salts were obtained through the kindness of the Euratom-CEA Association (Niveau de Pollution) from the Société Ugine Kuhlmann, Levallois, France.

The ^{106}Ru salts were prepared as mentioned earlier[10]. The original stock solutions were made up by adding filtered tap water (with characteristics very close to the local surface water as detailed previously[10]) to the solid salts or to neutralized acidic solutions of the nitrosylnitrate complexes and of the chloride complexes.

These solutions were assayed by high-voltage electrophoresis (Camag, Muttenz, Switzerland) at $2 \cdot 10^3$ V and 10 mA on 40 cm × 3 cm cellulose acetate strips (Sartorius SM 11200; Göttingen, W. Germany) bufered at pH 7 by Na_2HPO_4–KH_2PO_4 Sørensen buffer[2]. Between 10 and 100 μl of the well shaken ^{106}Ru solution was transferred by means of a glass capillary onto the dry strip which was then moistened with buffer. After a 30-min electrophoretic separation, the strips were exposed on Agfa-Gevaert (Mortsel, Belgium) Structurix D 10 X-Ray film.

Under identical experimental conditions, the migration distances to the cathode of $^{85}Sr^{2+}$ and $^{134}Cs^{+}$ were 20 and 5.5 cm, respectively. Reproducibility of the results was very good not only in terms of the number of observed bands but also their location (better than 5 mm on 40 cm). To achieve this, the strips had to be handled one by one; and the current had to be kept constant by small manual voltage corrections during the separation. Handling several strips together made it impossible

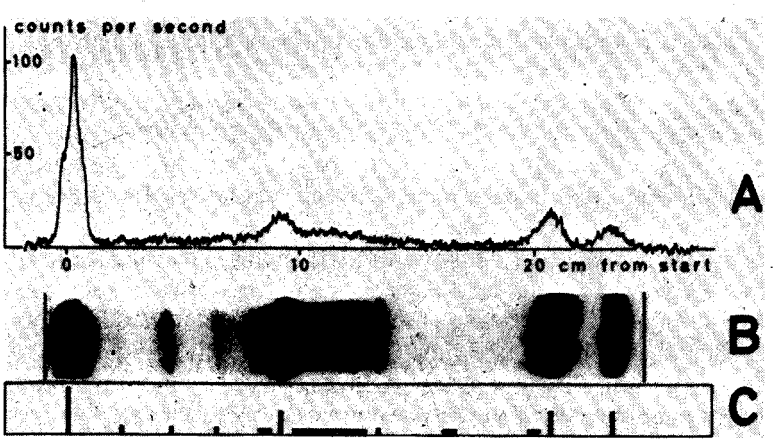

Fig. 1. High-voltage electrophoresis of a freshly prepared, concentrated solution of ruthenium nitrosylnitrate in fresh water. Comparison of: (A) radioactivity scan of the cellulose acetate strip (methane proportional flow counter, window slit 2 mm × 16 mm, time constant 10 s, strip speed 120 mm h^{-1}); (B) autoradiogram on X-Ray film; (C) schematic representation as used in Fig. 2.

to check the current transported through each strip.

Both diluted (10-fold by tap water, or 10-fold by sea water) and undiluted solutions were studied for the effect of ageing. For this purpose, they were analysed by high-voltage electrophoresis immediately after dilution (within 0.5 h), after 7 days, and after 45 days. The sea water used was collected at high tide near the Belgian coast, south of Ostend, and had a chloride content of 19% (Volhard method).

Results and discussion

In order to simplify description of the results, a coding system based on autoradiographic darkening was worked out. An example is given in Fig. 1, in which the result of radioactivity scanning is compared with the autoradiogram and with a sample of the code system used. Figure 2 gives the coded results of the autoradiograms of the electrophoresis strips from the five salts under the different experimental conditions.

Published data on the elution of diluted and filtered neutral nitrosyl and nitrate solutions from ion-exchange columns always mention a certain amount of cations[8], although this amount is less than in acidic medium[1,3,7]. In contrast, no cationic species were found in the present work. In agreement with Marazovic and Pucar[7], the electrophoretic separation pattern found for the chloride was different from that of nitrosylnitrate solutions, but the cations of the chloride solution detected in sea water medium by Marazovic and Pucar did not adsorb on a cation-exchange paper. This raises questions about their occurrence and stability in untreated solutions in which all equilibria have time to develop. Marazovic and Pucar also found differences between the results obtained with their own solutions and with commercial stock solutions, such as were used here.

Guegueniat[8], in his study of nitrosyl and nitrate complexes in sea water, confirmed the possible transition of anionic species to cationic forms on ageing. In the present experiments, the mobility and total number of anionic species also decreased strongly on ageing, and in the older nitrate solutions, more of the ^{106}Ru remained adsorbed at the starting line in the h.v. strips; but again cations were never observed. In the concentrated ruthenium–nitrite solutions, ageing even induced the appearance of a very mobile anion.

Ishikawa *et al.*[13] indicated the presence of 4% cations in their high-voltage electrophoresis (basic electrolyte $NaClO_4$) of nitrosylchloride solutions; ageing for 9 days altered neither the mobility nor the number of the three migrating complexes. This lack of evolution is in agreement with the present results, although only one broad migrating band of negative complexes was detected here. In ruthenium chloride solutions, however, Ishikawa *et al.* found that two new anionic and one new cationic species appeared after 3 days ageing of the sea water solutions, whereas a decreasing number of species was observed here. The fact that Ishikawa *et al.* only used supernates, without shaking, may explain why they found a decreasing quantity of neutral ^{106}Ru, whereas a high amount of non-migrating ^{106}Ru was detected throughout ageing in the present work.

If cations really occur in these ruthenium solutions, without being an artefact caused by electro-osmosis[15], the use of phosphate buffer as current carrier instead of sodium perchlorate[13] or sea water[7] could be responsible for masking these cations by complex formation with orthophosphate ions.

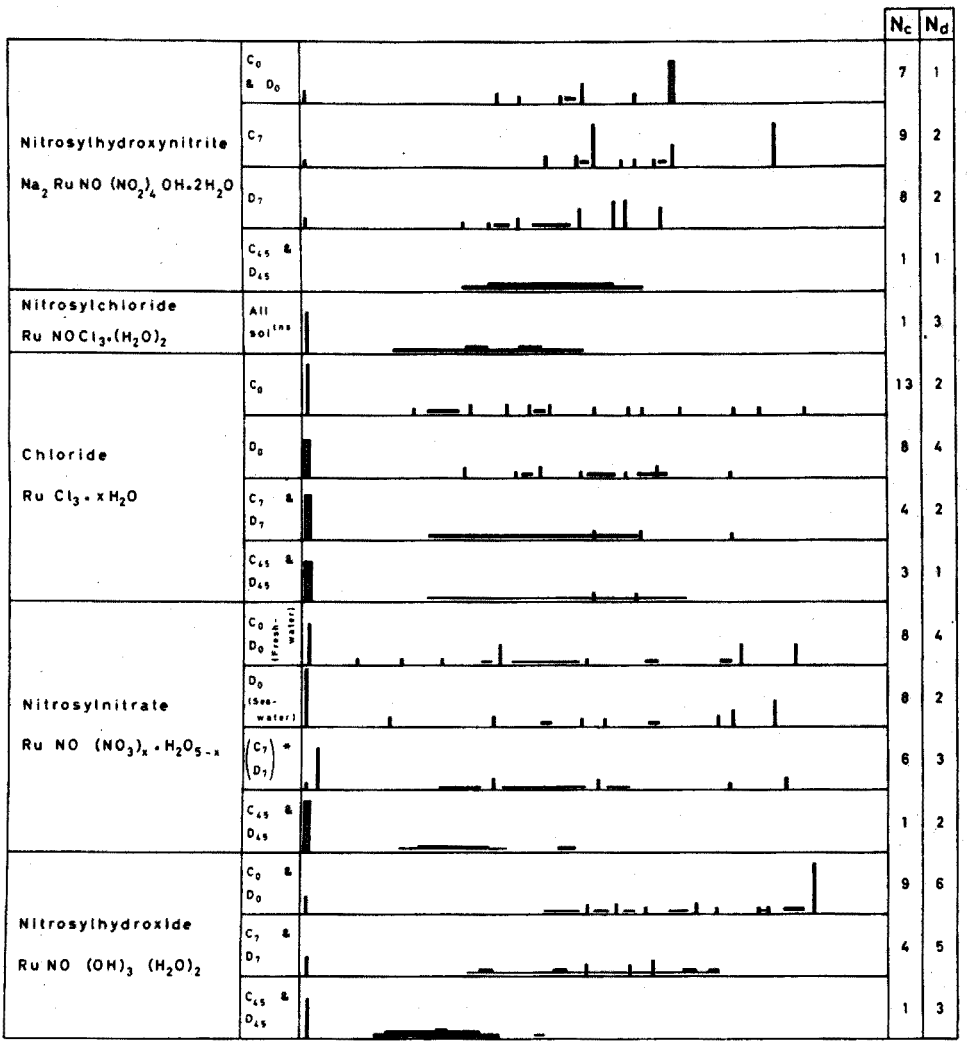

Fig. 2. Diagram of the location of ^{106}Ru on autoradiograms of high-voltage electrophoretic separation. Starting line at left, positive pole at right. C = concentrated stock solution; D = 10 times diluted (with fresh or sea water) stock solution; 0,7,45 = solutions after 0, 7 and 45 days ageing at room temperature in closed clear glass bottles with air-space kept in subdued light.

* Quality of these separations was minor, indicative value only.

Conclusions

This study provides further evidence of the complexity of ruthenium in aqueous neutral solutions and emphasizes the following points, which are important for waste release management.

1. The behaviour of the ruthenium salts is in general similar in filtered sea water and fresh water, except for fresh nitrosylnitrate solutions. A similar behaviour was also observed in biological uptake experiments[9].

2. Ageing is still incomplete after one week except for the ruthenium–nitrosylchloride complexes where there are no such effects.

3. Ageing of the ruthenium solutions results generally in a decrease of the number of complexes, a decrease of their mobility and a severe decrease or total disappearance of the resolution of the separation pattern.

4. Ten-fold dilution had no important influence except for the fresh ruthenium chloride and the 7-day old nitrosylnitrate.

5. Nitrosylnitrite, and especially the aged solutions, contains an exceptionally low amount of ^{106}Ru adsorbed on the starting line. This confirms observations in biological uptake experiments[10].

6. The characteristics of nitrosylhydroxide solutions in fresh and sea water, are similar to the other salts. The freshly prepared solutions contain about 30% of negative complexes with comparatively high mobility in the electric field.

7. The number of species detected by high-voltage electrophoresis in phosphate buffer ranges up to 13 clearly defined bands and 2 vaguer tailings for freshly prepared concentrated neutral ruthenium–chloride complexes. Each salt gives a different electrophoretic separation picture, although complexes at 20–20.5 cm from the starting line appear in most solutions. Between 9 and 9.5 cm, and between 16 and 17.5 cm, complexes appear in one or more of the tested solutions of every salt except nitrosylchloride.

These observations emphasize that ruthenium forms a large number of complexes in neutral medium. These could be due to the multiple possibilities of hydrolysis, which finally results in the displacement of all co-ordinated ligands by hydroxyl groups. Polymerization also could yield other complexes, in which the increasing number of positive charges could be compensated by hydroxyl ligands.

REFERENCES

1 J. M. Fletcher, F. Jenkins, F. Lever, F. Martin, A. Powell and R. Todd, *J. Inorg. Nucl Chem.*, 1 (1955) 378.
2 R. Bittel, *CEA-BIB-123*, 1968, 66 pp.
3 W. Kraak, *KR-3*, 1959.
4 I. G. Van Raaphorst and R. A. Deurloo, *KR-52*, 1963.
5 S. K. Bhagat and E. F. Gloyna, *EHE-11-6502*, 1965.
6 S. Keckes, Z. Pucar and L. Marazovic, *Publ. Ruder Boskovic Inst. Zagreb*, 1966, pp. 213–225 *(Ann. Rep. Res. Contr. no. 201/R2/RB)*.
7 L. Marazovic and Z. Pucar, *J. Chromatogr.*, 27 (1967) 405.
8 P. Guegueniat, *CEA-R-4125*, 1972, 44 pp.
9 O. Van der Borght and S. Van Puymbroeck, *Health Phys.*, 19 (1970) 801.
10 H. Beque, S. Van Puymbroeck, J. Jaumier, R. Bittel and O. Van der Borght, *Environ. Physiol.*, 1 (1971) 37.
11 L. Morpurgo, *Ric. Sci.*, 36 (5) (1966) 4/460.

12 A. Ohyoshi, *Radiochem. Acta*, 13 (1) (1970) 10.
13 M. Ishikawa, M. Sumiya and M. Saiki, *I.A.E.A. Symp. on Interaction of Radioactive Contaminants with Marine Environment, Seattle, July 1972*, IAEA-SM-158/22.
14 H. Peperstraete, J. Vos, S. Van Puymbroeck and O. Van der Borght, *IAEA-SM-158/52.*
15 I. Smith, *Chromatographic and Electrophoretic Techniques*, Vol. II, Heineman, London, 1962, p. 161–2.
16 O. Van der Borght, R. Bittel, S. Van Puymbroeck and J. Colard, *I.A.E.A.-SM-180/53*, 1973.

Analytica Chimica Acta, 67 (1973) 486–488

SHORT COMMUNICATION

Solid-state distribution analysis of sulfisoxazole tablets

L. V. ALLEN, V. A. YANCHICK and D. D. MANESS
College of Pharmacy, The University of Texas at Austin
M. A. WILKOV
Department of Aerospace Engineering and Engineering Mechanics, The University of Texas at Austin, Austin, Texas 78712 (U.S.A.)
(Received 18th March 1973)

Distribution analysis of a drug in solid dosage form can provide valuable information concerning the uniformity of the therapeutic component within the dosage form. Conventional analytical techniques are directed at qualitative identification or bulk quantitative analysis of the therapeutic component of a dosage form. For example, the USP content uniformity test[1] specifies that twenty whole tablets be assayed. Depending on the particular drug, several assays may be available to the analyst, yet few of these are specifically adaptable to distribution analysis. The electron microprobe, combining features of electron microscopy with those of X-ray diffraction spectroscopy[2], may be used to define the distribution of a drug on an individual tablet basis. If the therapeutic agent in the solid matrix possesses an element unique from other formulation components, that element will act as a tracer of the drug in a distribution analysis of the solid sample by moving the beam to scan the surface. It is apparent then, that a major criterion in microprobe distribution analysis of pharmaceuticals is that the drug moiety contains an element different from the remainder of the matrix.

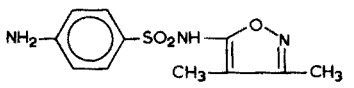

(I)

Sulfisoxazole (I) in 500-mg tablet form, was selected to demonstrate the feasibility of using the electron microprobe for the proposed method of distribution analysis. In this compound, sulfur was chosen to act as the tracer element for analysis.

These scored tablets were particularly suited for this experiment since uniform drug distribution throughout each tablet is necessary if a half-tablet dose were given.

Experimental

Sulfisoxazole tablets from eight different manufacturers were obtained. Instrumentation included a Japan Electron Optics Vacuum Evaporator and a Norelco

Electron Probe, model AMR3. Chemicals used for sulfisoxazole analysis were of reagent grade quality and were used without additional purification. Sulfur analyses of the tablets were performed by Galbraith Laboratories Inc., Knoxville, Tenn.

Sample preparation for microprobe analysis was as follows. The tablets were fixed edgewise on an aluminum disc with the bisecting groove of the score perpendicular to the disc surface. A mixture of Duco-cement and charcoal adhesive (5% charcoal) was used to secure the samples to the disc and provided a conductive medium between the disc and the tablets. Half of each tablet was removed by a lathe, exposing the halved edge as a flat, smooth surface.

Results and discussion

The tablets were analyzed for sulfur content to insure that extraneous sulfur, other than that contributed by the sulfisoxazole, was not present. Also, the sulfisoxazole content was determined titrimetrically to a thymol blue end-point with standard sodium methoxide in dimethylformamide[3]. The sulfur and sulfisoxazole analyses verified that all the sulfur present was contained in the sulfisoxazole entity, and could thus act as a tracer for sulfisoxazole.

A conductive carbon layer of *ca.* 20.0 nm thickness was deposited onto the tablets in the evaporator, and subsequently, these tablets were subjected to microprobe analysis. To minimize surface destruction, an operating voltage of 20,000 V was used. Although the beam diameter was 0.5 μm, all analyses were done with an oscillating beam, producing an effective beam width of 320 μm. The 320-μm

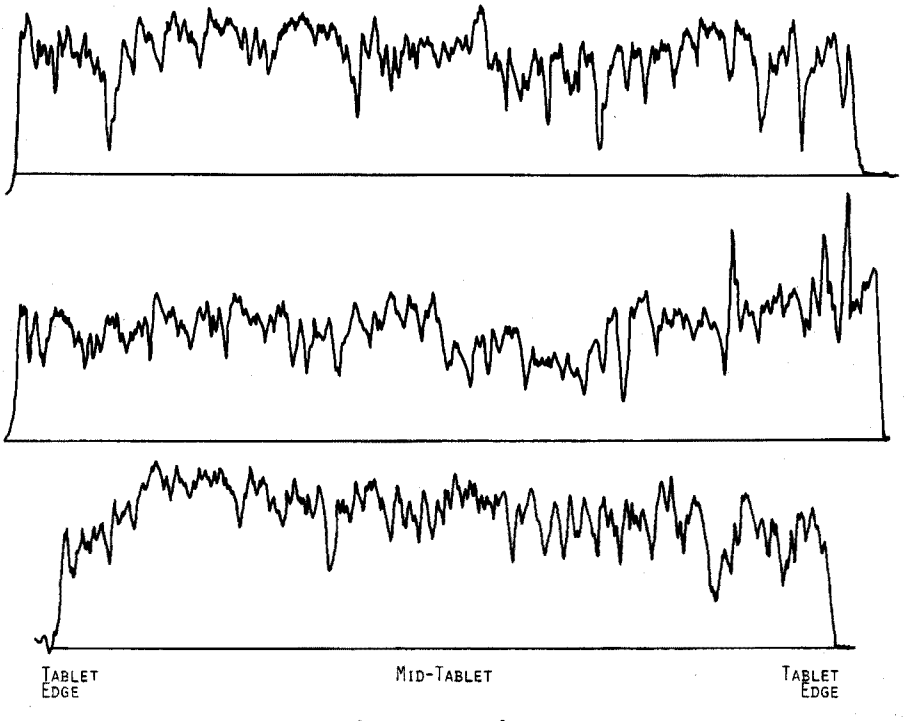

Fig. 1. Representative scans of tablets from one manufacturer.

beam width analyzed a larger surface area and thus yielded a better representation of the distribution of the sulfisoxazole in the tablet. The intensity level appeared to be more uniform, because of the averaging over a larger area. There was a concomitant reduction in signal intensity when the oscillating beam was used; this reduction resulted from the decreased energizing period that the beam was on a surface point. The scans were run lengthwise at a rate of 625 μm min^{-1}, so that each scan required *ca.* 20 min for completion. These scans depicted the relative sulfur content on the exposed surface and were considered to reflect the sulfisoxazole content in various segments of the tablets. A representative scan is shown in Fig. 1. The area under the scan is proportional to the concentration: thus the peaks are areas of high concentration of sulfisoxazole while the valleys are sulfisoxazole-deficient areas in the tablet. The minor irregularities in the distribution most probably are a result of the granulation procedures used before tabletting. All tablets tested showed an even distribution of the sulfisoxazole throughout the tablet.

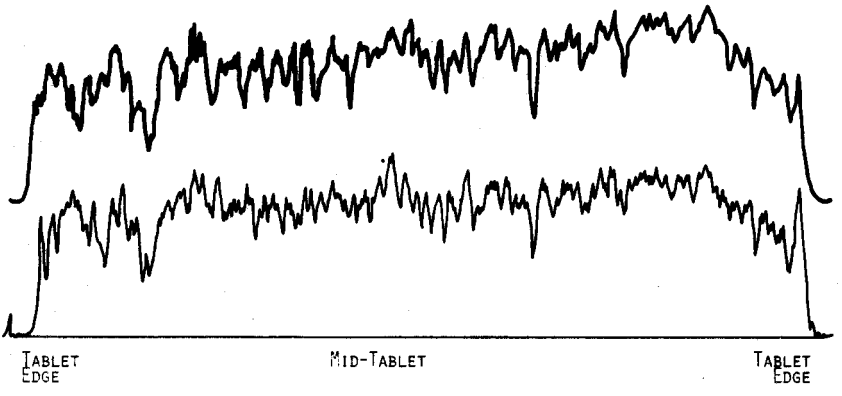

Fig. 2. A demonstration of the reproducibility of the microprobe scan. These are two consecutive scans of the same tablet over the same path.

In Fig. 2, the reproducibility of the microprobe scan is demonstrated. Two consecutive scans of the same tablet over the same path are shown. A 1:1 intensity correlation between the peaks and valleys is observed.

The scans themselves are distribution curves of the sulfisoxazole in the tablet matrix. Thus, microprobe analysis provides unique instrumentation for obtaining distribution of a drug in a solid dosage form.

REFERENCES

1 *The United States Pharmacopeia*, XVIII, Mack Publishing Co., Easton, Pa., 1970, p. 930.
2 L. E. Murr, *Electron Optical Applications in Materials Science*, McGraw-Hill, New York, 1970.
3 *The United States Pharmacopeia*, XVIII, Mack Publishing Co., Easton, Pa., 1970, p. 699.

ANALYTICA CHIMICA ACTA, VOL. 67 (1973)

AUTHOR INDEX

ANALYTICA CHIMICA ACTA, VOL. 67 (1973)

SUBJECT INDEX

(Continued from page 4 of cover)

CONTENTS

(continued on inside page of cover)